

The Two-Loop Lipatov Vertex in QCD

Samuel Abreu,^{a,b} Giuseppe De Laurentis,^a Giulio Falcioni,^{c,d} Einan Gardi,^a Calum Milloy,^e Leonardo Vernazza^e

^a*Higgs Centre for Theoretical Physics, School of Physics and Astronomy,
The University of Edinburgh, Edinburgh EH9 3FD, Scotland, UK*

^b*Theoretical Physics Department, CERN, Geneva 1211, Switzerland*

^c*Physik-Institut, Universität Zürich, Winterthurerstrasse 190, 8057 Zürich, Switzerland*

^d*Dipartimento di Fisica, Università di Torino, Via Pietro Giuria 1, I-10125 Torino, Italy*

^e*INFN, Sezione di Torino, Via Pietro Giuria 1, I-10125 Torino, Italy*

E-mail: Samuel.Abreu@ed.ac.uk, Giuseppe.DeLaurentis@ed.ac.uk,
Giulio.Falcioni@physik.uzh.ch, Einan.Gardi@ed.ac.uk,
calummilloy526@gmail.com, Leonardo.Vernazza@to.infn.it

ABSTRACT: High-energy factorization of $2 \rightarrow 2$ amplitudes in QCD has been recently pushed to the next-to-next-to-leading logarithmic order by determining the three-loop gluon Regge trajectory. This was based on computing multi-Reggeon exchanges using rapidity evolution in the shock-wave formalism, and disentangling between the Regge pole and Regge cut contributions. In the present paper we extend the relevant theoretical framework to $2 \rightarrow 3$ processes, and compute all multi-Reggeon exchanges necessary for extracting the two-loop Reggeon-gluon-Reggeon Lipatov vertex from $2 \rightarrow 3$ amplitudes. Then, specializing general amplitude methods to multi-Regge kinematics, we derive analytic expressions for non-planar two-loop $gg \rightarrow ggg$, $gq \rightarrow ggq$ and $qq \rightarrow qgq$ QCD amplitudes in that limit. Matching these to the multi-Reggeon computation, we determine the QCD Lipatov vertex in dimensional regularization at two loops through finite terms. We also determine the one-loop vertex through $\mathcal{O}(\epsilon^4)$. All results are expressed in a compact form in terms of a basis of single-valued generalised polylogarithms, manifesting target-projectile symmetry and reality properties. Furthermore, our basis of functions is explicitly finite in the soft limit, featuring delicate cancellation of spurious rational poles by transcendental functions. Agreement between all three partonic channels, as well agreement of the maximal weight contributions with the super Yang-Mills Lipatov vertex provide robust checks of the result.

Contents

1	Introduction	1
2	$2 \rightarrow 3$ amplitudes in multi-Regge kinematics	4
2.1	Kinematics	4
2.2	Colour	8
2.3	Signature	9
3	Taking the MRK limit of QCD amplitudes	11
3.1	Expansion of the transcendental functions	11
3.2	Reconstruction of the rational coefficients in the MRK limit	14
3.3	Assembly of the remainders	16
4	Reggeization and the Lipatov vertex	17
4.1	Regge-pole factorization in $2 \rightarrow 3$ scattering	17
4.2	The analytic structure and symmetries of the Lipatov Vertex	19
5	The QCD Lipatov vertex at one loop	22
6	The theory of multi-Reggeon interactions	29
6.1	From the shock-wave formalism to Reggeon fields	29
6.2	Real emission from Reggeons	33
6.3	Identifying single Reggeon contributions to $2 \rightarrow 3$ amplitudes	36
7	Multi-Reggeon computations	38
7.1	Multi-Reggeon contributions to the one-loop amplitude	38
7.2	Multi-Reggeon contributions to the two-loop amplitude	47
7.3	Odd-odd Amplitude	51
8	The QCD Lipatov vertex at two loops	58
8.1	Extracting the Reggeon-gluon-Reggeon vertex	58
8.2	Vertex structure through two loop	62
8.2.1	Basis of transcendental functions	64
8.2.2	Another look at the QCD vertex at one loop	67
8.2.3	QCD vertex at two loop	69
9	Conclusions	72
A	Tree level impact factors and Lipatov vertex for gluon scattering	75

B	Colour basis definition	78
B.1	$qq \rightarrow qgq$	79
B.2	$qg \rightarrow qgg$	79
B.3	$gq \rightarrow ggg$	80
B.4	$gg \rightarrow ggg$	81
B.5	Color space formalism	82
C	Variables conversion in the MRK power expansion	83
D	Gluon Regge trajectory, impact factors and vertex	84
E	The dipole formula in multi-Regge kinematics	88

1 Introduction

The Regge limit of QCD scattering, $s \gg -t$, has long inspired physicists, leading to profound theoretical developments. In the early days, important observations were made based on general scattering theory [1], where the asymptotic behaviour of amplitudes was studied in terms of their singularities in the complex angular momentum plane, corresponding to Regge poles and Regge cuts. It emerged that high-energy asymptotic properties are naturally attributed to amplitude components with a definite signature, namely ones that are either even (symmetric) or odd (antisymmetric) under kinematic $s \leftrightarrow u$ interchange. The leading power behaviour of an amplitude of a given signature is then governed by the t -channel exchange of the highest spin particle.

After the birth of QCD, it soon emerged [2] that the effective degree of freedom exchanged in the t -channel is a *Reggeized gluon*, also dubbed *Reggeon*. This object inherits its basic properties of odd signature and octet colour charge from the gluon, and is understood to govern the power-like growth of partonic amplitudes as $(s/(-t))^{1+\alpha_g(t)}$ where $\alpha_g(t)$ is the gluon Regge trajectory [3–9]. The concept of a Reggeon has subsequently played a key role in studying the Regge limit over the past half a century. In particular, compound states of two Reggeons are understood to dominate the high-energy behaviour of even-signature amplitudes and cross sections [10]. In the framework of BFKL [11–15], where unitarity is used to relate the forward limit of elastic amplitudes to multi-parton inelastic ones, interactions between Reggeons generate rapidity evolution. The same equation governs the small Bjorken- x limit of parton density functions (see e.g. [16]).

While questions such as the asymptotic behaviour of hadronic scattering cross sections are fundamentally non-perturbative, the Regge limit is rich and fascinating already at the perturbative level. In particular, one may address a broad range of questions pertaining to the structure of partonic amplitudes, their factorization and exponentiation properties, as well as their Regge singularities. In this context, the past decade has seen exciting progress due to the development of effective methods which directly describe the Regge limit: the

multi-Reggeon effective theory [17–26] based on the shock-wave formalism (see also [27–29] for an alternative approach) and Glauber SCET [30–33]. These effective methods are synergic with the computation of multi-loop partonic scattering amplitude in general kinematics, where much progress has been made in recent years. The synergy also motivates the present study.

At leading power in the Regge limit, $s \gg -t$, partonic scattering amplitudes feature major simplifications already at tree level, including the dominance of t -channel gluon exchange and flavour and helicity conservation of the scattered partons. More profoundly, partonic amplitudes of odd signature feature all-order factorization and exponentiation of high-energy logarithms. At leading (LL) and next-to-leading (NLL) logarithmic accuracy, these all-order properties can be understood directly as a manifestation of the fact that the amplitude is governed by the exchange of a single Reggeon, and hence features a Regge pole. Starting at next-to-next-to-leading logarithmic accuracy (NNLL), this is no more the case: at this logarithmic order factorization violating terms appear [34–37]. This has been first observed at two loops [34] by noting that a pure Regge-pole factorization ansatz would be inconsistent with explicit amplitude results of the three partonic channels (qq , qg and gg). It is now understood [18, 22–24, 27] that these factorization violations are generated by the t -channel exchange of multiple Reggeons – specifically three Reggeons and their mixing under evolution with a single Reggeon – giving rise to Regge cuts.

Key to pushing our understanding of amplitudes in the Regge limit to NNLL accuracy has been the development of a theoretical framework for direct computation of multi-Reggeon exchange [17–26]. This framework is based on the shock-wave formalism in which the scattered projectile is described by a set of infinite lightlike Wilson lines $U(z_\perp)$ in the background of the target. In this formalism, correlators of products of Wilson lines admit the Balitsky-JIMWLK [38–41] rapidity evolution equation, which provides a non-linear generalization of BFKL. While the original goal of setting up this formalism was to describe high gluon density saturation effects at cross-section level (see e.g. [16]), Simon Caron-Huot [17] has demonstrated its applicability to partonic amplitudes in the dilute, perturbative regime. Essential to this was to trade the use of correlators of Wilson lines $U(z_\perp) = e^{ig_s \mathbf{T}^a W^a(z_\perp)}$, where $U(z_\perp) \simeq 1$ in said regime, for those of their exponent $W^a(z_\perp)$, and to interpret the W fields as individual Reggeons. By construction, W fields have odd signature and carry octet colour charge, consistent with Reggeons. More profoundly, their interaction in the $2 - 2\epsilon$ transverse space, which generates rapidity evolution according to the Balitsky-JIMWLK equation (solved order by order in perturbation theory), matches partonic QCD amplitudes in $4 - 2\epsilon$ dimensions in the high-energy limit.

The interpretation of W as the Reggeon field has far-reaching consequences [17–26]. First, conceptually, it decouples the two-dimensional transverse space dynamics from that involving the collision energy, realising Lipatov’s ambitious goal of [42], at least in part. Second, it provides an efficient¹ and practical framework to perform computations of the multi-Reggeon components of partonic QCD amplitudes – precisely these components which

¹These computations are done directly in the $2 - 2\epsilon$ transverse space, and hence require no rapidity cutoffs. Furthermore, they typically involve planar integrals, even when the colour factors are non-planar.

break Regge-pole factorization and give rise to Regge cuts.

With these multi-Reggeon predictions at hand, a precise separation between Regge pole and Regge cut contributions to amplitudes is within reach. It requires, however, one more essential element [24], namely the special nature of the planar theory. Specifically, one uses the fact that in the planar limit, four and five-point amplitudes only have Regge poles.² Indeed, it has been shown through explicit computations through four loops [18–24] that while multi-Reggeon interactions (t -channel exchange of multiple W fields) contain contributions that are leading in the large- N_c limit, the latter are universal: they do not depend on the partonic process considered, and hence do not lead to Regge-pole factorization violations. This stands in sharp contrast to contributions that are subleading in the large- N_c limit, which do differ between partonic processes (starting at two loops) and necessarily generate factorization violation. It is thus only the latter, namely non-planar multi-Reggeon contributions, which generate a Regge cut.

These theoretical developments allowed [23, 24, 50, 51] to disentangle between Regge pole and Regge cut contributions in $2 \rightarrow 2$ scattering, and hence uniquely determine the Regge pole parameters, the gluon Regge trajectory and the impact factors, from three-loop results of $2 \rightarrow 2$ QCD amplitudes for qq , qg and gg scattering [50–52]. With these parameters fixed, NNLL corrections associated with the Regge pole have been fixed to all orders in perturbation theory, while the corresponding Regge cut corrections have been shown to be non-planar to all orders, and have been explicitly determined to four loops.

The aim of the present paper is to take a step towards extending these results to n -point scattering amplitudes in the so-called Multi-Regge Kinematic (MRK) limit [2, 53–56], where the final-state particles are all strongly ordered in rapidity, while their transverse momenta are unconstrained. It has been established [9] through NLL accuracy that the dispersive part of any n -point $2 \rightarrow n-2$ amplitude admits a similar factorization structure in MRK to that of $2 \rightarrow 2$ amplitudes in the Regge limit, with the same universal impact factors and gluon Regge trajectory, with one additional ingredient, namely the vertex by which a real gluon is emitted from the Reggeon. This Reggeon-gluon-Reggeon vertex [2], referred to as the Lipatov vertex, is a key element in BFKL theory, which is needed in particular to determine the BFKL kernel. The Lipatov vertex appears for the first time in five-point amplitudes, providing the natural setting to extract it. This quantity was determined in the tree approximation in [2], and at one loop in [55, 57–62]. In this paper we determine it at two loops.³

Given the recent completion of the calculation of all $2 \rightarrow 3$ amplitudes in QCD [63–69], and given that the impact factor and gluon Regge trajectory have already been fixed based on $2 \rightarrow 2$ amplitudes [23, 24, 50–52], one might naively expect that the determination of the two-loop vertex would be straightforward. However, this is not so. Similarly to the

²Focusing here on $2 \rightarrow 3$ amplitudes, Regge cuts do not feature in the planar limit. For higher-point amplitudes, $n \geq 6$, Regge cuts appear in certain kinematic regions even in the planar limit, see e.g. [43–48]. For the same reason, the Bern-Dixon-Smirnov ansatz [49] describing the exponentiation of planar amplitudes in super Yang-Mills (sYM) theory, is exact for four and five point amplitudes, while it receives non-trivial corrections (the so-called remainder function) for higher point amplitudes.

³An independent computation by another group has recently appeared, see ref. [26].

case of $2 \rightarrow 2$ scattering, at two loops the relevant (odd-odd signature, octet) component of the amplitude, starts to receive contributions from multiple Reggeon exchange, giving rise to Regge cuts in the non-planar theory. Thus, in order to isolate the single Reggeon contribution, which factorizes in the MRK limit at NNLL accuracy, one needs once again to separately determine the non-factorizing non-planar (and process-dependent) multi-Reggeon contributions and set them aside before using the usual Regge-pole factorization formula (which is fully governed by a Regge pole) to extract the Lipatov vertex. To this end we first need to set up the shockwave formalism in the context of $2 \rightarrow 3$ scattering (for previous work in this direction, see [17, 21]), and then compute all multi-Reggeon contributions to the relevant component of the amplitude. The final results of this computation have been reported in [25] (see also [26]); their derivation will be presented here, before turning to extract the two-loop vertex from the $gg \rightarrow ggg$, $gq \rightarrow ggq$ and $qq \rightarrow qqg$ amplitudes in MRK.

The structure of the paper is as follows. In section 2 we define the MRK limit and set up our notations for $2 \rightarrow 3$ massless scattering momenta, helicities, colour and signature. In section 3 we briefly explain how we compute the two-loop QCD $gg \rightarrow ggg$, $gq \rightarrow ggq$ and $qq \rightarrow qqg$ amplitudes in MRK. In section 4 we discuss the factorization structure in $2 \rightarrow 3$ scattering, define the Lipatov vertex, and analyze its symmetries and analytic properties based on general considerations. Next, in section 5 we determine the QCD Lipatov vertex at one loop through $\mathcal{O}(\epsilon^4)$ and discuss its properties. At this point, in section 6, we turn to discuss the theory of multi-Reggeon interactions within the shock-wave formalism. This theory is then used in section 7 to compute all multi-Reggeon contributions to $2 \rightarrow 3$ amplitudes at one loop, and the odd-odd component at two loops, in order to facilitate the extraction of the two-loop Lipatov vertex in section 8. The result is presented in section 8.2. We also provide the expressions for the MRK amplitude and the vertex components in ancillary files [70].

2 $2 \rightarrow 3$ amplitudes in multi-Regge kinematics

2.1 Kinematics

We consider $2 \rightarrow 3$ scattering amplitudes in any massless gauge theory in multi-Regge kinematics (MRK), as depicted in figure 1. The amplitude $\mathcal{M}_{ij \rightarrow i'g j'}$ corresponds to a scattering process $ij \rightarrow i'g j'$ where g is an emitted gluon while i (i') and j (j') may each be a quark (q) or a gluon (g). We will often drop the subscript when we do not need to specify the process. We label four-vector momenta in terms of capital letters P_i , and take all momenta to be outgoing: $\sum_i P_i = 0$. With this notation the scattering process in figure 1 reads

$$i[(-P_1)^{-\lambda_1}, a_1] + j[(-P_2)^{-\lambda_2}, a_2] \rightarrow j'[P_3^{\lambda_3}, a_3] + g[P_4^{\lambda_4}, a_4] + i'[P_5^{\lambda_5}, a_5], \quad (2.1)$$

where $P_i^2 = 0$, a_i is the colour index of parton i and the superscript $\lambda_i = \oplus$ or \ominus labels the helicity of particle i . Using momentum conservation, the amplitudes in generic kinematics depend on five independent Mandelstam invariants. Defining $s_{kl} = (P_k + P_l)^2$, the physical

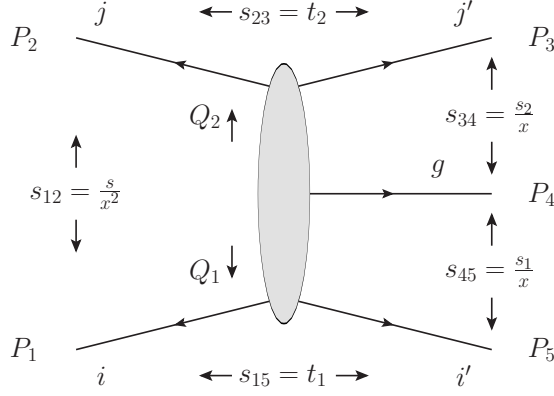


Figure 1. Momentum label for $2 \rightarrow 3$ scattering processes. Capital letters are used to indicate 4-vector momenta.

scattering region is defined by

$$s_{12} > 0, \quad s_{34} > 0, \quad s_{45} > 0, \quad s_{23} < 0, \quad s_{15} < 0, \quad \Delta < 0, \quad (2.2)$$

where $\Delta = \det(s_{kl})_{k,l=1\dots 4}$ is the Gram determinant of the external momenta and is also related to the pseudoscalar invariant

$$\text{tr}_5 \equiv -4i \epsilon_{\mu\nu\sigma\rho} P_1^\mu P_2^\nu P_3^\sigma P_5^\rho \quad (2.3)$$

through $\Delta = (\text{tr}_5)^2$, and where the convention for the Levi-Civita tensor $\epsilon_{\mu\nu\sigma\rho}$ is $\epsilon_{0123} = +1$. It implies that tr_5 is purely imaginary in the physical region, and while the absolute value of the imaginary part is dependent on s_{ij} , the sign of tr_5 is required to fully specify a phase-space point.

In the centre of mass frame P_1 and P_2 are back to back, and we choose coordinates such that

$$P_1 = \frac{\sqrt{s_{12}}}{2}(1, 0, 0, -1), \quad P_2 = \frac{\sqrt{s_{12}}}{2}(1, 0, 0, 1). \quad (2.4)$$

In this way we define two light-like directions along which a generic momentum Q can be decomposed as follows:

$$Q = (q^+, q^-, \mathbf{q}), \quad \text{where} \quad q^\pm = q^0 \pm q^3. \quad (2.5)$$

Therefore P_1 (P_2) is solely in the $-$ ($+$) direction. The transverse momentum \mathbf{q} can be expressed in terms of the complex-valued coordinates $\mathbf{q} = q^1 + i q^2$ with $\bar{\mathbf{q}} = q^1 - i q^2$ and then $Q^2 = q^+ q^- - \bar{\mathbf{q}}\mathbf{q}$.

The multi-Regge kinematic (MRK) limit is defined by strong ordering in rapidity, which is alternatively described by the conditions

$$|p_3^+| \gg |p_4^+| \gg |p_5^+|, \quad |p_3^-| \ll |p_4^-| \ll |p_5^-|, \quad |\mathbf{p}_3| \simeq |\mathbf{p}_4| \simeq |\mathbf{p}_5|. \quad (2.6)$$

The limit can also be described by defining an auxiliary parameter x which relates a point in generic kinematics to a point in the MRK limit. This can be done through

$$s_{12} = \frac{s}{x^2}, \quad s_{15} = t_1, \quad s_{45} = \frac{s_1}{x}, \quad s_{23} = t_2, \quad s_{34} = \frac{s_2}{x}, \quad (2.7)$$

and then considering the limit $x \rightarrow 0$. We will also find it convenient to introduce the variables z and \bar{z} , defined through

$$t_1 = -(1-z)(1-\bar{z})\frac{s_1 s_2}{s}, \quad t_2 = -z\bar{z}\frac{s_1 s_2}{s}. \quad (2.8)$$

The variables $\{s, s_1, s_2, t_1, t_2\}$, or equivalently $\{s, s_1, s_2, z, \bar{z}\}$, describe a point in generic kinematics, which can be mapped to a point in the MRK limit by taking $x \rightarrow 0$ in eq. (2.7). In this limit, the invariant tr_5 in eq. (2.3) becomes

$$\text{tr}_5 \simeq \frac{s_1 s_2}{x^2}(z - \bar{z}), \quad (2.9)$$

where we use \simeq to denote equalities that are valid at leading order in $x \rightarrow 0$. As mentioned after eq. (2.3), tr_5 is purely imaginary in the physical scattering region, which is consistent with taking $\bar{z} = z^*$. Furthermore, because the definition of eq. (2.8) is symmetric under $z \leftrightarrow \bar{z}$, there remains a residual ambiguity in distinguishing which solution to the quadratic is z and which is \bar{z} . Eq. (2.9) effectively removes this ambiguity.

In the MRK limit, we can relate the transverse components of the various final state momenta using the z and \bar{z} variables. Explicitly, at leading order in $x \rightarrow 0$, we have:

$$\mathbf{p}_3 \simeq -z\mathbf{p}_4, \quad \bar{\mathbf{p}}_3 \simeq -\bar{z}\bar{\mathbf{p}}_4, \quad \mathbf{p}_5 \simeq -(1-z)\mathbf{p}_4, \quad \bar{\mathbf{p}}_5 \simeq -(1-\bar{z})\bar{\mathbf{p}}_4. \quad (2.10)$$

Throughout this paper, we will by default choose a frame where \mathbf{p}_4 only has a real component, $\bar{\mathbf{p}}_4 = \mathbf{p}_4$. Momentum conservation in the transverse plane then implies that

$$\mathbf{p}_4 = -\mathbf{p}_3 - \mathbf{p}_5 \simeq -\sqrt{\frac{s_1 s_2}{s}}, \quad t_1 \simeq -|\mathbf{p}_5|^2, \quad t_2 \simeq -|\mathbf{p}_3|^2. \quad (2.11)$$

Note that eq. (2.10) is consistent with $\bar{z} = z^*$, as also argued below eq. (2.9).

In what follows it will be convenient to introduce a notation also for the momenta exchanged in the t -channel, that we define as follows:

$$Q_i \equiv Q_1 = P_1 + P_5, \quad Q_j \equiv Q_2 = P_2 + P_3, \quad (2.12)$$

such that

$$\mathbf{q}_1 = \mathbf{p}_5, \quad \mathbf{q}_2 = \mathbf{p}_3, \quad Q_1^2 = t_1, \quad Q_2^2 = t_2. \quad (2.13)$$

It can be shown that the tree-level amplitude $\mathcal{M}_{ij \rightarrow i'g'j'}^{\text{tree}}$ in MRK assumes a factorized structure [55, 71]

$$\begin{aligned} \mathcal{M}_{ij \rightarrow i'g'j'}^{\text{tree}} &= 2s \left[g_s \delta_{-\lambda_5, \lambda_1} \mathbf{T}_{a_5 a_1}^x C_i^{(0)}(P_1^{\lambda_1}, P_5^{\lambda_5}) \right] \frac{1}{t_1} \\ &\times \left[g_s \mathbf{T}_{yx}^{a_4} V_\mu^{(0)}(Q_1, P_4, Q_2) \varepsilon_{\lambda_4}^\mu(P_4) \right] \frac{1}{t_2} \left[g_s \delta_{-\lambda_3, \lambda_2} \mathbf{T}_{a_3 a_2}^y C_j^{(0)}(P_2^{\lambda_2}, P_3^{\lambda_3}) \right]. \end{aligned} \quad (2.14)$$

In this equation, $C_{i/j}^{(0)}$ represent tree-level impact factors, describing the coupling between the external states i/j and a gluon exchanged in the t -channel. In appendix A, we provide their expression for the gluon amplitude. The factors $\delta_{-\lambda_3, \lambda_2}$, $\delta_{-\lambda_5, \lambda_1}$ represent helicity conservation along the lines i and j , and $\mathbf{T}_{a_i a_{i'}}^x$ are the color generator associated to incoming/outgoing particles a_i , $a_{i'}$: $\mathbf{T}_{a_i a_{i'}}^x = (T_F^x)_{a_i a_{i'}}$ for quarks, $\mathbf{T}_{a_i a_{i'}}^x = -(T_F^x)_{a_{i'} a_i}$ for anti-quarks, $\mathbf{T}_{a_i a_{i'}}^x = i f^{a_i x a_{i'}}$ for gluons.

The vector $V_\mu^{(0)}(Q_1, P_4, Q_2)$ is the Lipatov vertex at tree level, which accounts for the emission of a gluon at central rapidity [2]:

$$V_\mu^{(0)}(Q_1, P_4, Q_2) = \mathcal{P}_\mu + \mathcal{Q}_\mu, \quad (2.15)$$

where \mathcal{P}^μ and \mathcal{Q}^μ are defined by

$$\begin{aligned} \mathcal{Q}^\mu &= (Q_1 - Q_2)_\perp^\mu + 2P_1^\mu \frac{|\mathbf{q}_1|^2}{s_{45}} - 2P_2^\mu \frac{|\mathbf{q}_2|^2}{s_{34}}, \\ \mathcal{P}^\mu &= -|\mathbf{p}_4|^2 \left(\frac{P_1^\mu}{s_{45}} - \frac{P_2^\mu}{s_{34}} \right), \end{aligned} \quad (2.16)$$

with $(Q_i)_\perp = (0, 0; \mathbf{q}_i)$. Note that \mathcal{P}^μ and \mathcal{Q}^μ are separately gauge invariant, as they vanish upon contraction with $P_{4\mu}$. These two also furnish the complete set of tensors that may appear in the vertex $V_\mu(Q_1, P_4, Q_2)$ at higher orders. For definiteness, we give the expression of the gluon polarisation $\varepsilon_\lambda^\mu(P_4)$ in the light-cone gauge $\varepsilon^-(P_4) = 0$, the left gauge (see (A.17)), which will be our default choice of gauge in this paper,

$$\varepsilon_\oplus^\mu(P_4) = \left(\frac{\mathbf{p}_4}{\sqrt{2}p_4^-}, \frac{1}{\sqrt{2}}, \frac{i}{\sqrt{2}}, \frac{\mathbf{p}_4}{\sqrt{2}p_4^-} \right), \quad (2.17)$$

$$\varepsilon_\ominus^\mu(P_4) = \left(\frac{\mathbf{p}_4}{\sqrt{2}p_4^-}, \frac{1}{\sqrt{2}}, -\frac{i}{\sqrt{2}}, \frac{\mathbf{p}_4}{\sqrt{2}p_4^-} \right). \quad (2.18)$$

It is convenient to express the polarisation vector in lightcone components, using the notation of eq. (2.5),

$$\varepsilon_\oplus^\mu(P_4) = \left(\frac{\sqrt{2}\mathbf{p}_4}{p_4^-}, 0; \varepsilon_\oplus(P_4) \right), \quad \text{with} \quad \varepsilon_\oplus(P_4) = \left(\frac{1}{\sqrt{2}}, \frac{i}{\sqrt{2}} \right). \quad (2.19)$$

With this notation one has

$$\varepsilon_\oplus(P_4) \cdot \mathbf{p}_k = \frac{1}{\sqrt{2}} \begin{cases} \mathbf{p}_k, & k \in \{3, 4, 5\}, \\ 0, & k \in \{1, 2\}. \end{cases} \quad (2.20)$$

In what follows we consider the helicity configuration $(\ominus, \ominus, \oplus, \oplus, \oplus)$. By contracting the Lipatov vertex, eq. (2.15) with the polarisation vector above, we get the scalar vertex

$$V^{(0)}(Q_1, P_4^\oplus, Q_2) \equiv V_\mu^{(0)}(Q_1, P_4, Q_2) \varepsilon_\oplus^\mu(P_4) = \sqrt{2} \frac{\bar{\mathbf{q}}_2 \mathbf{q}_1}{\bar{\mathbf{p}}_4} = \sqrt{2} \frac{\bar{\mathbf{p}}_3 \mathbf{p}_5}{\bar{\mathbf{p}}_4}, \quad (2.21)$$

such that the tree level amplitude takes the form

$$\mathcal{M}_{ij \rightarrow i' g j'}^{\text{tree}} = C_i^{(0)}(P_1^\ominus, P_5^\oplus) \mathcal{K}^{(0)} C_{ij}^{(0)} C_j^{(0)}(P_2^\ominus, P_3^\oplus), \quad (2.22)$$

where for future use we have introduced the kinematic and colour factors

$$\mathcal{K}^{(0)} = 2\sqrt{2} g_s^3 \frac{s_{12}}{\mathbf{P}_3 \bar{\mathbf{P}}_4 \bar{\mathbf{P}}_5}, \quad (2.23)$$

$$\mathcal{C}_{ij}^{(0)} = i f^{y a_4 x} (\mathbf{T}_i^x)_{a_5 a_1} (\mathbf{T}_j^y)_{a_3 a_2}. \quad (2.24)$$

2.2 Colour

The tree amplitude in eq. (2.14) is the leading term in the coupling expansion

$$\mathcal{M}_{ij \rightarrow i' g j'} = \sum_{n=0}^{\infty} \left(\frac{\alpha_s}{\pi} \right)^n \mathcal{M}^{(n)}, \quad (2.25)$$

i.e. $\mathcal{M}^{(0)} = \mathcal{M}_{ij \rightarrow i' g j'}^{\text{tree}}$. In general, the coefficients $\mathcal{M}^{(n)}$ develop a non-trivial color structure for $n \geq 1$. This is conveniently described in the colour space formalism [72–74]. We begin by expanding the amplitude coefficients on a basis of colour tensors

$$\mathcal{M}^{(n)} = \sum_i c_{a_1 \dots a_5}^{[i]} \mathcal{M}^{(n), [i]}, \quad (2.26)$$

where the sum includes all linearly independent tensors $c_{a_1 \dots a_5}^{[i]}$ with indices $a_1 \dots a_5$ in the representation of the five external particles. Denoting the colour operator in the representation of the k -th parton as \mathbf{T}_k , we have

$$\mathbf{T}_k^b c_{a_1 \dots a_5}^{[i]} = (\mathbf{T}_k^b)_{a_k a'_k} c_{a_1 \dots a'_k \dots a_5}^{[i]}, \quad (2.27)$$

for $k = 1 \dots 5$, with

$$(\mathbf{T}_k^b)_{a a'} = \begin{cases} (T_F^b)_{a a'} & \text{for } k = \text{quark,} \\ -(T_F^b)_{a' a} & \text{for } k = \text{antiquark,} \\ i f^{a b a'} & \text{for } k = \text{gluon,} \end{cases} \quad (2.28)$$

where T_F are the $\text{SU}(N_c)$ generators in the fundamental representation and f are the structure constants. In this language, colour conservation is guaranteed by the condition

$$\sum_{k=1}^5 (\mathbf{T}_k^b) c_{a_1 \dots a_5}^{[i]} = 0, \quad \forall c^{[i]}. \quad (2.29)$$

Following from eq. (2.27) it is clear that generators associated with different particles trivially commute, so one has

$$[\mathbf{T}_k^a, \mathbf{T}_l^b] = i f^{abc} \mathbf{T}_k^c \delta_{kl} \quad (2.30)$$

and

$$(\mathbf{T}_k^b \mathbf{T}_k^b) \equiv \mathbf{T}_k \cdot \mathbf{T}_k = C_k \mathbf{1}, \quad (2.31)$$

where C_k is the quadratic Casimir operator of the corresponding colour representation, i.e. $C_q = C_F = (N_c^2 - 1)/(2N_c)$ for quarks and $C_g = C_A = N_c$ for gluons.

In the Multi-Regge limit, it is natural to use a t -channel colour basis [35, 75], which diagonalises the operators

$$\mathbf{T}_{t_1}^2 \equiv (\mathbf{T}_1 + \mathbf{T}_5)^2 = 2 \mathbf{T}_1 \cdot \mathbf{T}_5 + C_1 \mathbf{1} + C_5 \mathbf{1}, \quad (2.32)$$

$$\mathbf{T}_{t_2}^2 \equiv (\mathbf{T}_2 + \mathbf{T}_3)^2 = 2 \mathbf{T}_2 \cdot \mathbf{T}_3 + C_2 \mathbf{1} + C_3 \mathbf{1}. \quad (2.33)$$

Since $\mathbf{T}_{t_1}^2$ and $\mathbf{T}_{t_2}^2$ are Hermitian and, by eq. (2.30), $[\mathbf{T}_{t_1}^2, \mathbf{T}_{t_2}^2] = 0$, we choose the tensors $c_{a_1 \dots a_5}^{[i]}$ such that *both* t -channel operators are simultaneously diagonal [75]. Therefore, the basis elements are identified by the eigenvalues of $\mathbf{T}_{t_1}^2$ and $\mathbf{T}_{t_2}^2$, which measure the colour charge exchanged in the t -channel. We modify the notation of eq. (2.26) accordingly

$$\mathcal{M}^{(n)} = \sum_{(r_1, r_2), r} c_{a_1 \dots a_5}^{[r_1, r_2]_r} \mathcal{M}^{(n), [r_1, r_2]_r}, \quad (2.34)$$

where r_1 and r_2 label the pairs of irreducible representations of $SU(N_c)$ that can flow in the t -channel and an additional subscript r is introduced to distinguish degenerate cases. The bases for $qq \rightarrow qqq$, $qg \rightarrow qgg$ and $gg \rightarrow ggg$ scattering are given in Appendix B, where we also provide the eigenvalues of $\mathbf{T}_{t_1}^2$ and $\mathbf{T}_{t_2}^2$.

In what follows it will be useful to introduce also a colour operator associated to the s -channel, as done in Ref. [75]

$$\mathbf{T}_s^2 = (\mathbf{T}_1 + \mathbf{T}_2)^2 = 2 \mathbf{T}_1 \cdot \mathbf{T}_2 + C_1 \mathbf{1} + C_2 \mathbf{1}. \quad (2.35)$$

The matrix representations of the operator \mathbf{T}_s are constructed using the color basis in appendix B. These matrices are non-diagonal and provided in an ancillary file [70].

2.3 Signature

Another important feature that characterises the structure of amplitudes in the high energy limit is the so-called signature symmetry. It is well known that in case of $2 \rightarrow 2$ scattering, the signature symmetry, i.e. the way the amplitude transforms under the exchange of the kinematic variables $s \leftrightarrow u$, plays a relevant role in determining the analytic structure of the amplitude itself. In order to derive the generalization of the signature symmetry to $2 \rightarrow 3$ scattering, we start by invoking momentum conservation, which allows us to determine all kinematic invariants in terms of the parameterization in eq. (2.7): considering the leading terms in the small x limit, one has

$$\begin{aligned} s_{12} &= \frac{s}{x^2}, & s_{45} &= \frac{s_1}{x}, & s_{34} &= \frac{s_2}{x}, & s_{15} &= t_1, & s_{23} &= t_2, & s_{35} &= \frac{s}{x^2}, \\ s_{14} &= -\frac{s_1}{x}, & s_{24} &= -\frac{s_2}{x}, & s_{13} &= -\frac{s}{x^2}, & s_{25} &= -\frac{s}{x^2}, \end{aligned} \quad (2.36)$$

which immediately reveals that the natural generalization of signature symmetry to the $2 \rightarrow 3$ case is realised via two independent permutations:

$$(1 \leftrightarrow 5) \quad \rightarrow \quad \{s \rightarrow -s, \quad s_1 \rightarrow -s_1\}, \quad (2.37a)$$

$$(2 \leftrightarrow 3) \quad \rightarrow \quad \{s \rightarrow -s, \quad s_2 \rightarrow -s_2\}. \quad (2.37b)$$

As for the $2 \rightarrow 2$ scattering, it proves useful to decompose the $2 \rightarrow 3$ amplitude into even and odd components under the exchange in eq. (2.37):

$$\mathcal{M}_{ij \rightarrow i'gj'} = \mathcal{M}_{ij \rightarrow i'gj'}^{(+,+)} + \mathcal{M}_{ij \rightarrow i'gj'}^{(+,-)} + \mathcal{M}_{ij \rightarrow i'gj'}^{(-,+)} + \mathcal{M}_{ij \rightarrow i'gj'}^{(-,-)}, \quad (2.38)$$

where

$$\begin{aligned} & \mathcal{M}_{ij \rightarrow i'gj'}^{(\sigma_1, \sigma_2)}(P_1^{\lambda_1}, P_2^{\lambda_2}, P_3^{\lambda_3}, P_4^{\lambda_4}, P_5^{\lambda_5}) \\ &= \frac{1}{4} \left[\mathcal{M}_{ij \rightarrow i'gj'}(P_1^{\lambda_1}, P_2^{\lambda_2}, P_3^{\lambda_3}, P_4^{\lambda_4}, P_5^{\lambda_5}) + \sigma_1 \mathcal{M}_{ij \rightarrow i'gj'}(P_1^{\lambda_1}, P_3^{\lambda_3}, P_2^{\lambda_2}, P_4^{\lambda_4}, P_5^{\lambda_5}) \right. \\ & \quad \left. + \sigma_2 \mathcal{M}_{ij \rightarrow i'gj'}(P_5^{\lambda_5}, P_2^{\lambda_2}, P_3^{\lambda_3}, P_4^{\lambda_4}, P_1^{\lambda_1}) + \sigma_1 \sigma_2 \mathcal{M}_{ij \rightarrow i'gj'}(P_5^{\lambda_5}, P_3^{\lambda_3}, P_2^{\lambda_2}, P_4^{\lambda_4}, P_1^{\lambda_1}) \right]. \end{aligned} \quad (2.39)$$

The two signature indices σ_1 and σ_2 can be separately $+1$ or -1 , and determine the transformation properties of the partial amplitudes $\mathcal{M}_{ij \rightarrow i'gj'}^{(\sigma_1, \sigma_2)}$ under the permutations in eq. (2.37). Comparing with eq. (2.14) one finds that the overall factor of s implies $\mathcal{M}_{ij \rightarrow i'gj'}^{\text{tree}} = \mathcal{M}_{ij \rightarrow i'gj'}^{(-,-)}|_{\text{tree}}$. In case of gluon scattering, because of Bose symmetry, the upper and lower vertices acquire a corresponding colour symmetry: at tree level the upper vertex is antisymmetric upon interchanging the colour indices a_2 and a_3 , while the lower vertex is antisymmetric upon interchanging a_1 and a_5 . At higher orders, all amplitudes (σ_1, σ_2) are nonzero: in case of the $gg \rightarrow ggg$ amplitude the upper vertex is thus symmetric/antisymmetric upon interchanging the colour indices a_2 and a_3 , for $\sigma_1 = +1$ and $\sigma_1 = -1$, respectively. Similarly, the lower vertex is symmetric/antisymmetric upon interchanging the colour indices a_1 and a_5 , for $\sigma_2 = +1$ and $\sigma_2 = -1$, respectively. Let us stress, however, that the correspondence between color symmetry and signature holds only for the all gluon amplitude, because of Bose Symmetry; it does not hold for scattering amplitudes involving quarks.

The operators $\mathbf{T}_{t_1}^2$ and $\mathbf{T}_{t_2}^2$ introduced in Sec 2.2 commute with the operation of exchanging particles $2 \leftrightarrow 3$ and $1 \leftrightarrow 5$, thus they are *even* under both exchanges and preserve the symmetry of the colour tensor on which they act. The operator \mathbf{T}_s^2 instead is clearly not invariant under $1 \leftrightarrow 5$ and $2 \leftrightarrow 3$. Therefore, the operator \mathbf{T}_s^2 mixes colour structures with different signatures. As we will see, it proves useful to describe the amplitude in terms of colour operators with a definite symmetry under the exchange $1 \leftrightarrow 5$ and $2 \leftrightarrow 3$, matching the symmetry properties of the amplitudes $\mathcal{M}_{ij \rightarrow i'gj'}^{(\sigma_1, \sigma_2)}$. To this end let us define the set of operators

$$\begin{aligned} \mathbf{T}_{(++)} &= (\mathbf{T}_1^a + \mathbf{T}_5^a) \cdot (\mathbf{T}_2^a + \mathbf{T}_3^a) : \text{signature-preserving operator on line } i, j ; \\ \mathbf{T}_{(+-)} &= (\mathbf{T}_1^a + \mathbf{T}_5^a) \cdot (\mathbf{T}_2^a - \mathbf{T}_3^a) : \text{signature-preserving on line } i, \text{ inverting on } j ; \\ \mathbf{T}_{(-+)} &= (\mathbf{T}_1^a - \mathbf{T}_5^a) \cdot (\mathbf{T}_2^a + \mathbf{T}_3^a) : \text{signature-preserving on line } j, \text{ inverting on } i ; \\ \mathbf{T}_{(--) } &= (\mathbf{T}_1^a - \mathbf{T}_5^a) \cdot (\mathbf{T}_2^a - \mathbf{T}_3^a) : \text{signature-inverting operator on lines } i, j. \end{aligned} \quad (2.40)$$

Using the definition above we get

$$\mathbf{T}_s^2 = \frac{1}{2} \left[\mathbf{T}_{(++)} + \mathbf{T}_{(+-)} + \mathbf{T}_{(-+)} + \mathbf{T}_{(--) } \right] + C_1 \mathbf{1} + C_2 \mathbf{1}. \quad (2.41)$$

In the forthcoming sections will see how colour operators with distinct signature symmetry, and corresponding colour structure $\mathbf{T}_{(\sigma_1 \sigma_2)}$ arise. We begin in Sec. 4 by reviewing the Reggeization property of the signature odd-odd amplitude $\mathcal{M}_{ij \rightarrow i'gj'}^{(-,-)}$.

3 Taking the MRK limit of QCD amplitudes

In order to compute the required amplitudes in the MRK limit, we will start from the amplitudes for 3-jet production at hadron colliders in general kinematics, which are known up to two loops [63–68]. Depending on the physical channel and the number of loops, the various QCD amplitudes are known in slightly different formats. In all cases, however, they are written as a decomposition of the form

$$\mathcal{F} = \sum_k r_k f_k, \quad (3.1)$$

where \mathcal{F} might be either an amplitude or a finite remainder (see eq. (E.1)), the r_k are rational coefficients, and the f_k are transcendental functions, such as Feynman integrals. If \mathcal{F} is an amplitude, then it also depends on the dimensional regulator ϵ . In order to compute the MRK limit of the QCD amplitudes, we must then compute the limit of both the rational coefficients and the transcendental functions.

Our QCD amplitudes in the MRK limit will be constructed out of the one- and two-loop remainders given in refs. [67, 68], and as such we focus our discussion on these expressions. However, the procedure can be easily adapted to other cases (such as, e.g., the expressions for one-loop amplitudes given in ref. [64], which are written as a decomposition in terms of one-loop master integrals, and valid to all orders in ϵ). In refs. [67, 68], the one- and two-loop remainders \mathcal{H} were expressed in the form

$$\mathcal{H} = \sum_{j,k} r_k M_{kj} h_j, \quad (3.2)$$

where the r_k are rational coefficients of (contractions of) the spinors λ_α and $\lambda_{\dot{\alpha}}$ ($\alpha, \dot{\alpha} \in \{1, \dots, 5\}$), M_{kj} is a rectangular matrix of rational numbers, and the h_j are a set of transcendental functions appearing in five-point massless scattering up to two loops, known as pentagon functions [76].

3.1 Expansion of the transcendental functions

The pentagon functions are functions of five Mandelstam variables $\{s_{12}, s_{23}, s_{34}, s_{45}, s_{15}\}$ and of the (sign of the) pseudoscalar invariant tr_5 defined in eq. (2.3). This set of functions is sufficient to express any master integral appearing in five-point massless scattering at two loops [76]. A convenient way to expand them in the MRK limit is to start from the differential equation they satisfy. By definition, this set of functions is closed under differentiation, and if one assembles all the pentagon functions into a vector \vec{h} , one can write a system of first-order differential equations for the pentagon functions of the form

$$d\vec{h} = \epsilon M(x, y) \vec{h}, \quad M(x, y) = \sum_k m_k d \log W_k(x, y), \quad (3.3)$$

where the m_k are matrices of rational numbers, and the W_k are the 31 letters of the alphabet for five-point massless scattering at two loops.⁴ In our case, the vector \vec{h} contains

⁴We thank Vasily Sotnikov for discussions on this topic, and for providing us with his own calculation of the differential equations satisfied by the pentagon functions.

1083 entries, each one being a pure function of weight smaller or equal to 4. In eq. (3.3), the parameter ϵ is strictly speaking not the dimensional regulator (since, by definition, the pentagon functions do not depend on the dimensional regulator), but rather a bookkeeping parameter that keeps track of the transcendental weight of each object.

The steps to expand the functions \vec{h} in the MRK limit starting from eq. (3.3) are well known [77] (see also ref. [21] for an application in the context of the MRK limit of five-point amplitudes). We summarise them here for completeness. The first step is to rewrite the letters W_k as functions of x , the variable that controls the approach to the MRK limit, and $\{s, s_1, s_2, t_1, t_2\}$ or $\{s, s_1, s_2, z, \bar{z}\}$ (see eq. (2.7) and (2.8)), which for simplicity we collectively denote as y in what follows. A point in generic kinematics corresponds to $(x = 1, y)$ and a point in the MRK limit corresponds to $(x = 0, y)$. From eq. (3.3), we can construct two differential equations that allow us to move in the x direction and in the y space, namely

$$\frac{d\vec{h}}{dx} = \epsilon M_x(x, y) \vec{h}, \quad \frac{d\vec{h}}{dy} = \epsilon M_y(x, y) \vec{h}, \quad (3.4)$$

with

$$M_\kappa(x, y) = \sum_j m_j \frac{d \log W_j(x, y)}{d\kappa}. \quad (3.5)$$

Given that the \vec{h} are pure functions, they have at most logarithmic divergences as $x \rightarrow 0$, which are generated by single poles at $x = 0$ in M_x . That is,

$$M_x(x, y) = \frac{M_x^{(-1)}}{x} + \sum_{k=0} M_x^{(k)}(y) x^k, \quad (3.6)$$

where $M_x^{(-1)}$ is a matrix of rational numbers. In contrast, the matrix $M_y(x, y)$ is regular at $x = 0$.

The solution to eq. (3.3) can be written as [21, 77]

$$\vec{h}(x, y, \epsilon) = T(x, y, \epsilon) \vec{h}(x, y, \epsilon) \quad (3.7)$$

where

$$\vec{h}(x, y, \epsilon) = x^{\epsilon M_x^{(-1)}} \mathbb{P} \exp \left(\epsilon \int_{y_0}^y M_y(0, v) dv \right) \vec{h}_0(\epsilon) \quad (3.8)$$

is a solution to the simpler system of equations

$$\frac{d\vec{h}}{dx} = \epsilon \frac{M_x^{(-1)}}{x} \vec{h}, \quad \frac{d\vec{h}}{dy} = \epsilon M_y(0, y) \vec{h}, \quad (3.9)$$

and it captures the non-analytic behaviour for $x \rightarrow 0$. The matrix $T(x, y, \epsilon)$ can be expanded in powers of x and ϵ , and be chosen to be the identity matrix at $x = 0$. We then write

$$T(x, y, \epsilon) = \mathbb{I} + \sum_{k, j \geq 1} x^k \epsilon^j T_{k, j}(y) \quad (3.10)$$

and the coefficients $T_{k,j}(y)$ can be recursively computed with

$$\begin{aligned} T_{k,1}(y) &= \frac{M_x^{(k)}(y)}{k}, \\ T_{k,j}(y) &= \frac{1}{k} \left(\left[M_x^{(-1)}, T_{k,j-1}(y) \right] + \sum_{l=1}^{k-1} M_x^{(k-l)}(y) T_{l,j-1}(y) \right), \quad \text{for } j > 1. \end{aligned} \quad (3.11)$$

In other words, we can write

$$\vec{h}(x, y, \epsilon) = \vec{h}(x, y, \epsilon) + \sum_{k \geq 1} x^k \vec{h}^{(k)}(x, y, \epsilon). \quad (3.12)$$

$\vec{h}(x, y, \epsilon)$ gives the leading behaviour in the $x \rightarrow 0$ limit, which contains (powers of) logarithms of x , and the higher-order terms $h^{(k)}(x, y, \epsilon)$ can be systematically generated through multiplication by (the expansion of) the matrix $T(x, y, \epsilon)$, which is explicitly given above.

In order to determine $\vec{h}(x, y, \epsilon)$, we must compute the boundary condition $\vec{h}_0(\epsilon)$. This corresponds to the evaluation of the pentagon functions at a point $(0, y_0)$ in the MRK limit. We start from the point

$$X_0 = \{x = 1; s = 3, s_1 = 1, s_2 = 1, t_1 = -1, t_2 = -1\}, \quad (3.13)$$

which is the point chosen as a boundary value for the pentagon functions $\vec{h}(1, y, \epsilon)$ in ref. [76], and use the differential equation (3.3) within `DiffExp` [78] to compute an expansion around

$$X_1 = \{x = 0; s = 1, s_1 = 1, s_2 = 1, t_1 = -1, t_2 = -1\}. \quad (3.14)$$

This point is in the MRK limit, and as such the expansion near X_1 contains powers of $\log(x)$. These logarithms correspond to the expansion of the $x^{\epsilon M_x^{(-1)}}$ factor in eq. (3.8), and we can indeed verify that the expansion we obtain from `DiffExp` contains the expected logarithms. The point X_1 was the boundary point chosen in ref. [21], and we could validate our setup by comparing our results with the ones given there. We note, however, that X_1 corresponds to a singular limit within MRK, namely the limit where the centrally emitted gluon is soft. To proceed with the computation of $\vec{h}(x, y, \epsilon)$ we therefore use a regular point within MRK at which we evaluate the boundary condition:

$$X_2 = \{x = 0; s = 1, s_1 = 1, s_2 = 1, z = i, \bar{z} = -i\}. \quad (3.15)$$

Given that both X_1 and X_2 lie in the MRK limit (with $x = 0$), we can simply use the second equation in (3.4) within `DiffExp` to obtain a numerical evaluation at X_2 starting from the one at X_1 . In summary, we can use `DiffExp` to obtain $\vec{h}_0(\epsilon)$ in eq. (3.8). At our boundary point X_2 these numbers do not correspond to simple constants, so we keep $\vec{h}_0(\epsilon)$ as a vector of numbers with 60 digit precision.

To complete the calculation of $\vec{h}(x, y, \epsilon)$, we must compute the integrals in the path-ordered exponential in eq. (3.8), starting at the point X_2 . As already noted in ref. [21], it turns out that the alphabet greatly simplifies in the MRK limit, and in particular the

letters either depend on $\{s, s_1, s_2\}$ or on $\{z, \bar{z}\}$. This makes the integration easy to perform in terms of multiple polylogarithms using e.g. `PolyLogTools` [79].

The most complicated functions appearing in the remainders we are interested in are of transcendental weight 4. We thus require the calculation of $\vec{h}_0(\epsilon)$ and of the integrals in the path-ordered exponentials in eq. (3.8) up to weight 4. Given the size of the differential equation (3.3) this is not a trivial calculation, but we found that `DiffExp` [78] and a combination of `PolyLogTools` [79] and `HyperInt` [80] was sufficient to handle it.

Having determined $\vec{h}(x, y, \epsilon)$ with the steps described above, we can then compute the subleading terms in the $x \rightarrow 0$ limit using eqs. (3.7), (3.10) and (3.11). As described in the next section, for the two-loop remainders of the QCD amplitudes we require expansions of the pentagon functions up to terms of order x^2 in the MRK limit.

We close this discussion with two comments. First, while our discussion was in the context of the MRK limit of pentagon functions, exactly the same procedure is applicable to Feynman integrals in a pure basis, since they satisfy a differential equation of the same form as in eq. (3.3) (and this is indeed what was done in [21]). In fact, this procedure is simpler when applied to a basis of master integrals, because the system of equations are typically smaller, and the solutions typically have more constrained analytic structure than individual pentagon functions. Second, given the current knowledge of the two-loop QCD amplitudes we cannot compute them beyond the finite term in the expansion in the dimensional regulator. However, at one-loop we do have expressions valid to all orders in the dimensional regulator [64]. We have thus implemented the same steps described above to compute the one-loop integrals in the MRK limit up to weight 6, allowing us to compute one-loop amplitudes in the MRK limit up to order ϵ^4 .

3.2 Reconstruction of the rational coefficients in the MRK limit

One might expect that the expansion in the MRK limit of the (rational) coefficients r_k in eq. (3.2) should be much simpler than that of the transcendental functions h_j . This would indeed be the case if the r_k were simply rational functions of the Mandelstam variables $\{s_{12}, s_{23}, s_{34}, s_{45}, s_{15}\}$, and if there were no spurious-pole cancellations. In such a scenario, one could directly substitute the relations in eq. (2.7) and analytically expand around $x = 0$. However, as already noted below eq. (3.2), the r_k given in refs. [67, 68] are rational functions of contractions of spinors, making this procedure more involved. Furthermore, if an r_k were to exhibit any spurious poles in x , retaining additional orders in the x expansion to manifest these cancellations analytically could become computationally prohibitive.

In this section, we describe how the expansion of the rational coefficients around $x = 0$ can be obtained through analytic reconstruction of p -adic numerical evaluations [81, 82]. This has two benefits. First, spinors no longer pose a complication since we only need to numerically evaluate the expressions. Second, any cancellation, if present, will happen numerically, which is computationally efficient. Fortunately, due to the simplicity of the rational functions given in refs. [67, 68], spurious-pole cancellations do not pose an obstacle to the present calculation. Nevertheless, this technique lays the groundwork for more complex scenarios. A preliminary investigation [83] of a similar calculation with higher-

multiplicity amplitudes [84] suggests that such cancellations become very relevant, and the p -adic approach offers a scalable solution.

In the computation of the Laurent expansion of the rational functions around $x = 0$, we employ a somewhat different minimal set of kinematic variables, which we denote by w, \bar{w}, X_{34} and X_{45} (see also refs. [85, 86]). We define them as

$$w = -\frac{\mathbf{p}_3}{\mathbf{p}_4}, \quad \bar{w} = -\frac{\bar{\mathbf{p}}_3}{\bar{\mathbf{p}}_4}, \quad X_{34} = \frac{p_3^+}{p_4^+}, \quad X_{45} = \frac{p_4^+}{p_5^+}. \quad (3.16)$$

The definition for w and \bar{w} is none other than eq. (2.10), now taken as exact. Given that z and \bar{z} are defined by eq. (2.8) instead, we have $w = z + \mathcal{O}(x)$ and $\bar{w} = \bar{z} + \mathcal{O}(x)$ as we move away from the MRK limit. Similarly, X_{34} and X_{45} are closely related to $s_{34} = s_2/x$ and $s_{45} = s_1/x$. In appendix C, we provide explicit formulae to relate $(w, \bar{w}, X_{34}, X_{45})$ to the set of variables $(z, \bar{z}, s_{34}, s_{45})$, and therefore (z, \bar{z}, s_1, s_2) , through the third order in the power expansion in x . In order to work with $\mathcal{O}(x^0)$ variables, we perform one more change of variables to

$$\tilde{X}_{34} = x X_{34}, \quad \tilde{X}_{45} = x X_{45}. \quad (3.17)$$

We shall work with the minimal set of independent variables $(w, \bar{w}, \tilde{X}_{34}, \tilde{X}_{45})$.

We consider the MRK limit of the r_k in eq. (3.2) normalised by a factor that removes the spinor weight. We choose such a factor to be the leading-colour tree amplitude in a reference permutation, which we denote $\mathcal{M}^{\text{tree}}$. We write

$$\tilde{r}_k = \frac{r_k}{\mathcal{M}^{\text{tree}}}, \quad (3.18)$$

and the expansion of the \tilde{r}_k takes the form

$$\tilde{r}_k = \frac{\tilde{r}_k^{(-2)}(w, \bar{w}, \tilde{X}_{34}, \tilde{X}_{45})}{x^2} + \frac{\tilde{r}_k^{(-1)}(w, \bar{w}, \tilde{X}_{34}, \tilde{X}_{45})}{x} + \tilde{r}_k^{(0)}(w, \bar{w}, \tilde{X}_{34}, \tilde{X}_{45}) + \mathcal{O}(x). \quad (3.19)$$

Our objective is to determine the expansion coefficients $\tilde{r}_k^{(-2)}$, $\tilde{r}_k^{(-1)}$ and $\tilde{r}_k^{(0)}$.

The structure of p -adic numbers lends itself well to the present task as, unlike finite-field numbers, they allow us to approach limits. Indeed, they can be thought of as a Laurent expansion in powers of the prime p . We compute the expansion of eq. (3.19) numerically over p -adic numbers, by setting $x = p$ (we recall that while p is generally chosen as a large prime to avoid accidental cancellations, p -adically it is actually a small quantity, $|p|_p \ll 1$), while the four minimal variables are chosen as random $\mathcal{O}(1)$ p -adic integers. We interpret the digits of the p -adic number as finite field evaluations of the corresponding terms in the x expansion of \tilde{r}_k , namely $\tilde{r}_k^{(-2)}$, $\tilde{r}_k^{(-1)}$ and $\tilde{r}_k^{(0)}$. Note that a direct computation over finite fields of these expansion coefficients would be impossible, since x would need to be either exactly zero, causing divisions by zero, or $\mathcal{O}(1)$, meaning it would be away from the limit. One may rely on a univariate interpolation in x , but this would require obtaining the full x dependence before truncating at $\mathcal{O}(x)$.

With p -adic evaluations at hand, we sequentially reconstruct each digit with finite field interpolation methods [87, 88]. Specifically, we obtain the denominators from a univariate slice by matching factors obtained from a univariate Thiele rational interpolation to a list

of expected singularities related to the letters of the symbol alphabet [63]. The set of possible denominator factors that we consider is

$$\{w, \bar{w}, w + 1, w - 1, \bar{w} + 1, \bar{w} - 1, 1 - w - \bar{w}, w - \bar{w}, \tilde{X}_{34}, \tilde{X}_{45}\}. \quad (3.20)$$

Subsequently, we perform a multivariate Newton interpolation of the numerators. Given the simplicity of the r_i , this reconstruction is trivially performed in least common denominator form.

Several components of this calculation are available in public software. The general kinematic results can be loaded using `antares` [89] from `antares-results` [90] and evaluated over p -adic numbers using the phase-space implementation of `lips` [91] and the p -adic number type implementation in `pyadic` [92]. Newton and Thiele interpolation algorithms are implemented in `pyadic.interpolation`.

We close this section with a comment on one-loop amplitudes. As already noted previously, in refs. [63, 64] expressions are given for the one-loop amplitudes (and not remainders) that are valid to all orders in the dimensional regulator ϵ . After normalisation by a factor that removes the spinor weight, the coefficients are written in terms of rational functions in the Mandelstam variables and tr_5 , and as such computing their MRK limit does not require the more advanced technology described here. We note, however, that for the amplitudes involving two and four quarks, the results of refs. [63, 64] are only sufficient for calculations in the leading-colour limit, so we computed the remaining amplitudes to order ϵ^2 with `Caravel` [93]. This allowed us to explicitly construct all the required amplitudes from the remainders.

3.3 Assembly of the remainders

After discussing the expansion of the pentagon functions in the MRK limit in section 3.1 and the expansion of the coefficients in 3.2, in this section we briefly comment on the assembly of the the one- and two-loop remainders.

For each remainder \mathcal{H} as in eq. (3.2), we combine the coefficients r_k with the corresponding transcendental functions h_k . In the most complicated cases the coefficients include terms starting at $\mathcal{O}(x^{-2})$, and we must include the expansion of the functions up to order $\mathcal{O}(x^2)$. As discussed in section 3.1, the boundary conditions $\vec{h}_0(\epsilon)$ were kept as numbers with 60 digit precision. The reason why we did not try to identify these numbers is that we do not expect the pentagon functions to only involve simple transcendental numbers. However, by the time we have assembled the remainders, we expect this to be the case. After constructing each remainder, we thus combine all numeric terms at each weight (which are linear combinations of the $\vec{h}_0(\epsilon)$ and the evaluation of the integrals in the path-ordered exponentials at y_0 , see eq. (3.8)) and use the PSLQ algorithm to fit them to a basis of zeta values. Up to weight four, this basis is rather small: $\{i\pi\}$ for weight 1, $\{\zeta_2\}$ for weight 2, $\{\zeta_3, i\pi^3\}$ for weight 3 and $\{\zeta_4, i\pi\zeta_3\}$ for weight 4. As such, the 60-digit evaluations of $\vec{h}_0(\epsilon)$ are sufficient to successfully fit the remaining numeric terms and obtain fully analytic expressions.

As a cross-check of our results, we compared the analytic expressions we obtained for the MRK limit of the one- and two-loop remainders with a numerical evaluation of the

expressions in refs. [67, 68] at a point very close to the MRK limit (we take $x = 10^{-10}$ and we run the pentagon functions to octuple precision). The agreement of these two calculations for at least 6 significant digits (which is consistent with the value of x chosen in the numerical calculations), provides a non-trivial check of the expansion procedures outlined in sections 3.1 and 3.2.

The analytic expressions for all components of the amplitudes of the three process (in the colour basis described in appendix B) at both one and two loops are provided in the ancillary files [70].

4 Reggeization and the Lipatov vertex

In the high-energy limit the scattering amplitude develops large logarithms proportional to the rapidity differences between the final-state particles. These contributions are dominated by the exchange of a single Reggeized gluon [2, 94–96]. In this section we discuss the amplitude in the Regge-pole approximation, where it is assumed that a single Reggeized gluon (or Reggeon) is exchanged across each of the rapidity spans, that is in each of the t_i channels. While this is not the complete description of high-energy amplitudes in MRK, it fully captures the planar limit of four and five-point amplitudes, and in the full non-planar theory it holds through next-to-leading logarithms for the dispersive part of the amplitude [9].

In terms of colour structure, the Reggeon has the same quantum number of the gluon, i.e. an antisymmetric octet. Thus, the amplitude in the Regge-pole approximation has the same colour structure of the tree-level one⁵, $C_{ij}^{(0)}$ defined in eq. (2.23). In terms of signature, each Reggeon has negative parity. Hence in this whole section we shall refer to the Regge-pole contribution as $\mathcal{M}_{ij \rightarrow i'g'j'}^{(-,-)}|^{1\text{-Reggeon}}$.

4.1 Regge-pole factorization in $2 \rightarrow 3$ scattering

At leading logarithmic (LL) accuracy, Reggeization of the t -channel gluons across each rapidity interval amounts to dressing the corresponding propagators in eq. (2.14) as follows:

$$\frac{1}{t_1} \rightarrow \frac{1}{t_1} \left(\frac{s_{45}}{\tau} \right)^{C_A \alpha_g(t_1)}, \quad \frac{1}{t_2} \rightarrow \frac{1}{t_2} \left(\frac{s_{34}}{\tau} \right)^{C_A \alpha_g(t_2)}, \quad (4.1)$$

where the scale $\tau \sim -t_1 \sim -t_2 \sim |\mathbf{p}_4|^2 > 0$ is a reference scale, and $\alpha_g(t)$ is the so-called *gluon Regge trajectory* [2]

$$\alpha_g(t_i) = \frac{\alpha_s(\mu^2)}{\pi} \alpha_g^{(1)}(t_i, \mu^2, \epsilon) + \left(\frac{\alpha_s(\mu)}{\pi} \right)^2 \alpha_g^{(2)}(t_i, \mu^2, \epsilon) + \dots \quad (4.2)$$

At LL accuracy, only the one-loop term in the Regge trajectory is relevant

$$\alpha_g^{(1)}(t_i, \mu^2, \epsilon) = \frac{r_\Gamma}{2\epsilon} \left(\frac{\mu^2}{-t_i} \right)^\epsilon, \quad r_\Gamma(\epsilon) = \frac{e^{\epsilon\gamma_E} \Gamma(1-\epsilon)^2 \Gamma(1+\epsilon)}{\Gamma(1-2\epsilon)} = 1 - \frac{\zeta_2}{2} \epsilon^2 - \frac{7\zeta_3}{3} \epsilon^3 + \dots, \quad (4.3)$$

⁵Other components in the basis, which appear due to multi-Reggeon exchange across either or both of these rapidity spans will be discussed in Sections 6 and 7.

and the LL amplitude reads

$$\mathcal{M}_{ij \rightarrow i'gj'}^{\text{LL}} = \left(\frac{s_{45}}{\tau} \right)^{C_A \alpha_g(t_1)} \left(\frac{s_{34}}{\tau} \right)^{C_A \alpha_g(t_2)} \mathcal{M}_{ij \rightarrow i'gj'}^{\text{tree}}. \quad (4.4)$$

Extending the Reggeization hypothesis beyond leading logarithms requires corrections to the gluon Regge trajectory (4.2), the impact factors and the Lipatov vertex. The impact factors are the effective vertices describing the emission of a Reggeon from the scattered partons i and j , while the Lipatov vertex is the emission vertex of a real gluon g from the Reggeon. Below we briefly define our notation for these quantities, while we delegate a more detailed exposition of their perturbative expansion to appendix D.

Let us parametrize the loop correction to the impact factors and Lipatov vertex as follows: for the impact factors we write

$$C_i(P_i, P_{i'}, \tau) = g_s C_i^{(0)}(P_i, P_{i'}) c_i(t_i, \tau), \quad (4.5)$$

where $t_i = Q_i^2 = (P_i + P_{i'})^2$ (cf. eqs. (2.12) and (2.13)), with

$$c_i(t_i, \tau) = 1 + \sum_{n=1}^{\infty} \left(\frac{\alpha_s}{\pi} \right)^n c_i^{(n)}(t_i, \tau, \mu^2). \quad (4.6)$$

In the rest of this section we will keep the dependence on the renormalization scale μ implicit, i.e. $c_{i/j}^{(n)}(t_k, \tau) \equiv c_{i/j}^{(n)}(t_k, \tau, \mu^2)$. We discuss the complete renormalization and factorization scale dependence of the impact factors in appendix D.

Concerning the Lipatov vertex, in a similar fashion we define

$$V_\mu(Q_1, P_4, Q_2, \tau) = g_s V^{(0)}(Q_1, P_4, Q_2) v_\mu(z, \bar{z}, |\mathbf{p}_4|^2, \tau), \quad (4.7)$$

with

$$v_\mu(z, \bar{z}, |\mathbf{p}_4|^2, \tau) = \frac{V_\mu^{(0)}(Q_1, P_4, Q_2)}{V^{(0)}(Q_1, P_4, Q_2)} + \sum_{n=1}^{\infty} \left(\frac{\alpha_s}{\pi} \right)^n v_\mu^{(n)}(z, \bar{z}, |\mathbf{p}_4|^2, \tau), \quad (4.8)$$

where $V_\mu^{(0)}(Q_1, P_4, Q_2)$ and $V^{(0)}(Q_1, P_4, Q_2)$ introduced in eq. (2.15) and (2.21), respectively. Note that this definition implies that v_μ is normalized similarly to (4.5) such that

$$v_\oplus(z, \bar{z}, |\mathbf{p}_4|^2, \tau) \equiv v_\mu(z, \bar{z}, |\mathbf{p}_4|^2, \tau) \varepsilon_\oplus^\mu(P_4) = 1 + \sum_{n=1}^{\infty} \left(\frac{\alpha_s}{\pi} \right)^n v_\oplus^{(n)}. \quad (4.9)$$

where we omitted the kinematic dependence for the coefficients, $v_\oplus^{(n)} = \varepsilon_\oplus^\mu(P_4) v_\mu^{(n)}$.

Under the Reggeization hypothesis, the amplitude takes the form

$$\begin{aligned} \mathcal{M}_{ij \rightarrow i'gj'}^{(-,-)} \Big|^{1\text{-Reggeon}} &= c_i(t_1, \tau) e^{\omega_1 \eta_1} v_\mu(t_1, t_2, |\mathbf{p}_4|^2, \tau) e^{\omega_2 \eta_2} c_j(t_2, \tau) \varepsilon_{\lambda_4}^\mu \mathcal{M}_{ij \rightarrow i'gj'}^{\text{tree}} \\ &= c_i(t_1, \tau) e^{\omega_1 \eta_1} v_{\lambda_4}(t_1, t_2, |\mathbf{p}_4|^2, \tau) e^{\omega_2 \eta_2} c_j(t_2, \tau) \mathcal{M}_{ij \rightarrow i'gj'}^{\text{tree}}, \end{aligned} \quad (4.10)$$

with

$$\eta_1 \equiv \log \left(\frac{s_{45}}{\tau} \right) - i \frac{\pi}{4}, \quad \eta_2 \equiv \log \left(\frac{s_{34}}{\tau} \right) - i \frac{\pi}{4}, \quad (4.11)$$

where the exponents are $\omega_k \equiv C_A \alpha_g(t_k)$ for $k = 1, 2$ and where the phases associated with the Reggeized gluons have been fixed based on the infrared singularity structure (see appendix E): these are the terms proportional to $\mathbf{T}_{t_1}^2$ and $\mathbf{T}_{t_2}^2$ in eqs. (E.16), which accompany the energy logarithms in (E.19).

4.2 The analytic structure and symmetries of the Lipatov Vertex

Because the impact factors c_i and c_j in (4.10) are real, the remaining phase of the single Reggeon amplitude (4.10), must be attributed to the Lipatov vertex v_μ . This phase is tightly constrained by *signature* and *analyticity*. The former requires the *antisymmetry* of the single Reggeon amplitude upon either $\{s_{12} \rightarrow -s_{12}, s_{45} \rightarrow -s_{45}\}$, or $\{s_{12} \rightarrow -s_{12}, s_{34} \rightarrow -s_{34}\}$, eq. (2.37). The latter forbids sequential discontinuities in partially overlapping channels, such as $s_{34}^{\text{power}} s_{45}^{\text{power}}$. Accounting for this, the Regge-pole ansatz takes the form

$$\mathcal{M}_{ij \rightarrow igj}^{(-,-)} \Big|^{1\text{-Reggeon}} = c_i(t_1, \tau) c_j(t_2, \tau) \mathcal{M}_{ij \rightarrow igj}^{\text{tree}} \varepsilon_{\lambda_4}^\mu(P_4) \mathcal{A}_\mu(z, \bar{z}, s_{45}, s_{34}, |\mathbf{p}_4|^2, \tau), \quad (4.12)$$

where the production amplitude \mathcal{A}_μ is [54, 55, 97, 98]

$$\begin{aligned} \mathcal{A}_\mu(z, \bar{z}, s_{45}, s_{34}, |\mathbf{p}_4|^2, \tau) = & \\ & \frac{1}{4} \left[\left(\frac{s_{34}}{\tau} \right)^{\omega_2 - \omega_1} + \left(\frac{-s_{34} - i\delta}{\tau} \right)^{\omega_2 - \omega_1} \right] \left[\left(\frac{s_{12}}{\tau} \right)^{\omega_1} + \left(\frac{-s_{12} - i\delta}{\tau} \right)^{\omega_1} \right] R_\mu(z, \bar{z}, |\mathbf{p}_4|^2, \tau) \\ & + \frac{1}{4} \left[\left(\frac{s_{45}}{\tau} \right)^{\omega_1 - \omega_2} + \left(\frac{-s_{45} - i\delta}{\tau} \right)^{\omega_1 - \omega_2} \right] \left[\left(\frac{s_{12}}{\tau} \right)^{\omega_2} + \left(\frac{-s_{12} - i\delta}{\tau} \right)^{\omega_2} \right] L_\mu(z, \bar{z}, |\mathbf{p}_4|^2, \tau), \end{aligned} \quad (4.13)$$

where the relation (2.11) $s_{12} = s_{34}s_{45}/|\mathbf{p}_4|^2$ can be used to restore the overall dependence on the powers of s_{45} and s_{34} , consistently with eq. (4.11). The *right* and *left* vertices, R_μ and L_μ , are *real* functions, obeying

$$R_\mu(z, \bar{z}, |\mathbf{p}_4|^2, \tau) = R_\mu^*(z, \bar{z}, |\mathbf{p}_4|^2, \tau) = R_\mu(\bar{z}, z, |\mathbf{p}_4|^2, \tau), \quad (4.14a)$$

$$L_\mu(z, \bar{z}, |\mathbf{p}_4|^2, \tau) = L_\mu^*(z, \bar{z}, |\mathbf{p}_4|^2, \tau) = L_\mu(\bar{z}, z, |\mathbf{p}_4|^2, \tau). \quad (4.14b)$$

Note that this reality property is no more manifest once the vertex is contracted into the gluon complex polarization vector in (4.12), defining the conventional left and right vertices

$$v_R^{(\lambda_4)} \equiv \varepsilon_{\lambda_4}^\mu(P_4) R_\mu(z, \bar{z}, |\mathbf{p}_4|^2, \tau), \quad v_L^{(\lambda_4)} \equiv \varepsilon_{\lambda_4}^\mu(P_4) L_\mu(z, \bar{z}, |\mathbf{p}_4|^2, \tau). \quad (4.15)$$

Hence, for now we proceed to consider the vectors quantities R_μ and L_μ .

In practice, R_μ and L_μ are written in terms of a basis of transcendental functions⁶ and their associated rational coefficients, so for example for R_μ

$$R_\mu(z, \bar{z}, |\mathbf{p}_4|^2, \tau) \Big|_{\tau=|\mathbf{p}_4|^2} = \mathcal{Q}_\mu \sum_i S_Q^{(i)}(z, \bar{z}) \Phi_i(z, \bar{z}) + \mathcal{P}_\mu \sum_i S_P^{(i)}(z, \bar{z}) \Phi_i(z, \bar{z}), \quad (4.16)$$

where \mathcal{P}_μ and \mathcal{Q}_μ are the gauge invariant tensors in eq. (2.16), Φ_i are the elements of the transcendental basis and $S_P^{(i)}$, $S_Q^{(i)}$ are rational coefficients. A similar expansion (with different coefficients) holds for L_μ . Given the reality property, it is natural to choose a basis in which neither the transcendental functions nor their rational coefficients would

⁶Example of such a basis, in which we express the result for the vertex through two loop is provided in section 8.2.

have any explicit imaginary i factors. Then, upon complex conjugation, equation (4.16) becomes

$$R_\mu^*(z, \bar{z}, |\mathbf{p}_4|^2, \tau)|_{\tau=|\mathbf{p}_4|^2} = \mathcal{Q}_\mu \sum_i S_Q^{(i)}(\bar{z}, z) \Phi_i(\bar{z}, z) + \mathcal{P}_\mu \sum_i S_P^{(i)}(\bar{z}, z) \Phi_i(\bar{z}, z). \quad (4.17)$$

The reality condition (4.14a) can then be satisfied if the functions and their respective rational coefficients are all either real, namely,

$$S_{Q/P}^{(i)}(\bar{z}, z) = S_{Q/P}^{(i)}(z, \bar{z}), \quad \Phi_i(\bar{z}, z) = \Phi_i(z, \bar{z}), \quad (4.18)$$

or purely imaginary

$$S_{Q/P}^{(i)}(\bar{z}, z) = -S_{Q/P}^{(i)}(z, \bar{z}), \quad \Phi_i(\bar{z}, z) = -\Phi_i(z, \bar{z}). \quad (4.19)$$

We recall that the amplitude will eventually be contracted with the complex polarization vector $\varepsilon_{\lambda_4}^\mu(P_4)$ in (4.12). Thus, the rational coefficients in the amplitude would no longer obey the symmetry conditions above. However, the transcendental functions $\Phi_i(z, \bar{z})$ cannot be affected by the contraction with ε^μ , and therefore can always be chosen such that each is either purely real (i.e. symmetric under $z \leftrightarrow \bar{z}$) or purely imaginary (antisymmetric under $z \leftrightarrow \bar{z}$). Equivalently, one may choose a basis of complex functions, but such that they are all hermitian:

$$\Phi_i^*(z, \bar{z}) = \Phi_i(\bar{z}, z). \quad (4.20)$$

In section 8 we will choose such a basis to express the vertex through two loops.

By comparing eq. (4.10) with eqs. (4.12) and (4.13), it follows that

$$\begin{aligned} v_\mu(t_1, t_2, |\mathbf{p}_4|^2, \tau) &= \left(\frac{|\mathbf{p}_4|^2}{\tau} \right)^{-\omega_1} \exp \left\{ i \frac{\pi}{4} (\omega_1 - \omega_2) \right\} \tilde{R}_\mu(z, \bar{z}, |\mathbf{p}_4|^2, \tau) \\ &+ \left(\frac{|\mathbf{p}_4|^2}{\tau} \right)^{-\omega_2} \exp \left\{ i \frac{\pi}{4} (\omega_2 - \omega_1) \right\} \tilde{L}_\mu(z, \bar{z}, |\mathbf{p}_4|^2, \tau), \end{aligned} \quad (4.21)$$

where we introduce the real functions

$$\tilde{R}_\mu(z, \bar{z}, |\mathbf{p}_4|^2, \tau) = R_\mu(z, \bar{z}, |\mathbf{p}_4|^2, \tau) \cos \left[\frac{\pi}{2} \omega_1 \right] \cos \left[\frac{\pi}{2} (\omega_1 - \omega_2) \right], \quad (4.22a)$$

$$\tilde{L}_\mu(z, \bar{z}, |\mathbf{p}_4|^2, \tau) = L_\mu(z, \bar{z}, |\mathbf{p}_4|^2, \tau) \cos \left[\frac{\pi}{2} \omega_2 \right] \cos \left[\frac{\pi}{2} (\omega_1 - \omega_2) \right]. \quad (4.22b)$$

By expanding the complex exponentials, we may now read off eq. (4.21) the dispersive and the absorptive parts [55] of the complex Lipatov vertex of eq. (4.10):

$$\text{Disp} [v_\mu(z, \bar{z}, |\mathbf{p}_4|^2, \tau)] = \left[\left(\frac{\tau}{|\mathbf{p}_4|^2} \right)^{\omega_1} \tilde{R}_\mu + \left(\frac{\tau}{|\mathbf{p}_4|^2} \right)^{\omega_2} \tilde{L}_\mu \right] \cos \left[\frac{\pi}{4} (\omega_1 - \omega_2) \right], \quad (4.23a)$$

$$\text{Absorp} [v_\mu(z, \bar{z}, |\mathbf{p}_4|^2, \tau)] = \left[\left(\frac{\tau}{|\mathbf{p}_4|^2} \right)^{\omega_1} \tilde{R}_\mu - \left(\frac{\tau}{|\mathbf{p}_4|^2} \right)^{\omega_2} \tilde{L}_\mu \right] \sin \left[\frac{\pi}{4} (\omega_1 - \omega_2) \right], \quad (4.23b)$$

where we drop the arguments of \tilde{R}_μ and \tilde{L}_μ to keep the expressions compact. We now contract $\text{Disp}[v_\mu]$ and $\text{Absorp}[v_\mu]$ with the gluon polarisations, given in eq. (2.17), to compute the Lipatov vertex for positive and negative helicity of the emitted gluon.

By introducing

$$\tilde{v}_R(z, \bar{z}, |\mathbf{p}_4|^2, \tau) \equiv \tilde{R}_\mu(z, \bar{z}, |\mathbf{p}_4|^2, \tau) \varepsilon_\oplus^\mu, \quad \tilde{v}_L(z, \bar{z}, |\mathbf{p}_4|^2, \tau) \equiv \tilde{L}_\mu(z, \bar{z}, |\mathbf{p}_4|^2, \tau) \varepsilon_\oplus^\mu, \quad (4.24)$$

and noting that the negative helicity polarization vector is the complex conjugate of the positive helicity one, $\varepsilon_\ominus^\mu(P_4) = (\varepsilon_\oplus^\mu(P_4))^*$, using the reality of the functions (4.22) we get:

$$\tilde{R}_\mu(z, \bar{z}, |\mathbf{p}_4|^2, \tau) \varepsilon_\ominus^\mu = \tilde{v}_R^*(z, \bar{z}, |\mathbf{p}_4|^2, \tau), \quad \tilde{L}_\mu(z, \bar{z}, |\mathbf{p}_4|^2, \tau) \varepsilon_\ominus^\mu = \tilde{v}_L^*(z, \bar{z}, |\mathbf{p}_4|^2, \tau), \quad (4.25)$$

The complex vertex of eq. (4.10), after contraction with a positive helicity polarization vector, may be expressed as

$$\begin{aligned} v_\oplus(z, \bar{z}, |\mathbf{p}_4|^2, \tau) &\equiv v_\mu(z, \bar{z}, |\mathbf{p}_4|^2, \tau) \varepsilon_\oplus^\mu \\ &= \text{Disp} [v_\oplus(z, \bar{z}, |\mathbf{p}_4|^2, \tau)] + i \text{Absorp} [v_\oplus(z, \bar{z}, |\mathbf{p}_4|^2, \tau)], \end{aligned} \quad (4.26)$$

where the definition of $\text{Disp} [v_\oplus]$ and $\text{Absorp} [v_\oplus]$ follows from eqs. (4.23a) and (4.23b)

$$\text{Disp} [v_\oplus(z, \bar{z}, |\mathbf{p}_4|^2, \tau)] = \left[\left(\frac{\tau}{|\mathbf{p}_4|^2} \right)^{\omega_1} \tilde{v}_R + \left(\frac{\tau}{|\mathbf{p}_4|^2} \right)^{\omega_2} \tilde{v}_L \right] \cos \left[\frac{\pi}{4} (\omega_1 - \omega_2) \right], \quad (4.27a)$$

$$\text{Absorp} [v_\oplus(z, \bar{z}, |\mathbf{p}_4|^2, \tau)] = \left[\left(\frac{\tau}{|\mathbf{p}_4|^2} \right)^{\omega_1} \tilde{v}_R - \left(\frac{\tau}{|\mathbf{p}_4|^2} \right)^{\omega_2} \tilde{v}_L \right] \sin \left[\frac{\pi}{4} (\omega_1 - \omega_2) \right]. \quad (4.27b)$$

Since the polarisation vector is complex, both $\text{Disp} [v_\oplus]$ and $\text{Absorp} [v_\oplus]$ are complex-valued functions of z and \bar{z} . However, they do not include explicit factors of i , namely, as a consequence of eq. (4.14a), one may take their complex conjugate using

$$\tilde{v}_R^*(z, \bar{z}) = \tilde{v}_R(\bar{z}, z), \quad \tilde{v}_L^*(z, \bar{z}) = \tilde{v}_L(\bar{z}, z). \quad (4.28)$$

Using eq. (4.25), we find the dispersive and absorptive part of the Lipatov vertex of negative helicity in terms of the quantities defined for positive helicity in eqs. (4.27a) and (4.27b),

$$\begin{aligned} \text{Re} \{ \text{Disp} [v_\ominus(z, \bar{z}, |\mathbf{p}_4|^2)] \} &= \text{Re} \{ \text{Disp} [v_\oplus(z, \bar{z}, |\mathbf{p}_4|^2)] \}, \\ \text{Im} \{ \text{Disp} [v_\ominus(z, \bar{z}, |\mathbf{p}_4|^2)] \} &= -\text{Im} \{ \text{Disp} [v_\oplus(z, \bar{z}, |\mathbf{p}_4|^2)] \}, \end{aligned} \quad (4.29)$$

$$\begin{aligned} \text{Re} \{ \text{Absorp} [v_\ominus(z, \bar{z}, |\mathbf{p}_4|^2)] \} &= \text{Re} \{ \text{Absorp} [v_\oplus(z, \bar{z}, |\mathbf{p}_4|^2)] \}, \\ \text{Im} \{ \text{Absorp} [v_\ominus(z, \bar{z}, |\mathbf{p}_4|^2)] \} &= -\text{Im} \{ \text{Absorp} [v_\oplus(z, \bar{z}, |\mathbf{p}_4|^2)] \}. \end{aligned} \quad (4.30)$$

In the rest of the paper, we will focus on the determination of the dispersive and of the absorptive parts of v_\oplus .

Another important property of the amplitude and the vertex is target-projectile symmetry. It is defined by the simultaneous swap of partons $1 \leftrightarrow 2$ along with $3 \leftrightarrow 5$ so $s_{34} \leftrightarrow s_{45}$ and $t_1 \leftrightarrow t_2$. This amounts to following transformation of the emitted gluon polarization vector: $\varepsilon_{L\perp}^\oplus(P_4) \leftrightarrow \varepsilon_{R\perp}^\ominus(P_4)$, i.e. changing from the L gauge to the R gauge and picking the negative helicity instead of the positive one. According to eqs. (A.10) and (A.9) this produces an overall minus sign that compensates in (2.21) for the change of sign of the two vectors P_μ and Q_μ of (2.16). In terms of the variables z and \bar{z} appearing in the vertex, target-projectile symmetry is a symmetry under

$$z \rightarrow 1 - \bar{z}, \quad \bar{z} \rightarrow 1 - z. \quad (4.31)$$

Note that this operation swaps $t_1 \leftrightarrow t_2$ according to eq. (2.8), while preserving the sign of tr_5 in (2.9). One may readily verify that (4.31) preserves the contracted expression for the tree-level vertex in (2.21). The same must happen at higher orders.

Considering now eqs. (4.23a) and (4.23b) under target-projectile symmetry, we observe that $t_1 \leftrightarrow t_2$ implies $\omega_1 \leftrightarrow \omega_2$, and since the left hand side flips sign, on the right hand side we must have $\tilde{R}_\mu \leftrightarrow -\tilde{L}_\mu$. Equivalently, after contraction with the polarization vector we observe that under target-projectile symmetry both the dispersive (4.27a) and absorptive parts (4.27b) of the vertex remain invariant, while $\tilde{v}_R(z, \bar{z}) \leftrightarrow \tilde{v}_L(z, \bar{z})$, which means

$$\tilde{v}_R(1 - \bar{z}, 1 - z) = \tilde{v}_L(z, \bar{z}). \quad (4.32)$$

This has immediate implications for the basis of transcendental functions and their coefficients. Rather than considering the separate expressions for \tilde{v}_R and \tilde{v}_L , it is now convenient to consider directly the quantities $\text{Disp} [v_\oplus(z, \bar{z}, |\mathbf{p}_4|^2, \tau)]$ and $\text{Absorp} [v_\oplus(z, \bar{z}, |\mathbf{p}_4|^2, \tau)]$ in terms of transcendental functions: both are symmetric under (4.31), hence, it is natural to express them both in terms of functions that admit

$$\Phi_i(1 - \bar{z}, 1 - z) = \pm \Phi_i(z, \bar{z}), \quad (4.33)$$

with rational coefficients that admit the same relation, respectively, so that the sign would cancel in the product, restoring the exact symmetry of the vertex.

We conclude that in expressing the dispersive and absorptive parts of the complex vertex $v_\oplus(z, \bar{z}, |\mathbf{p}_4|^2, \tau)$ it should be possible, and indeed natural, to choose a basis of transcendental functions satisfying the two properties of hermiticity (4.20) and target-projectile symmetry (4.33). In the next section we shall see that these properties are realized straightforwardly for the one-loop vertex. In section 8 these properties will guide our choice of basis of transcendental functions for the two-loop vertex.

5 The QCD Lipatov vertex at one loop

In this section we derive the Lipatov vertex $v_\oplus(t_1, t_2, |\mathbf{p}_4|^2, \tau, \mu^2)$ at one loop in QCD through $\mathcal{O}(\epsilon^4)$. The gluon-loop contribution to the one-loop Lipatov vertex was originally computed in Ref. [55] through finite terms as $\epsilon \rightarrow 0$. The terms proportional to n_f , originating from quark loop diagrams, were calculated to all orders in ϵ soon afterwards [57]. The complete vertex to $\mathcal{O}(\epsilon^0)$ was also extracted from the one-loop five-gluon amplitude in [59], finding agreement with the previous results. In addition, the soft limit of the one-loop vertex has been computed in Ref. [58] to all orders in ϵ . A representation of the vertex in general kinematics, which is valid to all orders in ϵ , is given in Ref. [99]. The latter has been evaluated recently up to $\mathcal{O}(\epsilon^2)$ [62], in terms of classical and Nielsen polylogarithms and of double sums, denoted as \mathcal{M} -functions, originating from the ϵ -expansion of Appell F_4 and Kampé de Fériet functions [60]. The same functions appear in the Lipatov vertex in planar $\mathcal{N} = 4$ super Yang Mills (sYM) theory, which has been determined to $\mathcal{O}(\epsilon^2)$ [61]. Here we follow the general strategy of ref. [59], that is, we determine $v^{(1)}$ by computing the $2 \rightarrow 3$ amplitude in the multi-Regge kinematic limit and then matching it with relevant

factorization formula. However, while Ref. [59] applied Regge factorisation only to the dispersive part of the amplitude, here we factorise the full, signaturised one, $\mathcal{M}_{gg \rightarrow ggg}^{(-,-)}$, which at one loop, features both dispersive and absorptive parts.⁷

To extract the vertex we match $\mathcal{M}_{gg \rightarrow ggg}^{(-,-)}$ with the factorization formula in eq. (4.10). Upon expansion we obtain

$$\begin{aligned} \mathcal{M}_{ij \rightarrow i'gg'}^{(-,-)} \Big|_{\text{NLL}} &= \mathcal{M}_{\text{tree}} \left(\frac{s_{45}}{\tau} \right)^{\omega_1} \left(\frac{s_{23}}{\tau} \right)^{\omega_2} \left[1 + \left(\frac{\alpha_s}{\pi} \right) \left(c_i^{(1)}(-t_1, \tau, \mu^2) + c_j^{(1)}(-t_2, \tau, \mu^2) \right. \right. \\ &\quad \left. \left. + v_{\oplus}^{(1)}(t_1, t_2, |\mathbf{p}_4|^2, \tau, \mu^2) - i \frac{C_A \pi}{4} (\alpha_g^{(1)}(\mu^2, -t_1) + \alpha_g^{(1)}(\mu^2, -t_2)) \right) \right. \\ &\quad \left. + C_A \left(\frac{\alpha_s}{\pi} \right)^2 \left(\alpha_g^{(2)}(\mu^2, -t_1) \log \frac{s_{45}}{\tau} + \alpha_g^{(2)}(\mu^2, -t_2) \log \frac{s_{23}}{\tau} \right) \right]. \end{aligned} \quad (5.1)$$

In the equation above, the one-loop Regge trajectory $\alpha^{(1)}(-t, \mu^2)$, eq. (4.3), and the one-loop gluon impact factor are known to all orders in ϵ . The latter reads

$$c_i^{(1)}(-t, \tau, \mu^2) = \left(\frac{\mu^2}{-t} \right)^\epsilon \left[c_i^{(1)} - C_A \frac{\alpha_g^{(1)}}{2} \log \left(\frac{-t}{\tau} \right) \right] - \frac{b_0}{8\epsilon} \left(1 - \left(\frac{\mu^2}{-t} \right)^\epsilon \right), \quad (5.2)$$

where b_0 is given in (D.8), $\alpha_g^{(1)} = \alpha_g^{(1)}(-t, -t) = \frac{r_\Gamma}{2\epsilon}$ [2] where r_Γ is given in eq. (4.3) and $c_i^{(1)} = c_i^{(1)}(-t, -t, -t)$. The latter has been computed in Ref. [100] and is given by

$$\begin{aligned} c_g^{(1)} &= r_\Gamma(\epsilon) \left[N_c \left(-\frac{1}{2\epsilon^2} + \frac{\psi(1+\epsilon) - 2\psi(1-\epsilon) + \psi(1)}{4\epsilon} - \frac{11-7\epsilon}{8\epsilon(3-2\epsilon)(1-2\epsilon)} \right) \right. \\ &\quad \left. + n_f \frac{(1-\epsilon)}{4\epsilon(1-2\epsilon)(3-2\epsilon)} \right] - \frac{b_0}{8\epsilon}. \end{aligned} \quad (5.3)$$

From eq. (5.1) it follows that the one-loop vertex is

$$\begin{aligned} v_{\oplus}^{(1)}(t_1, t_2, |\mathbf{p}_4|^2, \tau, \mu^2) &= \frac{\mathcal{M}_{gg \rightarrow ggg}^{(-,-),(1)}}{\mathcal{M}_{gg \rightarrow ggg}^{\text{tree}}} - \left[C_A \left(\alpha^{(1)}(-t_1, \mu^2) \log \frac{s_{45}}{\tau} + \alpha^{(1)}(-t_2, \mu^2) \log \frac{s_{34}}{\tau} \right) \right. \\ &\quad \left. + c_g^{(1)}(-t_1, \tau, \mu^2) + c_g^{(1)}(-t_2, \tau, \mu^2) - i C_A \frac{\pi}{4} \left(\alpha^{(1)}(-t_1, \mu^2) + \alpha^{(1)}(-t_2, \mu^2) \right) \right]. \end{aligned} \quad (5.4)$$

The signaturised amplitude $\mathcal{M}_{gg \rightarrow ggg}^{(-,-),(1)}$ is the colour projection of the five gluon scattering amplitude $\mathcal{M}_{gg \rightarrow ggg}^{(1)}$ onto the component $c^{[8_a, 8_a]}$ of the orthonormal basis in appendix B. To compute the amplitude we used the results of ref. [64] for the five-gluon amplitudes, which are given as a decomposition in terms of one-loop master integrals valid to all orders in ϵ . They are written as

$$\mathcal{M}_{gg \rightarrow ggg}^{(1)} = \sum_{\sigma \in \mathcal{S}_5} \sum_{i=1}^{11} R_{\sigma,i} I_{\sigma,i}, \quad (5.5)$$

⁷Similarly to the tree amplitude, $\mathcal{M}_{gg \rightarrow ggg}^{(-,-)}$ at one loop consists exclusively of the $[8_a, 8_a]$ colour component, and corresponds to a single Reggeon exchange. However, in contrast to the tree amplitude, it features both dispersive and absorptive parts, as is evident from eq. (4.13).

where σ is a permutation of the 5 external gluons and the $I_{\sigma,i}$ are a basis of one-loop master integrals. This is a particular case of the type of decompositions we discussed in section 3, and these expressions can be expanded in the MRK limit with the techniques described there (see in particular the comments at the end of sections 3.1 and 3.2). All the master integrals have been written in terms of powers of logarithms of $s_{34} > 0$, $s_{45} > 0$, $|\mathbf{p}_4|^2 > 0$, and Goncharov multiple polylogarithms (GPLs) [101, 102] with the symbol alphabet

$$\{z, \bar{z}, 1-z, 1-\bar{z}, z-\bar{z}, 1-z-\bar{z}\}, \quad (5.6)$$

where we recall the relations in eq. (2.8) in the physical region, which to leading power in the MRK limit read

$$-t_1 \simeq (1-z)(1-\bar{z})|\mathbf{p}_4|^2 > 0 \quad \text{and} \quad -t_2 \simeq z\bar{z}|\mathbf{p}_4|^2 > 0,$$

so z and \bar{z} are complex conjugate. Notably, the latter transcendental functions appear only in single-valued combinations, and we used the Maple code `HyperlogProcedures` [103] to write all the master integrals, up to transcendental weight 6, in terms of Single Valued Multiple Polylogarithms (SVMPLs) [20, 21, 79, 103–109]. Note that the notation used for SVMPLs (\mathcal{I}) in the `HyperlogProcedures` code, relates to the one we use here (\mathcal{G}) via

$$\mathcal{G}(a_1, \dots, a_n, z) \equiv \mathcal{I}(z, a_1, \dots, a_n, 0) \quad (5.7)$$

where the heading z and the trailing 0 represent the limits of the final (single-valued) integration. By plugging these results for the master integrals into eq. (5.5), we obtained the amplitude $\mathcal{M}^{(-,-),(1)}$ up to $\mathcal{O}(\epsilon^4)$ and, via eq. (5.1), the one-loop Lipatov vertex $v^{(1)}(t_1, t_2, |\mathbf{p}_4|^2, \tau, \mu^2)$ to the same order in ϵ . We provide a replacement list for the single-valued functions \mathcal{G} into ordinary GPLs, G , which may be evaluated numerically using the GiNaC library [110] via `PolyLogTools` [79].

The dependence of $v^{(1)}(t_1, t_2, |\mathbf{p}_4|^2, \tau, \mu^2)$ on the factorisation and the renormalisation scales can be described to all-orders in ϵ by

$$\begin{aligned} v^{(1)}(t_1, t_2, |\mathbf{p}_4|^2, \tau, \mu^2) &= \left(\frac{\mu^2}{|\mathbf{p}_4|^2}\right)^\epsilon v^{(1)}(t_1, t_2, |\mathbf{p}_4|^2) + \frac{b_0}{8\epsilon} \left[\left(\frac{\mu^2}{|\mathbf{p}_4|^2}\right)^\epsilon - 1 \right] \\ &\quad - \frac{\alpha_g^{(1)} C_A}{2} \log\left(\frac{|\mathbf{p}_4|^2}{\tau}\right) \left[\left(\frac{\mu^2}{-t_1}\right)^\epsilon + \left(\frac{\mu^2}{-t_2}\right)^\epsilon \right]. \end{aligned} \quad (5.8)$$

The procedure of obtaining eq. (5.8) is described in appendix D, and it can be straightforwardly extended to higher-loop orders. Using appendix D and eq. (5.8) we have defined

$$v^{(1)}(z, \bar{z}) \equiv v^{(1)}(t_1, t_2, |\mathbf{p}_4|^2) \equiv v^{(1)}(t_1, t_2, |\mathbf{p}_4|^2, \tau = |\mathbf{p}_4|^2, \mu^2 = |\mathbf{p}_4|^2). \quad (5.9)$$

This single complex function captures the complexity of the one-loop Lipatov vertex, due to its dependence on the three transverse momenta \mathbf{q}_1 , \mathbf{q}_2 and \mathbf{p}_4 . $v^{(1)}(z, \bar{z})$ is an analytic function of the complex conjugate pair of variables z and \bar{z} , introduced in eq. (2.10). Figure 2 describes the location of singularities and potential singularities of the vertex as a function of z and \bar{z} . The lines $z = 0, 1$ and $\bar{z} = 0, 1$ in the (z, \bar{z}) plane mark the physical singularities

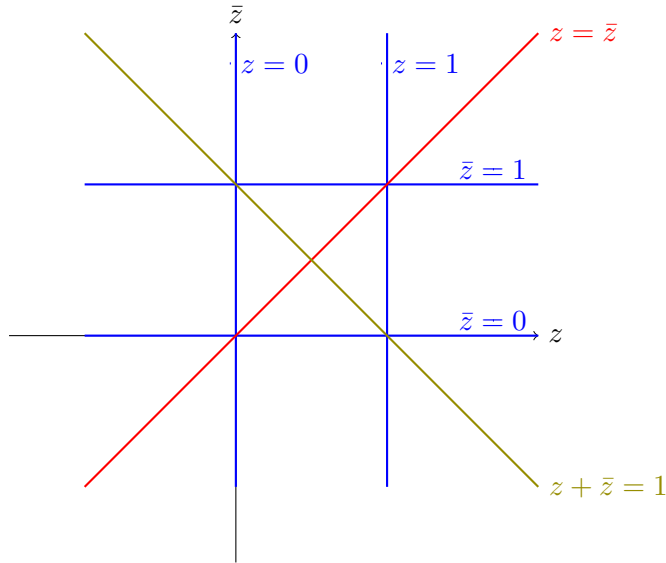


Figure 2. Lines in the z and \bar{z} plane identifying the position of physical ($z = 0, 1$ and $\bar{z} = 0, 1$) and spurious ($z = \bar{z}$ and $z + \bar{z} = 1$) singularities of the Lipatov vertex (or the amplitude at MRK). The physical singularities (drawn in blue) represent the zeros of the squared transverse momentum t_1 or t_2 of (2.8) carried by the Reggeized gluons (additional singularities appear when these invariants diverge, at $z \rightarrow \infty$ and $\bar{z} \rightarrow \infty$). The spurious singularity at $z = \bar{z}$ (in red) represents, at the level of the amplitude, the limit where $\text{tr}_5 \equiv -4i \epsilon_{\mu\nu\sigma\rho} P_1^\mu P_2^\nu P_3^\sigma P_5^\rho = 0$, as can be seen from eq. (2.9). Finally, spurious singularity at $z + \bar{z} = 1$ (in olive green) corresponds to the soft limit where $|\mathbf{p}_4|^2 \rightarrow 0$ and $t_1 = t_2 \equiv t$.

of the amplitude. These lines correspond to the poles associated to the Reggeized gluon propagators with virtualities t_1 and t_2 going on shell. There are two more regions in the (z, \bar{z}) plane associated to potential singularities of the amplitude. One is the line $z = \bar{z}$, where the invariant tr_5 , defined in eq. (2.3), vanishes, following eq. (2.9). This corresponds to the situation where all 5 parton 3-momenta are lying in a plane, or alternatively that the three transverse momenta of the vertex are aligned, i.e. they admit

$$(\mathbf{q}_1 \cdot \mathbf{q}_2)^2 - |\mathbf{q}_1|^2 |\mathbf{q}_2|^2 = \frac{|\mathbf{p}_4|^4 (z - \bar{z})^2}{4} \rightarrow 0. \quad (5.10)$$

The second potential singularity is the line $1 - z - \bar{z} = 0$, corresponding to the soft limit, $|\mathbf{p}_4|^2 \rightarrow 0$, where all components of the emitted gluon momentum vanish and the two t channel invariants become equal, $t_1 = t_2 \equiv t$.

It is interesting to examine the soft limit of the vertex in more detail. In Figure 2 the line $z + \bar{z} = 1$ corresponds to this limit. We note that reflection about this line, eq. (4.31), correspond to target-projectile symmetry. Because the $|\mathbf{p}_4|^2 \rightarrow 0$ limit is taken keeping $t_1 = -|\mathbf{q}_1|^2$ and $t_2 = -|\mathbf{q}_2|^2$ finite, the variables z and \bar{z} develop in this limit large imaginary parts (see eq. (2.8)):

$$z(\bar{z}) \rightarrow \frac{1 + \delta}{2} \pm i \sqrt{\frac{|\mathbf{q}_2|^2}{|\mathbf{p}_4|^2} - \frac{(1 - \delta)^2}{4}}, \quad |\mathbf{p}_4| \rightarrow 0, \quad \delta = \frac{|\mathbf{q}_1|^2 - |\mathbf{q}_2|^2}{|\mathbf{p}_4|^2} \rightarrow 0. \quad (5.11)$$

In ref. [58, 59, 62] the sum and the difference of the right and left vertices⁸ of eq. (4.15), have been computed to all orders in ϵ . Using these results in eqs. (4.27a) and (4.27b) respectively, we derive the soft limit of the dispersive and absorptive parts of the complex vertex v_{\oplus} at one loop (defined by eq. (4.10) for positive helicity) to all orders in ϵ :

$$\lim_{|\mathbf{p}_4|^2 \rightarrow 0} v_{\oplus}^{(1)}(t_1, t_2, |\mathbf{p}_4|^2, \tau) = 1 + \frac{\alpha_s(\mu^2)}{\pi} \left\{ -\frac{b_0}{8\epsilon} + \frac{N_c}{4} \frac{r_{\Gamma}(\epsilon)}{\epsilon} \left[2 \left(\frac{\mu^2}{-t} \right)^{\epsilon} \ln \left(\frac{\tau}{|\mathbf{p}_4|^2} \right) - \left(\frac{\mu^2}{|\mathbf{p}_4|^2} \right)^{\epsilon} \left(\frac{1}{\epsilon} + \Psi(1-\epsilon) - \Psi(1+\epsilon) + \frac{i\pi}{2} \right) \right] \right\} \quad (5.12)$$

where

$$\lim_{|\mathbf{p}_4|^2 \rightarrow 0} t_1 = \lim_{|\mathbf{p}_4|^2 \rightarrow 0} t_2 \equiv t,$$

and $r_{\Gamma}(\epsilon)$ is defined in eq. (4.3). This result in the soft limit (5.12) provides a useful check of our general kinematics calculation below.

We stress that while there are alphabet letters (5.6) which vanish on $z = \bar{z}$ or on $z + \bar{z} = 1$, there are no physical singularities in these kinematic limits, only spurious poles. In fact, spurious poles only appear as $z + \bar{z} \rightarrow 1$, and the terms containing these poles are known to all orders in ϵ [57, 62, 99] and it is convenient to single them out as follows, and separate the one-loop vertex as follows

$$v_{\oplus}^{(1)}(t_1, t_2, |p_4|^2) = v_{\text{sYM}}^{(1)}(t_1, t_2, |p_4|^2) + v_{\text{spurious}}^{(1)}(t_1, t_2, |p_4|^2) + v_{\beta}^{(1)}(\epsilon), \quad (5.13)$$

where we isolate the renormalisation term

$$v_{\beta}^{(1)}(\epsilon) = -\frac{11N_c - 2n_f}{24\epsilon}, \quad (5.14)$$

and where $v_{\text{spurious}}^{(1)}$ reads

$$v_{\text{spurious}}^{(1)}(t_1, t_2, |p_4|^2) = c_a v_a^{(1)}(t_1, t_2, |p_4|^2) + c_b v_b^{(1)}(t_1, t_2, |p_4|^2), \quad (5.15)$$

with

$$c_a = N_c(1-\epsilon) - n_f, \quad c_b = -(11-7\epsilon)N_c + 2(1-\epsilon)n_f \quad (5.16)$$

and

$$v_a^{(1)} = e^{\epsilon \gamma_E} \frac{\Gamma(\epsilon)\Gamma(1\epsilon)^2(|\mathbf{p}_4|^2)^{\epsilon}}{\Gamma(4-2\epsilon)\bar{z}(1-z)} \left[-\frac{\epsilon}{4} \frac{(-t_1)^{1-\epsilon} - (-t_2)^{1-\epsilon}}{(t_1-t_2)} + \frac{|\mathbf{p}_4|^2(1+z-\bar{z})}{2} \left(\frac{t_1 t_2 ((-t_1)^{-\epsilon} - (-t_2)^{-\epsilon})}{(t_1-t_2)^3} - \epsilon \frac{(-t_1)^{1-\epsilon} + (-t_2)^{1-\epsilon}}{2(t_1-t_2)^2} \right) \right] \quad (5.17a)$$

$$v_b^{(1)} = -e^{\epsilon \gamma_E} |\mathbf{p}_4|^2 (1+z-\bar{z}) \frac{\Gamma(\epsilon)\Gamma(1-\epsilon)\Gamma(2-\epsilon)(|\mathbf{p}_4|^2)^{\epsilon}}{\Gamma(4-2\epsilon)} \frac{(-t_1)^{-\epsilon} - (-t_2)^{-\epsilon}}{4(t_1-t_2)}. \quad (5.17b)$$

⁸Equivalently, one may use \tilde{v}_R and \tilde{v}_L defined here in (4.24), since the expansion of the cosine functions in (4.22) does not contribute at one loop.

The expansion in ϵ of eq. (5.17) is straightforward: $v_{\text{spurious}}^{(1)}$ is finite as $\epsilon \rightarrow 0$ and the only transcendental functions appearing are (single-valued) logarithms of $|z|^2$ or of $|1-z|^2$.

Importantly, both $v_a^{(1)}$ and $v_b^{(1)}$ vanish in the soft limit, eq. (5.11), despite the denominators $t_1 - t_2$ in eq. (5.17). This can be checked to all orders in ϵ , by writing t_1 and t_2 in terms of z and \bar{z} and taking the (commuting) expansions around $|\mathbf{p}_4| \rightarrow 0$ and $\delta \rightarrow 0$ to find that both $v_a^{(1)}$ and $v_b^{(1)}$ are power suppressed.

We note that $v_{\text{spurious}}^{(1)}$ does not contribute at maximal transcendental weight, hence it should not [111, 112] contribute to the $\mathcal{N} = 4$ super Yang Mills (sYM) vertex. Indeed, by inspecting the limit $\epsilon \rightarrow 0$ of the colour factors entering $v_{\text{spurious}}^{(1)}$, eq. (5.16), we recover the supersymmetric decomposition presented in Ref. [59]

$$c_a \rightarrow N_c - n_f, \quad c_b \rightarrow -(11N_c - 2n_f). \quad (5.18)$$

This shows that neither c_a or c_b can contribute to the sYM vertex: the former vanishes in the supersymmetric limit, while the latter is proportional to the running of the coupling, much like $v_\beta^{(1)}$, which vanishes for $\mathcal{N} = 4$ sYM.

The remaining contribution to the one-loop vertex in eq. (5.13) is $v_{\text{sYM}}^{(1)}(t_1, t_2, |p_4|^2)$, which can be identified as the Lipatov vertex in $\mathcal{N} = 4$ sYM. This contribution is free of spurious poles, and is expressed exclusively in terms of SVMPLs of maximal weight, in line with general expectations [111, 112]. We extracted this function through $\mathcal{O}(\epsilon^4)$ (weight 6). We also present below the explicit expression for $v_{\text{sYM}}^{(1)}$ through $\mathcal{O}(\epsilon^2)$, separated into its dispersive and absorptive components:

$$\begin{aligned} \text{Disp.}\{v_{\text{sYM}}^{(1)}\} &= -\frac{N_c}{4\epsilon^2} + \frac{N_c}{8} \left[\frac{5\pi^2}{6} - \log^2 \left(\frac{|z|^2}{|1-z|^2} \right) \right] \\ &+ \epsilon N_c \left[\frac{\mathcal{G}^3(0, z) + \mathcal{G}^3(1, z)}{12} - \frac{1}{4} \left(\mathcal{G}(0, 0, 1, z) - \mathcal{G}(0, 1, 0, z) + \mathcal{G}(0, 1, 1, z) \right. \right. \\ &+ 2\mathcal{G}(0, 1 - \bar{z}, 0, z) - 2\mathcal{G}(0, 1 - \bar{z}, 1, z) + \mathcal{G}(1, 0, 0, z) + \mathcal{G}(1, 0, 1, z) + \mathcal{G}(1, 1, 0, z) \Big) \\ &+ \frac{\pi^2}{24} \log(|z|^2|1-z|^2) + \frac{13}{12} \zeta_3 \Big] \\ &+ \epsilon^2 N_c \left[\frac{1}{4} \left(\mathcal{G}(0, 0, 0, 1, z) - \mathcal{G}(0, 0, 1, 0, z) - \mathcal{G}(0, 1, 0, 0, z) + \mathcal{G}(0, 0, 1, 1, z) \right. \right. \\ &+ 2\mathcal{G}(0, 0, 1 - \bar{z}, 0, z) - 2\mathcal{G}(0, 0, 1 - \bar{z}, 1, z) + \mathcal{G}(0, 1, 0, 1, z) - \mathcal{G}(0, 1, 1, 0, z) \\ &+ \mathcal{G}(0, 1, 1, 1, z) + 2\mathcal{G}(0, 1, 1 - \bar{z}, 0, z) - 2\mathcal{G}(0, 1, 1 - \bar{z}, 1, z) + 2\mathcal{G}(0, 1 - \bar{z}, 0, 0, z) \\ &- 2\mathcal{G}(0, 1 - \bar{z}, 1, 1, z) + \mathcal{G}(1, 0, 0, 0, z) + \mathcal{G}(1, 0, 0, 1, z) - \mathcal{G}(1, 0, 1, 0, z) + \mathcal{G}(1, 0, 1, 1, z) \\ &+ 2\mathcal{G}(1, 0, 1 - \bar{z}, 0, z) - 2\mathcal{G}(1, 0, 1 - \bar{z}, 1, z) + \mathcal{G}(1, 1, 0, 0, z) + \mathcal{G}(1, 1, 0, 1, z) \\ &+ \mathcal{G}(1, 1, 1, 0, z), + 2\mathcal{G}(\bar{z}, 0, 1, 0, z) - 2\mathcal{G}(\bar{z}, 0, 1 - \bar{z}, 0, z) + 2\mathcal{G}(\bar{z}, 0, 1 - \bar{z}, 1, z) \\ &- 2\mathcal{G}(\bar{z}, 1, 0, 1, z) - 2\mathcal{G}(\bar{z}, 1, 1 - \bar{z}, 0, z) + 2\mathcal{G}(\bar{z}, 1, 1 - \bar{z}, 1, z) \Big) - \frac{\mathcal{G}^4(0, z) + \mathcal{G}^4(1, z)}{32} \\ &- \frac{\pi^2}{96} \left(\mathcal{G}^4(0, z) + \mathcal{G}^2(1, z) + 2(9\mathcal{G}(0, 1, z) + \mathcal{G}(1, 0, z) - 8\mathcal{G}(\bar{z}, 1, z)) \right) \\ &- \frac{\zeta_3}{4} (\mathcal{G}(0, z) + \mathcal{G}(1, z)) + \frac{13\pi^4}{1920} \Big], \quad (5.19a) \end{aligned}$$

$$\begin{aligned}
\text{Absorp.}\{v_{\text{sYM}}^{(1)}\} &= \frac{\pi N_c}{8} \left[\frac{1}{\epsilon} + \epsilon \left(\mathcal{G}(0, 1, z) - \mathcal{G}(1, 0, z) + \frac{\pi^2}{12} \right) - \epsilon^2 \left(\mathcal{G}(0, 0, 1, z) - \mathcal{G}(0, 1, 0, z) \right. \right. \\
&\quad \left. \left. + \mathcal{G}(0, 1, 1, z) - \mathcal{G}(1, 0, 0, z) + \mathcal{G}(1, 0, 1, z) - \mathcal{G}(1, 1, 0, z) - 2\mathcal{G}(\bar{z}, 0, 1, z) \right. \right. \\
&\quad \left. \left. + 2\mathcal{G}(\bar{z}, 1, 0, z) - \frac{7\zeta_3}{3} \right) \right], \tag{5.19b}
\end{aligned}$$

where the functions \mathcal{G} are SVMPLs, which can be converted to multi-valued Goncharov multiple polylogarithms using the package `HyperlogProcedures` [103] (recall the relation between notations in (5.7)). In the ancillary files [70], we provide both expressions of $v_{\text{sYM}}^{(1)}$ up to $\mathcal{O}(\epsilon^4)$. The expression written in terms of SVMPL is very compact. Writing it in terms of these functions manifests the absence of branch points in the physical region, where z and \bar{z} are complex conjugates.

In order to compare with the literature [62, 99] it is useful to relate the dispersive (absorptive) part of the vertex to the sum (difference) of the left and right vertices \tilde{v}_L and \tilde{v}_R using eq. (4.27a) and (4.27b), respectively. These, we recall, are related through contraction with the polarization vector $v_R \pm v_L = \varepsilon_{\oplus}^{\mu}(P_4)(R_{\mu} \pm L_{\mu})$ to the quantities $R^{\mu} \pm L^{\mu}$ that were determined in Ref. [62] through $\mathcal{O}(\epsilon^2)$, in terms of polylogarithmic functions and of \mathcal{M} -functions [60]. The latter arise in one of the master integrals computed in Refs. [62, 99], named $\mathcal{I}_5 - \mathcal{L}_3$, which involves the 4-dimensional scalar pentagon integral. To better compare with our results in eqs. (5.19a) and (5.19b), we derived a different representation of the 4-dimensional pentagon integral in terms of the master integrals $I_{\sigma,i}$ of eq. (5.5). We find that $R^{\mu} + L^{\mu}$ contains spurious poles at $t_1 = t_2$, which match $v_{\text{spurious}}^{(1)}$ of eq. (5.16). The remaining terms in $R^{\mu} + L^{\mu}$ and $R^{\mu} - L^{\mu}$ agree with eqs. (5.19a) and (5.19b), respectively.

It is interesting to see how the two properties we discussed in section 4.2, reality and target-projectile symmetry, are realised in the one loop vertex. We have seen that the reality property is only expected to hold prior to contraction with the polarization vector, so while the transcendental functions can be chosen hermitian (4.33), the rational coefficients would not be so. In turn, target-projectile symmetry holds for the complex vertex, and the expectation is that if the transcendental functions are chosen to be invariant under

$$\{z \rightarrow 1 - \bar{z}, \bar{z} \rightarrow 1 - z\}. \tag{5.20}$$

so will be their rational coefficients.

Let's now examine the results for the one-loop vertex. Consider first the contribution $v_{\text{spurious}}^{(1)}$. We see immediately that this term is real: it trivially obeys $z \leftrightarrow \bar{z}$ symmetry, since it depends only on t_i of (2.8). We also observe that this contribution is manifestly symmetric under the target-projectile symmetry (5.20): in eq. (5.17) both the rational prefactors and each of the terms depending on t_1 and t_2 separately have this symmetry.

Consider next $v_{\text{sYM}}^{(1)}(t_1, t_2, |p_4|^2)$. Also here our expectations hold, but the way this is realised is more interesting, as the symbol alphabet (5.6) transforms non-trivially under both $z \leftrightarrow \bar{z}$ and under $z \leftrightarrow 1 - \bar{z}$. While $\text{Disp.}\{v_{\text{sYM}}^{(1)}\}$ and $\text{Absorp.}\{v_{\text{sYM}}^{(1)}\}$ separately satisfy the target-projectile symmetry (5.20), they transform nontrivially under $z \leftrightarrow \bar{z}$, as indeed expected, and they both have an even (symmetric) as well as an odd (antisymmetric) components under this transformation.

We note in passing that while both the even and odd components of the dispersive part of $v_{\text{sYM}}^{(1)}(z, \bar{z})$, as well as the odd component of the absorptive part of $v_{\text{sYM}}^{(1)}(z, \bar{z})$, are all non-trivial (uniform weight) single-valued GPLs functions of the alphabet in eq. (5.6), $\text{Absorp.} \left\{ v_{\text{sYM.Even}}^{(1)}(z, \bar{z}) \right\}$ is merely a uniform weight transcendental constant at any given order in ϵ , consisting of both even and odd ζ values. We obtain:

$$\text{Absorp.} \left\{ v_{\text{sYM.Even}}^{(1)}(z, \bar{z}) \right\} = \frac{\pi^3}{96} \epsilon + \frac{7\pi}{24} \zeta_3 \epsilon^2 + \frac{47\pi^5}{11520} \epsilon^3 + \left(-\frac{7\pi^3}{288} \zeta_3 + \frac{31\pi}{40} \zeta_5 \right) \epsilon^4 + \dots \quad (5.21)$$

6 The theory of multi-Reggeon interactions

As discussed in section 4 and 5, up to NLL accuracy the $(-, -)$ component of the amplitude is entirely captured by the exchange of a single Reggeon. Beyond this logarithmic accuracy for $\mathcal{M}^{(-,-)}$, and in general for the other signature components of the amplitude, a correct description requires to take into account the exchange of multiple Reggeons. A framework to calculate their contribution efficiently has been developed in Refs. [17, 18, 22–24, 113]. The method is based on an effective-theory approach, in which rapidity evolution equations in the shockwave formalism are used to determine all multi-Reggeon contributions to the amplitude. Subsequently, by matching to the high-energy expansion of the full amplitude, it is possible to extract matching coefficients which are not determined by the rapidity evolution, namely the impact factors, the Regge trajectory and (starting with $2 \rightarrow 3$ amplitudes) the Lipatov vertex. In this section we review the formalism and extend its application to the calculation of $2 \rightarrow 3$ amplitudes, building on earlier work in Ref. [17, 21].

6.1 From the shock-wave formalism to Reggeon fields

In the shockwave formalism [17, 18, 23, 38–41] one describes the projectile as a product of (an indefinite number of) Wilson-line operators, $U(z_{1\perp})U(z_{2\perp})\dots$, each of which extends over the infinite $+$ lightcone direction and located as a distinct transverse position z_{\perp} :

$$U(z_{\perp}) = \mathcal{P} \exp \left[\int_{-\infty}^{\infty} T^a A_+^a(x^+, x^- = 0, z_{\perp}) dx^+ \right]. \quad (6.1)$$

The Wilson lines (6.1) have rapidity divergences, so the operators $U(z_{1\perp})U(z_{2\perp})\dots$ admit rapidity evolution equations

$$-\frac{d}{d\eta} [U(z_{1\perp})U(z_{2\perp})\dots] = H [U(z_{1\perp})U(z_{2\perp})\dots], \quad (6.2)$$

known as the Balitsky-JIMWLK equations [38–41], where the leading-order Hamiltonian is given by

$$H = \frac{\alpha_s}{2\pi^2} \mu^{2\epsilon} \int [dz_0] \frac{z_{0i} \cdot z_{0j}}{(z_{0i}^2 z_{0j}^2)^{1-\epsilon}} \left(T_{i,L}^a T_{j,L}^a + T_{i,R}^a T_{j,R}^a - U_{\text{adj}}^{ab}(z_0) (T_{i,L}^a T_{j,R}^b + T_{j,L}^a T_{i,R}^b) \right), \quad (6.3)$$

where $z_{0i} \equiv z_0 - z_i$ and $[dz] \equiv d^{2-2\epsilon}z$. Here we work exclusively in the $2 - 2\epsilon$ dimensional transverse plane, and therefore we drop the boldface notation we used earlier for the

transverse components. In eq. (6.3) we used functional derivative operators, $T_{i,L}^a$ and $T_{i,R}^a$, which generate colour rotation. They are defined by

$$T_{i,L}^a \equiv T^a U(z_i) \frac{\delta}{\delta U(z_i)}, \quad T_{i,R}^a \equiv U(z_i) T^a \frac{\delta}{\delta U(z_i)}. \quad (6.4)$$

The action of the Hamiltonian H on the product of Wilson lines involves an additional Wilson line in the adjoint representation $U_{\text{adj}}^{ab}(z_0)$ generated through the interaction with the target shockwave. Thus this system of equations is non-linear and each iteration of the evolution involves an increasing number of Wilson lines. Clearly it is very hard to solve this system in general. However, in the perturbative regime where fields are weak, each Wilson $U(z_\perp)$ is close to unity. The dynamics is then best described in terms of its logarithm W , defined via [17]

$$U(z_\perp) = e^{ig_s T^a W^a(z_\perp)}. \quad (6.5)$$

The field W can be identified as sourcing a single Reggeon exchanged in the t channel. Wilson lines U (and products thereof) can be thus described perturbatively, order by order in g_s as an expansion in W fields, all at the same transverse position,

$$\begin{aligned} U = e^{ig_s W^a T^a} &= 1 + ig_s W^a T^a - \frac{g_s^2}{2} W^a W^b T^a T^b - i \frac{g_s^3}{6} W^a W^b W^c T^a T^b T^c \\ &+ \frac{g_s^4}{24} W^a W^b W^c W^d T^a T^b T^c T^d + \mathcal{O}(g_s^5 W^5), \end{aligned} \quad (6.6)$$

where n fields W source n Reggeons [17]. We can also express the action of the colour rotation operators $iT_{j,L/R}^a$ defined in (6.4) in terms of functional derivatives of W

$$\begin{aligned} iT_{j,L/R}^a &= \frac{1}{g_s} \frac{\delta}{\delta W_j^a} \pm \frac{1}{2} f^{abx} W_j^x \frac{\delta}{\delta W_j^b} - \frac{g_s}{12} W_j^x W_j^y (F^x F^y)^a_b \frac{\delta}{\delta W_j^b} \\ &- \frac{g_s^3}{720} W_j^x W_j^y W_j^z W_j^t (F^x F^y F^z F^t)^a_b \frac{\delta}{\delta W_j^b} + \dots, \end{aligned} \quad (6.7)$$

where we call $W_j \equiv W(z_j)$. In eq. (6.7) we have introduced the Hermitian colour matrix $(F^x)^a_b \equiv i f^{axb}$ for simplicity.

Through this expansion, Refs. [18, 23] have translated the action of the Balitsky-JIMWLK Hamiltonian in eq. (6.2) to an action on a vector of increasing order in the number of W fields, which schematically takes the form

$$\begin{aligned} H \begin{pmatrix} W \\ WW \\ WWW \\ \dots \end{pmatrix} &\equiv \begin{pmatrix} H_{1 \rightarrow 1} & 0 & H_{3 \rightarrow 1} & \dots \\ 0 & H_{2 \rightarrow 2} & 0 & \dots \\ H_{1 \rightarrow 3} & 0 & H_{3 \rightarrow 3} & \dots \\ \dots & \dots & \dots & \dots \end{pmatrix} \begin{pmatrix} W \\ WW \\ WWW \\ \dots \end{pmatrix} \\ &\sim \begin{pmatrix} g_s^2 & 0 & g_s^4 & \dots \\ 0 & g_s^2 & 0 & \dots \\ g_s^4 & 0 & g_s^2 & \dots \\ \dots & \dots & \dots & \dots \end{pmatrix} \begin{pmatrix} W \\ WW \\ WWW \\ \dots \end{pmatrix}, \end{aligned} \quad (6.8)$$

where the first line defines the components of the Hamiltonian $H_{k \rightarrow m}$ mediating between a state with k Reggeons and one with m Reggeons (note that transitions between odd and even number of Reggeons are forbidden) while the second line indicates the order in g_s at which each such component of the Hamiltonian begins. In this way the perturbative expansion of the Wilson lines in effect linearises the non-linear evolution, and upon working to a given order in the coupling, the system involves a restricted number of Reggeons.

In $2 \rightarrow 2$ scattering $ij \rightarrow i'j'$ one defines (see [23] for more details⁹):

$$|\psi_i\rangle \equiv \frac{(Z_i C_i^{(0)})^{-1}}{2p_i^+} a_{i'}(p_{i'}) a_i^\dagger(p_i) |0\rangle, \quad \langle\psi_j| \equiv \frac{(Z_j C_j^{(0)})^{-1}}{2p_j^-} \langle 0| a_{j'}(p_{j'}) a_j^\dagger(p_j), \quad (6.9)$$

where a_i^\dagger and $a_{i'}$ are respectively creation and annihilation operators associated with the projectile, while a_j^\dagger and $a_{j'}$ are associated with the target. Next, modelling these states in terms of products of (an indefinite number of) Wilson lines U , one may represent them as an expansion in terms of states with a definite number n of Reggeons W ,

$$|\psi_i\rangle = \sum_{n=1}^{\infty} |\psi_{i,n}\rangle, \quad \langle\psi_j| = \sum_{n=1}^{\infty} \langle\psi_{j,n}|. \quad (6.10)$$

An n Reggeon state $|\psi_i\rangle$ can in turn be expanded

$$|\psi_{i,n}\rangle = |\psi_{i,n}\rangle^{\text{LO}} + \sum_{k=1}^{\infty} |\psi_{i,n}\rangle^{\text{N}^k\text{LO}}. \quad (6.11)$$

Here leading order (LO) contributions arise from the expansion of a single Wilson line $U(z_\perp)$, in which case

$$|\psi_{i,1}\rangle^{\text{LO}} = ig_s \mathbf{T}_i^a W^a(p) |0\rangle, \quad (6.12a)$$

$$|\psi_{i,2}\rangle^{\text{LO}} = -\frac{g_s^2}{2} \mathbf{T}_i^a \mathbf{T}_i^b \int [\vec{d}q] W^a(q) W^b(p-q) |0\rangle, \quad (6.12b)$$

$$|\psi_{i,3}\rangle^{\text{LO}} = -\frac{ig_s^3}{6} \mathbf{T}_i^a \mathbf{T}_i^b \mathbf{T}_i^c \int [\vec{d}q_1][\vec{d}q_2] W^a(q_1) W^b(q_2) W^c(p-q_1-q_2) |0\rangle, \quad (6.12c)$$

where we use the following convention for the Fourier transform of the W fields:

$$W^a(p) = \int [dz] e^{-ipz} W^a(z), \quad W^a(z) = \int [\vec{d}p] e^{ipz} W^a(p). \quad (6.13)$$

and the measure is

$$[dz] \equiv d^{2-2\epsilon} z, \quad [\vec{d}p] \equiv \frac{d^{2-2\epsilon} p}{(2\pi)^{2-2\epsilon}}. \quad (6.14)$$

At next-to-leading order (NLO) two Wilson lines at distinct transverse positions play a role, and then non-trivial impact factors for the emission of a given number of Reggeons arise:

$$|\psi_{i,1}\rangle^{\text{NLO}} = ig_s \mathbf{T}_i^a \frac{\alpha_s}{\pi} d_i^{(1)}(-p^2) W^a(p) |0\rangle, \quad (6.15a)$$

⁹Notice that we divide by the unobservable phase associated with the tree-level impact factors $C_{i/j}^{(0)}$, see e.g. eq. (A.25). The removal of this phase is taken into account also in [23], although not explicitly stated.

$$|\psi_{i,2}\rangle^{\text{NLO}} = -\frac{g_s^2}{2} \mathbf{T}_i^a \mathbf{T}_i^b \int [d\bar{q}] \frac{\alpha_s}{\pi} \psi_i^{(1)}(p, q) W^a(q) W^b(p-q) |0\rangle. \quad (6.15b)$$

Similarly, at next-to-next-to-leading order (NNLO) one has

$$|\psi_{i,1}\rangle^{\text{NNLO}} = ig_s \mathbf{T}_i^a \left(\frac{\alpha_s}{\pi}\right)^2 d_i^{(2)}(-p^2, \tau) W^a(p) |0\rangle, \quad (6.16)$$

and so on. In particular, the all orders generalization of the 1-Reggeon wavefunction reads

$$|\psi_{i,1}\rangle = ig_s \mathbf{T}_i^a d_i(-p^2, \tau) W^a(p) |0\rangle, \quad (6.17)$$

where the impact factor $d_i(-p^2, \tau)$ has perturbative expansion

$$d_i(-p^2, \tau) = 1 + \sum_n \left(\frac{\alpha_s}{\pi}\right)^n d_i^{(n)}(-p^2, \tau). \quad (6.18)$$

Comparing with eqs. (4.5), (4.6) and (6.9), it is easy to see that the functions d_i represent the perturbative correction to the impact factors with collinear singularities removed:

$$C_i^{\text{SR}}(p_i, p_{i'}, \tau) = C_i^{(0)}(p_i, p_{i'}) Z_i(t_i, \tau) d_i(t_i, \tau), \quad (6.19)$$

or, equivalently,

$$c_i^{\text{SR}}(t_i, \tau) = Z_i(t_i, \tau) d_i(t_i, \tau). \quad (6.20)$$

Notice that in eqs. (6.19) and (6.20) and in what follows we add a superscript ‘‘SR’’, for ‘‘single Reggeon’’, in order to stress that the perturbative correction to the impact factors are defined as matching coefficients that arise naturally within the multi-Reggeon effective theory, identifying a Reggeon with a W field. To be precise, they are defined such that any contribution of the amplitude associated exclusively with a single W field, throughout the entire rapidity span between the target and the projectile, is considered a SR transition, while all other contributions to the amplitude in which more than one W field is involved in the transition (at any stage, even over part of the rapidity span or through mixing under evolution), is considered a MR transition. Matching in the SR/MR scheme means factorizing only the SR component of the amplitude when defining the impact factors, the Regge trajectory and the Reggeon-gluon-Reggeon vertex, while excluding all MR transitions. The alternative, pole/cut scheme originally defined in [23, 24] will be discussed in section 8.

Having expressed the projectile and the target in terms of states consisting of a definite number of Reggeons, and additionally knowing how the Hamiltonian acts on these states (see (6.8)) to generate rapidity evolution, we can determine how the projectile (and likewise the target) evolves, namely

$$-\frac{d}{d\eta} |\psi_i\rangle = H |\psi_i\rangle \quad (6.21)$$

With this we can compute $2 \rightarrow 2$ amplitudes in the high-energy limit via

$$\frac{i}{2s} \bar{\mathcal{M}}_{ij \rightarrow ij} \equiv \frac{i(Z_i Z_j C_i^{(0)} C_j^{(0)})^{-1}}{2s} \mathcal{M}_{ij \rightarrow ij} \equiv \langle \psi_j | e^{-H\eta} | \psi_i \rangle \quad (6.22)$$

where the factor $e^{-H\eta}$ corresponds to the evolution of the target to the rapidity of the projectile (or vice versa) where η is logarithm of the energy ratio. This technique was developed and used in Ref. [18] to compute the NNLL tower of logarithms of $2 \rightarrow 2$ amplitudes to three loops and in Refs. [22–24] to four loops.

6.2 Real emission from Reggeons

In eq. (6.22) we expressed $2 \rightarrow 2$ high-energy amplitude through a rapidity evolution of target and projectile states that can be expanded in terms of a fixed number of Reggeons. In a similar way, one writes the $2 \rightarrow 3$ amplitude $i(p_1)j(p_2) \rightarrow i'(p_5)g(p_4)j'(p_3)$ in MRK as follows [17, 18, 21]:

$$\frac{i}{2s_{12}} \bar{\mathcal{M}}_{ij \rightarrow i'g j'} \equiv \frac{i(Z_i Z_j C_i^{(0)} C_j^{(0)})^{-1}}{2s_{12}} \mathcal{M}_{ij \rightarrow i'g j'} = \langle \psi_j | e^{-H\eta_2} a_4(p_4) e^{-H\eta_1} | \psi_i \rangle, \quad (6.23)$$

where $\eta_{1,2} \gg 1$ represents the large energy logarithms. These can be chosen to coincide with the logarithms in eq. (4.11), namely

$$\eta_1 = \log\left(\frac{s_{45}}{\tau}\right) - i\frac{\pi}{4}, \quad \eta_2 = \log\left(\frac{s_{34}}{\tau}\right) - i\frac{\pi}{4}, \quad (6.24)$$

The new element of eq. (6.23) compared to the case of $2 \rightarrow 2$ scattering is the presence of the annihilation operator for the gluon $a_4(p_4)$. The first evolution operator $e^{-H\eta_1}$ evolves the Reggeons appearing in the expansion of $|\psi_i\rangle$ to the rapidity of the produced gluon with momentum p_4 (similarly, $e^{-H\eta_2}$ evolves the Reggeons appearing in $|\psi_j\rangle$ to the rapidity of the gluon p_4). Therefore, we need to determine the action of the operator $a_4(p_4)$ on a set of Wilson lines $U(z_i)$, and the corresponding linearised action of $a_4(p_4)$ on Reggeon fields W . This has been determined in [17], and we review the derivation in what follows before proceeding to use it in evaluating (6.23).

First of all, we need the action of the operator a_4 on a Wilson line $U(z_1)$, which reads [17]

$$U(z_1) a^a(p_2) = 2g_s \int [\bar{d}q][dz_2] \frac{q \cdot \varepsilon(p_2)}{q^2} e^{iq \cdot (z_2 - z_1)} e^{-ip_2 \cdot z_2} \left(U_{\text{ad}}^{ab}(z_2) T_{1,R}^b - T_{1,L}^a \right) U(z_1), \quad (6.25)$$

where the polarization vector $\varepsilon(p_2) \equiv \varepsilon(p_2)$ refers to the transverse component of the full gluon polarization vector¹⁰. Recall that $U_{\text{ad}}^{ab}(z_2)$ is a Wilson line in the adjoint representation at position z_2 , where the gluon crosses the shockwave, and the colour rotations $T_{R/L,i}^a$ are defined in eq. (6.4). Using eqs. (6.6) and (6.7) to expand $U_{\text{ad}}^{ab}(z_2)$ and $T_{R/L,i}^a$ we obtain the master equation

$$\begin{aligned} U(z_1) a^a(p_2) &\sim 2i g_s \int [\bar{d}q][dz_2] \frac{q \cdot \varepsilon(p_2)}{q^2} e^{iq \cdot (z_2 - z_1)} e^{-ip_2 \cdot z_2} \left\{ i(F^c)^a_b \left[W_1^c - W_2^c \right] \right. \\ &- \frac{g_s}{2} (F^{cd})^a_b \left[W_2^c (W_1^d - W_2^d) \right] + \frac{g_s^2}{12} i(F^{cde})^a_b \left[W_2^c W_1^d W_1^e - 3W_2^c W_2^d W_1^e + 2W_2^c W_2^d W_2^e \right] \\ &\left. - \frac{g_s^3}{24} (F^{cdef})^a_b \left[W_2^c W_2^d W_1^e W_1^f - 2W_2^c W_2^d W_2^e W_1^f + W_2^c W_2^d W_2^e W_2^f \right] \right\} \frac{\delta}{\delta W_1^b} U(z_1). \quad (6.26) \end{aligned}$$

where we included in the expansion up to terms of $\mathcal{O}(W^4)$, using the shorthand notation for $W_i^c = W^a(z_i)$ and $F^{a_1 a_2 \dots a_n} \equiv F^{a_1} F^{a_2} \dots F^{a_n}$. Eq. (6.25) determines the action of the

¹⁰Taking into account our convention for Fourier transformation in eq. (6.13), eq. (6.25) is equivalent to the definition given in eq. (5.7) of [17]. We check in section 6.3 that starting from eq. (6.25) we reproduce the correct tree level amplitude.

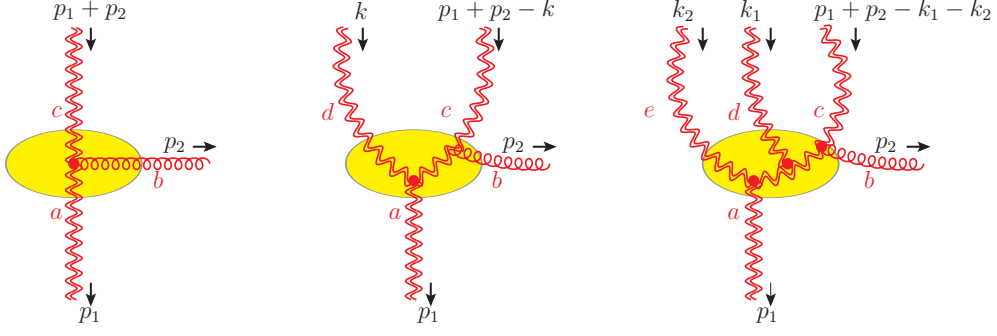


Figure 3. Diagrams describing the three vertices as one Reggeon into one, two or three Reggeons plus an emitted real gluon.

operator $a^a(p_2)$ on an arbitrary number of Reggeon fields. The corresponding vertices are obtained by expanding the Wilson line $U(z_1)$ up to the required number of Reggeons.

First, we consider the action of $a^a(p_2)$ on a single Reggeon, by expanding $U(z_1)$ to the linear order in $W^a(z_1)$ and then taking the Fourier transform according to eq. (6.13). We get

$$\begin{aligned}
W^a(p_1) a^b(p_2) \sim & \left\{ -2i g_s f^{abc} W^c(p_1 + p_2) \left[\frac{p_1^\mu}{p_1^2} + \frac{p_2^\mu}{p_2^2} \right] \right. \\
& - i g_s^2 f^{bce} f^{ead} \int [\vec{d}k] W^c(p_1 + p_2 - k) W^d(k) \left[\frac{p_1^\mu}{p_1^2} - \frac{(p_1 - k)^\mu}{(p_1 - k)^2} \right] \\
& + i \frac{g_s^3}{6} f^{bcx} f^{xdy} f^{yae} \int [\vec{d}k_1][\vec{d}k_2] W^c(p_1 + p_2 - k_1 - k_2) W^d(k_1) W^e(k_2) \\
& \left. \cdot \left[\frac{(p_1 - k_1 - k_2)^\mu}{(p_1 - k_1 - k_2)^2} - 3 \frac{(p_1 - k_2)^\mu}{(p_1 - k_2)^2} + 2 \frac{p_1^\mu}{p_1^2} \right] \right\} \varepsilon_\mu(p_2) + \dots, \quad (6.27)
\end{aligned}$$

These contributions are described by figure 3. The terms of higher order, which are omitted here, involve the coupling between a gluon and five or more Reggeons. These vertices start to contribute to N³LL and therefore are beyond the scope of the present paper. Next, we consider the term containing two W fields from the expansion of $U(z_1)$. At leading order we obtain

$$\begin{aligned}
\int [\vec{d}q] W^a(q) W^b(p_1 - q) a^c(p_2) \sim & \\
-2i g_s \int [\vec{d}q] \left\{ f^{acd} W^d(p_2 + q) W^b(p_1 - q) \left[\frac{p_2^\mu}{p_2^2} + \frac{q^\mu}{q^2} \right] \right. & (6.28) \\
& \left. + f^{bcd} W^a(q) W^d(p_1 + p_2 - q) \left[\frac{p_2^\mu}{p_2^2} + \frac{(p_1 - q)^\mu}{(p_1 - q)^2} \right] \right\} \varepsilon_\mu(p_2) + \dots,
\end{aligned}$$

where the ellipses stand for $WW \rightarrow WWW$ and $WW \rightarrow WWWW$ transitions not yet calculated, which will enter only at N³LL. The two-to-two Reggeon vertex is shown in figure 4. The last contribution necessary to achieve NNLL accuracy is given by the exchange

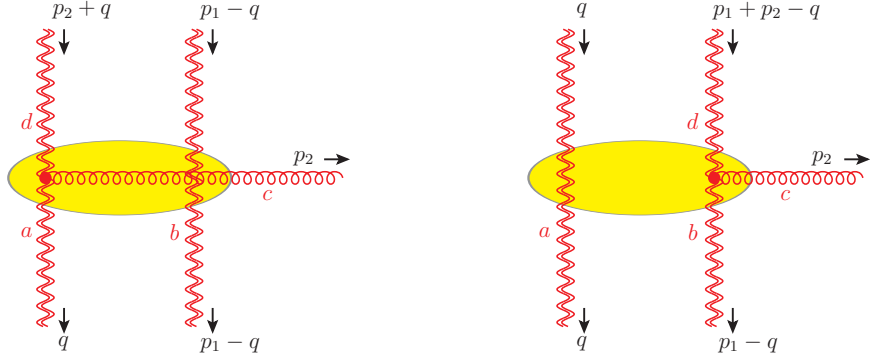


Figure 4. A Diagram describing the two-to-two Reggeon vertex associated with the emission of a real gluon.

of three Reggeons with emission of a gluon, which originates from considering the term containing three W fields from the expansion of $U(z_1)$. At leading order this gives

$$\begin{aligned}
& \int [\vec{d}q_1] \int [\vec{d}q_2] W^a(q_1) W^b(q_2) W^c(p_1 - q_1 - q_2) a^d(p_2) \sim \\
& -2i g_s \int [\vec{d}q_1] \int [\vec{d}q_2] \left\{ f^{ade} W^e(p_2 + q_1) W^b(q_2) W^c(p_1 - q_1 - q_2) \left[\frac{p_2^\mu}{p_2^2} + \frac{q_1^\mu}{q_1^2} \right] \right. \\
& + f^{bde} W^a(q_1) W^e(p_2 + q_2) W^c(p_1 - q_1 - q_2) \left[\frac{p_2^\mu}{p_2^2} + \frac{q_2^\mu}{q_2^2} \right] \\
& \left. + f^{cde} W^a(q_1) W^b(q_2) W^e(p_1 + p_2 - q_1 - q_2) \left[\frac{p_2^\mu}{p_2^2} + \frac{(p_1 - q_1 - q_2)^\mu}{(p_1 - q_1 - q_2)^2} \right] \right\} \varepsilon_\mu(p_2) + \dots,
\end{aligned} \tag{6.29}$$

where the ellipses stand for $WWW \rightarrow WWWW$ and $WWW \rightarrow WWWW$ transitions not yet calculated, which will enter starting at $N^3\text{LL}$. The three-to-three Reggeon vertex is shown in figure 5. Note that, as discussed in [17], at this logarithmic accuracy, eqs. (6.28) and (6.29) corresponds to summing the application of the first line of eq. (6.27) respectively on W^a , W^b and W^a , W^b and W^c , with the Reggeons not involved in the emission acting as spectators.

So far, all the vertices given in eqs. (6.27) and (6.28) are derived in the framework of the shockwave formalism to leading order, see eq. (6.25). In general, each vertex will receive new contributions beyond the leading order. In particular, the Reggeon-gluon-Reggeon vertex, which we denote by $\mathcal{R}g\mathcal{R}$, has the structure

$$W^a(p_1) a^b(p_2) \sim -2i g_s f^{abc} v^{\text{SR}}[(p_1 + p_2)^2, p_1^2, p_2^2, \tau] W^c(p_1 + p_2) \left[\frac{p_1^\mu}{p_1^2} + \frac{p_2^\mu}{p_2^2} \right] \varepsilon_\mu(p_2), \tag{6.30}$$

where the function $v^{\text{SR}}[p_1^2, (p_1 + p_2)^2, p_2^2, \tau] = 1 + \mathcal{O}(\alpha_s)$ identifies loop corrections to the Lipatov vertex: as we will see below, it coincides with the function defined in eq. (4.10), barring the scheme in which Regge factorization is applied: as explained following eqs. (6.19) and (6.20), here, within the context of the multi-Reggeon effective theory, we naturally use the SR/MR scheme, hence the superscript “SR” on v^{SR} . In section 8 the vertex will be

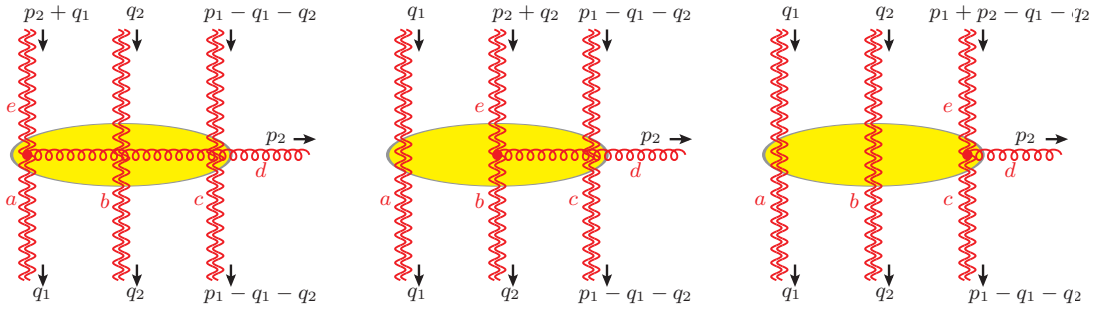


Figure 5. A Diagram describing the three-to-three Reggeon vertex associated with the emission of a real gluon.

related, along with the impact factors and Regge trajectory, to the alternative, pole/cut scheme of [23, 24]. Note also that in the present section we use simplified notation, omitting the polarization index (λ_4) corresponding to the helicity of the emitted gluon. The one-loop correction contributes to the $2 \rightarrow 3$ amplitude at NLL in the high-energy limit; the two-loop corrections will become relevant at NNLL.

6.3 Identifying single Reggeon contributions to $2 \rightarrow 3$ amplitudes

We are now in a position to consider again the amplitude in eq. (6.23), and separate single-Reggeon from multiple-Reggeon exchanges, with the aim to reproduce the Regge factorisation formula in eq. (4.10). To this end we split the amplitude in eq. (6.23) into single Reggeon (SR) and *Multi-Reggeon* (MR) components:

$$\bar{\mathcal{M}}_{ij \rightarrow i'gj'} = \bar{\mathcal{M}}_{ij \rightarrow i'gj'}^{\text{SR}} + \bar{\mathcal{M}}_{ij \rightarrow i'gj'}^{\text{MR}}, \quad (6.31)$$

and we decompose the Hamiltonian H in eq. (6.21) accordingly, i.e. we separate the evolution of a single Reggeon from the remaining Multi-Reggeon components:

$$H = H_{1 \rightarrow 1} + H_{\text{MR}}, \quad \text{where} \quad H_{\text{MR}} \equiv \sum_{n,m} H_{n \rightarrow m} (1 - \delta_{n1} \delta_{m1}), \quad (6.32)$$

where we identify the single-Reggeon term $H_{1 \rightarrow 1}$ with the gluon Regge trajectory $\alpha_g^{\text{SR}}(t)$ times the t -channel colour charge $-\mathbf{T}_{t_i}^2$:

$$H_{1 \rightarrow 1} \eta_i = -\mathbf{T}_{t_i}^2 \alpha_g^{\text{SR}}(t_i) \eta_i. \quad (6.33)$$

Let us stress once again that the superscript “SR” indicates that $\alpha_g^{\text{SR}}(t)$ identifies the Regge trajectory in the SR/MR scheme, as explained following eqs. (6.19) and (6.20). The relation with the pole/cut scheme [23, 24], will be presented in section 8.

The single Reggeon amplitude involves exclusively the exchange of a single Reggeon in both the η_1 and η_2 rapidity spans, thus we have

$$\frac{i}{2s_{12}} \bar{\mathcal{M}}_{ij \rightarrow i'gj'}^{\text{SR}} = \langle \psi_{j,1} | e^{-H_{1 \rightarrow 1} \eta_2} a_4(p_4) e^{-H_{1 \rightarrow 1} \eta_1} | \psi_{i,1} \rangle. \quad (6.34)$$

Instead, the Multi-Reggeon amplitude $\bar{\mathcal{M}}_{ij \rightarrow i'gj'}^{\text{MR}}$ involves H_{MR} in either or both of the rapidity spans, and we postpone its analysis to section 7. Here we proceed by elaborating the SR component. Using eq. (6.33), as well as eqs. (6.17) and (6.19) in eq. (6.23) we obtain

$$\frac{i}{2s_{12}} \mathcal{M}_{ij \rightarrow i'gj'}^{\text{SR}} = - \left[g_s \mathbf{T}_i^x C_i^{\text{SR}}(p_i, p'_i, \tau) \right] e^{C_A \alpha_g^{\text{SR}}(t_1) \eta_1} \left[g_s \mathbf{T}_j^y C_j^{\text{SR}}(p_j, p'_j, \tau) \right] e^{C_A \alpha_g^{\text{SR}}(t_2) \eta_2} \times \langle 0 | W^y(-q_2) a_4(p_4) W^x(q_1) | 0 \rangle. \quad (6.35)$$

We can now take into account the emission of a central gluon by means of eq. (6.30). This gives

$$\langle 0 | W^y(-q_2) a_4^{a_4}(p_4) W^x(q_1) | 0 \rangle = -2i g_s f^{xa_4y'} v^{\text{SR}}(t_1, t_2, p_4^2, \tau) \left[\frac{q_1^\mu}{q_1^2} + \frac{p_4^\mu}{p_4^2} \right] \varepsilon_\mu(p_4) \times \langle 0 | W^y(-q_2) W^{y'}(q_1 + p_4) | 0 \rangle. \quad (6.36)$$

At this point we are left with the expectation value in the last line, which simply gives the free Reggeon propagator¹¹ [17, 18]:

$$\langle 0 | W^y(-q_2) W^{y'}(q_1 + p_4) | 0 \rangle = \frac{i\delta^{yy'}}{q_2^2} (2\pi)^{2-2\epsilon} \delta^{(2-2\epsilon)}(q_1 + q_2 + p_4). \quad (6.37)$$

Inserting this result into eq. (6.36) we obtain

$$\langle 0 | W^y(-q_2) a_4^{a_4}(p_4) W^x(q_1) | 0 \rangle = 2 g_s f^{xa_4y} v(t_1, t_2, p_4^2, \tau) \frac{(2\pi)^{2-2\epsilon} \delta^{(2-2\epsilon)}(q_1 + q_2 + p_4)}{q_1^2 q_2^2} \times \left[\frac{q_1^\mu}{q_1^2} + \frac{p_4^\mu}{p_4^2} \right] \varepsilon_\mu(p_4). \quad (6.38)$$

We can easily check that this is indeed proportional to the tree-level Lipatov vertex. Taking into account that $v(t_1, t_2, p_4^2, \tau) = 1 + \mathcal{O}(\alpha_s)$, at tree level we can evaluate eq. (6.38) in $d = 2$, such that the relation in eq. (2.20) applies; one has $(q_1^\mu/q_1^2 + p_4^\mu/p_4^2)\varepsilon_\mu(p_4) = -1/\sqrt{2}(\bar{\mathbf{q}}_2 \mathbf{q}_1)/\bar{\mathbf{p}}_4$; enforcing momentum conservation according to eqs. (2.11) and (2.13) we get

$$\begin{aligned} & \langle 0 | W^y(-q_2) a_4^{a_4}(p_4) W^x(q_1) | 0 \rangle \Big|_{\text{tree}} \\ &= \sqrt{2} g_s f^{ya_4x} \frac{\bar{\mathbf{p}}_3 \mathbf{p}_5}{\bar{\mathbf{p}}_4} \frac{(2\pi)^{2-2\epsilon} \delta^{(2-2\epsilon)}(\mathbf{p}_3 + \mathbf{p}_4 + \mathbf{p}_5)}{t_1 t_2} \\ &= g_s f^{ya_4x} V^{(0)}(Q_1, P_4^\oplus, Q_2) \frac{(2\pi)^{2-2\epsilon} \delta^{(2-2\epsilon)}(\mathbf{p}_3 + \mathbf{p}_4 + \mathbf{p}_5)}{t_1 t_2}, \end{aligned} \quad (6.39)$$

where in the last line we have identified the tree-level Lipatov vertex $V^{(0)} = \sqrt{2} \bar{\mathbf{p}}_3 \mathbf{p}_5 / \bar{\mathbf{p}}_4$ as given in eq. (2.21). Beyond tree level, comparing eq. (6.38) with eq. (6.39) we readily obtain

$$\langle 0 | W^y(-q_2) a_4^{a_4}(p_4) W^x(q_1) | 0 \rangle$$

¹¹Note that we follow the convention that Reggeons emitted from the projectile i have incoming momentum, while Reggeons Absorbed into the target j have outgoing momentum, such that momentum in the transverse plane flows from j to i .

$$= g_s f^{ya_4x} V^{(0)}(Q_1, P_4^\oplus, Q_2) v^{\text{SR}}(t_1, t_2, \mathbf{p}_4^2, \tau) \frac{(2\pi)^{2-2\epsilon} \delta^{(2-2\epsilon)}(\mathbf{p}_3 + \mathbf{p}_4 + \mathbf{p}_5)}{t_1 t_2}. \quad (6.40)$$

Inserting eq. (6.40) into eq. (6.35) we finally obtain

$$\begin{aligned} \mathcal{M}_{ij \rightarrow i'gj'}^{\text{SR}} &= 2s_{12} \left[g_s \mathbf{T}_i^x C_i^{\text{SR}}(p_i, p'_i, \tau) \right] e^{C_A \alpha_g^{\text{SR}}(t_1) \eta_1} \left[g_s \mathbf{T}_j^y C_j^{\text{SR}}(p_j, p'_j, \tau) \right] e^{C_A \alpha_g^{\text{SR}}(t_2) \eta_2} \\ &\times g_s (i f^{ya_4x}) V^{(0)}(Q_1, P_4^\oplus, Q_2) v^{\text{SR}}(t_1, t_2, \mathbf{p}_4^2, \tau) \frac{(2\pi)^{2-2\epsilon} \delta^{(2-2\epsilon)}(\mathbf{p}_3 + \mathbf{p}_4 + \mathbf{p}_5)}{t_1 t_2} \\ &= c_i^{\text{SR}}(p_i, p'_i, \tau) e^{C_A \alpha_g^{\text{SR}}(t_1) \eta_1} v^{\text{SR}}(t_1, t_2, \mathbf{p}_4^2, \tau) \\ &\quad \times e^{C_A \alpha_g^{\text{SR}}(t_2) \eta_2} c_j^{\text{SR}}(p_j, p'_j, \tau) \mathcal{M}_{ij \rightarrow i'gj'}^{\text{tree}}, \end{aligned} \quad (6.41)$$

where in the second line we have identified the tree-level amplitude according to eqs. (2.14) and (2.22). We see that the 1-Reggeon transition as obtained within the shockwave formalism reproduces the classical Regge factorization formula of eq. (4.10), when the rapidity factors are identified as in eq. (6.24). Notice, however, that within the shockwave formalism (at least in the present formulation) one only determines rapidity evolution, therefore the impact factors and the Lipatov vertex appears as effective matching coefficients. In particular, this means that the shockwave formalism cannot predict the analytic structure in eq. (4.12). The impact factors and Lipatov vertex are not predicted within the theory, and need to be extracted by matching the factorization formula on the r.h.s. to the amplitude on the l.h.s of eq. (6.41). In this respect, we see that the contribution due to the multi-Reggeon transitions in the last line of eq. (6.41) plays a relevant role. In particular, they become essential, starting at NNLL accuracy, for a consistent extraction of the Lipatov vertex. The shockwave formalism provides a method to systematically compute multi-Reggeon transitions, expressing them in terms of integrals which solve iteratively the Balitsky-JIMWLK evolution equation, as discussed above. We will compute explicitly their contribution at one and two loops in section 7. The consistent extraction of the Lipatov vertex at two loops will be then discussed in Section 8.

7 Multi-Reggeon computations

In section 4 we have discussed the factorized structure of the amplitude in presence of a single Reggeon exchange. In section 6 we presented the formalism for computing multi-Reggeon exchanges. We now compute their contribution to the $2 \rightarrow 3$ scattering amplitude. As an illustration, in section 7.1 we calculate the complete multi-Reggeon contribution at one loop. Subsequently, in section 7.2 we describe the structure of all multi-Reggeon contributions to the two-loop amplitude, and finally in section 7.3 compute explicitly the respective $(-, -)$ component.

7.1 Multi-Reggeon contributions to the one-loop amplitude

The expansion of eq. (6.23) to one loop shows that there are two possible transitions involving multiple Reggeons. One entails the exchange of two Reggeons between the target and the projectile, as shown in Fig. 6 (a). In this case the emission of the central gluon

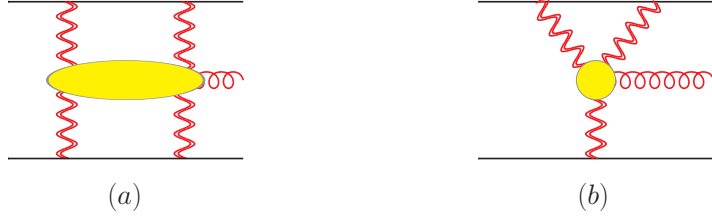


Figure 6. Multi-Reggeon exchange contribution to the one-loop $2 \rightarrow 3$ amplitude. Diagram (a) involves the exchange of two Reggeons between the target and the projectile, labelled as $\mathcal{R}^2 g \mathcal{R}^2$ in the main text. Diagram (b) represents the one-to-two Reggeon transition amplitude, denoted by $\mathcal{R} g \mathcal{R}^2$ in the main text. At one loop there is an additional diagram, involving the two-to-one Reggeon transition, or $\mathcal{R}^2 g \mathcal{R}$ amplitude. The latter is not shown here, because it is identical to the $\mathcal{R} g \mathcal{R}^2$ amplitude by target-projectile symmetry.

is governed by eq. (6.28), whose diagrammatic representation is given in Fig. 4. The other transition involves the emission of a single Reggeon from the projectile i which subsequently, upon emission of the central gluon, is turned into two Reggeons on the target side, as shown in Fig. 6 (b), or its symmetric counterpart under target-projectile interchange. This transition is governed by the second line of eq. (6.27), which in turn is represented diagrammatically by the central diagram in Fig. 3. In what follows we evaluate both transitions in some detail, to be able to discuss the techniques involved in the calculation.

The $\mathcal{R}^2 g \mathcal{R}^2$ transition. Using eq. (6.12b) in eq. (6.23) one has

$$\begin{aligned} \frac{i}{2s_{12}} \bar{\mathcal{M}}_{ij \rightarrow i' g j'} \Big|_{\mathcal{R}^2 g \mathcal{R}^2}^{\text{1-loop}} &= \left(\frac{g_s^2}{2} \right)^2 \mathbf{T}_i^a \mathbf{T}_i^b \mathbf{T}_j^{a'} \mathbf{T}_j^{b'} \int [dk_1] \int [dk_2] \\ &\times \langle 0 | W^{a'}(k_2) W^{b'}(-q_2 - k_2) a_4^c(p_4) W^a(k_1) W^b(q_1 - k_1) | 0 \rangle, \end{aligned} \quad (7.1)$$

Next, using eq. (6.28) we get

$$\begin{aligned} \frac{i}{2s_{12}} \bar{\mathcal{M}}_{ij \rightarrow i' g j'} \Big|_{\mathcal{R}^2 g \mathcal{R}^2}^{\text{1-loop}} &= -2i g_s \left(\frac{g_s^2}{2} \right)^2 \mathbf{T}_i^a \mathbf{T}_i^b \mathbf{T}_j^{a'} \mathbf{T}_j^{b'} \int [dk_1] \int [dk_2] \\ &\times \left\{ f^{acd} \langle 0 | W^{a'}(k_2) W^{b'}(-q_2 - k_2) W^d(k_1 + p_4) W^b(q_1 - k_1) | 0 \rangle \left[\frac{p_4^\mu}{p_4^2} + \frac{k_1^\mu}{k_1^2} \right] \right. \\ &\left. + f^{bcd} \langle 0 | W^{a'}(k_2) W^{b'}(-q_2 - k_2) W^a(k_1) W^d(-q_1 - k_1 + p_4) | 0 \rangle \left[\frac{p_4^\mu}{p_4^2} + \frac{(q_1 - k_1)^\mu}{(q_1 - k_1)^2} \right] \right\} \varepsilon_\mu(p_4). \end{aligned} \quad (7.2)$$

We contract a Reggeon in the target with one in the projectile according to

$$\langle 0 | W^x(p_1) W^y(p_2) | 0 \rangle = \frac{i \delta^{xy}}{p_1^2} (2\pi)^{2-2\epsilon} \delta^{(2-2\epsilon)}(p_1 - p_2), \quad (7.3)$$

which identifies the momenta defined in the same orientation. Wick contractions between two W s both originating from i or both originating with j lead to vanishing (scaleless)

integrals. Integrating over k_2 using the δ functions from the Reggeon propagators gives

$$\begin{aligned} \frac{i}{2s_{12}} \bar{\mathcal{M}}_{ij \rightarrow i'gj'} \Big|_{\mathcal{R}^2 g \mathcal{R}^2}^{\text{1-loop}} &= 2i g_s \left(\frac{g_s^2}{2} \right)^2 \mathbf{T}_i^a \mathbf{T}_i^b \mathbf{T}_j^{a'} \mathbf{T}_j^{b'} (2\pi)^{2-2\epsilon} \delta^{(2-2\epsilon)}(p_4 + q_1 + q_2) \\ &\times \int [d\bar{k}_1] \left\{ \left(f^{acb'} \delta^{a'b} + f^{aca'} \delta^{bb'} \right) \frac{1}{(q_1 - k_1)^2 (q_1 + q_2 - k_1)^2} \left[\frac{p_4^\mu}{p_4^2} + \frac{k_1^\mu}{k_1^2} \right] \right. \\ &\quad \left. + \left(f^{bca'} \delta^{ab'} + f^{bcb'} \delta^{aa'} \right) \frac{1}{k_1^2 (k_1 + q_2)^2} \left[\frac{p_4^\mu}{p_4^2} + \frac{(q_1 - k_1)^\mu}{(q_1 - k_1)^2} \right] \right\} \varepsilon_\mu(p_4). \end{aligned} \quad (7.4)$$

The kinematic factor in first term in the curly brackets is equal to the second one, upon performing the shift of the loop momentum $q_1 - k_1 \rightarrow k_1$. After this manipulation we combine terms and get

$$\begin{aligned} \frac{i}{2s_{12}} \bar{\mathcal{M}}_{ij \rightarrow i'gj'} \Big|_{\mathcal{R}^2 g \mathcal{R}^2}^{\text{1-loop}} &= 2i g_s \left(\frac{g_s^2}{2} \right)^2 \mathbf{T}_i^a \mathbf{T}_i^b \mathbf{T}_j^{a'} \mathbf{T}_j^{b'} (2\pi)^{2-2\epsilon} \delta^{(2-2\epsilon)}(p_4 + q_1 + q_2) \quad (7.5) \\ &\times \left(f^{acb'} \delta^{a'b} + f^{aca'} \delta^{bb'} + f^{bca'} \delta^{ab'} + f^{bcb'} \delta^{aa'} \right) \int \frac{[d\bar{k}_1]}{k_1^2 (k_1 + q_2)^2} \left[\frac{p_4^\mu}{p_4^2} + \frac{(q_1 - k_1)^\mu}{(q_1 - k_1)^2} \right] \varepsilon_\mu(p_4). \end{aligned}$$

Thus, we showed that the result factorises as a single colour factor multiplying the entire integral. Defining

$$\mathbf{T}_i^{\{a,b\}} = \frac{1}{2} \left(\mathbf{T}_i^a \mathbf{T}_i^b + \mathbf{T}_i^b \mathbf{T}_i^a \right), \quad (7.6)$$

we may write this colour factor as follows:

$$i \mathbf{T}_i^a \mathbf{T}_i^b \mathbf{T}_j^{a'} \mathbf{T}_j^{b'} \left(f^{acb'} \delta^{a'b} + f^{aca'} \delta^{bb'} + f^{bca'} \delta^{ab'} + f^{bcb'} \delta^{aa'} \right) = -4i f^{a'ca} \mathbf{T}_i^{\{a,b\}} \mathbf{T}_j^{\{a',b'\}}, \quad (7.7)$$

hence we obtain

$$\begin{aligned} \frac{i}{2s_{12}} \bar{\mathcal{M}}_{ij \rightarrow i'gj'} \Big|_{\mathcal{R}^2 g \mathcal{R}^2}^{\text{1-loop}} &= -8i\pi^2 g_s^3 \frac{\alpha_s}{\pi} f^{a'ca} \mathbf{T}_i^{\{a,b\}} \mathbf{T}_j^{\{a',b'\}} (2\pi)^{2-2\epsilon} \delta^{(2-2\epsilon)}(p_4 + q_1 + q_2) \\ &\times \int \frac{[d\bar{k}_1]}{k_1^2 (k_1 + q_2)^2} \left[\frac{p_4^\mu}{p_4^2} + \frac{(q_1 - k_1)^\mu}{(q_1 - k_1)^2} \right] \varepsilon_\mu(p_4). \end{aligned} \quad (7.8)$$

As for the case of $2 \rightarrow 2$ amplitude (see [18, 23]), we want to express this result in terms of loop integrals and color operators acting on the tree-level amplitude. Indeed, we observe that the color structure in eq. (7.8) can be written as follows:

$$\begin{aligned} \mathbf{T}_i^{\{a,b\}} i f^{a'ca} \mathbf{T}_j^{\{a',b'\}} &= \frac{1}{4} (\mathbf{T}_1 \cdot \mathbf{T}_2 - \mathbf{T}_1 \cdot \mathbf{T}_3 - \mathbf{T}_2 \cdot \mathbf{T}_5 + \mathbf{T}_3 \cdot \mathbf{T}_5) [\mathbf{T}_i^a i f^{a'ca} \mathbf{T}_j^{a'}] \\ &= \frac{1}{4} \mathbf{T}_{(-)} \mathcal{C}_{ij}^{(0)}, \end{aligned} \quad (7.9)$$

where in the first line we have used techniques discussed in Refs. [18, 23] to express the color factor in terms of operators acting on the tree-level color structure. In the second line we have then identified the operators with $\mathbf{T}_{(-)}$, defined in eq. (2.40), and the tree-level colour structure with the factor $\mathcal{C}_{ij}^{(0)}$, defined in eq. (2.24).

We can now consider the full amplitude, switching from $\bar{\mathcal{M}}_{ij \rightarrow i'gj'}$ to $\mathcal{M}_{ij \rightarrow i'gj'}$ according to eq. (6.23). We take into account eq. (7.9) and also the fact that $Z_{i/j} = 1 + \mathcal{O}(\alpha_s)$. Furthermore, in order to evaluate the loop integral, it is useful to notice that $q_1 = p_5$, $q_2 = p_3$, and momentum conservation fixes $p_4 = -p_3 - p_5$. Also, we work in dimensional regularization in the $\overline{\text{MS}}$ scheme, thus we make now the renormalization scale explicit by replacing $\alpha_s \rightarrow \alpha_s [\mu^2 e^{\gamma_E} / (4\pi)]^\epsilon$. In the end we get

$$\begin{aligned} \mathcal{M}_{ij \rightarrow i'gj'} \Big|_{\mathcal{R}^2 g \mathcal{R}^2}^{\text{1-loop}} &= 4i\pi^2 s_{12} g_s^3 \frac{\alpha_s}{\pi} C_i^{(0)} C_j^{(0)} \mathbf{T}_{(--)} C_{ij}^{(0)} (2\pi)^{2-2\epsilon} \delta^{(2-2\epsilon)}(p_3 + p_4 + p_5) \\ &\quad \times \left(\frac{\mu^2 e^{\gamma_E}}{4\pi} \right)^\epsilon \int \frac{[dk_1]}{k_1^2 (k_1 + p_3)^2} \left[\frac{p_4^\mu}{p_4^2} - \frac{(k_1 - p_5)^\mu}{(k_1 - p_5)^2} \right] \varepsilon_\mu(p_4). \end{aligned} \quad (7.10)$$

The loop integration can be reduced to a set of master integrals by means of IBPs. One has

$$\begin{aligned} \pi \left(\frac{\mu^2 e^{\gamma_E}}{4\pi} \right)^\epsilon \int \frac{[dk_1]}{k_1^2 (k_1 + p_3)^2} \left[\frac{p_4^\mu}{p_4^2} - \frac{(k_1 - p_5)^\mu}{(k_1 - p_5)^2} \right] \varepsilon_\mu(p_4) \\ = \left\{ \frac{\mathcal{I}_{(1,1,0)}}{p_3^2} \left[\frac{p_4^\mu}{p_4^2} + \frac{1}{2} \frac{p_3 \cdot p_5 p_3^\mu - p_3^2 p_5^\mu}{(p_3 \cdot p_5)^2 - p_3^2 p_5^2} \right] + \frac{\mathcal{I}_{(1,0,1)}}{2p_5^2} \frac{p_5^2 p_3^\mu - p_3 \cdot p_5 p_5^\mu}{(p_3 \cdot p_5)^2 - p_3^2 p_5^2} \right. \\ \left. - \frac{\mathcal{I}_{(0,1,1)}}{2p_3^2 p_5^2} \frac{(p_3 \cdot p_5 + p_5^2) p_3^\mu - (p_3^2 + p_3 \cdot p_5) p_5^\mu}{(p_3 \cdot p_5)^2 - p_3^2 p_5^2} \right. \\ \left. + \frac{\mathcal{I}_{(1,1,1)}}{2p_3^2 p_5^2} \frac{[2(p_3 \cdot p_5)^2 + p_3^2 (p_3 \cdot p_5 - p_5^2)] p_5^\mu - (p_3^2 + p_3 \cdot p_5) p_3^2 p_5^\mu}{(p_3 \cdot p_5)^2 - p_3^2 p_5^2} \right\} \varepsilon_\mu(p_4), \end{aligned} \quad (7.11)$$

where we have introduced the family of master integrals

$$\mathcal{I}_{(a,b,c)} = \pi \left(\frac{\mu^2 e^{\gamma_E}}{4\pi} \right)^\epsilon \int [dk] \frac{(p_5^2)^b (p_3^2)^c}{[k^2]^a [(k+p_3)^2]^{b+b'\epsilon} [(k-p_5)^2]^{c+c'\epsilon}}. \quad (7.12)$$

All the scalar products on the r.h.s. of eq. (7.11) can be evaluated in two transverse dimension by means of eqs. (2.10), (2.11) and (2.20), except for the integrals $\mathcal{I}_{(a,b,c)}$ which needs to be evaluated in dimensional regularization in $d = 2 - 2\epsilon$. Inserting eq. (7.11) into eq. (7.10), after some elaboration we get

$$\begin{aligned} \mathcal{M}_{ij \rightarrow i'gj'} \Big|_{\mathcal{R}^2 g \mathcal{R}^2}^{\text{1-loop}} &= -i\pi \frac{\alpha_s}{\pi} \frac{1}{z - \bar{z}} \left[(1 - \bar{z}) \mathcal{I}_{(1,1,0)} + z \mathcal{I}_{(1,0,1)} - \frac{\mathcal{I}_{(0,1,1)}}{|\mathbf{p}_4|^2 \bar{z} (1 - z)} - \mathcal{I}_{(1,1,1)} \right] \\ &\quad \times \mathbf{T}_{(--)} \mathcal{M}_{ij \rightarrow igj}^{\text{tree}}, \end{aligned} \quad (7.13)$$

where we have identified $\mathcal{M}_{ij \rightarrow igj}^{\text{tree}}$ according to eq. (2.22).

Eq. (7.13) contains three bubble integrals and a triangle integral. The bubbles are easy to calculate by means of the formula

$$B_{a,b}^{(2-2\epsilon)}(p^2, \epsilon) = \pi \left(\frac{\mu^2 e^{\gamma_E}}{4\pi} \right)^\epsilon \int [dk] \frac{1}{[k^2]^a [(k+p)^2]^b} = \frac{B_{a,b}(\epsilon)}{2\epsilon} \left(\frac{\mu^2}{p^2} \right)^\epsilon (p^2)^{1-a-b}, \quad (7.14)$$

where

$$B_{a,b}(\epsilon) = 2\epsilon \frac{e^{\epsilon\gamma_E} \Gamma(1-a-\epsilon)\Gamma(1-b-\epsilon)\Gamma(a+b-1+\epsilon)}{4 \Gamma(a)\Gamma(b)\Gamma(2-2\epsilon-a-b)}. \quad (7.15)$$

It is easy to identify

$$\begin{aligned} \mathcal{I}_{(1,1,0)} &= p_3^2 B_{(1,1)}^{(2-2\epsilon)}(p_3^2, \epsilon), \\ \mathcal{I}_{(1,0,1)} &= p_5^2 B_{(1,1)}^{(2-2\epsilon)}(p_5^2, \epsilon), \\ \mathcal{I}_{(0,1,1)} &= p_3^2 p_5^2 B_{(1,1)}^{(2-2\epsilon)}[(p_3 + p_5)^2, \epsilon] = p_3^2 p_5^2 B_{(1,1)}^{(2-2\epsilon)}(p_4^2, \epsilon). \end{aligned} \quad (7.16)$$

The triangle integral for generic powers a, b, c has been provided to all order in ϵ in [114, 115]. Here we need the case $a = b = c = 1$, which allows for some simplification. In the end one has

$$\begin{aligned} \mathcal{I}_{(1,1,1)} &= \pi \left(\frac{\mu^2 e^{\gamma_E}}{4\pi} \right)^\epsilon \int [dk] \frac{p_5^2 p_3^2}{k^2 (k+p_3)^2 (k-p_5)^2} \\ &= -\frac{e^{\gamma_E \epsilon} \Gamma(1-\epsilon)\Gamma(1+\epsilon)^2}{4\epsilon} (z-\bar{z}) \left(\frac{\mu^2 (z-\bar{z})^2}{z\bar{z}(1-z)(1-\bar{z})p_4^2} \right)^\epsilon \\ &\quad + \frac{e^{\gamma_E \epsilon} (1+2\epsilon)\Gamma(1-\epsilon)^2\Gamma(1+\epsilon)}{2\epsilon(1+\epsilon)\Gamma(1-2\epsilon)} z\bar{z}(1-z)(1-\bar{z}) \left(\frac{\mu^2}{p_4^2} \right)^\epsilon \\ &\quad \times \left\{ \frac{1}{z(1-\bar{z})} {}_2F_1 \left(1, -\epsilon, 2+\epsilon, \frac{\bar{z}(1-z)}{z(1-\bar{z})} \right) \right. \\ &\quad \quad - \frac{(z\bar{z})^{-1-\epsilon}}{z-\bar{z}} {}_2F_1 \left(1, 2(1+\epsilon), 2+\epsilon, -\frac{1-z}{z-\bar{z}} \right) \\ &\quad \quad \left. - \frac{[(1-z)(1-\bar{z})]^{-1-\epsilon}}{z-\bar{z}} {}_2F_1 \left(1, 2(1+\epsilon), 2+\epsilon, -\frac{\bar{z}}{z-\bar{z}} \right) \right\}. \end{aligned} \quad (7.17)$$

Inserting eq. (7.17) as well as the expression for the bubble integrals from eq. (7.14) into eq. (7.13), expanding in powers of ϵ , after some elaboration one has

$$\mathcal{M}_{ij \rightarrow i'gj'} \Big|_{\mathcal{R}^2 g \mathcal{R}^2}^{1\text{-loop}} = i\pi \frac{\alpha_s}{4\pi} G_{\mathcal{R}^2 g \mathcal{R}^2}^{(1)}(z, \bar{z}, |\mathbf{p}_4|^2, \mu^2) \mathbf{T}_{(--)} \mathcal{M}_{ij \rightarrow igj}^{\text{tree}}, \quad (7.18)$$

where the function $G_{\mathcal{R}^2 g \mathcal{R}^2}^{(1)}$ reads

$$\begin{aligned} G_{\mathcal{R}^2 g \mathcal{R}^2}^{(1)}(z, \bar{z}, |\mathbf{p}_4|^2, \mu^2) &= \frac{1}{\epsilon} + \ln \left(\frac{\mu^2 |\mathbf{p}_4|^2}{|\mathbf{p}_3|^2 |\mathbf{p}_5|^2} \right) + \epsilon \left[-\frac{\pi^2}{12} - 2D_2(z, \bar{z}) \right. \\ &\quad \left. + \frac{1}{2} \ln \left(\frac{\mu^2}{|\mathbf{p}_3|^2} \right)^2 - \frac{1}{2} \ln \left(\frac{\mu^2}{|\mathbf{p}_4|^2} \right)^2 + \frac{1}{2} \ln \left(\frac{\mu^2}{|\mathbf{p}_5|^2} \right)^2 \right] + \mathcal{O}(\epsilon^2), \end{aligned} \quad (7.19)$$

with $|\mathbf{p}_3|^2 = z\bar{z}|\mathbf{p}_4|^2$, $|\mathbf{p}_5|^2 = (1-z)(1-\bar{z})|\mathbf{p}_4|^2$ and the function $D_2(z, \bar{z})$ represents a single-valued combination of dilogarithms

$$D_2(z, \bar{z}) = \text{Li}_2(z) - \text{Li}_2(\bar{z}) + \frac{1}{2} \ln \left(\frac{1-z}{1-\bar{z}} \right) \ln(z\bar{z}), \quad (7.20)$$

which is referred to as the Bloch-Wigner dilogarithm [116].

Before concluding, it is instructive to have an explicit look at the action of the color operator $\mathbf{T}_{(--)}$ on the tree level amplitude $\mathcal{M}_{ij \rightarrow igj}^{\text{tree}}$. Let us recall that in color space the amplitude is written as a vector, according to eq. (2.26). An operator \mathbf{T}_X then acts as a matrix, according to (see appendix B.5 for more details)

$$\sum_{ji} c^{[j]} \mathbf{T}_X^{[j][i]} \mathcal{M}^{[i]} = \sum_j c^{[j]} \mathcal{M}^{[j]}. \quad (7.21)$$

Decomposing the amplitude on an orthonormal basis in the t -channel, as in eq. (2.34), the tree level amplitudes $\mathcal{M}_{ij \rightarrow igj}^{\text{tree}}$ are given by a single element: explicitly one has

$$\begin{aligned} \mathcal{M}_{qq \rightarrow qq}^{\text{tree}} &= c^{[8,8]_a} (\mathcal{M}_{qq \rightarrow qq}^{\text{tree}})^{[8,8]_a}, \\ \mathcal{M}_{gg \rightarrow gg}^{\text{tree}} &= c^{[8,8_a]_a} (\mathcal{M}_{gg \rightarrow gg}^{\text{tree}})^{[8,8_a]_a}, \\ \mathcal{M}_{gg \rightarrow ggg}^{\text{tree}} &= c^{[8_a,8_a]} (\mathcal{M}_{gg \rightarrow ggg}^{\text{tree}})^{[8_a,8_a]}, \end{aligned} \quad (7.22)$$

where the basis elements $c^{[r_1, r_2]_r}$ for the respective scattering processes are defined in eqs. (B.1), (B.4), (B.7) and (B.10), and the explicit coefficients $(\mathcal{M}_{ij \rightarrow igj}^{\text{tree}})^{[J]}$ are provided in eq. (B.16). Taking this into account, the action of the operator $\mathbf{T}_{(--)}$ on these tree level amplitudes gives

$$\sum_j c^{[j]} \mathbf{T}_{(--)}^{[j][8,8]_a} (\mathcal{M}_{qq \rightarrow qq}^{\text{tree}})^{[8,8]_a} = \frac{N_c^2 - 4}{2N_c} c^{[8,8]_a} (\mathcal{M}_{qq \rightarrow qq}^{\text{tree}})^{[8,8]_a}, \quad (7.23)$$

$$\sum_j c^{[j]} \mathbf{T}_{(--)}^{[j][8,8_a]_a} (\mathcal{M}_{gg \rightarrow gg}^{\text{tree}})^{[8,8_a]_a} = \frac{\sqrt{N_c^2 - 4}}{2} c^{[8,8_s]_a} (\mathcal{M}_{gg \rightarrow gg}^{\text{tree}})^{[8,8_a]_a}, \quad (7.24)$$

$$\sum_j c^{[j]} \mathbf{T}_{(--)}^{[j][8_a,8_a]} (\mathcal{M}_{gg \rightarrow ggg}^{\text{tree}})^{[8_a,8_a]} = \frac{\sqrt{N_c^2 - 4}}{2} c^{[8_s,8]_a} (\mathcal{M}_{gg \rightarrow ggg}^{\text{tree}})^{[8_a,8_a]}, \quad (7.25)$$

$$\begin{aligned} \sum_j c^{[j]} \mathbf{T}_{(--)}^{[j][8_a,8_a]} (\mathcal{M}_{gg \rightarrow ggg}^{\text{tree}})^{[8_a,8_a]} &= 2 \left(\sqrt{\frac{N_c - 3}{2N_c}} c^{[0,0]} + \sqrt{\frac{N_c + 3}{2N_c}} c^{[27,27]} \right. \\ &\quad \left. + \frac{N_c}{4} c^{[8_s,8_s]} \right) (\mathcal{M}_{gg \rightarrow ggg}^{\text{tree}})^{[8_a,8_a]}. \end{aligned} \quad (7.26)$$

Notice that for completeness we provide both the case in which $i = q$, $j = g$, namely $\mathcal{M}_{gg \rightarrow qgg}$, and the case in which $i = g$, $j = q$, i.e. $\mathcal{M}_{qq \rightarrow ggg}$. As it is evident, the action of $\mathbf{T}_{(--)}$ on these amplitudes is obviously symmetric. Comparing with the color basis in eq. (B.10) it is interesting to note that, for the $gg \rightarrow ggg$ amplitude, the color operator $\mathbf{T}_{(--)}$ projects onto the color basis elements which are even both under $1 \leftrightarrow 5$ and $2 \leftrightarrow 3$, as expected from Bose symmetry.

The $\mathcal{R}g\mathcal{R}^2$ and $\mathcal{R}^2g\mathcal{R}$ transitions. At one loop there are two additional contributions, namely, the one-to-two ($\mathcal{R}g\mathcal{R}^2$) and the two-to-one ($\mathcal{R}^2g\mathcal{R}$) Reggeon transition amplitudes. These transitions are related by the target-projectile (or top-bottom) symmetry, therefore we focus on the calculation of the $\mathcal{R}g\mathcal{R}^2$ amplitude, represented in Fig. 6 (b). In the end we will obtain the $\mathcal{R}^2g\mathcal{R}$ amplitude by symmetry.

The $\mathcal{R}g\mathcal{R}^2$ amplitude at one loop reads

$$\begin{aligned} \frac{i}{2s_{12}} \bar{\mathcal{M}}_{ij \rightarrow i'gj'} \Big|_{\mathcal{R}g\mathcal{R}^2}^{1\text{-loop}} &= -i g_s \frac{g_s^2}{2} \mathbf{T}_i^a \mathbf{T}_j^{a'} \mathbf{T}_j^{b'} \int [dk_1] \\ &\times \langle 0 | W^{a'}(k_2) W^{b'}(-q_2 - k_2) a_4^c(p_4) W^a(q_1) | 0 \rangle. \end{aligned} \quad (7.27)$$

In this case we need the second line of eq. (6.27), represented by the central diagram in Fig. 3. We get

$$\begin{aligned} \frac{i}{2s_{12}} \bar{\mathcal{M}}_{ij \rightarrow i'gj'} \Big|_{\mathcal{R}g\mathcal{R}^2}^{1\text{-loop}} &= -\frac{g_s^5}{2} f^{cc'e} f^{ead} \mathbf{T}_i^a \mathbf{T}_j^{a'} \mathbf{T}_j^{b'} \int [dk_1] \int [dk_2] \\ &\times \langle 0 | W^{a'}(k_2) W^{b'}(-q_2 - k_2) W^{c'}(q_1 - k_1 + p_4) W^d(k_1) | 0 \rangle \left[\frac{q_1^\mu}{q_1^2} - \frac{(q_1 - k_1)^\mu}{(q_1 - k_1)^2} \right] \varepsilon_\mu(p_4). \end{aligned} \quad (7.28)$$

Contracting the Reggeon fields according to eq. (7.3) and integrating over k_2 using the δ functions from the Reggeon propagators, after some elaboration gives

$$\begin{aligned} \frac{i}{2s_{12}} \bar{\mathcal{M}}_{ij \rightarrow i'gj'} \Big|_{\mathcal{R}g\mathcal{R}^2}^{1\text{-loop}} &= -4\pi^2 g_s^3 \frac{\alpha_s}{\pi} f^{a'ce} f^{eab'} \mathbf{T}_i^a \mathbf{T}_j^{\{a',b'\}} (2\pi)^{2-2\epsilon} \delta^{(2-2\epsilon)}(p_4 + q_1 + q_2) \\ &\times \int \frac{[dk_1]}{k_1^2(k_1 + q_2)^2} \left[\frac{q_1^\mu}{q_1^2} + \frac{(k_1 - q_1)^\mu}{(k_1 - q_1)^2} \right] \varepsilon_\mu(p_4), \end{aligned} \quad (7.29)$$

where we have expressed the color structure on the line i in terms of the operator defined in eq. (7.6). As for the $\mathcal{R}^2g\mathcal{R}^2$ transition amplitude, we want to write the result in eq. (7.29) in terms of loop integrals and color operators acting on the tree level amplitude. To this end we first use the Jacobi identity as follows:

$$f^{eab'} \mathbf{T}_i^a = i(\mathbf{T}_i^e \mathbf{T}_i^{b'} - \mathbf{T}_i^{b'} \mathbf{T}_i^e). \quad (7.30)$$

Inserting this result into the full color structure of eq. (7.29), and proceeding as before with methods described in [18, 23] we obtain

$$\begin{aligned} i f^{a'ce} (\mathbf{T}_i^e \mathbf{T}_i^{b'} - \mathbf{T}_i^{b'} \mathbf{T}_i^e) \mathbf{T}_j^{\{a',b'\}} &= \frac{1}{2} (\mathbf{T}_3 \cdot \mathbf{T}_5 - \mathbf{T}_2 \cdot \mathbf{T}_5 + \mathbf{T}_1 \cdot \mathbf{T}_3 - \mathbf{T}_1 \cdot \mathbf{T}_2) [\mathbf{T}_i^a i f^{a'ca} \mathbf{T}_j^{a'}] \\ &= \frac{1}{2} \mathbf{T}_{(+)} \mathcal{C}_{ij}^{(0)}, \end{aligned} \quad (7.31)$$

where in the second line we have identified the color operators in the first line with $\mathbf{T}_{(+)}$, defined in eq. (2.40), and the tree-level colour structure with the factor $\mathcal{C}_{ij}^{(0)}$, defined in eq. (2.24).

We can now consider the full amplitude, switching from $\bar{\mathcal{M}}_{ij \rightarrow i'gj'}$ to $\mathcal{M}_{ij \rightarrow i'gj'}$ according to eq. (6.23). Taking into account eq. (7.9), and also that $Z_{i/j} = 1 + \mathcal{O}(\alpha_s)$, at one loop we have

$$\begin{aligned} \mathcal{M}_{ij \rightarrow i'gj'} \Big|_{\mathcal{R}g\mathcal{R}^2}^{1\text{-loop}} &= 4i\pi^2 s_{12} g_s^3 \frac{\alpha_s}{\pi} C_i^{(0)} C_j^{(0)} \mathbf{T}_{(+)} \mathcal{C}_{ij}^{(0)} (2\pi)^{2-2\epsilon} \delta^{(2-2\epsilon)}(p_4 + q_1 + q_2) \\ &\times \int \frac{[dk_1]}{k_1^2(k_1 + q_2)^2} \left[\frac{q_1^\mu}{q_1^2} + \frac{(k_1 - q_1)^\mu}{(k_1 - q_1)^2} \right] \varepsilon_\mu(p_4). \end{aligned} \quad (7.32)$$

As before, we set $q_1 = p_5$, $q_2 = p_3$, and make the renormalization scale explicit by replacing $\alpha_s \rightarrow \alpha_s [\mu^2 e^{\gamma_E} / (4\pi)]^\epsilon$, obtaining

$$\begin{aligned} \mathcal{M}_{ij \rightarrow i'gj'} \Big|_{\mathcal{R}g\mathcal{R}^2}^{\text{1-loop}} &= 4i\pi^2 s_{12} g_s^3 \frac{\alpha_s}{\pi} C_i^{(0)} C_j^{(0)} \mathbf{T}_{(+ -)} C_{ij}^{(0)} (2\pi)^{2-2\epsilon} \delta^{(2-2\epsilon)} (p_3 + p_4 + p_5) \\ &\quad \times \left(\frac{\mu^2 e^{\gamma_E}}{4\pi} \right)^\epsilon \int \frac{[d\mathbf{k}_1]}{k_1^2 (k_1 + p_3)^2} \left[\frac{p_5^\mu}{p_5^2} + \frac{(k_1 - p_5)^\mu}{(k_1 - p_5)^2} \right] \varepsilon_\mu(p_4). \end{aligned} \quad (7.33)$$

The loop integration in eq. (7.33) can be reduced to a set of master integrals by means of IBPs. In this case we obtain

$$\begin{aligned} \pi \left(\frac{\mu^2 e^{\gamma_E}}{4\pi} \right)^\epsilon \int \frac{[d\mathbf{k}_1]}{k_1^2 (k_1 + p_3)^2} \left[\frac{p_5^\mu}{p_5^2} + \frac{(k_1 - p_5)^\mu}{(k_1 - p_5)^2} \right] \varepsilon_\mu(p_4) \\ = \left\{ \frac{\mathcal{I}_{(1,1,0)}}{2p_3^2} \left[\frac{2(p_3 \cdot p_5)^2 - p_3^2 p_5^2 p_5^\mu}{(p_3 \cdot p_5)^2 - p_3^2 p_5^2} - \frac{p_3 \cdot p_5 p_3^\mu}{(p_3 \cdot p_5)^2 - p_3^2 p_5^2} \right] \right. \\ + \frac{\mathcal{I}_{(1,0,1)}}{2p_5^2} \frac{p_3 \cdot p_5 p_5^\mu - p_5^2 p_3^\mu}{(p_3 \cdot p_5)^2 - p_3^2 p_5^2} + \frac{\mathcal{I}_{(0,1,1)}}{2p_3^2 p_5^2} \frac{(p_3 \cdot p_5 + p_5^2) p_3^\mu - (p_3^2 + p_3 \cdot p_5) p_5^\mu}{(p_3 \cdot p_5)^2 - p_3^2 p_5^2} \\ \left. + \frac{\mathcal{I}_{(1,1,1)}}{2p_3^2 p_5^2} \frac{(p_3^2 + p_3 \cdot p_5) p_5^2 p_3^\mu - [2(p_3 \cdot p_5)^2 + p_3^2 (p_3 \cdot p_5 - p_5^2)] p_5^\mu}{(p_3 \cdot p_5)^2 - p_3^2 p_5^2} \right\} \varepsilon_\mu(p_4), \end{aligned} \quad (7.34)$$

where the family of integrals is the same introduced in eq. (7.12). All the scalar products on the r.h.s. of eq. (7.34) can be evaluated in two transverse dimension by means of eqs. (2.10), (2.11) and (2.20), except for the integrals $\mathcal{I}_{(a,b,c)}$ which needs to be evaluated in dimensional regularization in $d = 2 - 2\epsilon$. Inserting eq. (7.34) into eq. (7.33), after some elaboration we obtain

$$\begin{aligned} \mathcal{M}_{ij \rightarrow i'gj'} \Big|_{\mathcal{R}g\mathcal{R}^2}^{\text{1-loop}} &= i\pi \frac{\alpha_s}{\pi} \frac{1}{z - \bar{z}} \left[(1 - z) \mathcal{I}_{(1,1,0)} + z \mathcal{I}_{(1,0,1)} \right. \\ &\quad \left. - \frac{\mathcal{I}_{(0,1,1)}}{|\mathbf{p}_4|^2 \bar{z} (1 - z)} - \mathcal{I}_{(1,1,1)} \right] \mathbf{T}_{(+ -)} \mathcal{M}_{ij \rightarrow igj}^{\text{tree}}. \end{aligned} \quad (7.35)$$

Inserting eq. (7.17) as well as the expression for the bubble integrals from eq. (7.14) into eq. (7.35), expanding in powers of ϵ we arrive at

$$\mathcal{M}_{ij \rightarrow i'gj'} \Big|_{\mathcal{R}g\mathcal{R}^2}^{\text{1-loop}} = i\pi \frac{\alpha_s}{4\pi} G_{\mathcal{R}g\mathcal{R}^2}^{(1)}(z, \bar{z}, |\mathbf{p}_4|^2, \mu^2) \mathbf{T}_{(+ -)} \mathcal{M}_{ij \rightarrow igj}^{\text{tree}}, \quad (7.36)$$

where

$$\begin{aligned} G_{\mathcal{R}g\mathcal{R}^2}^{(1)}(z, \bar{z}, |\mathbf{p}_4|^2, \mu^2) &= \frac{1}{\epsilon} + \ln \left(\frac{\mu^2 |\mathbf{p}_5|^2}{|\mathbf{p}_3|^2 |\mathbf{p}_4|^2} \right) + \epsilon \left[-\frac{\pi^2}{12} + 2D_2(z, \bar{z}) \right. \\ &\quad \left. + \frac{1}{2} \ln \left(\frac{\mu^2}{|\mathbf{p}_3|^2} \right)^2 + \frac{1}{2} \ln \left(\frac{\mu^2}{|\mathbf{p}_4|^2} \right)^2 - \frac{1}{2} \ln \left(\frac{\mu^2}{|\mathbf{p}_5|^2} \right)^2 \right] + \mathcal{O}(\epsilon^2). \end{aligned} \quad (7.37)$$

As for the $\mathcal{R}^2 g\mathcal{R}^2$ transition, it is instructive to have an explicit look at the action of the color operator $\mathbf{T}_{(+ -)}$ on the tree level amplitude $\mathcal{M}_{ij \rightarrow igj}^{\text{tree}}$. Using the same notation as

in eq. (7.9), we have

$$\sum_j c^{[j]} \mathbf{T}_{(+ -)}^{[j][8,8]_a} (\mathcal{M}_{qq \rightarrow qgg}^{\text{tree}})^{[8,8]_a} = - \left(\sqrt{2} c^{[8,1]} + \frac{\sqrt{N_c^2 - 4}}{2} c^{[8,8]_s} \right) (\mathcal{M}_{qq \rightarrow qgg}^{\text{tree}})^{[8,8]_a}, \quad (7.38)$$

$$\sum_j c^{[j]} \mathbf{T}_{(+ -)}^{[j][8,8_a]_a} (\mathcal{M}_{gg \rightarrow ggg}^{\text{tree}})^{[8,8_a]_a} = - \left(\frac{2N_c}{\sqrt{N_c^2 - 1}} c^{[8,1]} + \frac{N_c}{2} c^{[8,8_s]_s} + \sqrt{\frac{N_c + 3}{N_c + 1}} c^{[8,27]} + \sqrt{\frac{N_c - 3}{N_c - 1}} c^{[8,0]} \right) (\mathcal{M}_{gg \rightarrow ggg}^{\text{tree}})^{[8,8_a]_a}, \quad (7.39)$$

$$\sum_j c^{[j]} \mathbf{T}_{(+ -)}^{[j][8_a,8]_a} (\mathcal{M}_{gg \rightarrow ggg}^{\text{tree}})^{[8_a,8]_a} = \left(\sqrt{2} c^{[8_a,1]} + \frac{\sqrt{N_c^2 - 4}}{2} c^{[8_a,8]_s} \right) (\mathcal{M}_{gg \rightarrow ggg}^{\text{tree}})^{[8_a,8]_a}, \quad (7.40)$$

$$\sum_j c^{[j]} \mathbf{T}_{(+ -)}^{[j][8_a,8_a]_a} (\mathcal{M}_{gg \rightarrow ggg}^{\text{tree}})^{[8_a,8_a]_a} = - \left(\frac{2N_c}{\sqrt{N_c^2 - 1}} c^{[8_a,1]} + \frac{N_c}{2} c^{[8_a,8_s]_s} + \sqrt{\frac{N_c + 3}{N_c + 1}} c^{[8_a,27]} + \sqrt{\frac{N_c - 3}{N_c - 1}} c^{[8_a,0]} \right) (\mathcal{M}_{gg \rightarrow ggg}^{\text{tree}})^{[8_a,8_a]_a}. \quad (7.41)$$

Comparing with the color basis in eq. (B.10) it is interesting to note that, for the $gg \rightarrow ggg$ amplitude, the color operator $\mathbf{T}_{(+ -)}$ projects onto the color basis elements which are odd under $1 \leftrightarrow 5$ and even under $2 \leftrightarrow 3$, as expected from Bose symmetry.

With the result for the $\mathcal{R}g\mathcal{R}^2$ in eq. (7.36), we can immediately obtain the $\mathcal{R}^2g\mathcal{R}$ transition amplitude by applying projectile-target symmetry. For the color operator, the symmetry implies $\mathbf{T}_{(+ -)} \rightarrow \mathbf{T}_{(- +)}$, while the kinematic dependence is obtained by applying the target-projectile symmetry $z \rightarrow 1 - \bar{z}$, $\bar{z} \rightarrow 1 - z$ to eq. (7.36). Taking into account the property

$$D_2(1 - \bar{z}, 1 - z) = D_2(z, \bar{z}), \quad (7.42)$$

we have

$$\mathcal{M}_{ij \rightarrow i'g'j'} \Big|_{\mathcal{R}^2g\mathcal{R}}^{\text{1-loop}} = i\pi \frac{\alpha_s}{4\pi} G_{\mathcal{R}^2g\mathcal{R}}^{(1)}(z, \bar{z}, |\mathbf{p}_4|^2, \mu^2) \mathbf{T}_{(- +)} \mathcal{M}_{ij \rightarrow i'g'j'}^{\text{tree}}, \quad (7.43)$$

where

$$G_{\mathcal{R}^2g\mathcal{R}}^{(1)}(z, \bar{z}, |\mathbf{p}_4|^2, \mu^2) = \frac{1}{\epsilon} + \ln \left(\frac{\mu^2 |\mathbf{p}_3|^2}{|\mathbf{p}_4|^2 |\mathbf{p}_5|^2} \right) + \epsilon \left[-\frac{\pi^2}{12} + 2D_2(z, \bar{z}) - \frac{1}{2} \ln \left(\frac{\mu^2}{|\mathbf{p}_3|^2} \right)^2 + \frac{1}{2} \ln \left(\frac{\mu^2}{|\mathbf{p}_4|^2} \right)^2 + \frac{1}{2} \ln \left(\frac{\mu^2}{|\mathbf{p}_5|^2} \right)^2 \right] + \mathcal{O}(\epsilon^2). \quad (7.44)$$

The action of the $\mathbf{T}_{(- +)}$ color operator on the tree level reads

$$\sum_j c^{[j]} \mathbf{T}_{(- +)}^{[j][8,8]_a} (\mathcal{M}_{qq \rightarrow qgg}^{\text{tree}})^{[8,8]_a} = \left(\sqrt{2} c^{[1,8]} + \frac{\sqrt{N_c^2 - 4}}{2} c^{[8,8]_s} \right) (\mathcal{M}_{qq \rightarrow qgg}^{\text{tree}})^{[8,8]_a}, \quad (7.45)$$

$$\sum_j c^{[j]} \mathbf{T}_{(- +)}^{[j][8,8_a]_a} (\mathcal{M}_{gg \rightarrow ggg}^{\text{tree}})^{[8,8_a]_a} = \left(\sqrt{2} c^{[1,8_a]} + \frac{\sqrt{N_c^2 - 4}}{2} c^{[8,8_a]_s} \right) (\mathcal{M}_{gg \rightarrow ggg}^{\text{tree}})^{[8,8_a]_a},$$

(7.46)

$$\sum_j c^{[j]} \mathbf{T}_{(-+)}^{[j][8_a, 8]_a} (\mathcal{M}_{gg \rightarrow gq}^{\text{tree}})^{[8_a, 8]_a} = - \left(\frac{2N_c}{\sqrt{N_c^2 - 1}} c^{[1, 8]} + \frac{N_c}{2} c^{[8_s, 8]_s} \right. \\ \left. + \sqrt{\frac{N_c + 3}{N_c + 1}} c^{[27, 8]} + \sqrt{\frac{N_c - 3}{N_c - 1}} c^{[0, 8]} \right) (\mathcal{M}_{gq \rightarrow gq}^{\text{tree}})^{[8_a, 8]_a}, \quad (7.47)$$

$$\sum_j c^{[j]} \mathbf{T}_{(-+)}^{[j][8_a, 8_a]} (\mathcal{M}_{gg \rightarrow ggg}^{\text{tree}})^{[8_a, 8_a]} = \left(\frac{2N_c}{\sqrt{N_c^2 - 1}} c^{[1, 8_a]} + \frac{N_c}{2} c^{[8_s, 8_a]} \right. \\ \left. + \sqrt{\frac{N_c + 3}{N_c + 1}} c^{[27, 8_a]} + \sqrt{\frac{N_c - 3}{N_c - 1}} c^{[0, 8_a]} \right) (\mathcal{M}_{gg \rightarrow ggg}^{\text{tree}})^{[8_a, 8_a]}. \quad (7.48)$$

As expected, for the $gg \rightarrow ggg$ amplitude, the color operator $\mathbf{T}_{(-+)}$ projects onto the color basis elements which are even under $1 \leftrightarrow 5$ and odd under $2 \leftrightarrow 3$, as expected from Bose symmetry.

The complete MR amplitude at one loop. The full one-loop multiple-Reggeon contribution is given by the sum of eqs. (7.18), (7.36) and (7.43), and reads

$$\mathcal{M}_{ij \rightarrow i'gj'}^{\text{MR}} \Big|^{1\text{-loop}} = \mathcal{M}_{ij \rightarrow i'gj'} \Big|_{\mathcal{R}^2 g \mathcal{R}^2}^{1\text{-loop}} + \mathcal{M}_{ij \rightarrow i'gj'} \Big|_{\mathcal{R} g \mathcal{R}^2}^{1\text{-loop}} + \mathcal{M}_{ij \rightarrow i'gj'} \Big|_{\mathcal{R}^2 g \mathcal{R}}^{1\text{-loop}} \\ = i\pi \frac{\alpha_s}{4\pi} \left\{ \frac{1}{\epsilon} \left[\mathbf{T}_{(--)} + \mathbf{T}_{(-+)} + \mathbf{T}_{(+-)} \right] \right. \\ + \ln \left(\frac{\mu^2 |\mathbf{p}_4|^2}{|\mathbf{p}_3|^2 |\mathbf{p}_5|^2} \right) \mathbf{T}_{(--)} + \ln \left(\frac{\mu^2 |\mathbf{p}_3|^2}{|\mathbf{p}_4|^2 |\mathbf{p}_5|^2} \right) \mathbf{T}_{(-+)} + \ln \left(\frac{\mu^2 |\mathbf{p}_5|^2}{|\mathbf{p}_4|^2 |\mathbf{p}_3|^2} \right) \mathbf{T}_{(+-)} \\ + \epsilon \left[\left(-\frac{\pi^2}{12} - 2D_2(z, \bar{z}) + \frac{1}{2} \ln^2 \left(\frac{\mu^2}{|\mathbf{p}_3|^2} \right) - \frac{1}{2} \ln^2 \left(\frac{\mu^2}{|\mathbf{p}_4|^2} \right) + \frac{1}{2} \ln^2 \left(\frac{\mu^2}{|\mathbf{p}_5|^2} \right) \right) \mathbf{T}_{(--)} \right. \\ + \left(-\frac{\pi^2}{12} + 2D_2(z, \bar{z}) - \frac{1}{2} \ln^2 \left(\frac{\mu^2}{|\mathbf{p}_3|^2} \right) + \frac{1}{2} \ln^2 \left(\frac{\mu^2}{|\mathbf{p}_4|^2} \right) + \frac{1}{2} \ln^2 \left(\frac{\mu^2}{|\mathbf{p}_5|^2} \right) \right) \mathbf{T}_{(-+)} \\ \left. + \left(-\frac{\pi^2}{12} + 2D_2(z, \bar{z}) + \frac{1}{2} \ln^2 \left(\frac{\mu^2}{|\mathbf{p}_3|^2} \right) + \frac{1}{2} \ln^2 \left(\frac{\mu^2}{|\mathbf{p}_4|^2} \right) - \frac{1}{2} \ln^2 \left(\frac{\mu^2}{|\mathbf{p}_5|^2} \right) \right) \mathbf{T}_{(+-)} \right] \\ \left. + \mathcal{O}(\epsilon^2) \right\} \mathcal{M}_{ij \rightarrow i'gj'}^{\text{tree}}. \quad (7.49)$$

7.2 Multi-Reggeon contributions to the two-loop amplitude

We are now ready to consider the amplitude at two loops. At this order we need to take into account several multi-Reggeon transitions, which contribute to all the amplitude components $\mathcal{M}^{(\pm, \pm)}$. As discussed in the introduction, purpose of this paper is to disentangle the Regge pole and cut contribution, such as to achieve an unambiguous definition of the Litpatov vertex at two loops. To this end we need to focus on the multi-Reggeon contribution to $\mathcal{M}^{(-, -)}$ only, that we will calculate in detail in what follows. For illustration, however, let us start by identifying all the contributions that appear at two loops.

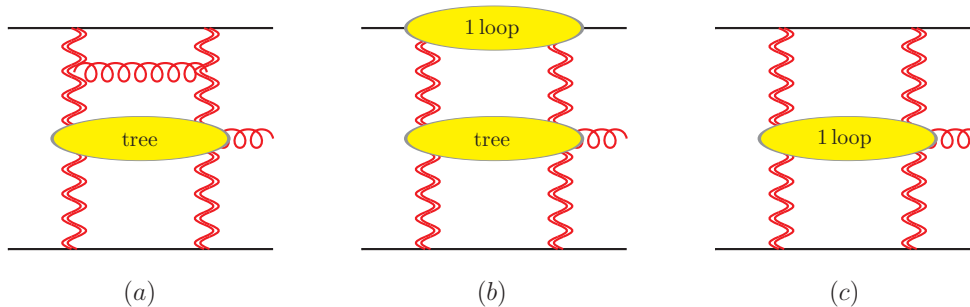


Figure 7. Multi-Reggeon exchange contribution to two-loop even-even amplitude $\mathcal{M}^{(+,+)}$. Adopting the notation from [18, 21, 23], the horizontal gluon in the ladder represents one application of the BFKL kernel, while the blob on the upper line j represents the two-Reggeon impact factor. There are two additional diagrams, in which the BFKL kernel is applied below the emission vertex, and one where the Two-Reggeon impact factor is taken on the leg i .

As usual, we obtain such terms by expanding eq. (6.23) to second order in the strong coupling constant. We recall at this point that the signature symmetry, i.e. the symmetry of the amplitude under the exchange of $1 \leftrightarrow 5$ for the projectile i , and $2 \leftrightarrow 3$ for the target j , is in direct correspondence with the parity of the number of Reggeons emitted: one Reggeon belong to the odd ($-$) sector, two Reggeons to the even ($+$) sector, three Reggeons to the odd sector again, and so on. Following this criterion, we can unambiguously assign all contributions to a specific amplitude component $\mathcal{M}^{(\pm,\pm)}$. Starting from the even-even amplitude, or $\mathcal{M}^{(+,+)}$, we have

$$\begin{aligned}
\frac{i}{2s_{12}} \bar{\mathcal{M}}_{ij \rightarrow i'gj'}^{(+,+)} \Big|^{2\text{-loops}} &= \frac{i}{2s_{12}} \bar{\mathcal{M}}_{ij \rightarrow i'gj'} \Big|_{\mathcal{R}^2 g \mathcal{R}^2}^{2\text{-loops}} \\
&= -\eta_2 \langle \psi_{j,2} | H_{2 \rightarrow 2} a_4(p_4) | \psi_{i,2} \rangle^{\text{LO}} - \eta_1 \langle \psi_{j,2} | a_4(p_4) H_{2 \rightarrow 2} | \psi_{i,2} \rangle^{\text{LO}} \\
&\quad + \langle \psi_{j,2} | a_4(p_4) | \psi_{i,2} \rangle^{\text{NLO}}. \tag{7.50}
\end{aligned}$$

In this equation, the term proportional to η_2 involves an application of the leading order BFKL kernel $H_{2 \rightarrow 2}$ between the target j and the emission of the central gluon, as represented in Fig. 7 (a); in the second term, proportional to η_1 , the BFKL kernel is applied between the central emission gluon and the projectile i . The last term, instead, involves the sum of three NLO contributions: the first is given by the insertion of the one-loop two-Reggeon impact factor on the target, as in Figure Fig. 7 (b); the second contribution is obtained by inserting the two-Reggeon impact factor at one loop on the projectile; the third term is given by the one-loop version of the two-Reggeon-gluon emission vertex in eq. (6.28), which is yet to be calculated. Notice that the two terms involving $H_{2 \rightarrow 2}$ in eq. (7.50) contributes at NLL to the amplitude, as evident from the rapidity factors η_1, η_2 multiplying them, while the last term contributes at NNLL.

Next, we consider the two-loop odd-even amplitude $\mathcal{M}^{(-,+)}$. In contrast to the one-loop case, where this amplitude only receives a contribution from the $\mathcal{R}g\mathcal{R}^2$ transition, at two loops we also need to take into account the transition $\mathcal{R}^3g\mathcal{R}^2$, which involves three Reggeons emission from the target. This is in correspondence to what happens in case of

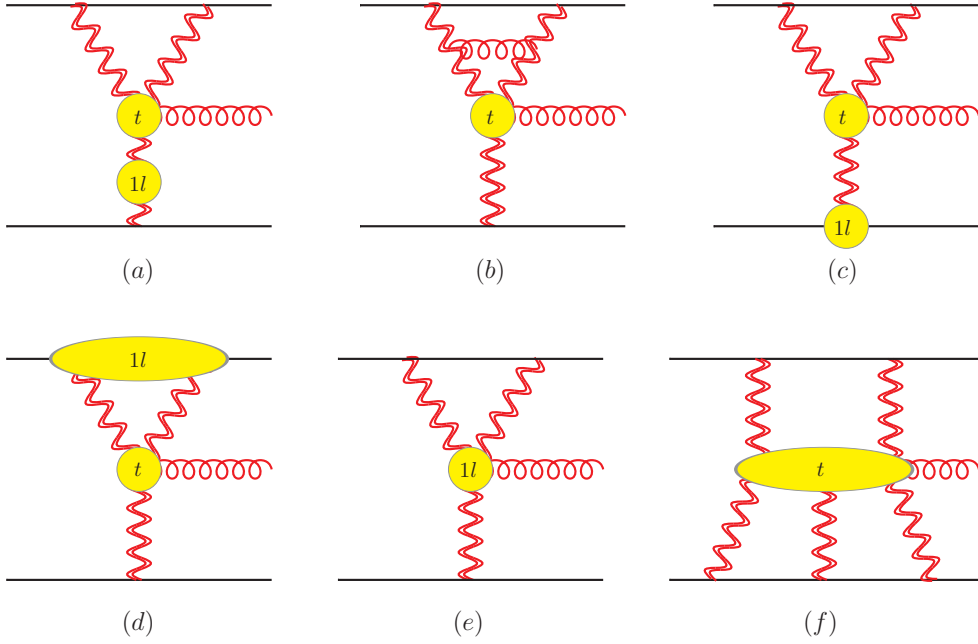


Figure 8. Multi-Reggeon exchange contribution to the two-loop odd-even amplitude $\mathcal{M}^{(-,+)}$. A small t indicates that the corresponding vertex is taken at tree level, while the label $1l$ indicates that one needs to consider the corresponding insertion at one loop. The two-loop even-odd amplitude $\mathcal{M}^{(+,-)}$ can be obtained from the diagrams above by exploiting the target-projectile (or top-bottom) symmetry.

the $2 \rightarrow 2$ scattering amplitudes: in that case, in fact, in the odd sector $\mathcal{M}_{ij \rightarrow ij}^{(-)}$, starting at two loops one needs to take into account the mixing between one and three Reggeons [18]. One has thus

$$\frac{i}{2s_{12}} \bar{\mathcal{M}}_{ij \rightarrow i'gj'}^{(-,+)} \Big|_{\mathcal{R}g\mathcal{R}^2}^{2\text{-loops}} = \frac{i}{2s_{12}} \left(\bar{\mathcal{M}}_{ij \rightarrow i'gj'} \Big|_{\mathcal{R}g\mathcal{R}^2}^{2\text{-loops}} + \bar{\mathcal{M}}_{ij \rightarrow i'gj'} \Big|_{\mathcal{R}^3g\mathcal{R}^2}^{2\text{-loops}} \right), \quad (7.51)$$

where in turn the two transitions reads

$$\begin{aligned} \frac{i}{2s_{12}} \bar{\mathcal{M}}_{ij \rightarrow i'gj'} \Big|_{\mathcal{R}g\mathcal{R}^2}^{2\text{-loops}} &= -\eta_2 \langle \psi_{j,2} | a_4(p_4) H_{1 \rightarrow 1} | \psi_{i,1} \rangle^{\text{LO}} - \eta_1 \langle \psi_{j,2} | H_{2 \rightarrow 2} a_4(p_4) | \psi_{i,1} \rangle^{\text{LO}} \\ &\quad + \langle \psi_{j,2} | a_4(p_4) | \psi_{i,1} \rangle^{\text{NLO}}, \end{aligned} \quad (7.52)$$

and

$$\frac{i}{2s_{12}} \bar{\mathcal{M}}_{ij \rightarrow i'gj'} \Big|_{\mathcal{R}^3g\mathcal{R}^2}^{2\text{-loops}} = \langle \psi_{j,2} | a_4(p_4) | \psi_{i,3} \rangle^{\text{LO}}.$$

The first term in eq. (7.52) is represented in fig. 8 (a), and involves the insertion of the $H_{1 \rightarrow 1}$ evolution kernel (i.e., the Regge trajectory at one loop) between the projectile and the gluon emission. The second term is represented by fig. 8 (b), and involves the insertion of the leading order BFKL kernel $H_{2 \rightarrow 2}$ between the central emission gluon and the target j . The third term denoted by the superscript NLO involves three contributions: the first term

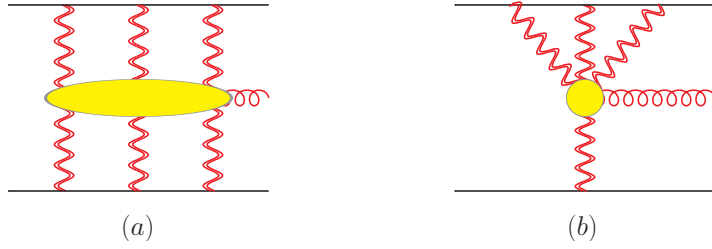


Figure 9. Multi-Reggeon exchange contribution to the two-loop odd-even amplitude $\mathcal{M}^{(-,-)}$.

is represented in fig. 8 (c), and involves the insertion of the one loop single Reggeon impact factor on the projectile; the second term, represented in fig. 8 (d), is obtained by inserting the two-Reggeon impact factor on the target. Last, the third term is represented in fig. 8 (e), and involves the one- to two-Reggeon-gluon emission vertex at one loop, which, as in case of the two-Reggeon-gluon emission vertex in Fig. 7, is yet to be calculated, and it would involve the BFKL kernel at NLO. The term in eq.(7.53) is given instead by the three- to two-Reggeon-gluon emission vertex. This term can be obtained either by expanding eq.(6.28) one additional order in g_s , thus taking into account the three-gluon terms on the r.h.s. of the equation; alternatively, this term is simply given by all possible combinations of the one- to two-Reggeon-gluon vertex given in the second line of eq.(6.27) (central diagram in Fig. 3), with an additional Reggeon propagating between the target and the projectile.

Last, we have the odd-odd amplitude, namely $\mathcal{M}^{(-,-)}$. In this case we need to take into account one-to-three, three-to-one and three-to three Reggeon transitions, on top of the single-Reggeon transition we described in section 6.3. We have

$$\frac{i}{2s_{12}} \bar{\mathcal{M}}_{ij \rightarrow i'gj'}^{(-,-)} \Big|^{2\text{-loops}} = \frac{i}{2s_{12}} \left(\bar{\mathcal{M}}_{ij \rightarrow i'gj'} \Big|_{\mathcal{R}g\mathcal{R}}^{2\text{-loops}} + \bar{\mathcal{M}}_{ij \rightarrow i'gj'} \Big|_{\mathcal{R}g\mathcal{R}^3}^{2\text{-loops}} + \bar{\mathcal{M}}_{ij \rightarrow i'gj'} \Big|_{\mathcal{R}^3g\mathcal{R}}^{2\text{-loops}} + \bar{\mathcal{M}}_{ij \rightarrow i'gj'} \Big|_{\mathcal{R}^3g\mathcal{R}^3}^{2\text{-loops}} \right). \quad (7.53)$$

The first term in this equation represents the single Reggeon transition, namely, considering the complete amplitude we have

$$\mathcal{M}_{ij \rightarrow i'gj'} \Big|_{\mathcal{R}g\mathcal{R}}^{2\text{-loops}} = \mathcal{M}_{ij \rightarrow i'gj'}^{\text{SR}} \Big|^{2\text{-loops}}, \quad (7.54)$$

which can be obtained by expanding eq.(6.41) consistently to second order in the strong coupling constant. The second term in eq.(7.53) reads

$$\frac{i}{2s_{12}} \bar{\mathcal{M}}_{ij \rightarrow i'gj'} \Big|_{\mathcal{R}g\mathcal{R}^3}^{2\text{-loops}} = \langle \psi_{j,3} | a_4(p_4) | \psi_{i,1} \rangle^{\text{LO}}, \quad (7.55)$$

and is represented in Fig. 9 (b), where the single-Reggeon to three-Reggeon-gluon vertex is given by the last term in eq.(6.27), also represented by the diagram on the right in Fig. 3. Next, the third term reads

$$\frac{i}{2s_{12}} \bar{\mathcal{M}}_{ij \rightarrow i'gj'} \Big|_{\mathcal{R}^3g\mathcal{R}}^{2\text{-loops}} = \langle \psi_{j,1} | a_4(p_4) | \psi_{i,3} \rangle^{\text{LO}}, \quad (7.56)$$

and can be obtained by target-projectile symmetry from the $\mathcal{R}g\mathcal{R}^3$ transition that we just described. Last, the term involving three Reggeons reads

$$\frac{i}{2s_{12}} \bar{\mathcal{M}}_{ij \rightarrow i'gj'} \Big|_{\mathcal{R}^3g\mathcal{R}^3}^{2\text{-loops}} = \langle \psi_{j,3} | a_4(p_4) | \psi_{i,3} \rangle^{\text{LO}}. \quad (7.57)$$

It is represented in Fig. 9 (a), and is obtained by using eq. (6.29) onto $a_4(p_4) | \psi_{i,3} \rangle$. In the following section we proceed to evaluate explicitly the terms giving rise eq. (7.53).

7.3 Odd-odd Amplitude

The $\mathcal{R}^3g\mathcal{R}^3$ transition. We start with the calculation of the three-Reggeon transition amplitude. Inserting eq. (6.12c) into eq. (7.52) one has

$$\begin{aligned} \frac{i}{2s_{12}} \bar{\mathcal{M}}_{ij \rightarrow i'gj'} \Big|_{\mathcal{R}^3g\mathcal{R}^3}^{2\text{-loops}} &= - \left(\frac{g_s^3}{6} \right)^2 (\mathbf{T}^a \mathbf{T}^b \mathbf{T}^c)_i (\mathbf{T}^{a'} \mathbf{T}^{b'} \mathbf{T}^{c'})_j \int [dk_1][dk_2] \int [dk_3][dk_4] \\ &\times \langle 0 | W^{a'}(k_3) W^{b'}(k_4) W^{c'}(-q_2 - k_3 - k_4) a_4^d(p_4) W^a(k_1) W^b(k_2) W^c(q_1 - k_1 - k_2) | 0 \rangle, \end{aligned} \quad (7.58)$$

Using eq. (6.29) with $q_1 = k_1$, $q_2 = k_2$, $p_1 = q_1$, $p_2 = p_4$, we get

$$\begin{aligned} \frac{i}{2s_{12}} \bar{\mathcal{M}}_{ij \rightarrow i'gj'} \Big|_{\mathcal{R}^3g\mathcal{R}^3}^{2\text{-loops}} &= 2i g_s \left(\frac{g_s^3}{6} \right)^2 (\mathbf{T}^a \mathbf{T}^b \mathbf{T}^c)_i (\mathbf{T}^{a'} \mathbf{T}^{b'} \mathbf{T}^{c'})_j \\ &\times \int [dk_1][dk_2] \int [dk_3][dk_4] \langle 0 | W^{a'}(k_3) W^{b'}(k_4) W^{c'}(-q_2 - k_3 - k_4) \\ &\times \left\{ f^{ade} \left[\frac{p_4^\mu}{p_4^2} + \frac{k_1^\mu}{k_1^2} \right] W^e(k_1 + p_4) W^b(k_2) W^c(q_1 - k_1 - k_2) | 0 \rangle \right. \\ &+ f^{bde} \left[\frac{p_4^\mu}{p_4^2} + \frac{k_2^\mu}{k_2^2} \right] W^a(k_1) W^e(k_2 + p_4) W^c(q_1 - k_1 - k_2) | 0 \rangle \\ &\left. + f^{cde} \left[\frac{p_4^\mu}{p_4^2} + \frac{(q_1 - k_1 - k_2)^\mu}{(q_1 - k_2 - k_2)^2} \right] W^a(k_1) W^b(k_2) W^c(q_1 - k_1 - k_2 + p_4) | 0 \rangle \right\} \varepsilon_\mu(p_4). \end{aligned} \quad (7.59)$$

From here one proceeds as illustrated in the previous sections, namely, we contract the Reggeon fields according to eq. (7.3), which gives rise to three Dirac deltas for each terms; subsequently we integrate over k_3 and k_4 , thus enforcing momentum conservation. In the end one can exploit the freedom to shift the remaining two integration variables, i.e. k_1 and k_2 , to express the momentum dependent part in a compact form. After some work one gets

$$\begin{aligned} \frac{i}{2s_{12}} \bar{\mathcal{M}}_{ij \rightarrow i'gj'} \Big|_{\mathcal{R}^3g\mathcal{R}^3}^{2\text{-loops}} &= i \frac{16\pi^4}{3} g_s^3 \left(\frac{\alpha_s}{\pi} \right)^2 (2\pi)^{2-2\epsilon} \delta^{(2-2\epsilon)}(p_4 + q_1 + q_2) \\ &\times \left\{ (\mathbf{T}^a \mathbf{T}^b \mathbf{T}^c)_i + (\mathbf{T}^b \mathbf{T}^a \mathbf{T}^c)_i + (\mathbf{T}^c \mathbf{T}^b \mathbf{T}^a)_i \right\} (i f^{a'da}) \mathbf{T}_j^{\{a',b,c\}} \\ &\times \int [dk_1][dk_2] \frac{1}{k_1^2 k_2^2 (k_1 + k_2 + q_2)^2} \left[\frac{p_4^\mu}{p_4^2} - \frac{(k_1 + k_2 - q_1)^\mu}{(k_1 + k_2 - q_1)^2} \right] \varepsilon_\mu(p_4), \end{aligned} \quad (7.60)$$

where, in analogy to eq. (7.6), we have used the notation

$$\mathbf{T}_i^{\{a,b,c\}} = \frac{1}{3!} \sum_{\sigma \in \mathcal{S}_3} \mathbf{T}_i^{\sigma(a)} \mathbf{T}_i^{\sigma(b)} \mathbf{T}_i^{\sigma(c)}. \quad (7.61)$$

In order to express this result in terms of loop integrals and color operators acting on the tree level amplitude, we first notice that the color structure in eq. (7.60) can be written as follows:

$$\begin{aligned} & \left\{ (\mathbf{T}^a \mathbf{T}^b \mathbf{T}^c)_i + (\mathbf{T}^b \mathbf{T}^a \mathbf{T}^c)_i + (\mathbf{T}^c \mathbf{T}^b \mathbf{T}^a)_i \right\} (i f^{a'da}) \mathbf{T}_j^{\{a',b,c\}} \\ &= \frac{1}{6} \left\{ \mathbf{T}_1 \cdot \mathbf{T}_2 (+ 2\mathbf{T}_1 \cdot \mathbf{T}_2 + \mathbf{T}_1 \cdot \mathbf{T}_3 - \mathbf{T}_2 \cdot \mathbf{T}_5 - \mathbf{T}_3 \cdot \mathbf{T}_5) \right. \\ & \quad + \mathbf{T}_1 \cdot \mathbf{T}_3 (-\mathbf{T}_1 \cdot \mathbf{T}_2 + 2\mathbf{T}_1 \cdot \mathbf{T}_3 + \mathbf{T}_2 \cdot \mathbf{T}_5 - \mathbf{T}_3 \cdot \mathbf{T}_5) \\ & \quad + \mathbf{T}_2 \cdot \mathbf{T}_5 (-\mathbf{T}_1 \cdot \mathbf{T}_2 + 2\mathbf{T}_2 \cdot \mathbf{T}_5 - \mathbf{T}_3 \cdot \mathbf{T}_5) \\ & \quad + \mathbf{T}_3 \cdot \mathbf{T}_5 (-\mathbf{T}_1 \cdot \mathbf{T}_3 - \mathbf{T}_2 \cdot \mathbf{T}_5 + 2\mathbf{T}_3 \cdot \mathbf{T}_5) \\ & \quad \left. + \frac{C_A}{2} (\mathbf{T}_1 + \mathbf{T}_5) (\mathbf{T}_2 + \mathbf{T}_3) \right\} [\mathbf{T}_i^a i f^{a'da} \mathbf{T}_j^{a'}] \\ &= \frac{1}{48} \left[9\mathbf{T}_{(--)}^2 + \mathbf{T}_{(++)}^2 + 3(\mathbf{T}_{(+-)}^2 + \mathbf{T}_{(-+)}^2) + 4C_A \mathbf{T}_{(++)} \right] C_{ij}^{(0)}. \quad (7.62) \end{aligned}$$

Inserting this result into eq. (7.60), switching from $\bar{\mathcal{M}}_{ij \rightarrow i'gj'}$ to $\mathcal{M}_{ij \rightarrow i'gj'}$ according to eq. (6.23), taking into account momentum conservation and the fact that $Z_{i/j} = 1 + \mathcal{O}(\alpha_s)$, at two loops we obtain

$$\begin{aligned} \mathcal{M}_{ij \rightarrow i'gj'} \Big|_{\mathcal{R}^3 g \mathcal{R}^3}^{2\text{-loops}} &= \frac{2\pi^4}{9} s_{12} g_s^3 \left(\frac{\alpha_s}{\pi} \right)^2 (2\pi)^{2-2\epsilon} \delta^{(2-2\epsilon)} (p_3 + p_4 + p_5) C_i^{(0)} C_j^{(0)} \\ & \times \left[9\mathbf{T}_{(--)}^2 + \mathbf{T}_{(++)}^2 + 3(\mathbf{T}_{(+-)}^2 + \mathbf{T}_{(-+)}^2) + 4C_A \mathbf{T}_{(++)} \right] C_{ij}^{(0)} \quad (7.63) \\ & \times \int [d\bar{k}_1][d\bar{k}_2] \frac{1}{k_1^2 k_2^2 (k_1 + k_2 + p_3)^2} \left[\frac{p_4^\mu}{p_4^2} - \frac{(k_1 + k_2 - p_5)^\mu}{(k_1 + k_2 - p_5)^2} \right] \varepsilon_\mu(p_4), \end{aligned}$$

This expression can be elaborates such that one of the two loop integrals reduces to a simple bubble integral, of the form given in eq. (7.14), and the second is given in terms of the same family of integrals defined in eq. (7.12). To this end, we shift $k_1 + k_2 \rightarrow k_2$, then perform the k_1 bubble integral, obtaining

$$\begin{aligned} & \pi^2 \int [d\bar{k}_1][d\bar{k}_2] \frac{1}{k_1^2 k_2^2 (k_1 + k_2 + p_3)^2} \left[\frac{p_4^\mu}{p_4^2} - \frac{(k_1 + k_2 - p_5)^\mu}{(k_1 + k_2 - p_5)^2} \right] \varepsilon_\mu(p_4) \\ &= \pi \frac{\mu^{2\epsilon} B_{1,1}(\epsilon)}{2\epsilon} \int [d\bar{k}_2] \frac{1}{(k_2^2)^{1+\epsilon} (k_2 + p_3)^2} \left[\frac{p_4^\mu}{p_4^2} - \frac{(k_2 - p_5)^\mu}{(k_2 - p_5)^2} \right] \varepsilon_\mu(p_4). \quad (7.64) \end{aligned}$$

The integral over k_2 can be reduced by means of IBPs to a set of master integrals belonging to the topology in eq. (7.12). After some elaboration we obtain

$$\mathcal{M}_{ij \rightarrow i'gj'} \Big|_{\mathcal{R}^3 g \mathcal{R}^3}^{2\text{-loops}} = (i\pi)^2 \left(\frac{\alpha_s}{\pi} \right)^2 \frac{\mu^{2\epsilon} B_{1,1}(\epsilon)}{2\epsilon} \frac{1}{18(z - \bar{z})}$$

$$\begin{aligned} & \times \left\{ (1 - \bar{z}) \mathcal{I}_{(1+\epsilon,1,0)} + z \mathcal{I}_{(1+\epsilon,0,1)} - \frac{\mathcal{I}_{(\epsilon,1,1)}}{|\mathbf{p}_4|^2 \bar{z} (1 - z)} - \mathcal{I}_{(1+\epsilon,1,1)} \right\} \quad (7.65) \\ & \times \left[9\mathbf{T}_{(--)}^2 + \mathbf{T}_{(++)}^2 + 3\left(\mathbf{T}_{(+-)}^2 + \mathbf{T}_{(-+)}^2\right) + 4C_A \mathbf{T}_{(++)} \right] \mathcal{M}_{ij \rightarrow igj}^{\text{tree}}. \end{aligned}$$

The first two master integrals are easily evaluated by means of eq. (7.14), while the last two integrals require a generalization of eq. (7.17). For conciseness, let us define the color operator involved in the $\mathcal{R}^3 g \mathcal{R}^3$ transition as follows:

$$\mathcal{C}_{\mathcal{R}^3 g \mathcal{R}^3} \equiv 9\mathbf{T}_{(--)}^2 + \mathbf{T}_{(++)}^2 + 3\left(\mathbf{T}_{(+-)}^2 + \mathbf{T}_{(-+)}^2\right) + 4C_A \mathbf{T}_{(++)}. \quad (7.66)$$

After some elaboration we obtain

$$\mathcal{M}_{ij \rightarrow i'gj'} \Big|_{\mathcal{R}^3 g \mathcal{R}^3}^{2\text{-loops}} = (i\pi)^2 \left(\frac{\alpha_s}{\pi}\right)^2 G_{\mathcal{R}^3 g \mathcal{R}^3}^{(2)}(z, \bar{z}, |\mathbf{p}_4|^2, \mu^2) \mathcal{C}_{\mathcal{R}^3 g \mathcal{R}^3} \mathcal{M}_{ij \rightarrow igj}^{\text{tree}}. \quad (7.67)$$

where, setting for simplicity $\mu^2 = |\mathbf{p}_4|^2$, $G_{\mathcal{R}^3 g \mathcal{R}^3}^{(2)}$ reads

$$\begin{aligned} G_{\mathcal{R}^3 g \mathcal{R}^3}^{(2)}(z, \bar{z}, |\mathbf{p}_4|^2, |\mathbf{p}_4|^2) &= \frac{1}{288} \left\{ \frac{1}{\epsilon^2} - \frac{2}{\epsilon} \log [z\bar{z}(1-z)(1-\bar{z})] - 6D_2(z, \bar{z}) - \zeta_2 \right. \quad (7.68) \\ & \left. + 2\log^2 [z\bar{z}] + 2\log^2 [(1-z)(1-\bar{z})] + \log [z\bar{z}] \log [(1-z)(1-\bar{z})] + \mathcal{O}(\epsilon) \right\}. \end{aligned}$$

To conclude the evaluation of the $\mathcal{R}^3 g \mathcal{R}^3$ transition, we report the explicit action of the color operator on the tree level amplitude, using the same notation used in eqs. (7.9) and (7.31): we have

$$\sum_j c^{[j]} \mathcal{C}_{\mathcal{R}^3 g \mathcal{R}^3}^{[j][8,8]_a} (\mathcal{M}_{qq \rightarrow qgq}^{\text{tree}})^{[8,8]_a} = \left(2N_c^2 - 12 + \frac{36}{N_c^2}\right) c^{[8,8]_a} (\mathcal{M}_{qq \rightarrow qgq}^{\text{tree}})^{[8,8]_a}, \quad (7.69)$$

$$\sum_j c^{[j]} \mathcal{C}_{\mathcal{R}^3 g \mathcal{R}^3}^{[j][8,8_a]_a} (\mathcal{M}_{qg \rightarrow qgg}^{\text{tree}})^{[8,8_a]_a} = (2N_c^2 + 12) c^{[8,8_a]_a} (\mathcal{M}_{qg \rightarrow qgg}^{\text{tree}})^{[8,8_a]_a}, \quad (7.70)$$

$$\sum_j c^{[j]} \mathcal{C}_{\mathcal{R}^3 g \mathcal{R}^3}^{[j][8_a,8]_a} (\mathcal{M}_{gq \rightarrow ggg}^{\text{tree}})^{[8_a,8]_a} = (2N_c^2 + 12) c^{[8_a,8]_a} (\mathcal{M}_{gq \rightarrow ggg}^{\text{tree}})^{[8_a,8]_a}, \quad (7.71)$$

$$\begin{aligned} \sum_j c^{[j]} \mathcal{C}_{\mathcal{R}^3 g \mathcal{R}^3}^{[j][8_a,8_a]_a} (\mathcal{M}_{gg \rightarrow ggg}^{\text{tree}})^{[8_a,8_a]_a} &= \left[(2N_c^2 + 72) c^{[8_a,8_a]_a} \right. \\ & \left. - 36\sqrt{N_c - 4} c^{[10,10]_1} \right] (\mathcal{M}_{gg \rightarrow ggg}^{\text{tree}})^{[8_a,8_a]_a}. \quad (7.72) \end{aligned}$$

The $\mathcal{R}g\mathcal{R}^3$ transition. We continue with the Reggeon to three Reggeon transition, represented by the diagram (b) in Fig. 9, which, to the best of our knowledge, has not been considered in previous works. This transition involve the state eq. (6.12c) for the target j and the state eq. (6.12a) for the projectile i . Inserting these states into eq. (7.55) we have

$$\begin{aligned} \frac{i}{2s_{12}} \bar{\mathcal{M}}_{ij \rightarrow i'gj'} \Big|_{\mathcal{R}g\mathcal{R}^3}^{2\text{-loops}} &= g_s \left(\frac{g_s^3}{6}\right) \mathbf{T}_i^a (\mathbf{T}^{a'} \mathbf{T}^{b'} \mathbf{T}^{c'})_j \int [d\bar{k}_1][d\bar{k}_2] \quad (7.73) \\ & \times \langle 0 | W^{a'}(k_3) W^{b'}(k_4) W^{c'}(-q_2 - k_3 - k_4) a_4^d(p_4) W^a(q_1) | 0 \rangle. \end{aligned}$$

Using the third line of eq. (6.27) with $p_1 = q_1$, $p_2 = p_4$, we get

$$\begin{aligned} \frac{i}{2s_{12}} \bar{\mathcal{M}}_{ij \rightarrow i'gj'} \Big|_{\mathcal{R}_g \mathcal{R}^3}^{2\text{-loops}} &= i \frac{g_s^7}{36} f^{dgx} f^{xfy} f^{yae} \mathbf{T}_i^a (\mathbf{T}^{a'} \mathbf{T}^{b'} \mathbf{T}^{c'})_j \int [dk_1][dk_2] \int [dk_3][dk_4] \\ &\times \langle 0 | W^{a'}(k_3) W^{b'}(k_4) W^{c'}(-q_2 - k_3 - k_4) W^g(q_1 + p_4 - k_1 - k_2) W^f(k_1) W^e(k_2) | 0 \rangle \\ &\times \left[\frac{(q_1 - k_1 - k_2)^\mu}{(q_1 - k_1 - k_2)^2} - 3 \frac{(q_1 - k_2)^\mu}{(q_1 - k_2)^2} + 2 \frac{q_1^\mu}{q_1^2} \right] \varepsilon_\mu(p_4). \end{aligned} \quad (7.74)$$

From here we contract the Reggeon fields according to eq. (7.3); this gives rise to three Dirac deltas for each terms, and subsequently we integrate over k_3 and k_4 , thus enforcing momentum conservation. In the end we exploit the freedom to shift the remaining two integration variables, i.e. k_1 and k_2 , to express the momentum dependent part in a compact form. After some work we get

$$\begin{aligned} \frac{i}{2s_{12}} \bar{\mathcal{M}}_{ij \rightarrow i'gj'} \Big|_{\mathcal{R}_g \mathcal{R}^3}^{2\text{-loops}} &= \frac{8\pi^4}{3} g_s^3 \left(\frac{\alpha_s}{\pi} \right)^2 (2\pi)^{2-2\epsilon} \delta^{(2-2\epsilon)}(p_4 + q_1 + q_2) \\ &\times f^{dgx} f^{xfy} f^{yae} \mathbf{T}_i^a \mathbf{T}_j^{\{e,f,g\}} \int [dk_1][dk_2] \frac{1}{k_1^2 k_2^2 (k_1 + k_2 + q_2)^2} \\ &\times \left[\frac{(q_1 - k_1 - k_2)^\mu}{(q_1 - k_1 - k_2)^2} - 3 \frac{(q_1 - k_2)^\mu}{(q_1 - k_2)^2} + 2 \frac{q_1^\mu}{q_1^2} \right] \varepsilon_\mu(p_4). \end{aligned} \quad (7.75)$$

The color structure can be written as follows:

$$\begin{aligned} &i f^{dgx} f^{xfy} f^{yae} \mathbf{T}_i^a \mathbf{T}_j^{\{e,f,g\}} \\ &= -\frac{1}{6} \left\{ \mathbf{T}_1 \cdot \mathbf{T}_2 (+2\mathbf{T}_1 \cdot \mathbf{T}_2 - \mathbf{T}_1 \cdot \mathbf{T}_3 + 2\mathbf{T}_2 \cdot \mathbf{T}_5 - 2\mathbf{T}_3 \cdot \mathbf{T}_5) \right. \\ &\quad + \mathbf{T}_1 \cdot \mathbf{T}_3 (-\mathbf{T}_1 \cdot \mathbf{T}_2 + 2\mathbf{T}_1 \cdot \mathbf{T}_3 - 2\mathbf{T}_2 \cdot \mathbf{T}_5 + 2\mathbf{T}_3 \cdot \mathbf{T}_5) \\ &\quad + \mathbf{T}_2 \cdot \mathbf{T}_5 (+2\mathbf{T}_1 \cdot \mathbf{T}_2 + 2\mathbf{T}_2 \cdot \mathbf{T}_5 - \mathbf{T}_3 \cdot \mathbf{T}_5) \\ &\quad + \mathbf{T}_3 \cdot \mathbf{T}_5 (+2\mathbf{T}_1 \cdot \mathbf{T}_3 - \mathbf{T}_2 \cdot \mathbf{T}_5 + 2\mathbf{T}_3 \cdot \mathbf{T}_5) \\ &\quad \left. + \frac{C_A}{2} (\mathbf{T}_1 + \mathbf{T}_5)(\mathbf{T}_2 + \mathbf{T}_3) \right\} [\mathbf{T}_i^a i f^{a'ca} \mathbf{T}_j^{a'}] \\ &= -\frac{1}{12} \left[\mathbf{T}_{(++)}^2 + 3\mathbf{T}_{(+-)}^2 + C_A \mathbf{T}_{(++)} \right] \mathcal{C}_{ij}^{(0)}. \end{aligned} \quad (7.76)$$

Inserting this result into eq. (7.60), switching from $\bar{\mathcal{M}}_{ij \rightarrow i'gj'}$ to $\mathcal{M}_{ij \rightarrow i'gj'}$ according to eq. (6.23), taking into account momentum conservation and the fact that $Z_{i/j} = 1 + \mathcal{O}(\alpha_s)$, at two loops we obtain

$$\begin{aligned} \mathcal{M}_{ij \rightarrow i'gj'} \Big|_{\mathcal{R}_g \mathcal{R}^3}^{2\text{-loops}} &= \frac{4\pi^4}{9} s_{12} g_s^3 \left(\frac{\alpha_s}{\pi} \right)^2 (2\pi)^{2-2\epsilon} \delta^{(2-2\epsilon)}(p_3 + p_4 + p_5) C_i^{(0)} C_j^{(0)} \\ &\times \left[\mathbf{T}_{(++)}^2 + 3\mathbf{T}_{(+-)}^2 + C_A \mathbf{T}_{(++)} \right] \mathcal{C}_{ij}^{(0)} \int [dk_1][dk_2] \frac{1}{k_1^2 k_2^2 (k_1 + k_2 + p_3)^2} \end{aligned}$$

$$\times \left[2 \frac{p_5^\mu}{p_5^2} + 3 \frac{(k_2 - p_5)^\mu}{(k_2 - p_5)^2} - \frac{(k_1 + k_2 - p_5)^\mu}{(k_1 + k_2 - p_5)^2} \right] \varepsilon_\mu(p_4). \quad (7.77)$$

We write the loop integral as follows:

$$\begin{aligned} \pi^2 \int \frac{[dk_1][dk_2]}{k_1^2 k_2^2 (k_1 + k_2 + p_3)^2} & \left[3 \left(\frac{p_5^\mu}{p_5^2} + \frac{(k_2 - p_5)^\mu}{(k_2 - p_5)^2} \right) - \left(\frac{p_5^\mu}{p_5^2} + \frac{(k_1 + k_2 - p_5)^\mu}{(k_1 + k_2 - p_5)^2} \right) \right] \varepsilon_\mu(p_4) \\ & = \pi \frac{\mu^{2\epsilon} B_{1,1}(\epsilon)}{2\epsilon} \int [dk_2] \left\{ \frac{1}{(k_2^2)^{1+\epsilon} (k_2 + p_3)^2} \left[2 \frac{p_5^\mu}{p_5^2} - \frac{(k_2 - p_5)^\mu}{(k_2 - p_5)^2} \right] \right. \\ & \quad \left. + \frac{3}{k_2^2 [(k_2 + p_3)^2]^{1+\epsilon}} \frac{(k_2 - p_5)^\mu}{(k_2 - p_5)^2} \right\} \varepsilon_\mu(p_4). \quad (7.78) \end{aligned}$$

The integral over k_2 can be reduced by means of IBPs to a set of master integrals belonging to the topology in eq. (7.12), obtaining

$$\begin{aligned} \mathcal{M}_{ij \rightarrow i'gj'} \Big|_{\mathcal{R}g\mathcal{R}^3}^{2\text{-loops}} & = -(i\pi)^2 \left(\frac{\alpha_s}{\pi} \right)^2 \frac{\mu^{2\epsilon} B_{1,1}(\epsilon)}{2\epsilon} \frac{1}{3(z - \bar{z})} \\ & \times \left\{ (1-z) \left(\mathcal{I}_{(1,1+\epsilon,0)} - \frac{1}{3} \mathcal{I}_{(1,1+\epsilon,0)} \right) + z \left(\mathcal{I}_{(1,\epsilon,1)} - \frac{1}{3} \mathcal{I}_{(1+\epsilon,0,1)} \right) \right. \\ & \quad \left. + \frac{1}{|\mathbf{p}_4|^2 \bar{z}(1-z)} \left(\frac{1}{3} \mathcal{I}_{(\epsilon,1,1)} - \mathcal{I}_{(0,1+\epsilon,1)} \right) - \mathcal{I}_{(1,1+\epsilon,1)} + \frac{1}{3} \mathcal{I}_{(1+\epsilon,1,1)} \right\} \\ & \quad \times \left[\mathbf{T}_{(++)}^2 + 3\mathbf{T}_{(+-)}^2 + C_A \mathbf{T}_{(++)} \right] \mathcal{M}_{ij \rightarrow i'gj'}^{\text{tree}}. \quad (7.79) \end{aligned}$$

The bubble integrals can be evaluated in terms of the general formula given in eq. (7.14), while the triangle integrals are given in terms of a generalization of eq. (7.17). For conciseness, let us define the color operator involved in the $\mathcal{R}g\mathcal{R}^3$ transition as follows:

$$\mathcal{C}_{\mathcal{R}g\mathcal{R}^3} \equiv \mathbf{T}_{(++)}^2 + 3\mathbf{T}_{(+-)}^2 + C_A \mathbf{T}_{(++)}, \quad (7.80)$$

Setting for simplicity $\mu^2 = |\mathbf{p}_4|^2$, after some elaboration we obtain

$$\mathcal{M}_{ij \rightarrow i'gj'} \Big|_{\mathcal{R}g\mathcal{R}^3}^{2\text{-loops}} = (i\pi)^2 \left(\frac{\alpha_s}{\pi} \right)^2 G_{\mathcal{R}g\mathcal{R}^3}^{(2)}(z, \bar{z}, |\mathbf{p}_4|^2, \mu^2) \mathcal{C}_{\mathcal{R}g\mathcal{R}^3} \mathcal{M}_{ij \rightarrow i'gj'}^{\text{tree}}, \quad (7.81)$$

where, setting $\mu^2 = |\mathbf{p}_4|^2$, we have

$$\begin{aligned} G_{\mathcal{R}g\mathcal{R}^3}^{(2)}(z, \bar{z}, |\mathbf{p}_4|^2, |\mathbf{p}_4|^2) & = \frac{1}{144} \left\{ \frac{1}{\epsilon^2} - \frac{2}{\epsilon} \log \left[\frac{z\bar{z}}{(1-z)^2(1-\bar{z})^2} \right] + 12 D_2(z, \bar{z}) - \zeta_2 \right. \\ & \quad \left. + 2 \log^2 [z\bar{z}] - \log^2 [(1-z)(1-\bar{z})] - 2 \log [z\bar{z}] \log [(1-z)(1-\bar{z})] + \mathcal{O}(\epsilon) \right\}. \quad (7.82) \end{aligned}$$

The color operator acting on the tree level can be evaluated explicitly, and following the notation of eq. (7.69) we have

$$\sum_j c^{[j]} \mathcal{C}_{\mathcal{R}g\mathcal{R}^3}^{[j][8,8]_a} (\mathcal{M}_{qq \rightarrow qqq}^{\text{tree}})^{[8,8]_a} = \left(\frac{N_c^2}{2} + 3 \right) c^{[8,8]_a} (\mathcal{M}_{qq \rightarrow qqq}^{\text{tree}})^{[8,8]_a}, \quad (7.83)$$

$$\sum_j c^{[j]} \mathcal{C}_{\mathcal{R}g\mathcal{R}^3}^{[j][8,8_a]a} (\mathcal{M}_{qq \rightarrow qgg}^{\text{tree}})^{[8,8_a]a} = \left[\left(\frac{N_c^2}{2} + 18 \right) c^{[8,8_a]a} - \frac{9\sqrt{N_c^2 - 4}}{\sqrt{2}} c^{[8,10+\overline{10}]} \right] (\mathcal{M}_{qq \rightarrow qgg}^{\text{tree}})^{[8,8_a]a}, \quad (7.84)$$

$$\sum_j c^{[j]} \mathcal{C}_{\mathcal{R}g\mathcal{R}^3}^{[j][8_a,8]a} (\mathcal{M}_{gq \rightarrow ggg}^{\text{tree}})^{[8_a,8]a} = \left(\frac{N_c^2}{2} + 3 \right) c^{[8_a,8]a} (\mathcal{M}_{gq \rightarrow ggg}^{\text{tree}})^{[8_a,8]a},$$

$$\sum_j c^{[j]} \mathcal{C}_{\mathcal{R}g\mathcal{R}^3}^{[j][8_a,8_a]} (\mathcal{M}_{gg \rightarrow ggg}^{\text{tree}})^{[8_a,8_a]} = \left[\left(\frac{N_c^2}{2} + 18 \right) c^{[8_a,8_a]} - \frac{9\sqrt{N_c^2 - 4}}{\sqrt{2}} c^{[8_a,10+\overline{10}]} \right] (\mathcal{M}_{gg \rightarrow ggg}^{\text{tree}})^{[8_a,8_a]}. \quad (7.85)$$

With the result in eq. (7.81) we immediately get the amplitude corresponding to the transition $\mathcal{R}^3 g \mathcal{R}$ by exploiting the target-projectile symmetry. Namely, starting from eq. (7.81) we replace $\mathbf{T}_{(+ -)} \rightarrow \mathbf{T}_{(- +)}$, as well as $z \rightarrow 1 - \bar{z}$, $\bar{z} \rightarrow 1 - z$ for the kinematic factors. Taking into account eq. (7.42) we get

$$\mathcal{M}_{ij \rightarrow i' g j'} \Big|_{\mathcal{R}^3 g \mathcal{R}}^{\text{2-loops}} = (i\pi)^2 \left(\frac{\alpha_s}{\pi} \right)^2 G_{\mathcal{R}^3 g \mathcal{R}}^{(2)}(z, \bar{z}, |\mathbf{p}_4|^2, \mu^2) \mathcal{C}_{\mathcal{R}^3 g \mathcal{R}} \mathcal{M}_{ij \rightarrow i' g j'}^{\text{tree}}, \quad (7.86)$$

where

$$G_{\mathcal{R}^3 g \mathcal{R}}^{(2)}(z, \bar{z}, |\mathbf{p}_4|^2, |\mathbf{p}_4|^2) = \frac{1}{144} \left\{ \frac{1}{\epsilon^2} - \frac{2}{\epsilon} \log \left[\frac{(1-z)(1-\bar{z})}{z^2 \bar{z}^2} \right] + 12 D_2(z, \bar{z}) - \zeta_2 - \log^2 [z\bar{z}] + 2 \log^2 [(1-z)(1-\bar{z})] - 2 \log [z\bar{z}] \log [(1-z)(1-\bar{z})] + \mathcal{O}(\epsilon) \right\}, \quad (7.87)$$

and the color operator reads

$$\mathcal{C}_{\mathcal{R}^3 g \mathcal{R}} \equiv \mathbf{T}_{(++)}^2 + 3\mathbf{T}_{(-+)}^2 + C_A \mathbf{T}_{(++)}. \quad (7.88)$$

Its action on the tree level amplitude explicitly gives

$$\sum_j c^{[j]} \mathcal{C}_{\mathcal{R}^3 g \mathcal{R}}^{[j][8,8]a} (\mathcal{M}_{qq \rightarrow qgg}^{\text{tree}})^{[8,8]a} = \left(\frac{N_c^2}{2} + 3 \right) c^{[8,8]a} (\mathcal{M}_{qq \rightarrow qgg}^{\text{tree}})^{[8,8]a}, \quad (7.89)$$

$$\sum_j c^{[j]} \mathcal{C}_{\mathcal{R}^3 g \mathcal{R}}^{[j][8_a,8]a} (\mathcal{M}_{gq \rightarrow ggg}^{\text{tree}})^{[8_a,8]a} = \left(\frac{N_c^2}{2} + 3 \right) c^{[8_a,8]a} (\mathcal{M}_{gq \rightarrow ggg}^{\text{tree}})^{[8_a,8]a}, \quad (7.90)$$

$$\sum_j c^{[j]} \mathcal{C}_{\mathcal{R}^3 g \mathcal{R}}^{[j][8_a,8_a]} (\mathcal{M}_{gg \rightarrow ggg}^{\text{tree}})^{[8_a,8_a]} = \left[\left(\frac{N_c^2}{2} + 18 \right) c^{[8_a,8_a]} - \frac{9\sqrt{N_c^2 - 4}}{\sqrt{2}} c^{[10+\overline{10},8]} \right] (\mathcal{M}_{gg \rightarrow ggg}^{\text{tree}})^{[8_a,8_a]}, \quad (7.91)$$

$$\sum_j c^{[j]} \mathcal{C}_{\mathcal{R}^3 g \mathcal{R}}^{[j][8_a,8_a]} (\mathcal{M}_{gg \rightarrow ggg}^{\text{tree}})^{[8_a,8_a]} = \left[\left(\frac{N_c^2}{2} + 18 \right) c^{[8_a,8_a]} + \frac{9\sqrt{N_c^2 - 4}}{\sqrt{2}} c^{[8_a,10+\overline{10}]} \right] (\mathcal{M}_{gg \rightarrow ggg}^{\text{tree}})^{[8_a,8_a]}. \quad (7.92)$$

The complete MR odd-odd amplitude at two loops. The complete multi-Reggeon contribution to the odd-odd amplitude is given by the sum of eqs. (7.67), (7.81) and (7.86):

$$\begin{aligned} \mathcal{M}_{ij \rightarrow i'gj'}^{(-,-)} \Big|_{\text{MR}}^{2\text{-loops}} &= (i\pi)^2 \left(\frac{\alpha_s}{\pi} \right)^2 \left\{ G_{\mathcal{R}^3 g \mathcal{R}^3}^{(2)}(z, \bar{z}, |\mathbf{p}_4|^2, \mu^2) \mathcal{C}_{\mathcal{R}^3 g \mathcal{R}^3} \right. \\ &\quad \left. + G_{\mathcal{R} g \mathcal{R}^3}^{(2)}(z, \bar{z}, |\mathbf{p}_4|^2, \mu^2) \mathcal{C}_{\mathcal{R} g \mathcal{R}^3} + G_{\mathcal{R}^3 g \mathcal{R}}^{(2)}(z, \bar{z}, |\mathbf{p}_4|^2, \mu^2) \mathcal{C}_{\mathcal{R}^3 g \mathcal{R}} \right\} \mathcal{M}_{ij \rightarrow igj}^{\text{tree}}, \end{aligned} \quad (7.93)$$

where the functions $G_i^{(2)}$ are given in eqs. (7.68), (7.82) and (7.87), and the color operators are listed in eqs. (7.66), (7.80) and (7.88).

For later convenience, let us provide the octet-octet component of eq. (7.93), i.e. the coefficient of $c^{[8,8]_a}$, $c^{[8,8a]_a}$ and $c^{[8a,8a]}$, respectively for $qq \rightarrow qgq$, $qq \rightarrow qgg$ and $gg \rightarrow ggg$ scattering, which can be obtained using eqs. (7.69), (7.83) and (7.89). We obtain

$$\begin{aligned} \mathcal{M}_{qq \rightarrow qgq}^{[8,8]_a} \Big|_{\text{MR}}^{2\text{-loops}} &= \frac{(i\pi)^2}{72} \left(\frac{\alpha_s}{\pi} \right)^2 \left[N_c^2 F_{\text{fact}}^{(2)}(z, \bar{z}, |\mathbf{p}_4|^2, \mu^2) \right. \\ &\quad \left. + F_{\text{non fact}}^{qq(2)}(z, \bar{z}, |\mathbf{p}_4|^2, \mu^2) \right] \mathcal{M}_{qq \rightarrow qgq}^{\text{tree}}, \end{aligned} \quad (7.94)$$

$$\begin{aligned} \mathcal{M}_{qq \rightarrow qgg}^{[8,8a]_a} \Big|_{\text{MR}}^{2\text{-loops}} &= \frac{(i\pi)^2}{72} \left(\frac{\alpha_s}{\pi} \right)^2 \left[N_c^2 F_{\text{fact}}^{(2)}(z, \bar{z}, |\mathbf{p}_4|^2, \mu^2) \right. \\ &\quad \left. + F_{\text{non fact}}^{qq(2)}(z, \bar{z}, |\mathbf{p}_4|^2, \mu^2) \right] \mathcal{M}_{qq \rightarrow qgg}^{\text{tree}}, \end{aligned} \quad (7.95)$$

$$\mathcal{M}_{gg \rightarrow ggg}^{[8a,8a]} \Big|_{\text{MR}}^{2\text{-loops}} = \frac{(i\pi)^2}{72} \left(\frac{\alpha_s}{\pi} \right)^2 (N_c^2 + 36) F_{\text{fact}}^{(2)}(z, \bar{z}, |\mathbf{p}_4|^2, \mu^2) \mathcal{M}_{gg \rightarrow ggg}^{\text{tree}}, \quad (7.96)$$

where

$$\begin{aligned} F_{\text{fact}}^{(2)}(z, \bar{z}, |\mathbf{p}_4|^2, |\mathbf{p}_4|^2) &= \frac{1}{\epsilon^2} - \frac{1}{2\epsilon} \log [z\bar{z}(1-z)(1-\bar{z})] + 3 D_2(z, \bar{z}) - \zeta_2 \\ &\quad + \frac{5}{4} \log^2 [z\bar{z}] + \frac{5}{4} \log^2 [(1-z)(1-\bar{z})] - \frac{1}{2} \log [z\bar{z}] \log [(1-z)(1-\bar{z})] + \mathcal{O}(\epsilon), \end{aligned} \quad (7.97)$$

and

$$\begin{aligned} F_{\text{non fact}}^{qq(2)}(z, \bar{z}, |\mathbf{p}_4|^2, |\mathbf{p}_4|^2) &= \frac{9}{\epsilon} \log [z\bar{z}(1-z)(1-\bar{z})] + 54 D_2(z, \bar{z}) \\ &\quad - \frac{9}{2} \log^2 [z\bar{z}(1-z)(1-\bar{z})] + \frac{9}{N_c^2} \left\{ \frac{1}{\epsilon^2} - \frac{2}{\epsilon} \log [z\bar{z}(1-z)(1-\bar{z})] - 6 D_2(z, \bar{z}) \right. \\ &\quad \left. + 2 \log^2 [z\bar{z}] + 2 \log^2 [(1-z)(1-\bar{z})] + \log [z\bar{z}] \log [(1-z)(1-\bar{z})] - \zeta_2 \right\} + \mathcal{O}(\epsilon), \end{aligned} \quad (7.98)$$

$$\begin{aligned} F_{\text{non fact}}^{qq(2)}(z, \bar{z}, |\mathbf{p}_4|^2, |\mathbf{p}_4|^2) &= \frac{27}{2\epsilon^2} - \frac{9}{\epsilon} \left(2 \log [z\bar{z}] - 3 \log [(1-z)(1-\bar{z})] \right) + 108 D_2(z, \bar{z}) \\ &\quad + \frac{45}{2} \log^2 [z\bar{z}] - 18 \log [z\bar{z}] \log [(1-z)(1-\bar{z})] - \frac{27}{2} \zeta_2 + \mathcal{O}(\epsilon). \end{aligned} \quad (7.99)$$

Given that no other color component is leading in color, as can be seen by inspecting eqs. (7.69), (7.83) and (7.89), we immediately deduce that the leading color planar limit is

universal, i.e. it does not depend on the representation of the scattered particles, and it is proportional to the function $F_{\text{fact}}^{(2)}$:

$$\mathcal{M}_{ij \rightarrow i'gj'}^{[8_a, 8_a]} \Big|_{\text{MR, planar}}^{2\text{-loops}} = (i\pi)^2 \left(\frac{\alpha_s}{\pi}\right)^2 \frac{N_c^2}{72} F_{\text{fact}}^{(2)}(z, \bar{z}, |\mathbf{p}_4|^2, \mu^2) \mathcal{M}_{ij \rightarrow igj}^{\text{tree}}. \quad (7.100)$$

This property will be important for extracting the two-loop vertex in the next section.

8 The QCD Lipatov vertex at two loops

8.1 Extracting the Reggeon-gluon-Reggeon vertex

As described in section 6, within the theory of multi-Reggeon interactions we express the amplitude as a sum over multi-Reggeon exchanges in the t_i channels

$$\mathcal{M}_{ij \rightarrow i'gj'} = \mathcal{M}_{ij \rightarrow i'gj'}^{\text{SR}} + \mathcal{M}_{ij \rightarrow i'gj'}^{\text{MR}}, \quad (8.1)$$

where we split the pure single-Reggeon (SR) exchange (involving a single W field through-out) from all other contributions involving multi-Reggeon (MR) exchange (i.e. multiple W fields). In particular, the SR component factorizes according to eq. (6.41), namely, one has

$$\mathcal{M}_{ij \rightarrow i'gj'}^{(-,-)\text{SR}} = c_i^{\text{SR}}(t_1, \tau) e^{C_A \alpha_g^{\text{SR}}(t_1) \eta_1} v^{\text{SR}}(t_1, t_2, |\mathbf{p}_4|^2, \tau) e^{C_A \alpha_g^{\text{SR}}(t_2) \eta_2} c_j^{\text{SR}}(t_2, \tau) \mathcal{M}_{ij \rightarrow i'gj'}^{\text{tree}}, \quad (8.2)$$

where $v^{\text{SR}}(t_1, t_2, |\mathbf{p}_4|^2, \tau)$ defines the perturbative corrections to the Reggeon-gluon-Reggeon ($\mathcal{R}g\mathcal{R}$) vertex within the so-called SR/MR scheme. With the perturbative corrections to the impact factors $c_i^{\text{SR}}(t_1, \tau)$, $c_j^{\text{SR}}(t_2, \tau)$ and Regge Trajectory $\alpha_g^{\text{SR}}(t_i)$ extracted from $2 \rightarrow 2$ parton scattering [23, 24], the calculation of $\mathcal{M}_{ij \rightarrow i'gj'}$ on the l.h.s. of eq. (8.1) to two loops, as discussed in section 3, allows one to extract $v^{\text{SR}}(t_1, t_2, |\mathbf{p}_4|^2, \tau)$ to the same loop accuracy.

While from a calculation perspective the separation of the amplitude according to (8.1) is convenient, physically, the amplitude $\mathcal{M}_{ij \rightarrow i'gj'}$ is expected to feature both a Regge pole and a Regge cut, with different factorization and exponentiation properties. Hence a separation into the pole and cut components is desirable [18, 22, 23, 27, 34, 36, 37, 117–120].

The pole and cut components of the amplitude do not immediately correspond to the single- and multi-Reggeon transitions. Furthermore, given that the high-energy analytic properties are only manifest upon resumming the perturbative series, it is a priori not obvious how to disentangle the Regge pole from the Regge cut in a fixed-order computation. Addressing this issue, a criterion has been proposed in [23, 24], building upon the fact that four and five point amplitudes are expected to have only a Regge pole in the large- N_c (planar) limit [1, 121]. The fact that MR exchanges are present in the planar limit is well known [18, 54, 122–126]. From this it follows [23, 24] that, while the Regge cut arises in $2 \rightarrow 2$ and $2 \rightarrow 3$ amplitudes exclusively from MR exchanges, planar MR exchanges contribute instead (only) to the Regge pole, along with the SR exchange. In turn, the Regge cut is associated exclusively to the non-planar¹² MR exchanges.

¹²An interesting precursor of this is the observation, due to Mandelstam [1, 127], analysing the high-energy asymptotic behaviour of individual scalar Feynman integrals, is that Regge cuts are present only in (particular) non-planar ones.

In $2 \rightarrow 2$ scattering amplitudes, this criterion has been shown [23, 24] to be consistent order by order in perturbation theory, to four loops. This consistency is tested by two properties:

1. The planar MR contributions are universal, i.e. they are the same in the three partonic processes, gg , qg and qq scattering, hence they cannot violate Regge-pole factorization. This stands in sharp contrast to the non-planar MR contributions, which do differ between partonic channels and violate factorization.
2. The planar MR contributions in $2 \rightarrow 2$ scattering vanishes identically at four loops, and conjecturally beyond (any non-vanishing contribution would invalidate the factorization structure at NNLL, since all parameters at this logarithmic accuracy are fixed at 3 loops).

We can now further test and then immediately use the same criterion to disentangle the Regge pole and cut in the $2 \rightarrow 3$ scattering amplitudes. The test has already been presented in the previous section, namely, the universality of the planar MR contributions in the three $2 \rightarrow 3$ scattering processes – see eq. (7.100) above. This universality is essential for the planar MR contributions to factorize together with the single Reggeon, as will be clear from what follows.

Applying the criterion of [23, 24] to $2 \rightarrow 3$ scattering, the pole part should be separated from the cut as follows:

$$\begin{aligned} \mathcal{M}_{ij \rightarrow i'gj'}^{(-,-)} &= \underbrace{\mathcal{M}_{ij \rightarrow i'gj'}^{(-,-)\text{SR}} + \mathcal{M}_{ij \rightarrow i'gj'}^{(-,-)\text{MR}} \Big|_{\text{planar}}}_{\mathcal{M}_{ij \rightarrow i'gj'}^{(-,-)\text{pole}}} + \mathcal{M}_{ij \rightarrow i'gj'}^{(-,-)\text{MR}} \Big|_{\text{nonplanar}} \\ &= \mathcal{M}_{ij \rightarrow i'gj'}^{(-,-)\text{pole}} + \mathcal{M}_{ij \rightarrow i'gj'}^{\text{cut}}, \end{aligned} \quad (8.3)$$

where, crucially, $\mathcal{M}_{ij \rightarrow i'gj'}^{(-,-)\text{pole}}$ has formally the same factorization structure of $\mathcal{M}_{ij \rightarrow i'gj'}^{(-,-)\text{SR}}$ in eq. (8.2), i.e.:

$$\mathcal{M}_{ij \rightarrow i'gj'}^{(-,-)\text{pole}} = c_i(t_1, \tau) e^{C_A \alpha_g(t_1) \eta_1} v(t_1, t_2, |\mathbf{p}_4|^2, \tau) e^{C_A \alpha_g(t_2) \eta_2} c_j(t_2, \tau) \mathcal{M}_{ij \rightarrow i'gj'}^{\text{tree}}, \quad (8.4)$$

where $c_i(t_1, \tau)$, $c_j(t_2, \tau)$, $\alpha_g(t_k)$ and $v(t_1, t_2, |\mathbf{p}_4|^2, \tau)$ represent respectively the impact factors, the Regge trajectory and the Reggeon-gluon-Reggeon Lipatov vertex in the *pole/cut scheme*.

The relation between the two schemes for the Regge trajectory and the impact factors has been determined from $2 \rightarrow 2$ scattering up to NNLL accuracy in [23, 24]: one has

$$\begin{aligned} c_{i/j}^{(1)} &= c_{i/j}^{\text{SR}(1)}, \\ c_{i/j}^{(2)} &= c_{i/j}^{\text{SR}(2)} + \frac{\pi^2}{12} N_c^2 (r_\Gamma(\epsilon))^2 S^{(2)}(\epsilon), \end{aligned} \quad (8.5)$$

where $r_\Gamma(\epsilon)$ is given in (4.3) and

$$S^{(2)}(\epsilon) = -\frac{1}{8\epsilon^2} + \frac{3}{4}\epsilon\zeta_3 + \frac{9}{8}\epsilon^2\zeta_4 + \mathcal{O}(\epsilon^3). \quad (8.6)$$

For the Regge trajectory we have

$$\begin{aligned}
\alpha_g^{(1)} &= \alpha_g^{\text{SR}(1)}, \\
\alpha_g^{(2)} &= \alpha_g^{\text{SR}(2)}, \\
\alpha_g^{(3)} &= \alpha_g^{\text{SR}(3)} - (r_\Gamma(\epsilon))^3 N_c^2 \frac{\pi^2}{18} \left(S_A^{(3)}(\epsilon) - S_B^{(3)}(\epsilon) \right),
\end{aligned} \tag{8.7}$$

where

$$\begin{aligned}
S_A^{(3)}(\epsilon) &= \frac{1}{48\epsilon^3} + \frac{37}{24}\zeta_3 + \frac{37}{16}\epsilon\zeta_4 + \mathcal{O}(\epsilon^2), \\
S_B^{(3)}(\epsilon) &= \frac{1}{24\epsilon^3} + \frac{1}{12}\zeta_3 + \frac{1}{8}\epsilon\zeta_4 + \mathcal{O}(\epsilon^2).
\end{aligned} \tag{8.8}$$

Taking into account these results, first of all we are able to determine the relation between the Lipatov vertex in the SR/MR and in the pole/cut scheme; then, using the explicit calculation of the two-loop $2 \rightarrow 3$ amplitudes together with the results for the MR contribution to the odd-odd $[8, 8]$ amplitude in section 7.3, we will determine the Lipatov vertex explicitly. We will present the result for the two-loop vertex and discuss the structure in section 8.2.

Let us start here by determining the relation between $v^{\text{SR}}(t_1, t_2, |\mathbf{p}_4|^2, \tau)$ in the SR/MR scheme and $v(t_1, t_2, |\mathbf{p}_4|^2, \tau)$ in the pole/cut scheme. Expanding eqs. (8.3), (8.2) and (8.4) to second order in the coupling constant, and restricting to the NNLL terms, the matching equations read

$$\begin{aligned}
&\mathcal{M}_{ij \rightarrow i'gj'}^{[8_a, 8_a]} \Big|_{2\text{-loops}}^{\text{NNLL}} - \mathcal{M}_{ij \rightarrow i'gj'}^{[8_a, 8_a]} \Big|_{2\text{-loops}}^{\text{MR}} \Big|_{2\text{-loops}}^{\text{NNLL}} \\
&= \left(\frac{\alpha_s}{\pi} \right)^2 \left[c_i^{\text{SR}(2)} + c_j^{\text{SR}(2)} + c_i^{\text{SR}(1)} c_j^{\text{SR}(1)} \right. \\
&\quad \left. + \left(c_i^{\text{SR}(1)} + c_j^{\text{SR}(1)} \right) v^{\text{SR}(1)} + v^{\text{SR}(2)} \right] \mathcal{M}_{ij \rightarrow i'gj'}^{[8_a, 8_a]} \Big|_{\text{tree}},
\end{aligned} \tag{8.9}$$

to extract the Lipatov vertex in the SR/MR scheme, and

$$\begin{aligned}
&\mathcal{M}_{ij \rightarrow i'gj'}^{[8_a, 8_a]} \Big|_{2\text{-loops}}^{\text{NNLL}} - \mathcal{M}_{ij \rightarrow i'gj'}^{[8_a, 8_a]} \Big|_{2\text{-loops}}^{\text{cut}} \Big|_{2\text{-loops}}^{\text{NNLL}} \\
&= \left(\frac{\alpha_s}{\pi} \right)^2 \left[c_i^{(2)} + c_j^{(2)} + c_i^{(1)} c_j^{(1)} + \left(c_i^{(1)} + c_j^{(1)} \right) v^{(1)} + v^{(2)} \right] \mathcal{M}_{ij \rightarrow i'gj'}^{[8_a, 8_a]} \Big|_{\text{tree}},
\end{aligned} \tag{8.10}$$

in the pole/cut scheme. All functions on the r.h.s. of eqs. (8.9) and (8.10) are known, except for $v^{\text{SR}(2)}$ and $v^{(2)}$. More in detail, $\mathcal{M}_{ij \rightarrow i'gj'}^{[8_a, 8_a]} \Big|_{2\text{-loops}}^{\text{MR}} \Big|_{2\text{-loops}}^{\text{NNLL}}$ in eq. (8.9) has been given for all cases $qq \rightarrow qgq$, $qg \rightarrow qgg$, and $gg \rightarrow ggg$ in eq. (7.94), while $\mathcal{M}_{ij \rightarrow i'gj'}^{[8_a, 8_a]} \Big|_{2\text{-loops}}^{\text{cut}} \Big|_{2\text{-loops}}^{\text{NNLL}}$ in eq. (8.10) can be easily determined according to eq. (8.3), namely one has

$$\mathcal{M}_{ij \rightarrow i'gj'}^{[8_a, 8_a]} \Big|_{2\text{-loops}}^{\text{cut}} = \mathcal{M}_{ij \rightarrow i'gj'}^{[8_a, 8_a]} \Big|_{2\text{-loops}}^{\text{MR}} - \mathcal{M}_{ij \rightarrow i'gj'}^{[8_a, 8_a]} \Big|_{2\text{-loops}}^{\text{planar}}, \tag{8.11}$$

where $\mathcal{M}_{ij \rightarrow i'gj'}^{[8_a, 8_a]} \Big|_{2\text{-loops}}^{\text{planar}}$ has been given in eq. (7.100). Exploiting this information, it is easy to realize that the relation between the Lipatov vertex in the two schemes is independent

on the exact form of the two loop amplitude: it relies solely on $\mathcal{M}_{ij \rightarrow i'gj'}^{[8_a, 8_a] \text{MR}}|_{2\text{-loops}}^{\text{planar}}$ and the relation between the impact factors in the two schemes: by taking the difference of eq. (8.9) with eq. (8.10), taking into account the fact that $v^{\text{SR}(1)} = v^{(1)}$, as well as eq. (8.5), we have

$$\mathcal{M}_{ij \rightarrow i'gj'}^{[8_a, 8_a] \text{MR}}|_{2\text{-loops}}^{\text{planar}} = \left(\frac{\alpha_s}{\pi}\right)^2 \left[v^{\text{SR}(2)} - v^{(2)} - \frac{\pi^2}{6} N_c^2 r_\Gamma^2 S^{(2)}(\epsilon) \right] \mathcal{M}_{ij \rightarrow i'gj'}^{[8_a, 8_a]}|_{\text{tree}}, \quad (8.12)$$

and upon using eq. (7.100) we get

$$\begin{aligned} v^{(2)} &= v^{\text{SR}(2)} + \pi^2 N_c^2 \left(\frac{F_{\text{fact}}^{(2)}(z, \bar{z}, |\mathbf{P}_4|^2, \mu^2)}{72} - \frac{r_\Gamma^2 S^{(2)}(\epsilon)}{6} \right) \\ &= v^{\text{SR}(2)} + \frac{\pi^2 N_c^2}{144} \left\{ \frac{5}{\epsilon^2} - \frac{1}{\epsilon} \log [z\bar{z}(1-z)(1-\bar{z})] + 6D_2(z, \bar{z}) - 2\zeta_2 + \frac{5}{2} \log^2 [z\bar{z}] \right. \\ &\quad \left. + \frac{5}{2} \log^2 [(1-z)(1-\bar{z})] - \log [z\bar{z}] \log [(1-z)(1-\bar{z})] + \mathcal{O}(\epsilon) \right\}. \end{aligned} \quad (8.13)$$

Let us stress that the relations in eqs. (8.5), (8.7) and (8.13) completely fix the factorization structure up to NNLL. That is, given the three-loop information from $2 \rightarrow 2$ scattering, and the two-loop information determined here for $2 \rightarrow 3$ scattering (i.e. the two-loop lipatov vertex) at this logarithmic accuracy the theory (i.e. the exponentiation of rapidity logarithms associated with the pole) becomes predictive for $2 \rightarrow 3$ scattering at three loops and beyond. To see this, let us consider the NNLL three-loops contributions to the amplitude. In the SR/MR scheme one has

$$\begin{aligned} \mathcal{M}_{ij \rightarrow i'gj'}^{[8_a, 8_a]}|_{3\text{-loops}}^{\text{NNLL}} &= \left(\frac{\alpha_s}{\pi}\right)^3 \sum_{k=1}^2 \left\{ \eta_k C_A \left[\alpha_g^{\text{SR}(1)}(t_k) \left(v^{\text{SR}(2)} + v^{\text{SR}(1)} \left(c_i^{\text{SR}(1)} + c_j^{\text{SR}(1)} \right) \right. \right. \right. \\ &\quad \left. \left. + c_i^{\text{SR}(1)} c_j^{\text{SR}(1)} + c_i^{\text{SR}(2)} + c_j^{\text{SR}(2)} \right) + \alpha_g^{\text{SR}(2)}(t_k) \left(v^{\text{SR}(1)} + c_i^{\text{SR}(1)} + c_j^{\text{SR}(1)} \right) \right. \right. \\ &\quad \left. \left. + \alpha_g^{\text{SR}(3)}(t_k) \right] \right\} \mathcal{M}_{ij \rightarrow i'gj'}^{[8_a, 8_a]}|_{\text{tree}} + \mathcal{M}_{ij \rightarrow i'gj'}^{[8_a, 8_a] \text{MR}}|_{3\text{-loops}}^{\text{NNLL}}, \end{aligned} \quad (8.14)$$

while in the pole/cut scheme one has

$$\begin{aligned} \mathcal{M}_{ij \rightarrow i'gj'}^{[8_a, 8_a]}|_{3\text{-loops}}^{\text{NNLL}} &= \left(\frac{\alpha_s}{\pi}\right)^3 \sum_{k=1}^2 \left\{ \eta_k C_A \left[\alpha_g^{(1)}(t_k) \left(v^{(2)} + v^{(1)} \left(c_i^{(1)} + c_j^{(1)} \right) \right. \right. \right. \\ &\quad \left. \left. + c_i^{(1)} c_j^{(1)} + c_i^{(2)} + c_j^{(2)} \right) + \alpha_g^{(2)}(t_k) \left(v^{(1)} + c_i^{(1)} + c_j^{(1)} \right) \right. \\ &\quad \left. \left. + \alpha_g^{(3)}(t_k) \right] \right\} \mathcal{M}_{ij \rightarrow i'gj'}^{[8_a, 8_a]}|_{\text{tree}} + \mathcal{M}_{ij \rightarrow i'gj'}^{[8_a, 8_a] \text{cut}}|_{3\text{-loops}}^{\text{NNLL}}. \end{aligned} \quad (8.15)$$

Comparing eq. (8.14) with eq. (8.15), we deduce the following: first of all, all terms in the pole component of eq. (8.15), namely $\alpha_g^{(1)}$, $\alpha_g^{(2)}$, $c_{i/j}^{(1)}$, $c_{i/j}^{(2)}$, $v^{(1)}$ and $v^{(2)}$ have been determined from previous loop orders, therefore, there is no room for a further redefinitions of these coefficients. Given that the amplitude in eqs. (8.14) and (8.15) are the same, equating them gives

$$\mathcal{M}_{ij \rightarrow i'gj'}^{[8_a, 8_a] \text{MR}}|_{3\text{-loops}}^{\text{NNLL}} = \left(\frac{\alpha_s}{\pi}\right)^3 N_c \left\{ \left[\eta_1 \alpha_g^{(1)}(t_1) + \eta_2 \alpha_g^{(1)}(t_2) \right] \right\}$$

$$\begin{aligned}
& \times \left[\left(v^{(2)} - v^{\text{SR}(2)} \right) + \left(c_i^{(2)} + c_j^{(2)} - c_i^{\text{SR}(2)} - c_j^{\text{SR}(2)} \right) \right] \\
& + \eta_1 \left(\alpha_g^{(3)}(t_1) - \alpha_g^{\text{SR}(3)}(t_1) \right) + \eta_2 \left(\alpha_g^{(3)}(t_2) - \alpha_g^{\text{SR}(3)}(t_2) \right) \Big\} \mathcal{M}_{ij \rightarrow i'gj'}^{[8_a, 8_a]} \Big|_{\text{tree}} \\
& + \mathcal{M}_{ij \rightarrow i'gj'}^{[8_a, 8_a] \text{cut}} \Big|_{3\text{-loops}}^{\text{NNLL}}. \tag{8.16}
\end{aligned}$$

Expressing $c_{i/j}^{(2)}$ and $v^{(2)}$ in terms of $c_{i/j}^{\text{SR}(2)}$ and $v^{\text{SR}(2)}$ as given in eqs. (8.5) and (8.13), we have

$$\begin{aligned}
\mathcal{M}_{ij \rightarrow i'gj'}^{[8_a, 8_a] \text{MR}} \Big|_{3\text{-loops}}^{\text{NNLL}} &= \left(\frac{\alpha_s}{\pi} \right)^3 \frac{\pi^2 N_c^3}{18} \left\{ \left[\eta_1 \alpha_g^{(1)}(t_1) + \eta_2 \alpha_g^{(1)}(t_2) \right] \frac{1}{4} F_{\text{fact}}^{(2)}(z, \bar{z}, |\mathbf{p}_4|^2, \mu^2) \right. \\
& \left. - (\eta_1 + \eta_2) (r_\Gamma)^3 \left(S_A^{(3)}(\epsilon) - S_B^{(3)}(\epsilon) \right) \right\} \mathcal{M}_{ij \rightarrow i'gj'}^{[8_a, 8_a]} \Big|_{\text{tree}} + \mathcal{M}_{ij \rightarrow i'gj'}^{[8_a, 8_a] \text{cut}} \Big|_{3\text{-loops}}^{\text{NNLL}}, \tag{8.17}
\end{aligned}$$

and recalling that, by definition,

$$\mathcal{M}_{ij \rightarrow i'gj'}^{[8_a, 8_a] \text{cut}} \Big|_{3\text{-loops}} = \mathcal{M}_{ij \rightarrow i'gj'}^{[8_a, 8_a] \text{MR}} \Big|_{3\text{-loops}} - \mathcal{M}_{ij \rightarrow i'gj'}^{[8_a, 8_a] \text{MR}} \Big|_{3\text{-loops}}^{\text{planar}}, \tag{8.18}$$

we finally obtain

$$\begin{aligned}
\mathcal{M}_{ij \rightarrow i'gj'}^{[8_a, 8_a] \text{MR}} \Big|_{3\text{-loops}}^{\text{planar}} &= \left(\frac{\alpha_s}{\pi} \right)^3 \frac{\pi^2 N_c^3}{18} \left\{ \left[\eta_1 \alpha_g^{(1)}(t_1) + \eta_2 \alpha_g^{(1)}(t_2) \right] \frac{1}{4} F_{\text{fact}}^{(2)}(z, \bar{z}, |\mathbf{p}_4|^2, \mu^2) \right. \\
& \left. - (\eta_1 + \eta_2) (r_\Gamma)^3 \left(S_A^{(3)}(\epsilon) - S_B^{(3)}(\epsilon) \right) \right\} \mathcal{M}_{ij \rightarrow i'gj'}^{[8_a, 8_a]} \Big|_{\text{tree}}, \tag{8.19}
\end{aligned}$$

i.e., we obtain a prediction for the three loop planar MR amplitude at NNLL, which, if verified, would in turn provide further evidence for the conjecture in eq. (8.3), besides the equivalent check already satisfied in case of the four loop $2 \rightarrow 2$ scattering amplitude, see [23, 24].

This observation completes our discussion concerning the extraction of the Lipatov vertex at two loops. One uses eq. (8.9), with $\mathcal{M}_{ij \rightarrow i'gj'}^{[8_a, 8_a] \text{MR}} \Big|_{2\text{-loops}}^{\text{NNLL}}$ calculated as in section 7.3, and $\mathcal{M}_{ij \rightarrow i'gj'}^{[8_a, 8_a]} \Big|_{2\text{-loops}}^{\text{NNLL}}$ as discussed in section 3, to obtain $v^{\text{SR}(2)}$. Subsequently, $v^{(2)}$ is obtained by simply resorting to eq. (8.13). In the next section we are going to discuss the structure and analytic properties of the Lipatov vertex in the pole/cut scheme, i.e. $v^{(2)}$.

8.2 Vertex structure through two loop

The sYM vertex constitutes the (pure, maximal weight) weight-4 component of the QCD vertex. We have already provided the full expression for $v_{\text{sYM}}^{(1)} = v_{\text{reg}}^{(1)}$ in section 5, see eqs. (5.19a) and (5.19b) there. The result was expressed in terms of the single-valued GPL functions \mathcal{G} (see eq. (5.7) above). The ancillary file [70] `svRL.m` provide a replacement list of these functions in terms of combinations of ordinary (multi-valued) GPLs of z and \bar{z} , which can be evaluated using the GiNaC library [110] via PolyLogTools [79]. Alternatively, one may use the replacement list `svpdRL.m` to obtain GPLs that are fibrated in terms of the variables p and q where

$$p = 1 - z - \bar{z}, \quad q = z - \bar{z}. \tag{8.20}$$

The latter set of variables is convenient to express the results and understand their symmetry properties under $z \rightarrow 1 - \bar{z}$, which corresponds to $p \rightarrow -p$ (with fixed q), and $z \rightarrow \bar{z}$, which corresponds to $q \rightarrow -q$ (with fixed p).

Here we proceed to provide a similar expressions for the two-loop vertex in sYM. The results in QCD will be presented in the following subsections.

$$\begin{aligned}
v_{\text{sYM}}^{(2)}(t_1, t_2, |p_4|^2) &= v_{\text{sYM}}^{(2)}(z, \bar{z}) = \text{Disp} \left\{ v_{\text{sYM}}^{(2)}(z, \bar{z}) \right\} + i \text{Absorp} \left\{ v_{\text{sYM}}^{(2)}(z, \bar{z}) \right\} \\
&\equiv v_{\text{sYM, Disp}}^{(2)}(z, \bar{z}) + i\pi v_{\text{sYM, Absorp}}^{(2)}(z, \bar{z})
\end{aligned} \tag{8.21}$$

Note that in the second line we extracted a power of π from the absorptive part of the vertex, which always appears together with the explicit factor of i . This implies in particular that $v_{\text{sYM, Absorp}}^{(2)}$ is of weight 3, in contrast to $v_{\text{sYM, Disp}}^{(2)}(z, \bar{z})$, which is of weight 4.

$$\begin{aligned}
v_{\text{sYM, Absorp}}^{(2)} &= \frac{N_c^2}{32\epsilon^3} + \frac{N_c^2}{\epsilon} \left(\frac{1}{32} \mathcal{G}(0, 0, z) - \frac{1}{16} \mathcal{G}(0, 1, z) + \frac{1}{32} \mathcal{G}(1, 1, z) - \frac{\pi^2}{96} \right) \\
&+ \frac{N_c^2}{16} \left(\mathcal{G}(0, 1 - \bar{z}, 0, z) - \mathcal{G}(0, 1 - \bar{z}, 1, z) - \mathcal{G}(\bar{z}, 0, 1, z) + \mathcal{G}(\bar{z}, 1, 0, z) \right) \\
&- \frac{\pi^2}{12} \mathcal{G}(0, z) - \frac{\pi^2}{12} \mathcal{G}(1, z) - \mathcal{G}(0, 0, 0, z) + \mathcal{G}(0, 0, 1, z) \\
&- \mathcal{G}(0, 1, 0, z) + \mathcal{G}(0, 1, 1, z) + \mathcal{G}(1, 0, 1, z) - \mathcal{G}(1, 1, 1, z) - \frac{17\zeta(3)}{6}
\end{aligned} \tag{8.22}$$

$$\begin{aligned}
v_{\text{sYM, Disp}}^{(2)} &= \frac{N_c^2}{32\epsilon^4} + \frac{N_c^2}{48\epsilon^2} (3\mathcal{G}(0,0,z) - 3\mathcal{G}(0,1,z) - 3\mathcal{G}(1,0,z) + 3\mathcal{G}(1,1,z) - \pi^2) \\
&+ \frac{N_c^2}{192\epsilon} (24\mathcal{G}(0,1-\bar{z},0,z) - 24\mathcal{G}(0,1-\bar{z},1,z) - 5\pi^2\mathcal{G}(0,z) - 5\pi^2\mathcal{G}(1,z) \\
&- 24\mathcal{G}(0,0,0,z) + 12\mathcal{G}(0,0,1,z) - 12\mathcal{G}(0,1,0,z) + 12\mathcal{G}(0,1,1,z) \\
&+ 12\mathcal{G}(1,0,0,z) + 12\mathcal{G}(1,0,1,z) + 12\mathcal{G}(1,1,0,z) - 24\mathcal{G}(1,1,1,z) - 46\zeta(3)) \\
&+ \frac{N_c^2}{11520} (-480\pi^2\mathcal{G}(\bar{z},1,z) - 1440\mathcal{G}(0,0,1-\bar{z},0,z) \\
&+ 1440\mathcal{G}(0,0,1-\bar{z},1,z) - 1440\mathcal{G}(0,1,1-\bar{z},0,z) + 1440\mathcal{G}(0,1,1-\bar{z},1,z) \\
&- 1440\mathcal{G}(0,1-\bar{z},0,0,z) + 1440\mathcal{G}(0,1-\bar{z},1,1,z) - 1440\mathcal{G}(1,0,1-\bar{z},0,z) \\
&+ 1440\mathcal{G}(1,0,1-\bar{z},1,z) - 1440\mathcal{G}(\bar{z},0,1,0,z) + 1440\mathcal{G}(\bar{z},0,1-\bar{z},0,z) \\
&- 1440\mathcal{G}(\bar{z},0,1-\bar{z},1,z) + 1440\mathcal{G}(\bar{z},1,0,1,z) + 1440\mathcal{G}(\bar{z},1,1-\bar{z},0,z) \\
&- 1440\mathcal{G}(\bar{z},1,1-\bar{z},1,z) + 720\zeta(3)\mathcal{G}(0,z) + 720\zeta(3)\mathcal{G}(1,z) + 1140\pi^2\mathcal{G}(0,1,z) \\
&- 60\pi^2\mathcal{G}(1,0,z) + 4320\mathcal{G}(0,0,0,0,z) - 2880\mathcal{G}(0,0,0,1,z) - 1440\mathcal{G}(0,0,1,0,z) \\
&+ 1440\mathcal{G}(0,0,1,1,z) - 1440\mathcal{G}(0,1,0,0,z) + 1440\mathcal{G}(0,1,0,1,z) \\
&+ 2880\mathcal{G}(0,1,1,0,z) - 2880\mathcal{G}(0,1,1,1,z) - 2880\mathcal{G}(1,0,0,0,z) \\
&+ 1440\mathcal{G}(1,0,0,1,z) + 2880\mathcal{G}(1,0,1,0,z) - 2880\mathcal{G}(1,0,1,1,z) \\
&+ 1440\mathcal{G}(1,1,0,0,z) - 2880\mathcal{G}(1,1,0,1,z) - 2880\mathcal{G}(1,1,1,0,z) \\
&+ 4320\mathcal{G}(1,1,1,1,z) - 53\pi^4)
\end{aligned} \tag{8.23}$$

We note that the symbol alphabet of the sYM two-loop vertex consists of 6 letters, $\{z, \bar{z}, 1-z, 1-\bar{z}, z-\bar{z}, 1-z-\bar{z}\}$ and is identical to the one found at one loop, eq. (5.6). We comment that the letters $z-\bar{z}$ and $1-z-\bar{z}$ appear at two loops already at the level of the $1/\epsilon$ singularities.

8.2.1 Basis of transcendental functions

Here we present a basis for the *additional* transcendental functions of weight 1 through 3, which are needed to express the QCD vertex through $\mathcal{O}(\epsilon^2)$ at one loop and $\mathcal{O}(\epsilon^0)$ at two loops. Similarly to the sYM results discussed above, each of the functions we introduce has the following properties:

1. It is expressed in terms of *single-valued polylogarithms* \mathcal{G} of the 5 letter alphabet $\{z, \bar{z}, 1-z, 1-\bar{z}, 1-z-\bar{z}\}$ (the additional letter $z-\bar{z}$ in (5.6), does not appear here);

2. It is finite in the soft limit;

3. It admits either

$$\Phi(z, \bar{z}) = +\Phi(1-\bar{z}, 1-z) \tag{8.24}$$

or

$$\Phi(z, \bar{z}) = -\Phi(1-\bar{z}, 1-z) \tag{8.25}$$

which, together with a similar property of the corresponding rational coefficients, manifests the exact target-projectile symmetry of the vertex;

4. It admits the hermiticity relation

$$\Phi(z, \bar{z}) = (\Phi(\bar{z}, z))^* , \quad (8.26)$$

which manifest the reality properties of the vertex prior to contraction with the polarization vector. Most of the functions are real, $\mathbb{C} \rightarrow \mathbb{R}$, so they simply admit $\Phi(z, \bar{z}) = \Phi(\bar{z}, z)$, but some are complex valued, $\mathbb{C} \rightarrow \mathbb{C}$, and admit (8.26).

$$\phi_1(z, \bar{z}) = \mathcal{G}(0, z) + \mathcal{G}(1, z), \quad (8.27a)$$

$$\phi_2(z, \bar{z}) = \mathcal{G}(1, z) - \mathcal{G}(0, z), \quad (8.27b)$$

$$\phi_3(z, \bar{z}) = \mathcal{G}(0, 0, z) - \mathcal{G}(0, 1, z) - \mathcal{G}(1, 0, z) + \mathcal{G}(1, 1, z), \quad (8.27c)$$

$$\phi_4(z, \bar{z}) = \mathcal{G}(0, 0, z) - \mathcal{G}(1, 1, z), \quad (8.27d)$$

$$\phi_5(z, \bar{z}) = \mathcal{G}(0, 0, z) + \mathcal{G}(1, 1, z), \quad (8.27e)$$

$$\phi_6(z, \bar{z}) = \frac{1}{4}\mathcal{G}(0, 1, z) - \frac{1}{4}\mathcal{G}(1, 0, z) + \frac{\pi^2}{16}, \quad (8.27f)$$

$$\begin{aligned} \phi_7(z, \bar{z}) &= \mathcal{G}(1 - \bar{z}, 0, 0, z) - \mathcal{G}(1 - \bar{z}, 0, 1, z) - \mathcal{G}(1 - \bar{z}, 1, 0, z) + \mathcal{G}(1 - \bar{z}, 1, 1, z) \\ &+ \mathcal{G}(0, 0, 0, z) - \mathcal{G}(0, 1, 1, z) - \mathcal{G}(1, 0, 0, z) + \mathcal{G}(1, 1, 1, z) + \frac{8\zeta(3)}{3}, \end{aligned} \quad (8.27g)$$

$$\begin{aligned} \phi_8(z, \bar{z}) &= \frac{1}{2}(-\mathcal{G}(0, 1 - \bar{z}, 0, z) + \mathcal{G}(0, 1 - \bar{z}, 1, z) - \mathcal{G}(1, 1 - \bar{z}, 0, z) + \mathcal{G}(1, 1 - \bar{z}, 1, z) \\ &+ \mathcal{G}(0, 1, 0, z) - \mathcal{G}(1, 0, 1, z)) + \frac{1}{12}\pi^2(\mathcal{G}(1, z) - \mathcal{G}(0, z)), \end{aligned} \quad (8.27h)$$

$$\phi_9(z, \bar{z}) = \mathcal{G}(1 - \bar{z}, 0, z) - \mathcal{G}(1 - \bar{z}, 1, z) + \frac{1}{2}\mathcal{G}(0, 1, z) - \frac{1}{2}\mathcal{G}(1, 0, z) - \frac{\pi^2}{6}, \quad (8.27i)$$

$$\phi_{10}(z, \bar{z}) = \mathcal{G}(0, 0, 0, z) - \mathcal{G}(1, 1, 1, z), \quad (8.27j)$$

$$\begin{aligned} \phi_{11}(z, \bar{z}) &= 3 \left[3\mathcal{G}(0, 1 - \bar{z}, 0, z) - 3\mathcal{G}(0, 1 - \bar{z}, 1, z) + 3\mathcal{G}(1, 1 - \bar{z}, 0, z) - 3\mathcal{G}(1, 1 - \bar{z}, 1, z) \right. \\ &+ 2\mathcal{G}(1 - \bar{z}, 0, 0, z) - 4\mathcal{G}(1 - \bar{z}, 0, 1, z) + 4\mathcal{G}(1 - \bar{z}, 1, 0, z) - 2\mathcal{G}(1 - \bar{z}, 1, 1, z) \\ &- 8\mathcal{G}(1 - \bar{z}, 1 - \bar{z}, 0, z) + 8\mathcal{G}(1 - \bar{z}, 1 - \bar{z}, 1, z) - 4\mathcal{G}(0, 0, 0, z) + 4\mathcal{G}(0, 0, 1, z) + \mathcal{G}(0, 1, 0, z) \\ &\left. - 2\mathcal{G}(0, 1, 1, z) + 2\mathcal{G}(1, 0, 0, z) - \mathcal{G}(1, 0, 1, z) - 4\mathcal{G}(1, 1, 0, z) + 4\mathcal{G}(1, 1, 1, z) + 4\zeta(3) \right] \\ &+ 4\pi^2\mathcal{G}(1 - \bar{z}, z) - 3\pi^2\mathcal{G}(1, z) \end{aligned} \quad (8.27k)$$

For easy reference we summarize the properties of the ϕ_i functions in table 1. The first row in the table represents the transcendental weight. The second row shows how each function realises the hermiticity property of (8.26), where S indicates real functions, $\phi_i(z, \bar{z}) = \phi_i(\bar{z}, z)$, while C stands for complex functions obeying (8.26). Finally, in the

Property	ϕ_1	ϕ_2	ϕ_3	ϕ_4	ϕ_5	ϕ_6	ϕ_7	ϕ_8	ϕ_9	ϕ_{10}	ϕ_{11}
Weight	1	1	2	2	2	2	3	3	2	3	3
$z \rightarrow \bar{z}$	S	S	S	S	S	C	S	C	S	S	S
$z \rightarrow 1 - \bar{z}$	S	A	S	A	S	S	S	S	A	A	A

Table 1. Table summarising the weight and symmetry properties of the transcendental functions entering the non-maximal weight part of the QCD Lipatov vertex through two loops.

third row S indicates symmetry under target-projectile swap, as in (8.24), while A indicates antisymmetry under this swap, as in (8.25).

Next, we define non-pure, mixed-weight transcendental functions involving rational prefactors. Notably, as we have seen at one loop in eqs. (5.15) through (5.17), these contain spurious poles in $p = 1 - z - \bar{z}$, corresponding to the soft limit of the emitted gluon p_4 . As already discussed these $1/p^n$ poles cancel in the combinations that enter the vertex. Here we make this manifest by defining a basis of functions where each has a finite $p \rightarrow 0$ limit. These are defined in terms of the basis of ϕ_i we defined in (8.27) above:

$$\mu_1(z, \bar{z}) = \frac{\phi_2}{p} \quad (8.28a)$$

$$\mu_2(z, \bar{z}) = -\frac{(q^2 - 1)\phi_2}{p^3} - \frac{4}{p^2} \quad (8.28b)$$

$$\mu_3(z, \bar{z}) = \frac{\phi_4}{p} \quad (8.28c)$$

$$\mu_4(z, \bar{z}) = \frac{\phi_9}{p} \quad (8.28d)$$

$$\mu_5(z, \bar{z}) = \frac{\phi_3}{p^2} \quad (8.28e)$$

$$\mu_6(z, \bar{z}) = \frac{2\phi_1}{p^2} - \frac{(q^2 - 1)\phi_4}{p^3} \quad (8.28f)$$

$$\mu_7(z, \bar{z}) = \frac{(q^2 - 1)(\phi_2 - 3\phi_9)}{p^3} + \frac{3(\phi_1 + 4) + 4}{p^2} \quad (8.28g)$$

$$\mu_8(z, \bar{z}) = \frac{\phi_{10}}{p} \quad (8.28h)$$

$$\mu_9(z, \bar{z}) = -\frac{\phi_{11}}{p} \quad (8.28i)$$

$$\mu_{10}(z, \bar{z}) = \frac{(q^2 - 1)\left(\frac{1}{12}\pi^2\phi_2 + \phi_{10}\right)}{p^3} + \frac{\frac{\pi^2}{3} - 2\phi_5}{p^2} \quad (8.28j)$$

$$\mu_{11}(z, \bar{z}) = -\frac{6(2\phi_1 - \phi_3 + \phi_5 + \pi^2 + 16)}{p^2(q^2 - 1)} - \frac{3\pi^2\phi_2 + \phi_{11}}{p^3} \quad (8.28k)$$

Since the functions $\mu_j(z, \bar{z})$ have been constructed as linear combinations of ϕ_i with coefficients that are symmetric under $z \rightarrow \bar{z}$, it immediately follows that they admit the hermiticity property (8.26). Furthermore, given that they do not involve the two complex

functions (ϕ_6 and ϕ_8), these functions are all *real*:

$$\mu_j(z, \bar{z}) = \mu_j(\bar{z}, z). \quad (8.29)$$

Finally, these functions are all symmetric under the target-projectile swap $z \rightarrow 1 - \bar{z}$, (corresponding to $p \rightarrow -p$) as in (8.24):

$$\mu_j(z, \bar{z}) = \mu_j(1 - \bar{z}, 1 - z). \quad (8.30)$$

This holds since the antisymmetric ϕ_i enter eqs. (8.28) along with odd powers of p , while the symmetric ϕ_i with even powers.

8.2.2 Another look at the QCD vertex at one loop

In section 5 we have presented one-loop QCD vertex by separating the terms containing non-maximal weight functions in a closed form, to all order in ϵ following refs. [57, 62, 99] – see eqs. (5.15) through (5.17). Here, in preparation to presenting the two-loop case, we expand the result and keep terms through $\mathcal{O}(\epsilon^2)$ (or weight 4). As explained in the previous subsection, we do so in order to express the one and two loop results using a common basis of transcendental functions and parallel notation for the coefficients.

At the outset we split the coefficients into dispersive and absorptive parts,

$$\begin{aligned} v_{\oplus}^{(n)}(t_1, t_2, |p_4|^2) &= v_{\oplus}^{(n)}(z, \bar{z}) = \text{Disp} \left\{ v_{\oplus}^{(n)}(z, \bar{z}) \right\} + i \text{Absorp} \left\{ v_{\oplus}^{(n)}(z, \bar{z}) \right\} \\ &\equiv v_{\text{Disp}}^{(n)}(z, \bar{z}) + i\pi v_{\text{Absorp}}^{(n)}(z, \bar{z}) \end{aligned} \quad (8.31)$$

At one loop ($n = 1$) we have

$$\begin{aligned} v_{\text{Disp}}^{(1)}(z, \bar{z}) &= v_{\text{sYM, Disp}}^{(1)}(z, \bar{z}) + \mathcal{R}_{\text{Disp}}^{(1)} \\ &+ \sum_{i \in \{1, 2, 4, 5\}} W_i(p, q) \phi_i(z, \bar{z}) + \sum_{j \in \{1, 2, 3, 6, 8, 10\}} R_j(p, q) \mu_j(z, \bar{z}) \end{aligned} \quad (8.32a)$$

$$v_{\text{Absorp}}^{(1)}(z, \bar{z}) = v_{\text{sYM, Absorp}}^{(1)}(z, \bar{z}) \quad (8.32b)$$

where p and q are given in (8.20), the uniform weight functions $\phi_i(z, \bar{z})$ are given in eq. (8.27) and the non-pure (and mixed-weight) functions $\mu_j(z, \bar{z})$ are given in eq. (8.28). The final three contributions to $v_{\text{Disp}}^{(1)}(z, \bar{z})$ in (8.32a) correspond to $v_{\text{spurious}}^{(1)}(t_1, t_2, |p_4|^2) + v_{\beta}^{(1)}(\epsilon)$ in eq.(5.13), expanded in ϵ . The coefficients W_i , R_j and $\mathcal{R}_{\text{Disp}}^{(1)}$ are rational functions of p , q , N_c and n_f (note that they do contain π^2 terms, but no other transcendental numbers or functions). They read as follows:

$$W_1 = \frac{q}{6(q-1)((q-1)^2 - p^2)} \left(\epsilon(n_f - N_c) + \frac{1}{3}\epsilon^2(11n_f - 8N_c) \right) \quad (8.33a)$$

$$W_2 = \frac{p}{1-q} W_1 \quad (8.33b)$$

$$W_4 = \frac{pq\epsilon^2(N_c - n_f)}{6(q-1)^2((q-1)^2 - p^2)} \quad (8.33c)$$

$$W_5 = \frac{q-1}{p} W_4. \quad (8.33d)$$

Note that W_2 and W_4 are antisymmetric under $p \rightarrow -p$ (with fixed q), precisely compensating for the antisymmetry of the corresponding transcendental functions they multiply, ϕ_2 and ϕ_4 . In turn, W_1 and W_5 are symmetric under $p \rightarrow -p$, in line with the symmetry of the corresponding ϕ_i .

Next, the coefficients of the non-pure, mixed-weight functions μ_j are given by

$$\begin{aligned} R_1 = & -\frac{1}{16}q(n_f - 7N_c) + \frac{1}{16}(7N_c - n_f) \\ & + \epsilon \left(-\frac{1}{16}q(n_f - 14N_c) - \frac{1}{6}\frac{q}{(1-q)^2}(n_f - N_c) + \frac{1}{48}(44N_c - 5n_f) \right) \\ & + \epsilon^2 \left(-\frac{1}{16}q(n_f - 28N_c) + \frac{1}{192}\pi^2(q+1)(n_f - 7N_c) - \frac{1}{18}\frac{q}{(1-q)^2}(11n_f - 8N_c) \right. \\ & \left. + \frac{1}{144}(268N_c - 31n_f) \right) \end{aligned} \quad (8.34a)$$

$$R_2 = \frac{(1+q)^2}{1-q} \left(\frac{1}{48}(N_c - n_f) - \frac{1}{144}\epsilon(11n_f - 8N_c) + \frac{1}{432}\epsilon^2(52N_c - 85n_f) \right) \quad (8.34b)$$

$$R_3 = -\frac{\epsilon}{16}(q+1)(n_f - 7N_c) + \epsilon^2 \left(-\frac{1}{16}q(n_f - 14N_c) - \frac{q(n_f - N_c)}{6(q-1)^2} + \frac{1}{48}(44N_c - 5n_f) \right) \quad (8.34c)$$

$$R_6 = \frac{(q+1)^2}{144(1-q)} (3\epsilon(N_c - n_f) + \epsilon^2(8N_c - 11n_f)) \quad (8.34d)$$

$$R_8 = -\frac{1}{16}(q+1)\epsilon^2(7N_c - n_f) \quad (8.34e)$$

$$R_{10} = \frac{(q+1)^2\epsilon^2(N_c - n_f)}{48(1-q)}, \quad (8.34f)$$

and finally

$$\begin{aligned} \mathcal{R}_{\text{Disp}}^{(1)} = & -\frac{11N_c - 2n_f}{24\epsilon} + \frac{q}{(q-1)((q-1)^2 - p^2)} \left(\frac{1}{3}(N_c - n_f) - \frac{\epsilon}{9}(11n_f - 8N_c) \right) \\ & + \epsilon^2 \left(-\frac{1}{27}(85n_f - 52N_c) + \frac{\pi^2}{36}(n_f - N_c) \right). \end{aligned} \quad (8.35)$$

We emphasise that the transcendental functions entering the one-loop vertex beyond sYM consist exclusively of the subset of functions which correspond to powers of *single-valued logarithms* – rather than GPLs. These include ϕ_i for $i = 1, 2, 4, 5$ and μ_j for $j = 1, 2, 3, 6, 8, 10$, which are in turn expressible in terms of ϕ_i for $i = 1, 2, 4, 5$ and 10. This must indeed be so, as we know that the non-maximal weight component of the one-loop vertex exponentiates to all orders in the ϵ expansion according to eqs. (5.15) through (5.17) [57, 62, 99]. Next, we consider the two-loop vertex, where no such simplification occurs. In particular, the non-maximal weight component of the vertex involves the complete basis of GPLs we presented in sec. 8.2.1 above.

8.2.3 QCD vertex at two loop

In analogy with the one-loop case, eq. (8.32) we write the two-loop QCD vertex separated into dispersive and absorptive parts as in eq. (8.31). These two components are expressed using the bases of transcendental functions introduced in section 8.2.1:

$$\begin{aligned}
v_{\text{Disp}}^{(2)}(z, \bar{z}) &= v_{\text{sYM, Disp}}^{(2)}(z, \bar{z}) + \mathcal{R}_{\text{Disp}}^{(2)} \\
&+ \sum_{i \in \{1,2,3,4,5,7,8\}} U_i^{\text{Disp}}(p, q) \phi_i(z, \bar{z}) + \sum_{j \in \{1,2,3,4,5,6,7,9,11\}} S_j^{\text{Disp}}(p, q) \mu_j(z, \bar{z})
\end{aligned} \tag{8.36a}$$

$$\begin{aligned}
v_{\text{Absorp}}^{(2)}(z, \bar{z}) &= v_{\text{sYM, Absorp}}^{(2)}(z, \bar{z}) + \mathcal{R}_{\text{Absorp}}^{(2)} \\
&+ \sum_{i \in \{1,2,3,6\}} U_i^{\text{Absorp}}(p, q) \phi_i(z, \bar{z}) + \sum_{j \in \{1,2,3,4,6,7\}} S_j^{\text{Absorp}}(p, q) \mu_j(z, \bar{z})
\end{aligned} \tag{8.36b}$$

where, in contrast to the one-loop case, also the absorptive part of the vertex receives non-pure lower-weight functions, including spurious poles, $1/p^n$.

The coefficients $\mathcal{R}^{(2)}$, U_i and S_j appearing in (8.36) are rational functions of p , q , N_c and n_f at each order in ϵ . They contain π^2 factors, but no other transcendental numbers or functions. The coefficients of ϕ_i in the dispersive part of the vertex are:

$$\begin{aligned}
U_1^{\text{Disp}} &= \frac{q}{(q-1)((q-1)^2 - p^2)} \left(-\frac{N_c(n_f - N_c)}{24\epsilon} + \frac{1}{24} q N_c (N_c - n_f) \right. \\
&\quad \left. - \frac{1}{144} (2n_f - N_c)(5N_c + n_f) \right) - \frac{1}{576} \pi^2 N_c (2n_f - 11N_c)
\end{aligned} \tag{8.37a}$$

$$\begin{aligned}
U_2^{\text{Disp}} &= \frac{pq}{(q-1)^2((q-1)^2 - p^2)} \left(\frac{N_c(n_f - N_c)}{24\epsilon} + \frac{1}{24} q N_c (n_f - N_c) \right. \\
&\quad \left. + \frac{1}{144} (35N_c n_f - 27N_c^2 - 2n_f^2) \right)
\end{aligned} \tag{8.37b}$$

$$\begin{aligned}
U_3^{\text{Disp}} &= \frac{N_c(2n_f - 11N_c)}{96\epsilon} + \frac{qN_c(n_f - N_c)}{12(q-1)((q-1)^2 - p^2)} + \frac{1}{576} (-7N_c n_f - 144N_c^2 + 4n_f^2)
\end{aligned} \tag{8.37c}$$

$$U_4^{\text{Disp}} = \frac{pq}{24(q-1)^2((q-1)^2 - p^2)} N_c (n_f - N_c) \tag{8.37d}$$

$$U_5^{\text{Disp}} = \frac{q-1}{p} U_4^{\text{Disp}} \tag{8.37e}$$

$$U_7^{\text{Disp}} = U_8^{\text{Disp}} = \frac{1}{48} N_c (11N_c - 2n_f), \tag{8.37f}$$

while those in the absorptive part read:

$$\begin{aligned}
U_1^{\text{Absorp}} &= \frac{q}{(q-1)((q-1)^2 - p^2)} \frac{1}{48} N_c (N_c - n_f) \\
U_2^{\text{Absorp}} &= \frac{p}{1-q} U_1^{\text{Absorp}} \\
U_3^{\text{Absorp}} &= \frac{1}{192} N_c (11N_c - 2n_f) \\
U_6^{\text{Absorp}} &= \frac{1}{48} N_c (11N_c - 2n_f) .
\end{aligned} \tag{8.38a}$$

Note that the only antisymmetric coefficients under $p \rightarrow -p$ are those multiplying the two antisymmetric transcendental functions ϕ_2 and ϕ_4 (see Table 1), realizing the exact target-projectile symmetry of the vertex.

Next, the coefficients of the non-pure, mixed weight functions μ_j entering the dispersive part of the two-loop vertex are:

$$\begin{aligned}
S_1^{\text{Disp}} &= -\frac{(q+1)N_c(7N_c - n_f)}{64\epsilon^2} \\
&+ \frac{1}{\epsilon} \left(\frac{qN_c(n_f - N_c)}{24(q-1)^2} + \frac{1}{384}(q+1)(31N_cn_f - 161N_c^2 - 2n_f^2) + \frac{1}{96}N_c(n_f - N_c) \right) \\
&+ \frac{(q+1)^2N_c(n_f - N_c)}{96(q-1)} - \frac{1}{96}qN_c(n_f - N_c) - \frac{q(-41N_cn_f + 33N_c^2 + 2n_f^2)}{144(q-1)^2} \\
&+ q \left(-\frac{43N_cn_f}{288} + \frac{5n_f}{128N_c} + \frac{133N_c^2}{576} + \frac{7n_f^2}{576} \right) - \frac{11N_cn_f}{192} - \frac{1}{32}N_c(n_f - N_c) \\
&+ \frac{5n_f}{128N_c} + \frac{11N_c^2}{72} + \frac{5n_f^2}{576}
\end{aligned} \tag{8.39a}$$

$$\begin{aligned}
S_2^{\text{Disp}} &= \frac{(q+1)^2}{1-q} \left(-\frac{N_c(N_c - n_f)}{192\epsilon^2} + \frac{35N_cn_f - 27N_c^2 - 2n_f^2}{1152\epsilon} + \frac{1}{192}\pi^2 N_c(N_c - n_f) \right. \\
&\left. - \frac{2N_cn_f^2 - 68N_c^3 + 27n_f^2}{3456N_c} \right)
\end{aligned} \tag{8.39b}$$

$$\begin{aligned}
S_3^{\text{Disp}} &= -\frac{(q+1)N_c(7N_c - n_f)}{64\epsilon} + \frac{qN_c(n_f - N_c)}{24(q-1)^2} + \frac{1}{384}(q+1)(-13N_cn_f - 13N_c^2 + 2n_f^2) \\
&+ \frac{1}{96}N_c(n_f - N_c)
\end{aligned} \tag{8.39c}$$

$$S_4^{\text{Disp}} = \frac{1}{16}(q+1)N_c(N_c - n_f) \tag{8.39d}$$

$$S_5^{\text{Disp}} = -\frac{(q+1)^2(q+5)N_c(N_c - n_f)}{192(q-1)} \tag{8.39e}$$

$$S_6^{\text{Disp}} = \frac{(q+1)^2}{1-q} \left(\frac{N_c(n_f - N_c)}{192\epsilon} + \frac{-9N_cn_f + 13N_c^2 + 2n_f^2}{1152} \right) \tag{8.39f}$$

$$S_7^{\text{Disp}} = \frac{(q+1)^2}{1-q} \left(-\frac{1}{48} N_c (N_c - n_f) \right) \quad (8.39g)$$

$$S_9^{\text{Disp}} = \frac{1}{192} (q+1) N_c (7N_c - n_f) \quad (8.39h)$$

$$S_{11}^{\text{Disp}} = \frac{1}{576} (q+1)^3 N_c (N_c - n_f) , \quad (8.39i)$$

while those entering the absorptive part read:

$$S_1^{\text{Absorp}} = -\frac{(q+1)N_c(7N_c - n_f)}{128\epsilon} + \frac{1}{128}(q+1)N_c(2n_f - 15N_c) \\ + \frac{qN_c(n_f - N_c)}{48(q-1)^2} + \frac{1}{192}N_c(n_f - N_c) \quad (8.40a)$$

$$S_2^{\text{Absorp}} = \frac{(q+1)^2}{1-q} \frac{1}{384} \left(\frac{N_c(n_f - N_c)}{\epsilon} + N_c^2 \right) \quad (8.40b)$$

$$S_3^{\text{Absorp}} = -\frac{1}{64}(q+1)N_c(7N_c - n_f) \quad (8.40c)$$

$$S_4^{\text{Absorp}} = -S_3^{\text{Absorp}} \quad (8.40d)$$

$$S_6^{\text{Absorp}} = \frac{(q+1)^2 N_c (N_c - n_f)}{192(q-1)} \quad (8.40e)$$

$$S_7^{\text{Absorp}} = -\frac{1}{3} S_6^{\text{Absorp}} . \quad (8.40f)$$

Finally,

$$\mathcal{R}_{\text{Disp}}^{(2)} = \frac{5}{192\epsilon^3} N_c (11N_c - 2n_f) \\ + \frac{1}{\epsilon^2} \left(\frac{-qN_c(N_c - n_f)}{12(q-1)((q-1)^2 - p^2)} + \frac{-112N_c n_f + 229N_c^2 + 12n_f^2}{1152} \right) \\ + \frac{1}{\epsilon} \left(\frac{q(35N_c n_f - 27N_c^2 - 2n_f^2)}{72(q-1)((q-1)^2 - p^2)} + \frac{155N_c n_f}{1728} + \frac{\pi^2}{288} N_c (2n_f - 11N_c) - \frac{n_f}{64N_c} \right. \\ \left. - \frac{173N_c^2}{432} \right) + \frac{11\pi^2 N_c (67N_c - 10n_f)}{3456} - \frac{N_c (1142N_c - 65n_f)}{2592} \\ + \frac{q}{(q-1)((q-1)^2 - p^2)} \left(\left(-\frac{2N_c}{3} - \frac{1}{8N_c} \right) n_f + \frac{\pi^2}{24} N_c (N_c - n_f) + \frac{53N_c^2}{54} - \frac{n_f^2}{108} \right) \quad (8.41)$$

and

$$\mathcal{R}_{\text{Absorp}}^{(2)} = \frac{N_c (11N_c - 2n_f)}{96\epsilon^2} - \frac{N_c (67N_c - 10n_f)}{576\epsilon} - \frac{1}{864} N_c (193N_c - 19n_f) \\ + \frac{q}{24(q-1)((q-1)^2 - p^2)} \left(\frac{N_c (n_f - N_c)}{\epsilon} + qN_c (N_c - n_f) + \frac{N_c}{3} (11n_f - 8N_c) \right) . \quad (8.42)$$

9 Conclusions

In this paper we took a step forward in developing the effective theory for multi-Reggeon calculations [17–26] based on the shock-wave formalism with the aim of applying it to multi-leg amplitudes in the multi-Regge kinematic (MRK) limit. In line with previous work on this [17, 21, 25, 26], we find that the coupling of a real gluon to the Reggeon field W is not restricted to a single Reggeon transition $\mathcal{R}g\mathcal{R}$, but it comes along with a variety of possible multi-Reggeon (MR) transitions. Specifically, besides the single Reggeon transition, the additional $\mathcal{R}g\mathcal{R}^2$ and $\mathcal{R}^2g\mathcal{R}^2$ MR transitions are relevant starting from one loop, while $\mathcal{R}g\mathcal{R}^3$, $\mathcal{R}^2g\mathcal{R}^3$ and $\mathcal{R}^3g\mathcal{R}^3$, are relevant starting at two loops. One interesting feature is that in sharp contrast to rapidity evolution, which is described by the JIMWLK Hamiltonian and preserves signature, real gluon emission involves transitions between odd signature across one rapidity span and even signature across another.

We applied this formalism to $2 \rightarrow 3$ scattering, classifying all multi-Reggeon (MR) transitions at both one and two loops. We explicitly computed all one-loop transitions and those contributing to the odd-odd signature component at two loops. This provides us with the essential information for extracting the Lipatov vertex at two loops.

Specializing general-kinematics amplitude computations to the MRK limit, we computed analytically the full set of (non-planar) QCD amplitudes for $gg \rightarrow ggg$, $qg \rightarrow qgg$ and $qq \rightarrow qgg$ scattering at one and two loops. We obtained a closed form analytic result for all components of these amplitudes at leading power in MRK and converted the result to the t -channel colour basis.

Based on the computed amplitudes in MRK and the effective MR computation described above, we isolated the Regge-pole component and used the factorisation formula (8.4) to extract the Lipatov vertex. In identifying the Regge-pole component we used the criterion (8.3) of ref. [23, 24], originally set in the context of $2 \rightarrow 2$ scattering, namely that the Regge-pole component, i.e. the part of the octet-octet colour component of the amplitude which factorizes, consists of the sum of the SR transition, $\mathcal{R}g\mathcal{R}$, plus the planar part of the MR transitions. In turn, the Regge-cut part, which does not factorize, is entirely non-planar.

The extraction of the two-loop Lipatov vertex has been done using the aforementioned three partonic processes, providing a robust check of both the amplitudes and the effective MR computation. Furthermore, the universality of the planar part of the MR contribution – in contrast with the process dependence of its non-planar counterpart – gives further assurance that we are using the correct separation between the pole and cut components. Analyzing the expansion of the factorization formula to three loops, we predict the form of the planar part of the MR contributions to the octet-octet channel at this order. This can be confirmed through explicit computation in the future, to provide further assurance that we understand well the interplay between the MR effective theory and the factorization properties in the MRK limit. We recall that for $2 \rightarrow 2$ scattering, computations have been performed to four loops, providing such evidence [23, 24]. We also computed the one-loop amplitudes analytically to $\mathcal{O}(\epsilon^4)$ (weight 6) and extracted the one-loop Lipatov vertex to this order. These results can be used in the context of future three-loop $2 \rightarrow 3$

computations.

In section 4 we studied the analytic properties of the vertex based on general considerations and clarified its symmetries and the properties of the transcendental functions it contains. A main ingredient of this analysis has been the comparison between the factorization of eq. (4.10) in terms of a complex vertex and eqs. (4.12) and (4.13) which involve, before contraction with the polarization vector, real-valued left and right vertices. The reality condition implies that a natural basis of transcendental functions to be used in expressing both the dispersive and absorptive parts of the complex vertex would consist of real-valued functions that are symmetric under a swap of z and \bar{z} as well as imaginary ones, which are antisymmetric, or equivalently, all transcendental functions should be hermitian. Another important constraint on the analytic structure of the vertex is that it must satisfy target-projectile symmetry. It implies that the transcendental functions can all be chosen to admit (4.33) and then the same symmetry property must be satisfied by the rational coefficients.

These conclusions have been tested in the context of the one and two loop results for the vertex. They have also been used to derive compact expressions with transparent symmetry properties. A short summary of the properties can be found in the beginning of section 8.2.1. Table 1 summarises the symmetries of the basis of transcendental functions of non-maximal weight appearing in the QCD vertex.

A salient property of the Lipatov vertex is that it is a single-valued function of the kinematic variables z and \bar{z} . This is expected on physical grounds, since this complex plane corresponds to a two-dimensional Euclidean space. We have used this in section 8.2 to write the complete result for the vertex through two loops in terms SVMPLs. In agreement with previous work on $2 \rightarrow 3$ amplitudes in MRK in sYM [21] and in QCD [26], we find a six-letter alphabet, $\{z, \bar{z}, 1 - z, 1 - \bar{z}, z - \bar{z}, 1 - z - \bar{z}\}$. The first four letters correspond to physical logarithmic singularities where one of the two t channel momenta vanishes, while the last two correspond respectively to the configurations where all final-state momenta are in a plane, and to the limit where the centrally-emitted gluon is soft. None of these lead to rational kinematic singularities in the vertex, but there are spurious rational poles in the soft limit, which cancel through combinations of transcendental functions. We make this manifest by a basis choice (8.28) where each function is itself finite.

We performed a series of checks on our calculations. At one loop we find agreement with ref. [28], which provides the dispersive and the absorptive parts of the Lipatov vertex through $\mathcal{O}(\epsilon^2)$. In addition, we checked that all the multi-Reggeon transitions at one loop agree with the effective theory calculation presented in ref. [26]. Proceeding to two loops, we compared the multi-Reggeon transitions that contribute to the odd-odd signature components of the amplitude [25] with the results of [26]. Concerning the final ingredient that enter the determination of the two-loop Lipatov vertex, namely the $gg \rightarrow ggg$, $qg \rightarrow qgg$ and $qq \rightarrow qgg$ amplitudes in the MRK limit, we verified that the terms of leading transcendental weight in the $gg \rightarrow ggg$ QCD amplitude reproduce the $\mathcal{N} = 4$ sYM result of ref. [21]. Finally, for all the three channels above we checked that the finite remainder of the QCD amplitudes are in agreement with the results of ref. [26].

Let us now provide some outlook regarding the use of the new results. The two-loop

vertex, along with the already known three-loop Regge trajectory and two-loop impact factors [23, 24, 52], completes the information required to use the MRK Regge-pole factorization formula to predict or resum rapidity logarithms at higher orders with NNLL accuracy. To achieve complete control of rapidity logarithms at this accuracy in the non-planar theory, the Regge-pole factorization formula needs to be supplemented by Regge cut contributions, corresponding to the non-planar MR components. While these are not yet known at three loops, we have a theory set up to compute these (recall that for $2 \rightarrow 2$ amplitudes, such MR corrections have already been computed to four loops).

We emphasise that the possibility of using the MRK Regge-pole factorization formula to predict or resum rapidity logarithms at higher orders is not limited to $2 \rightarrow 3$ scattering. The same information, extracted from $2 \rightarrow 2$ and $2 \rightarrow 3$ transitions should be applicable to $2 \rightarrow 4$ and higher-point scattering amplitudes. Note though that a new feature arises starting from $2 \rightarrow 4$ amplitudes, namely that Regge cuts start to contribute also in the planar limit [43–48]. It would be very interesting to push the MR theory further and apply it in this context, where in the planar limit contact can be made with predictions for the remainder functions in sYM.

Finally, the two-loop Lipatov vertex is a key element for determining the BFKL kernel at NNLO. In order to compute this kernel (along the lines of the NLO computation in refs. [15, 128, 129]) one needs to sum interference diagrams of different multiplicity, including: *i*) virtual corrections involving the three-loop gluon Regge trajectory [23, 24, 52]; *ii*) single-particle production involving the two-loop Lipatov vertex computed here, interfering with the tree-level vertex, as well as the interference of two one-loop Lipatov vertices; *iii*) the central emission of two partons at one loop [85] interfering with its tree counterpart; and finally *iv*) the central emission of three partons at tree level. Recent progress has been made on determining several of these ingredients [83, 85], making BFKL theory at NNLL a realistic goal to pursue.

Acknowledgments

We wish to thank Emmet Byrne, Vittorio Del Duca, Claude Duhr, Michael Fucilla, Jenni Smillie, Vasily Sotnikov and Simone Zoia for useful discussions. We also wish to thank Federico Buccioni, Fabrizio Caola, Federica Devoto and Giulio Gambuti, who have recently published [26] an independent extraction of the Lipatov vertex following similar methods, for conducting a careful comparison between our results for the effective MR computation [25]. G.D.L.’s work is supported in part by the U.K. Royal Society through Grant URF/R1/20109; G.F. is supported by the EU’s Horizon Europe research and innovation programme under the Marie Skłodowska-Curie grant 101104792, *QCDchallenge*; EG is supported by the STFC Consolidated Grant “Particle Physics at the Higgs Centre”; CM has been partially supported by the Italian Ministry of University and Research (MUR) through grant PRIN20172LNEEZ and by Compagnia di San Paolo through grant TORPS1921EX-POST2101. GF and EG are grateful to the Galileo Galilei Institute in Florence for hospitality and support during the scientific program *Mathematical Structures in Scattering Amplitudes*, where part of this work was done.

A Tree level impact factors and Lipatov vertex for gluon scattering

In this appendix we calculate explicitly the tree level expressions for the impact factors and the Lipatov vertex for the process

$$g[(-P_1)^\oplus, a_1] + g[(-P_2)^\oplus, a_2] \rightarrow g[P_3^\oplus, a_3] + g[P_4^\oplus, a_4] + g[P_5^\oplus, a_5]. \quad (\text{A.1})$$

To this end we start from the high-energy limit of the tree level amplitude, where the polarization vectors are written explicitly, taking as a starting point eq. (20) of [71]. With the notation used in this paper, and keeping for now generic helicity states, we have

$$\begin{aligned} \mathcal{M}_{gg \rightarrow ggg} &= 2s \left[i g_s f^{a_2 a_3 y} \Gamma^{\mu_2 \mu_3} \right] \varepsilon_{\mu_2}^{\lambda_2^*}(P_2) \varepsilon_{\mu_3}^{\lambda_3}(P_3) \frac{1}{t_2} \\ &\quad \times \left[i g_s f^{y a_4 x} C^{\mu_4}(Q_1, Q_2) \right] \varepsilon_{\mu_4}^{\lambda_4}(P_4) \frac{1}{t_1} \\ &\quad \times \left[i g_s f^{a_1 a_5 x} \Gamma^{\mu_1 \mu_5} \right] \varepsilon_{\mu_1}^{\lambda_1^*}(P_1) \varepsilon_{\mu_5}^{\lambda_5}(P_5). \end{aligned} \quad (\text{A.2})$$

Comparing this amplitude with the one in eq. (2.14) specialised for gluons:

$$\begin{aligned} \mathcal{M}_{gg \rightarrow ggg}^{\text{tree}} &= 2s \left[g_s \delta_{-\lambda_3, \lambda_2} i f^{a_2 a_3 y} C_j^{(0)}(P_2^{\lambda_2}, P_3^{\lambda_3}) \right] \frac{1}{t_2} \\ &\quad \times \left[g_s i f^{y a_4 x} V^{(0)}(Q_1, P_4^{\lambda_4}, Q_2) \right] \frac{1}{t_1} \\ &\quad \times \left[g_s \delta_{-\lambda_5, \lambda_1} i f^{a_1 a_5 x} C_i^{(0)}(P_1^{\lambda_1}, P_5^{\lambda_5}) \right], \end{aligned} \quad (\text{A.3})$$

we immediately identify

$$\begin{aligned} C_g^{(0)}(P_2^{\lambda_2}, P_3^{\lambda_3}) &= \Gamma^{\mu_2 \mu_3} \varepsilon_{\mu_2}^{\lambda_2^*}(P_2) \varepsilon_{\mu_3}^{\lambda_3}(P_3), \\ V^{(0)}(Q_1, P_4^{\lambda_4}, Q_2) &= C^{\mu_4}(Q_1, Q_2) \varepsilon_{\mu_4}^{\lambda_4}(P_4), \\ C_g^{(0)}(P_1^{\lambda_1}, P_5^{\lambda_5}) &= \Gamma^{\mu_1 \mu_5} \varepsilon_{\mu_1}^{\lambda_1^*}(P_1) \varepsilon_{\mu_5}^{\lambda_5}(P_5). \end{aligned} \quad (\text{A.4})$$

The expression for $\Gamma^{\mu_2 \mu_3}$, $\Gamma^{\mu_1 \mu_5}$ and $C^{\mu_4}(Q_1, Q_2)$ can be found respectively in eqs. (21) and (22) of [71]. Taking all momenta outgoing we have

$$\begin{aligned} \Gamma^{\mu_2 \mu_3} &= g^{\mu_2 \mu_3} - \frac{P_2^{\mu_3} P_1^{\mu_2} - P_1^{\mu_3} P_3^{\mu_2}}{P_1 \cdot P_2} - t_2 \frac{P_1^{\mu_3} P_1^{\mu_2}}{2(P_1 \cdot P_2)^2}, \\ \Gamma^{\mu_1 \mu_5} &= g^{\mu_1 \mu_5} - \frac{P_2^{\mu_1} P_1^{\mu_5} - P_2^{\mu_5} P_5^{\mu_1}}{P_1 \cdot P_2} - t_1 \frac{P_2^{\mu_5} P_2^{\mu_1}}{2(P_1 \cdot P_2)^2}, \end{aligned} \quad (\text{A.5})$$

and

$$C^\mu(Q_1, Q_2) = \left[(Q_1 - Q_2)_\perp^\mu + \left(\frac{P_2 \cdot P_4}{P_1 \cdot P_2} + \frac{Q_1^2}{P_1 \cdot P_4} \right) P_1^\mu - \left(\frac{P_1 \cdot P_4}{P_1 \cdot P_2} + \frac{Q_2^2}{P_2 \cdot P_4} \right) P_2^\mu \right], \quad (\text{A.6})$$

Notice that e.g. $Q_{1\perp}$ is still a 4-momentum, i.e. given $Q_1 = (q_1^+, q_1^-; \mathbf{q}_1)$ one has $Q_{1\perp} = (0, 0; \mathbf{q}_1)$.

In order to proceed we need to define the polarization vectors. To this end we follow appendix C of [71], and define the polarization vectors in the left (L) or right (R) gauge, following eq. (50) of [71]: we have

$$\varepsilon_L^\mu(P) = \varepsilon_{L\perp}^\mu(P) - \frac{P \cdot \varepsilon_{L\perp}(P)}{P \cdot P_2} P_2^\mu, \quad (\text{A.7})$$

$$\varepsilon_R^\mu(P) = \varepsilon_{R\perp}^\mu(P) - \frac{P \cdot \varepsilon_{R\perp}(P)}{P \cdot P_1} P_1^\mu. \quad (\text{A.8})$$

In turn, the perpendicular component of the polarization vectors, are given in eq. (52), (53), (54) of [71]: in our notation one has

$$\begin{aligned} \varepsilon_{L\perp}^{\mu\oplus}(P) &= \left(0, 0; \varepsilon_{L\perp}^\oplus(P)\right), & \text{with} & \quad \varepsilon_{L\perp}^\oplus(P) = \left(\frac{1}{\sqrt{2}}, \frac{i}{\sqrt{2}}\right), \\ \varepsilon_{L\perp}^{\mu\ominus}(P) &= \left(0, 0; \varepsilon_{L\perp}^\ominus(P)\right), & \text{with} & \quad \varepsilon_{L\perp}^\ominus(P) = \left(\frac{1}{\sqrt{2}}, -\frac{i}{\sqrt{2}}\right), \end{aligned} \quad (\text{A.9})$$

$$\begin{aligned} \varepsilon_{R\perp}^{\mu\oplus}(P) &= \left(0, 0; \varepsilon_{R\perp}^\oplus(P)\right), & \text{with} & \quad \varepsilon_{R\perp}^\oplus(P) = -\frac{\mathbf{p}}{\mathbf{p}} \left(\frac{1}{\sqrt{2}}, -\frac{i}{\sqrt{2}}\right), \\ \varepsilon_{R\perp}^{\mu\ominus}(P) &= \left(0, 0; \varepsilon_{R\perp}^\ominus(P)\right), & \text{with} & \quad \varepsilon_{R\perp}^\ominus(P) = -\frac{\mathbf{p}}{\mathbf{p}} \left(\frac{1}{\sqrt{2}}, \frac{i}{\sqrt{2}}\right), \end{aligned} \quad (\text{A.10})$$

with $P \neq P_2$ or P_1 , and

$$\begin{aligned} \varepsilon_{L\perp}^{\mu\oplus}(P_1) &= \left(0, 0; \varepsilon_{L\perp}^\oplus(P_1)\right), & \text{with} & \quad \varepsilon_{L\perp}^\oplus(P_1) = \left(\frac{1}{\sqrt{2}}, -\frac{i}{\sqrt{2}}\right), \\ \varepsilon_{L\perp}^{\mu\ominus}(P_1) &= \left(0, 0; \varepsilon_{L\perp}^\ominus(P_1)\right), & \text{with} & \quad \varepsilon_{L\perp}^\ominus(P_1) = \left(\frac{1}{\sqrt{2}}, \frac{i}{\sqrt{2}}\right), \end{aligned} \quad (\text{A.11})$$

$$\begin{aligned} \varepsilon_{R\perp}^{\mu\oplus}(P_2) &= \left(0, 0; \varepsilon_{R\perp}^\oplus(P_2)\right), & \text{with} & \quad \varepsilon_{R\perp}^\oplus(P_2) = \left(\frac{1}{\sqrt{2}}, \frac{i}{\sqrt{2}}\right), \\ \varepsilon_{R\perp}^{\mu\ominus}(P_2) &= \left(0, 0; \varepsilon_{R\perp}^\ominus(P_2)\right), & \text{with} & \quad \varepsilon_{R\perp}^\ominus(P_2) = \left(\frac{1}{\sqrt{2}}, -\frac{i}{\sqrt{2}}\right). \end{aligned} \quad (\text{A.12})$$

In order to write explicitly the polarization vectors in eqs. (A.7) and (A.8) we need also $P \cdot P_1 = \frac{1}{2}p^+p_1^-$, $P \cdot P_2 = \frac{1}{2}p^-p_2^+$, which follows from $P_1 = (0, p_1^-, \mathbf{0})$ and $P_2 = (p_2^+, 0, \mathbf{0})$. The initial state particle polarization vector are fixed to be respectively in the L gauge for P_1 and in the R gauge, for P_2 : inserting eqs. (A.11) and (A.12) into eqs. (A.7) and (A.8), and choosing negative helicity, we immediately get

$$\varepsilon_L^{\mu\ominus}(P_1) = \varepsilon_{L\perp}^{\mu\ominus}(P_1) = \left(0, 0; \frac{1}{\sqrt{2}}, +\frac{i}{\sqrt{2}}\right), \quad (\text{A.13})$$

$$\varepsilon_R^{\mu\ominus}(P_2) = \varepsilon_{R\perp}^{\mu\ominus}(P_2) = \left(0, 0; \frac{1}{\sqrt{2}}, -\frac{i}{\sqrt{2}}\right), \quad (\text{A.14})$$

which follows from the fact that $P_1 \cdot \varepsilon_{L\perp}(P_1) = P_2 \cdot \varepsilon_{R\perp}(P_2) = 0$. Consider now the outgoing particles 3, 4 and 5. For particle 3 and 5, whose momenta P_3 and P_5 are mostly along P_2 and P_1 respectively, we adopt the same gauge of particles 1 and 5; furthermore, we choose the positive helicity. We obtain

$$\varepsilon_L^{\mu\oplus}(P_5) = \varepsilon_{L\perp}^\oplus(P_5) - \frac{P_5 \cdot \varepsilon_{L\perp}^\oplus(P_5)}{P_5 \cdot P_2} P_2^\mu = \left(\frac{\sqrt{2}\mathbf{p}_5}{p_5^-}, 0; \frac{1}{\sqrt{2}}, \frac{i}{\sqrt{2}}\right), \quad (\text{A.15})$$

$$\varepsilon_R^{\mu\oplus}(P_3) = \varepsilon_{R\perp}^{\mu\oplus}(P_3) - \frac{P_3 \cdot \varepsilon_{R\perp}^{\oplus}(P_3)}{P_3 \cdot P_1} P_1^\mu = -\frac{\mathbf{p}_3}{\bar{\mathbf{p}}_3} \left(0, \frac{\sqrt{2}\bar{\mathbf{p}}_3}{p_3^+}; \frac{1}{\sqrt{2}}, -\frac{i}{\sqrt{2}} \right). \quad (\text{A.16})$$

Last, we need the polarization vector for particle 4, which we choose to have positive helicity as well. In this case we are free to choose between L and R gauge. In the two cases we have

$$\varepsilon_L^{\mu\oplus}(P_4) = \varepsilon_{L\perp}^{\oplus}(P_4) - \frac{P_4 \cdot \varepsilon_{L\perp}^{\oplus}(P_4)}{P_4 \cdot P_2} P_2^\mu = \left(\frac{\sqrt{2}\mathbf{p}_4}{p_4^-}, 0; \frac{1}{\sqrt{2}}, \frac{i}{\sqrt{2}} \right), \quad (\text{A.17})$$

$$\varepsilon_R^{\mu\oplus}(P_4) = \varepsilon_{R\perp}^{\mu\oplus}(P_4) - \frac{P_4 \cdot \varepsilon_{R\perp}^{\oplus}(P_4)}{P_4 \cdot P_1} P_1^\mu = -\frac{\mathbf{p}_4}{\bar{\mathbf{p}}_4} \left(0, \frac{\sqrt{2}\bar{\mathbf{p}}_4}{p_4^+}; \frac{1}{\sqrt{2}}, -\frac{i}{\sqrt{2}} \right). \quad (\text{A.18})$$

At this point we still need to remember that in the tree-level amplitude of eq. (A.2) the initial state polarization vectors appear as complex conjugate, i.e. we need: $\varepsilon_{\mu_2}^{\ominus*}(P_2)$, $\varepsilon_{\mu_1}^{\ominus*}(P_1)$, and $\varepsilon_{\mu_3}^{\oplus}(P_3)$, $\varepsilon_{\mu_4}^{\oplus}(P_4)$, $\varepsilon_{\mu_5}^{\oplus}(P_5)$ for the final-state polarization vectors. Summarising, choosing the L gauge for $\varepsilon_L^{\mu\oplus}(P_4)$, we have

$$\begin{aligned} \varepsilon_L^{\mu\ominus*}(P_1) &= \left(0, 0; \frac{1}{\sqrt{2}}, -\frac{i}{\sqrt{2}} \right), \\ \varepsilon_R^{\mu\ominus*}(P_2) &= \left(0, 0; \frac{1}{\sqrt{2}}, \frac{i}{\sqrt{2}} \right), \\ \varepsilon_R^{\mu\oplus}(P_3) &= -\frac{\mathbf{p}_3}{\bar{\mathbf{p}}_3} \left(0, \frac{\sqrt{2}\bar{\mathbf{p}}_3}{p_3^+}; \frac{1}{\sqrt{2}}, -\frac{i}{\sqrt{2}} \right), \\ \varepsilon_L^{\mu\oplus}(P_4) &= \left(\frac{\sqrt{2}\mathbf{p}_4}{p_4^-}, 0; \frac{1}{\sqrt{2}}, \frac{i}{\sqrt{2}} \right), \\ \varepsilon_L^{\mu\oplus}(P_5) &= \left(\frac{\sqrt{2}\mathbf{p}_5}{p_5^-}, 0; \frac{1}{\sqrt{2}}, \frac{i}{\sqrt{2}} \right). \end{aligned} \quad (\text{A.19})$$

We can now determine the impact factors by inserting eqs. (A.5) and (A.19) into eq. (A.4): we obtain

$$\begin{aligned} C_g^{(0)}(P_2^\ominus, P_3^\oplus) &= \Gamma^{\mu_2\mu_3} \varepsilon_{\mu_2}^{\ominus*}(P_2) \varepsilon_{\mu_3}^{\oplus}(P_3) = \frac{\mathbf{p}_3}{\bar{\mathbf{p}}_3}, \\ C_g^{(0)}(P_1^\ominus, P_5^\oplus) &= \Gamma^{\mu_1\mu_5} \varepsilon_{\mu_1}^{\ominus*}(P_1) \varepsilon_{\mu_5}^{\oplus}(P_5) = -1. \end{aligned} \quad (\text{A.20})$$

Similarly, using the definitions in eqs. (A.6) and (A.19) we calculate $V^{(0)}(Q_1, P_4^\oplus, Q_2)$:

$$\begin{aligned} V^{(0)}(Q_1, P_4^\oplus, Q_2) &= \frac{1}{\sqrt{2}} \left[\mathbf{p}_3 - \mathbf{p}_5 + \left(\frac{p_2^+ p_4^-}{p_1^- p_2^+} + \frac{-\mathbf{p}_5 \bar{\mathbf{p}}_5}{\frac{1}{2} p_1^- p_4^+} \right) \frac{\mathbf{p}_4 p_1^-}{p_4^-} \right] \\ &= \sqrt{2} \frac{\bar{\mathbf{p}}_3 \mathbf{p}_5}{\bar{\mathbf{p}}_4}, \end{aligned} \quad (\text{A.21})$$

in agreement with eq. (25) of [130]. Eq. (A.21) is obtained by recalling that $P \cdot Q = \frac{1}{2}(p^+ q^- + p^- q^+ - \mathbf{p}\bar{\mathbf{q}} - \bar{\mathbf{p}}\mathbf{q})$, and also that $P_1 \sim p_1^-$, $P_2 \sim p_2^+$, and $P_k^2 = p_k^+ p_k^- - \mathbf{p}_k \bar{\mathbf{p}}_k = 0$, i.e. $p_k^+ p_k^- = \mathbf{p}_k \bar{\mathbf{p}}_k$ for $k = 3, 4, 5$.

Inserting eq. (A.21) into eq. (A.3) we have

$$\mathcal{M}_{ij \rightarrow i' g j'}^{\text{tree}} = 2s \left[g_s \mathbf{T}_{a_3 a_2}^y C_j^{(0)}(P_2^\ominus, P_3^\oplus) \right] \frac{1}{t_2}$$

$$\begin{aligned}
& \times \left[g_s i f^{y a_4 x} \sqrt{2} \frac{\bar{\mathbf{p}}_3 \mathbf{p}_5}{\bar{\mathbf{p}}_4} \right] \frac{1}{t_1} \\
& \times \left[g_s \mathbf{T}_{a_5 a_1}^x C_i^{(0)}(P_1^\ominus, P_5^\oplus) \right], \tag{A.22}
\end{aligned}$$

which can be used to match with eq. (2.22) in the main text, and extract the factors $\mathcal{K}^{(0)}$ and $C_{ij}^{(0)}$ respectively in eqs. (2.23) and (2.24).

To conclude, let us express the results above in terms of the standard helicity basis representation of the amplitude. The relation between the polarization vectors in eq. (A.19) and the polarization vectors expressed in the basis

$$\varepsilon_\mu^\pm(P, K) = \pm \frac{\langle P \pm | \gamma_\mu | K \pm \rangle}{\sqrt{2} \langle K \mp | P \pm \rangle}, \tag{A.23}$$

where K is a reference vector, has been derived in appendix C of [71]. In particular, one has (eq. (55) of [71])

$$\begin{aligned}
\varepsilon_\mu^\oplus(P_i, P_2) &= -\frac{\bar{\mathbf{p}}_i}{\mathbf{p}_i} \varepsilon_{L\mu}^\oplus(P_i), \\
\varepsilon_\mu^\oplus(P_i, P_1) &= -\frac{\bar{\mathbf{p}}_i}{\mathbf{p}_i} \varepsilon_{R\mu}^\oplus(P_i), \\
\varepsilon_\mu^\oplus(P_1, P_2) &= -\varepsilon_{L\mu}^\oplus(P_1), \\
\varepsilon_\mu^\oplus(P_2, P_1) &= \varepsilon_{R\mu}^\oplus(P_2). \tag{A.24}
\end{aligned}$$

Taking into account these relations, we determine eqs. (A.20) and (A.21) in the helicity basis:

$$\begin{aligned}
C_g^{(0)}(P_2^\ominus, P_3^\oplus) &= \Gamma^{\mu_2 \mu_3} \varepsilon_{\mu_2}^{\ominus*}(P_2, P_1) \varepsilon_{\mu_3}^\oplus(P_3, P_1) = -1, \\
C_g^{(0)}(P_1^\ominus, P_5^\oplus) &= \Gamma^{\mu_1 \mu_5} \varepsilon_{\mu_1}^{\ominus*}(P_1, P_2) \varepsilon_{\mu_5}^\oplus(P_5, P_2) = -\frac{\bar{\mathbf{p}}_5}{\mathbf{p}_5}, \tag{A.25}
\end{aligned}$$

in agreement with eq.(26) of [71], and

$$V^{(0)}(Q_1, P_4^\oplus, Q_2) = -\sqrt{2} \frac{\bar{\mathbf{p}}_3 \mathbf{p}_5}{\mathbf{p}_4}, \tag{A.26}$$

in agreement with eq.(27) of [71].

B Colour basis definition

We label the element of the colour basis as $[c_1, c_2]$, where c_i labels the representation in the t_i -channel in terms of its multiplicity number for the group SU(3). We label indices in the fundamental representation of SU(3) as lower indices i_x , while indices in the adjoint representation are labelled as upper indices a_x for particle x . Summed indices in the adjoint representation are labelled as w, x, y, z .

B.1 $qq \rightarrow qgq$

In case of $qq \rightarrow qgq$ the colour basis is labelled by the indices $(i_1, i_2, i_3, a_4, i_5)$. One has

$$\begin{aligned}
c^{[1,8]} &= \frac{\sqrt{2}}{\sqrt{N_c}\sqrt{N_c^2-1}} \delta_{i_5 i_1} (t^{a_4})_{i_3 i_2}, \\
c^{[8,1]} &= \frac{\sqrt{2}}{\sqrt{N_c}\sqrt{N_c^2-1}} \delta_{i_3 i_2} (t^{a_4})_{i_5 i_1}, \\
c^{[8,8]_s} &= \frac{2\sqrt{N_c}}{\sqrt{N_c^2-4}\sqrt{N_c^2-1}} (t^x)_{i_5 i_1} (t^y)_{i_3 i_2} d^{y a_4 x}, \\
c^{[8,8]_a} &= \frac{2}{\sqrt{N_c}\sqrt{N_c^2-1}} (t^x)_{i_5 i_1} (t^y)_{i_3 i_2} i f^{y a_4 x}.
\end{aligned} \tag{B.1}$$

We have for the $\mathbf{T}_{t_i}^2$ matrices

$$\mathbf{T}_{t_1}^2 = \begin{pmatrix} 0 & 0 & 0 & 0 \\ 0 & N_c & 0 & 0 \\ 0 & 0 & N_c & 0 \\ 0 & 0 & 0 & N_c \end{pmatrix}, \quad \mathbf{T}_{t_2}^2 = \begin{pmatrix} N_c & 0 & 0 & 0 \\ 0 & 0 & 0 & 0 \\ 0 & 0 & N_c & 0 \\ 0 & 0 & 0 & N_c \end{pmatrix}. \tag{B.2}$$

B.2 $qg \rightarrow qgg$

It is useful to introduce projectors onto the $\mathbf{10} \pm \overline{\mathbf{10}}$, $\mathbf{27}$, and $\mathbf{0}$ representations, defined respectively as

$$P_{\mathbf{10}+\overline{\mathbf{10}}}^{abcd} = \frac{1}{2} (\delta^{ac} \delta^{bd} - \delta^{ad} \delta^{bc}) - \frac{f^{abe} f^{cde}}{N_c}, \tag{B.3a}$$

$$P_{\mathbf{10}-\overline{\mathbf{10}}}^{abcd} = \frac{1}{2} i d^{ace} f^{bed} - \frac{1}{2} i f^{ace} d^{bed} \tag{B.3b}$$

$$P_{\mathbf{27}}^{abcd} = \frac{N_c d^{abe} d^{cde}}{4(N_c+2)} + \frac{1}{2} f^{ade} f^{cbe} - \frac{1}{4} f^{abe} f^{cde} + \frac{\delta^{ab} \delta^{cd}}{2(N_c+1)} + \frac{1}{4} \delta^{ad} \delta^{bc} + \frac{1}{4} \delta^{ac} \delta^{bd}, \tag{B.3c}$$

$$P_{\mathbf{0}}^{abcd} = -\frac{N_c d^{abe} d^{cde}}{4(N_c-2)} - \frac{1}{2} f^{ade} f^{cbe} + \frac{1}{4} f^{abe} f^{cde} - \frac{\delta^{ab} \delta^{cd}}{2(N_c-1)} + \frac{1}{4} \delta^{ad} \delta^{bc} + \frac{1}{4} \delta^{ac} \delta^{bd}. \tag{B.3d}$$

Note that $P_{\mathbf{0}}^{abce} P_{\mathbf{0}}^{abce} = \frac{1}{4}(N_c-3)N_c^2(N_c+1)$ which vanishes for $N_c = 3$.

In case of $qg \rightarrow qgg$ scattering the quark q is associated to the line $i \rightarrow i'$, while the gluon g is associated to the line $j \rightarrow j'$. The colour basis elements are labelled by the indices $(i_1, a_2, a_3, a_4, i_5)$, and reads

$$\begin{aligned}
c^{[1,8_s]} &= \frac{1}{\sqrt{(N_c^2-4)(N_c^2-1)}} \delta_{i_5 i_1} d^{a_3 a_4 a_2}, \\
c^{[1,8_a]} &= \frac{1}{N_c \sqrt{(N_c^2-1)}} \delta_{i_5 i_1} i f^{a_3 a_4 a_2}, \\
c^{[8,1]} &= \frac{\sqrt{2}}{N_c^2-1} (t^{a_4})_{i_5 i_1} \delta^{a_3 a_2},
\end{aligned}$$

$$\begin{aligned}
c^{[8,8_s]_s} &= \frac{\sqrt{2}N_c}{(N_c^2 - 4)\sqrt{N_c^2 - 1}} (t^x)_{i_5 i_1} d^{a_3 y a_2} d^{y a_4 x} \\
c^{[8,8_s]_a} &= \frac{\sqrt{2}}{\sqrt{(N_c^2 - 4)(N_c^2 - 1)}} (t^x)_{i_5 i_1} d^{a_3 y a_2} i f^{y a_4 x} , \\
c^{[8,8_a]_s} &= \frac{\sqrt{2}}{\sqrt{(N_c^2 - 4)(N_c^2 - 1)}} (t^x)_{i_5 i_1} i f^{a_3 y a_2} d^{y a_4 x} , \\
c^{[8,8_a]_a} &= \frac{\sqrt{2}}{N_c \sqrt{(N_c^2 - 1)}} (t^x)_{i_5 i_1} i f^{a_3 y a_2} i f^{y a_4 x} , \\
c^{[8,10+\overline{10}]} &= \frac{2}{\sqrt{(N_c^2 - 4)(N_c^2 - 1)}} (t^x)_{i_5 i_1} P_{\mathbf{10}+\overline{\mathbf{10}}}^{a_3 a_2 x a_4} , \\
c^{[8,10-\overline{10}]} &= \frac{2}{\sqrt{(N_c^2 - 4)(N_c^2 - 1)}} (t^x)_{i_5 i_1} P_{\mathbf{10}-\overline{\mathbf{10}}}^{a_3 a_2 x a_4} , \\
c^{[8,27]} &= \frac{2\sqrt{2}}{N_c \sqrt{(N_c + 3)(N_c - 1)}} (t^x)_{i_5 i_1} P_{\mathbf{27}}^{a_3 a_2 x a_4} , \\
c^{[8,0]} &= \frac{2\sqrt{2}}{N_c \sqrt{(N_c - 3)(N_c + 1)}} (t^x)_{i_5 i_1} P_{\mathbf{0}}^{a_3 a_2 x a_4} .
\end{aligned} \tag{B.4}$$

In this basis, the quadratic operators measuring the colour flow in the t channel reads

$$\mathbf{T}_{t_1}^2 = \text{diag} [0, 0, N_c, N_c, N_c, N_c, N_c, N_c, N_c, N_c, N_c] , \tag{B.5}$$

and

$$\mathbf{T}_{t_2}^2 = \text{diag} [N_c, N_c, 0, N_c, N_c, N_c, N_c, 2N_c, 2N_c, 2(N_c + 1), 2(N_c - 1)] . \tag{B.6}$$

B.3 $gq \rightarrow ggq$

In case of $gq \rightarrow ggq$ scattering the gluon g is associated to the line $i \rightarrow i'$, while the quark q is associated to the line $j \rightarrow j'$. The colour basis elements are labelled by the indices $(a_1, i_2, i_3, a_4, a_5)$, and reads

$$\begin{aligned}
c^{[8_s,1]} &= \frac{1}{\sqrt{(N_c^2 - 4)(N_c^2 - 1)}} \delta_{i_3 i_2} d^{a_5 a_4 a_1} , \\
c^{[8_a,1]} &= \frac{1}{N_c \sqrt{(N_c^2 - 1)}} \delta_{i_3 i_2} i f^{a_5 a_4 a_1} , \\
c^{[1,8]} &= \frac{\sqrt{2}}{N_c^2 - 1} (t^{a_4})_{i_3 i_2} \delta^{a_5 a_1} , \\
c^{[8_s,8]_s} &= \frac{\sqrt{2}N_c}{(N_c^2 - 4)\sqrt{N_c^2 - 1}} (t^x)_{i_3 i_2} d^{a_5 y a_1} d^{y a_4 x} \\
c^{[8_s,8]_a} &= \frac{\sqrt{2}}{\sqrt{(N_c^2 - 4)(N_c^2 - 1)}} (t^x)_{i_3 i_2} d^{a_5 y a_1} i f^{y a_4 x} , \\
c^{[8_a,8]_s} &= \frac{\sqrt{2}}{\sqrt{(N_c^2 - 4)(N_c^2 - 1)}} (t^x)_{i_3 i_2} i f^{a_5 y a_1} d^{y a_4 x} ,
\end{aligned} \tag{B.7}$$

$$\begin{aligned}
c^{[8_a,8]_a} &= \frac{\sqrt{2}}{N_c \sqrt{(N_c^2 - 1)}} (t^x)_{i_3 i_2}, i f^{a_5 y a_1} i f^{y a_4 x}, \\
c^{[10+\overline{10},8]} &= \frac{2}{\sqrt{(N_c^2 - 4)(N_c^2 - 1)}} (t^x)_{i_3 i_2} P_{\mathbf{10}+\overline{\mathbf{10}}}^{a_5 a_1 x a_4}, \\
c^{[10-\overline{10},8]} &= \frac{2}{\sqrt{(N_c^2 - 4)(N_c^2 - 1)}} (t^x)_{i_3 i_2} P_{\mathbf{10}-\overline{\mathbf{10}}}^{a_5 a_1 x a_4}, \\
c^{[27,8]} &= \frac{2\sqrt{2}}{N_c \sqrt{(N_c + 3)(N_c - 1)}} (t^x)_{i_3 i_2} P_{\mathbf{27}}^{a_5 a_1 x a_4}, \\
c^{[0,8]} &= \frac{2\sqrt{2}}{N_c \sqrt{(N_c - 3)(N_c + 1)}} (t^x)_{i_3 i_2} P_{\mathbf{0}}^{a_5 a_1 x a_4}.
\end{aligned}$$

With this basis choice, it is easy to check that the value of $\mathbf{T}_{t_1}^2$ and $\mathbf{T}_{t_2}^2$ are exchanged compared to the case $qg \rightarrow qgg$, i.e. for $gq \rightarrow gqg$ one has

$$\mathbf{T}_{t_1}^2 = \text{diag} [N_c, N_c, 0, N_c, N_c, N_c, N_c, 2N_c, 2N_c, 2(N_c + 1), 2(N_c - 1)], \quad (\text{B.8})$$

and

$$\mathbf{T}_{t_2}^2 = \text{diag} [0, 0, N_c, N_c, N_c, N_c, N_c, N_c, N_c, N_c, N_c]. \quad (\text{B.9})$$

B.4 $gq \rightarrow gqg$

Using the projectors defined in eq. (B.3) we get

$$\begin{aligned}
c^{[1,8_a]} &= \frac{1}{(N_c^2 - 1)\sqrt{N_c}} \delta^{a_5 a_1} i f^{a_3 a_4 a_2}, \\
c^{[8_a,1]} &= \frac{1}{(N_c^2 - 1)\sqrt{N_c}} \delta^{a_3 a_2} i f^{a_1 a_5 a_4}, \\
c^{[8_s,8_s]} &= \frac{\sqrt{N_c}}{(N_c^2 - 4)\sqrt{N_c^2 - 1}} d^{a_1 a_5 x} i f^{y a_4 x} d^{a_2 a_3 y}, \\
c^{[8_s,8_a]} &= \frac{\sqrt{N_c}}{(N_c^2 - 4)\sqrt{N_c^2 - 1}} d^{a_1 a_5 x} d^{y a_4 x} i f^{a_2 a_3 y}, \\
c^{[8_a,8_s]} &= \frac{\sqrt{N_c}}{(N_c^2 - 4)\sqrt{N_c^2 - 1}} i f^{a_1 a_5 x} d^{y a_4 x} d^{a_2 a_3 y}, \\
c^{[8_a,8_a]} &= \frac{1}{\sqrt{N_c^3(N_c^2 - 1)}} i f^{a_1 a_5 x} i f^{y a_4 x} i f^{a_2 a_3 y}, \\
c^{[8_s,10-\overline{10}]} &= \frac{\sqrt{2N_c}}{(N_c^2 - 4)\sqrt{N_c^2 - 1}} d^{a_1 a_5 x} P_{\mathbf{10}-\overline{\mathbf{10}}}^{a_3 a_2 x a_4}, \\
c^{[10-\overline{10},8_s]} &= \frac{\sqrt{2N_c}}{(N_c^2 - 4)\sqrt{N_c^2 - 1}} d^{a_2 a_3 x} P_{\mathbf{10}-\overline{\mathbf{10}}}^{a_1 a_5 a_4 x}, \\
c^{[8_a,10+\overline{10}]} &= \frac{\sqrt{2}}{\sqrt{N_c(N_c^2 - 4)(N_c^2 - 1)}} i f^{a_1 a_5 x} P_{\mathbf{10}+\overline{\mathbf{10}}}^{a_3 a_2 x a_4}, \\
c^{[10+\overline{10},8_a]} &= \frac{\sqrt{2}}{\sqrt{N_c(N_c^2 - 4)(N_c^2 - 1)}} i f^{a_2 a_3 x} P_{\mathbf{10}+\overline{\mathbf{10}}}^{a_1 a_5 a_4 x},
\end{aligned}$$

$$\begin{aligned}
c^{[8_a,27]} &= \frac{2}{\sqrt{N_c^3(N_c+3)(N_c-1)}} if^{a_1 a_5 x} P_{\mathbf{27}}^{a_3 a_2 x a_4}, \\
c^{[27,8_a]} &= \frac{2}{\sqrt{N_c^3(N_c+3)(N_c-1)}} if^{a_2 a_3 x} P_{\mathbf{27}}^{a_1 a_5 a_4 x}, \\
c^{[8_a,0]} &= \frac{2}{\sqrt{N_c^3(N_c-3)(N_c+1)}} if^{a_1 a_5 x} P_{\mathbf{0}}^{a_3 a_2 x a_4}, \\
c^{[0,8_a]} &= \frac{2}{\sqrt{N_c^3(N_c-3)(N_c+1)}} if^{a_2 a_3 x} P_{\mathbf{0}}^{a_1 a_5 a_4 x}, \\
c^{[10,\overline{10}]_1} &= \frac{2}{\sqrt{N_c(N_c^2-4)(N_c^2-1)}} P_{\mathbf{10+\overline{10}}}^{a_1 a_5 z x} if^{y a_4 x} P_{\mathbf{10+\overline{10}}}^{a_3 a_2 y z}, \\
c^{[10,\overline{10}]_2} &= \frac{2\sqrt{N_c}}{\sqrt{(N_c^2-4)(N_c^2-1)(N_c+3)(N_c-3)}} \left(P_{\mathbf{10-\overline{10}}}^{a_1 a_5 z x} d^{y a_4 x} P_{\mathbf{10+\overline{10}}}^{a_3 a_2 y z} \right. \\
&\quad \left. + \frac{1}{N_c} P_{\mathbf{10+\overline{10}}}^{a_1 a_5 z x} if^{y a_4 x} P_{\mathbf{10+\overline{10}}}^{a_3 a_2 y z} \right), \\
c^{[10+\overline{10},27]} &= \frac{2\sqrt{2}}{\sqrt{N_c(N_c^2-1)(N_c-2)(N_c+3)}} P_{\mathbf{10+\overline{10}}}^{a_1 a_5 z x} if^{y a_4 x} P_{\mathbf{27}}^{a_3 a_2 y z}, \\
c^{[27,10+\overline{10}]} &= \frac{2\sqrt{2}}{\sqrt{N_c(N_c^2-1)(N_c-2)(N_c+3)}} P_{\mathbf{27}}^{a_1 a_5 z x} if^{y a_4 x} P_{\mathbf{10+\overline{10}}}^{a_3 a_2 y z}, \\
c^{[10+\overline{10},0]} &= \frac{2\sqrt{2}}{\sqrt{N_c(N_c^2-1)(N_c+2)(N_c-3)}} P_{\mathbf{10+\overline{10}}}^{a_1 a_5 z x} if^{y a_4 x} P_{\mathbf{0}}^{a_3 a_2 y z}, \\
c^{[0,10+\overline{10}]} &= \frac{2\sqrt{2}}{\sqrt{N_c(N_c^2-1)(N_c+2)(N_c-3)}} P_{\mathbf{0}}^{a_1 a_5 z x} if^{y a_4 x} P_{\mathbf{10+\overline{10}}}^{a_3 a_2 y z}, \\
c^{[27,27]} &= \frac{2\sqrt{2}}{N_c \sqrt{(N_c^2-1)(N_c+3)}} P_{\mathbf{27}}^{a_1 a_5 z x} if^{y a_4 x} P_{\mathbf{27}}^{a_3 a_2 y z}, \\
c^{[0,0]} &= \frac{2\sqrt{2}}{N_c \sqrt{(N_c^2-1)(N_c-3)}} P_{\mathbf{0}}^{a_1 a_5 z x} if^{y a_4 x} P_{\mathbf{0}}^{a_3 a_2 y z}.
\end{aligned} \tag{B.10}$$

In this basis, the quadratic operators measuring the colour flow in the t channel reads

$$\mathbf{T}_{t_1}^2 = \text{diag}[0, N_c, N_c, N_c, N_c, N_c, N_c, 2N_c, N_c, 2N_c, N_c, 2(N_c+1), N_c, 2(N_c-1), \\
2N_c, 2N_c, 2N_c, 2(N_c+1), 2N_c, 2(N_c-1), 2(N_c+1), 2(N_c-1)], \tag{B.11}$$

and

$$\mathbf{T}_{t_2}^2 = \text{diag}[N_c, 0, N_c, N_c, N_c, N_c, 2N_c, N_c, 2N_c, N_c, 2(N_c+1), N_c, 2(N_c-1), N_c, \\
2N_c, 2N_c, 2(N_c+1), 2N_c, 2(N_c-1), 2N_c, 2(N_c+1), 2(N_c-1)]. \tag{B.12}$$

B.5 Color space formalism

Given the color basis defined above, an amplitude is interpreted as a vector in color space. This is best expressed by writing the amplitude in vector form $\mathcal{M}_{ij \rightarrow igj} = |\mathcal{M}_{ij \rightarrow igj}\rangle$, [72–74], then one has

$$\mathcal{M}_{ij \rightarrow igj} = \sum_i |c^{[i]}\rangle \langle c^{[i]} | \mathcal{M}_{ij \rightarrow igj}\rangle = \sum_i c^{[i]} \mathcal{M}_{ij \rightarrow igj}^{[i]}, \tag{B.13}$$

where in the second equality we have implicitly defined the vector of color basis element $|c^{[i]}\rangle \equiv c^{[i]}$, and the corresponding coefficients $\mathcal{M}_{ij \rightarrow igj}^{[i]} \equiv \langle c^{[i]} | \mathcal{M}_{ij \rightarrow igj} \rangle$, as used in the main text, for instance in eq. (2.26). Within this formalism, the action of a color operator \mathbf{T}_X on the amplitude reads

$$\mathbf{T}_X \mathcal{M}_{ij \rightarrow igj} = \sum_{ij} |c^{[j]}\rangle \underbrace{\langle c^{[j]} | \mathbf{T}_X | c^{[i]}\rangle}_{\langle c^{[j]} | \mathcal{M}_{ij \rightarrow igj} \rangle} \langle c^{[i]} | \mathcal{M}_{ij \rightarrow igj} \rangle = \sum_{ji} c^{[j]} \underbrace{\mathbf{T}_X^{[j][i]}}_{\mathcal{M}_{ij \rightarrow igj}^{[j]}} \mathcal{M}_{ij \rightarrow igj}^{[i]}, \quad (\text{B.14})$$

where $\mathbf{T}_X^{[j][i]} \equiv \langle c^{[j]} | \mathbf{T}_X | c^{[i]}\rangle$ represents the matrix in color space associated with the color operator \mathbf{T}_X . In the main text we have used the notation in the second equality in eq. (B.14), for instance in eq. (7.21).

The tree level amplitudes for the processes $qq \rightarrow qqq$, $qg \rightarrow qgg$, $gg \rightarrow ggg$ have a single non-zero element, corresponding to the propagation of a gluon from the projectile i to the target j , with emission of a gluon g , as indicated in eq. (7.22):

$$\begin{aligned} \mathcal{M}_{qq \rightarrow qqq}^{\text{tree}} &= c^{[8,8]_a} (\mathcal{M}_{qq \rightarrow qqq}^{\text{tree}})^{[8,8]_a}, \\ \mathcal{M}_{qg \rightarrow qgg}^{\text{tree}} &= c^{[8,8_a]_a} (\mathcal{M}_{qg \rightarrow qgg}^{\text{tree}})^{[8,8_a]_a}, \\ \mathcal{M}_{gg \rightarrow ggg}^{\text{tree}} &= c^{[8_a,8_a]} (\mathcal{M}_{gg \rightarrow ggg}^{\text{tree}})^{[8_a,8_a]}. \end{aligned} \quad (\text{B.15})$$

Comparison between eqs. (2.22), (2.24) and the color bases in eqs. (B.1), (B.4), (B.7) and (B.10) immediately gives

$$\begin{aligned} (\mathcal{M}_{qq \rightarrow qqq}^{\text{tree}})^{[8,8]_a} &= \frac{\sqrt{N_c} \sqrt{N_c^2 - 1}}{2} C_i^{(0)} \mathcal{K}^{(0)} C_j^{(0)}, \\ (\mathcal{M}_{qg \rightarrow qgg}^{\text{tree}})^{[8,8_a]_a} &= \frac{N_c \sqrt{(N_c^2 - 1)}}{\sqrt{2}} C_i^{(0)} \mathcal{K}^{(0)} C_j^{(0)}, \\ (\mathcal{M}_{gg \rightarrow ggg}^{\text{tree}})^{[8_a,8_a]} &= \sqrt{N_c^3 (N_c^2 - 1)} C_i^{(0)} \mathcal{K}^{(0)} C_j^{(0)}. \end{aligned} \quad (\text{B.16})$$

C Variables conversion in the MRK power expansion

We provide here details about the conversion between the minimal set of variables $(w, \bar{w}, X_{34}, X_{45}, |\mathbf{q}_2|^2)$ used in section 3.2 and the one used elsewhere, $(z, \bar{z}, s_1, s_2, r)$. Since X_{34} and X_{45} are dimensionless, while s_1 , s_2 , and r carry mass dimension squared, we need one more variable to normalize by in the conversion, which we pick to be $|\mathbf{q}_2|^2$ (see eq. (2.13)). Nevertheless, since we consider dimensionless functions, $r_i/\mathcal{M}^{(0)}$, this additional variable $|\mathbf{q}_2|^2$ never appears in the reconstruction. The relations read,

$$X_{34} = \frac{1}{x} \frac{s_2 w \bar{w}}{|\mathbf{q}_2|^2} - w - \bar{w} - x \frac{|\mathbf{q}_2|^2}{s_2} \quad (\text{C.1})$$

$$X_{45} = \frac{1}{x} \frac{s_1 w \bar{w}}{|\mathbf{q}_2|^2 (1-w)(1-\bar{w})} + \frac{-2+w+\bar{w}}{(1-w)(1-\bar{w})} - x \frac{|\mathbf{q}_2|^2}{s_1 w \bar{w}} \quad (\text{C.2})$$

$$w = z + x \frac{r z (1-z)}{s_1 s_2 (z - \bar{z})} [s_1 (1-z) + s_2 z] - x^2 \frac{r^2 z (1-z)}{s_1^2 s_2^2 (z - \bar{z})^3} \times$$

$$\left[s_1^2(1-z)^2(z^2 + \bar{z} - z\bar{z} - \bar{z}^2) + s_2^2 z^2(z^2 + \bar{z}(2 - \bar{z}) - z(1 + \bar{z})) + s_1 s_2 z(1-z)(-z(1-z) + 3\bar{z}(1 - \bar{z})) \right] \quad (\text{C.3})$$

where $r = s_1 s_2 / s$. Similarly, for \bar{w} , through a $z \leftrightarrow \bar{z}$ swap of eq. (C.3).

D Gluon Regge trajectory, impact factors and vertex

In this appendix we provide the impact factors at one loop and the Regge trajectory up to two loops. Furthermore, we discuss their factorization and renormalization scale dependence, for ease of comparison with appendix A of [23], where impact factors and Regge trajectory are given for $\mu^2 = \tau = -t$.

Let us start by recalling the perturbative expansions introduced in eqs. (4.2), (4.5), (4.6), (4.7), indicating the full scale dependence: we have

$$\alpha_g(-t, \mu^2) = \frac{g(\mu^2)^2}{4\pi^2} \alpha_g^{(1)}(-t, \mu^2) + \left(\frac{g(\mu^2)^2}{4\pi^2} \right)^2 \alpha_g^{(2)}(-t, \mu^2) + \dots, \quad (\text{D.1})$$

for the Regge trajectory, then

$$C_i(-t, \tau, \mu^2) = g(\mu^2) C_i^{(0)}(-t, \tau, \mu^2) \left[1 + \frac{g(\mu^2)^2}{4\pi^2} c_i^{(1)}(-t, \tau, \mu^2) + \dots \right], \quad (\text{D.2})$$

for the impact factors, and

$$V(t_1, t_2, |\mathbf{p}_4|^2, \tau, \mu^2) = g(\mu^2) V^{(0)}(t_1, t_2, |\mathbf{p}_4|^2, \tau, \mu^2) \times \left[1 + \frac{g(\mu^2)^2}{4\pi^2} v^{(1)}(t_1, t_2, |\mathbf{p}_4|^2, \tau, \mu^2) + \dots \right], \quad (\text{D.3})$$

for the Lipatov vertex. The perturbative coefficients reads respectively

$$\alpha_g^{(1)}(-t, \mu^2) = \left(\frac{\mu^2}{-t} \right)^\epsilon \frac{r_\Gamma}{2\epsilon} = \left(\frac{\mu^2}{-t} \right)^\epsilon \frac{e^{\epsilon\gamma_E} \Gamma^2(1 - \epsilon) \Gamma(1 + \epsilon)}{2\epsilon \Gamma(1 - 2\epsilon)}, \quad (\text{D.4a})$$

$$\alpha_g^{(2)}(-t, \mu^2) = \left(\frac{\mu^2}{-t} \right)^{2\epsilon} \left\{ -\frac{b_0}{16\epsilon^2} + \frac{1}{8\epsilon} \left[\left(\frac{67}{18} - \zeta_2 \right) C_A - \frac{10T_R n_f}{9} \right] + C_A \left(\frac{101}{108} - \frac{\zeta_3}{8} \right) - \frac{7T_R n_f}{27} + \mathcal{O}(\epsilon) \right\}, \quad (\text{D.4b})$$

for the Regge trajectory, and [59, 131]

$$c_q^{(1)} = \frac{r_\Gamma}{4} \left(\frac{\mu^2}{-t} \right)^\epsilon \frac{1}{\epsilon(1 - 2\epsilon)} \left\{ C_A \left[(1 - 2\epsilon) \left(\log \frac{\tau}{-t} + \psi(1 + \epsilon) - 2\psi(-\epsilon) + \psi(1) \right) + \frac{1}{4(3 - 2\epsilon)} + \frac{1}{\epsilon} - \frac{7}{4} \right] + \frac{1}{N_c} \left(\frac{1}{\epsilon} - \frac{1 - 2\epsilon}{2} \right) - n_f \frac{1 - \epsilon}{3 - 2\epsilon} \right\} - \frac{b_0}{8\epsilon}, \quad (\text{D.5})$$

$$c_g^{(1)} = \frac{r_\Gamma}{4} \left(\frac{\mu^2}{-t} \right)^\epsilon \left\{ C_A \left[-\frac{2}{\epsilon^2} + \frac{1}{\epsilon} \left(\log \frac{\tau}{-t} + \psi(1 + \epsilon) - 2\psi(-\epsilon) + \psi(1) \right) + \frac{1}{\epsilon(1 - 2\epsilon)} \left(\frac{1 - \epsilon}{2(3 - 2\epsilon)} - 2 \right) \right] + n_f \frac{1 - \epsilon}{\epsilon(1 - 2\epsilon)(3 - 2\epsilon)} \right\} - \frac{b_0}{8\epsilon}, \quad (\text{D.6})$$

respectively for the quark and gluon impact factor. Note that in these equations, the parameter δ_R related to the regularization scheme has been set to 1, corresponding to the HV or CDR scheme, see [59, 131] for further details. In these equations b_0 represents the one loop coefficient of the beta function: defining

$$\mu^2 \frac{d}{d\mu^2} a_s = -\epsilon a_s - b_0 a_s^2 - b_1 a_s^3 + \dots \quad (\text{D.7})$$

with $a_s = g_s^2/(4\pi)^2$, we have

$$b_0 = \frac{11C_A - 2n_f}{3}, \quad (\text{D.8a})$$

$$b_1 = \frac{34}{3}C_A^2 - \frac{10}{3}C_A n_f - 2C_F n_f. \quad (\text{D.8b})$$

In order to relate the coefficients in eqs. (D.4) and (D.5) to the one in appendix A of [23], given at $\mu^2 = \tau = -t$, we consider the factorised expression for the $2 \rightarrow 2$ amplitude

$$\text{Disp.}\{\mathcal{M}_{ij \rightarrow ij}\} = 2\frac{s}{t} C_i(-t, \tau, \mu^2) \left(\frac{s}{\tau}\right)^{C_A \alpha_g(-t, \mu^2)} C_j(-t, \tau, \mu^2). \quad (\text{D.9})$$

Expanding to one-loop order one finds

$$\begin{aligned} \text{Disp.}\{\mathcal{M}_{ij \rightarrow ij}\} &= 2\frac{s}{t} g(\mu^2)^2 C_i^{(0)}(-t, \tau, \mu^2) C_j^{(0)}(-t, \tau, \mu^2) \left[1 + \right. \\ &\quad \left. + \frac{g(\mu^2)^2}{4\pi^2} \left(c_i^{(1)}(-t, \tau, \mu^2) + c_j^{(1)}(-t, \tau, \mu^2) + C_A \alpha_g^{(1)}(-t, \mu^2) \log \frac{s}{\tau} \right) + \dots \right], \end{aligned} \quad (\text{D.10})$$

Since the amplitude itself is renormalisation group invariant, equating the perturbative expansion above for generic μ^2 and for $\mu^2 = -t$:

$$\begin{aligned} g(-t) C_i^{(0)}(-t, \tau, -t) + \frac{g(-t)^3}{4\pi^2} C_i^{(0)}(-t, \tau, -t) c_i^{(1)}(-t, \tau, -t) + \dots \\ = g(\mu^2) C_i^{(0)}(-t, \tau, \mu^2) + \frac{g(\mu^2)^3}{4\pi^2} C_i^{(0)}(-t, \tau, \mu^2) c_i^{(1)}(-t, \tau, \mu^2) + \dots \end{aligned} \quad (\text{D.11})$$

we are able to relate $C_i(-t, \tau, -t)$ and $C_i(-t, \tau, \mu^2)$. To this end we need to solve eq. (D.7) perturbatively: up to $\mathcal{O}[\alpha(\mu_0^2)^3]$ we have

$$a(\mu^2) = \frac{a(\mu_0^2) \left(\frac{\mu_0^2}{\mu^2}\right)^\epsilon}{1 + \frac{a(\mu_0^2)}{\epsilon} \left[1 - \left(\frac{\mu_0^2}{\mu^2}\right)^\epsilon \right] \left[b_0 + \frac{a(\mu_0^2)}{2} b_1 \left(1 + \left(\frac{\mu_0^2}{\mu^2}\right)^\epsilon \right) \right]} + \mathcal{O}[a(\mu_0^2)^4]. \quad (\text{D.12})$$

We use the equation above to write the coupling $g(-t) = 4\pi\sqrt{a(-t)}$, on the LHS of eq. (D.11), in terms of $g(\mu^2)$, obtaining

$$C_g^{(0)}(-t, \tau, \mu^2) = \left(\frac{\mu^2}{-t}\right)^{\frac{\epsilon}{2}} C_g^{(0)}(-t, \tau, -t), \quad (\text{D.13a})$$

$$c_g^{(1)}(-t, \tau, \mu^2) = \left(\frac{\mu^2}{-t}\right)^\epsilon c_g^{(1)}(-t, \tau, -t) - \frac{b_0}{8\epsilon} \left[1 - \left(\frac{\mu^2}{-t}\right)^\epsilon \right], \quad (\text{D.13b})$$

$$c_g^{(2)}(-t, \tau, \mu^2) = \left(\frac{\mu^2}{-t}\right)^{2\epsilon} c_g^{(2)}(-t, \tau, -t) + \frac{3b_0^2}{128\epsilon^2} \left[1 - \left(\frac{\mu^2}{-t}\right)^\epsilon\right]^2 - \frac{1}{64\epsilon} \left[1 - \left(\frac{\mu^2}{-t}\right)^\epsilon\right] \left\{ b_1 \left[1 + \left(\frac{\mu^2}{-t}\right)^\epsilon\right] + 24b_0 \left(\frac{\mu^2}{-t}\right)^\epsilon c_g^{(1)}(-t, \tau, -t) \right\}. \quad (\text{D.13c})$$

At this point we still need to relate the impact factors $C_i(-t, \tau, -t)$, where the factorization scale is generic, to the impact factors evaluated at the scale $\tau = -t$. Once again, this can be easily done by exploiting the scale invariance of the amplitude. We obtain

$$C_g(t, \tau, -t) = C_g(-t, -t, -t) \left(\frac{-t}{\tau}\right)^{-C_A \frac{\alpha_g(-t, -t)}{2}}, \quad (\text{D.14})$$

which expanding to second order in α_s gives

$$C_g^{(0)}(-t, \tau, -t) = C_g^{(0)}(-t, -t, -t), \quad (\text{D.15a})$$

$$c_g^{(1)}(-t, \tau, -t) = c_g^{(1)} - \frac{C_A \alpha_g^{(1)}}{2} \log\left(\frac{-t}{\tau}\right), \quad (\text{D.15b})$$

$$c_g^{(2)}(-t, \tau, -t) = c_g^{(2)} + \frac{1}{2} \left(\frac{C_A \alpha_g^{(1)}}{2} \log\frac{-t}{\tau}\right)^2 - \frac{C_A}{2} \log\frac{-t}{\tau} [c_g^{(1)} \alpha_g^{(1)} + \alpha_g^{(2)}]. \quad (\text{D.15c})$$

where $c_g^{(1)} \equiv c_g^{(1)}(-t, -t, -t)$, $\alpha_g^{(1)} \equiv \alpha_g^{(1)}(-t, -t)$, and similarly $c_g^{(2)} \equiv c_g^{(2)}(-t, -t, -t)$, $\alpha_g^{(2)} \equiv \alpha_g^{(2)}(-t, -t)$, are given in the ancillary file of [23]. Combining eq.(D.13) with eq.(D.15) we obtain

$$C_g^{(0)}(-t, \tau, \mu^2) = \left(\frac{\mu^2}{-t}\right)^{\frac{\epsilon}{2}} C_g^{(0)}(-t, -t, -t), \quad (\text{D.16a})$$

$$c_g^{(1)}(-t, \tau, \mu^2) = \left(\frac{\mu^2}{-t}\right)^\epsilon \left[c_g^{(1)} - \frac{C_A \alpha_g^{(1)}}{2} \log\left(\frac{-t}{\tau}\right) \right] - \frac{b_0}{8\epsilon} \left[1 - \left(\frac{\mu^2}{-t}\right)^\epsilon\right], \quad (\text{D.16b})$$

$$c_g^{(2)}(-t, \tau, \mu^2) = \left(\frac{\mu^2}{-t}\right)^{2\epsilon} \left\{ c_g^{(2)} + \frac{C_A^2}{8} (\alpha_g^{(1)})^2 \log^2\left(\frac{-t}{\tau}\right) - \frac{C_A}{2} \log\left(\frac{-t}{\tau}\right) (c_g^{(1)} \alpha_g^{(1)} + \alpha_g^{(2)}) \right\} - \frac{1}{64\epsilon} \left[1 - \left(\frac{\mu^2}{-t}\right)^\epsilon\right] \left\{ b_1 \left[1 + \left(\frac{\mu^2}{-t}\right)^\epsilon\right] + 24b_0 \left(\frac{\mu^2}{-t}\right)^\epsilon \left[c_g^{(1)} - \frac{C_A \alpha_g^{(1)}}{2} \log\left(\frac{-t}{\tau}\right) \right] \right\} + \frac{3}{128\epsilon^2} b_0^2 \left[1 - \left(\frac{\mu^2}{-t}\right)^\epsilon\right]^2. \quad (\text{D.16c})$$

Repeating the same procedure for the Regge trajectory we find

$$\alpha_g^{(1)}(-t, \mu^2) = \alpha_g^{(1)}(-t, -t) \left(\frac{\mu^2}{-t}\right)^\epsilon, \quad (\text{D.17a})$$

$$\alpha_g^{(2)}(-t, \mu^2) = \alpha_g^{(2)}(-t, -t) \left(\frac{\mu^2}{-t} \right)^{2\epsilon} - \alpha_g^{(1)}(-t, -t) \left(\frac{\mu^2}{-t} \right)^\epsilon \frac{b_0}{4\epsilon} \left[1 - \left(\frac{\mu^2}{-t} \right)^\epsilon \right]. \quad (\text{D.17b})$$

Once the scale dependence for the impact factors and Regge trajectory has been obtained, it can be used in the factorization formula for the $2 \rightarrow 3$ scattering amplitudes (eq. (4.10) in the main text) to derive the scale dependence of the Lipatov vertex. After some work we find that the Lipatov vertex evaluated at a generic renormalization scale μ^2 is related to the vertex at the scale $\mu^2 = |\mathbf{p}_4|^2$ as follows:

$$V_0(t_1, t_2, |\mathbf{p}_4|^2, \tau, \mu^2) = V_0(t_1, t_2, |\mathbf{p}_4|^2, \tau, |\mathbf{p}_4|^2) \left(\frac{\mu^2}{|\mathbf{p}_4|^2} \right)^{\frac{\epsilon}{2}}, \quad (\text{D.18a})$$

$$v^{(1)}(t_1, t_2, |\mathbf{p}_4|^2, \tau, \mu^2) = v^{(1)}(t_1, t_2, |\mathbf{p}_4|^2, \tau, |\mathbf{p}_4|^2) \left(\frac{\mu^2}{|\mathbf{p}_4|^2} \right)^\epsilon - \frac{b_0}{8\epsilon} \left[1 - \left(\frac{\mu^2}{|\mathbf{p}_4|^2} \right)^\epsilon \right], \quad (\text{D.18b})$$

$$v^{(2)}(t_1, t_2, |\mathbf{p}_4|^2, \tau, \mu^2) = v^{(2)}(t_1, t_2, |\mathbf{p}_4|^2, \tau, |\mathbf{p}_4|^2) \left(\frac{\mu^2}{|\mathbf{p}_4|^2} \right)^{2\epsilon} + \frac{3b_0^2}{128\epsilon^2} \left[\left(\frac{\mu^2}{|\mathbf{p}_4|^2} \right)^\epsilon - 1 \right]^2 - \frac{1}{64\epsilon} \left[1 - \left(\frac{\mu^2}{|\mathbf{p}_4|^2} \right)^\epsilon \right] \left\{ b_1 \left[1 + \left(\frac{\mu^2}{|\mathbf{p}_4|^2} \right)^\epsilon \right] + 24b_0 \left(\frac{\mu^2}{|\mathbf{p}_4|^2} \right)^\epsilon v^{(1)}(t_1, t_2, |\mathbf{p}_4|^2, \tau, |\mathbf{p}_4|^2) \right\}. \quad (\text{D.18c})$$

Furthermore, the relation between the Lipatov vertex evaluated at a generic factorization scale τ and the vertex at $\tau = |\mathbf{p}_4|^2$ is given by

$$V(t_1, t_2, |\mathbf{p}_4|^2, \tau, \mu^2) = V(t_1, t_2, |\mathbf{p}_4|^2, |\mathbf{p}_4|^2, \mu^2) \left(\frac{|\mathbf{p}_4|^2}{\tau} \right)^{-\frac{1}{2} [\alpha_g(t_1, \mu^2) + \alpha_g(t_2, \mu^2)]}, \quad (\text{D.19})$$

and expanding to second order in α_s we obtain

$$V_0(t_1, t_2, |\mathbf{p}_4|^2, \tau, |\mathbf{p}_4|^2) = V_0(t_1, t_2, |\mathbf{p}_4|^2, |\mathbf{p}_4|^2, |\mathbf{p}_4|^2), \quad (\text{D.20a})$$

$$v^{(1)}(t_1, t_2, |\mathbf{p}_4|^2, \tau, |\mathbf{p}_4|^2) = v^{(1)}(t_1, t_2, |\mathbf{p}_4|^2) - \frac{\alpha_g^{(1)} C_A}{2} \log \frac{|\mathbf{p}_4|^2}{\tau} \left[\left(\frac{|\mathbf{p}_4|^2}{-t_1} \right)^\epsilon + \left(\frac{|\mathbf{p}_4|^2}{-t_2} \right)^\epsilon \right], \quad (\text{D.20b})$$

$$v^{(2)}(t_1, t_2, |\mathbf{p}_4|^2, \tau, |\mathbf{p}_4|^2) = v^{(2)}(t_1, t_2, |\mathbf{p}_4|^2) - v^{(1)}(t_1, t_2, |\mathbf{p}_4|^2) \frac{\alpha_g^{(1)} C_A}{2} \log \frac{|\mathbf{p}_4|^2}{\tau} \left[\left(\frac{|\mathbf{p}_4|^2}{-t_1} \right)^\epsilon + \left(\frac{|\mathbf{p}_4|^2}{-t_2} \right)^\epsilon \right] - \frac{\alpha_g^{(1)} C_A b_0}{8\epsilon} \log \frac{|\mathbf{p}_4|^2}{\tau} \left[\left(\frac{|\mathbf{p}_4|^2}{-t_1} \right)^{2\epsilon} + \left(\frac{|\mathbf{p}_4|^2}{-t_2} \right)^{2\epsilon} - \left(\frac{|\mathbf{p}_4|^2}{-t_1} \right)^\epsilon - \left(\frac{|\mathbf{p}_4|^2}{-t_2} \right)^\epsilon \right] + \frac{C_A}{8} \log \frac{|\mathbf{p}_4|^2}{\tau} \left\{ (\alpha_g^{(1)})^2 C_A \log \frac{|\mathbf{p}_4|^2}{\tau} \left[\left(\frac{|\mathbf{p}_4|^2}{-t_1} \right)^\epsilon + \left(\frac{|\mathbf{p}_4|^2}{-t_2} \right)^\epsilon \right]^2 - 4\alpha_g^{(2)} \left[\left(\frac{|\mathbf{p}_4|^2}{-t_1} \right)^{2\epsilon} + \left(\frac{|\mathbf{p}_4|^2}{-t_2} \right)^{2\epsilon} \right] \right\} \quad (\text{D.20c})$$

Combining eq. (D.18) with eq. (D.20) we have

$$V_0(t_1, t_2, |\mathbf{p}_4|^2, \tau, \mu^2) = V_0(t_1, t_2, |\mathbf{p}_4|^2, |\mathbf{p}_4|^2, |\mathbf{p}_4|^2) \left(\frac{\mu^2}{|\mathbf{p}_4|^2} \right)^{\frac{\epsilon}{2}}, \quad (\text{D.21a})$$

$$v^{(1)}(t_1, t_2, |\mathbf{p}_4|^2, \tau, \mu^2) = v^{(1)}(t_1, t_2, |\mathbf{p}_4|^2) \left(\frac{\mu^2}{|\mathbf{p}_4|^2} \right)^{\epsilon} + \frac{b_0}{8\epsilon} \left[\left(\frac{\mu^2}{|\mathbf{p}_4|^2} \right)^{\epsilon} - 1 \right] \\ - \frac{\alpha_g^{(1)} C_A}{2} \log \frac{|\mathbf{p}_4|^2}{\tau} \left[\left(\frac{|\mathbf{p}_4|^2}{-t_1} \right)^{\epsilon} + \left(\frac{|\mathbf{p}_4|^2}{-t_2} \right)^{\epsilon} \right], \quad (\text{D.21b})$$

$$v^{(2)}(t_1, t_2, |\mathbf{p}_4|^2, \tau, \mu^2) = v^{(2)}(t_1, t_2, |\mathbf{p}_4|^2) \left(\frac{\mu^2}{|\mathbf{p}_4|^2} \right)^{2\epsilon} \\ + v^{(1)}(t_1, t_2, |\mathbf{p}_4|^2) \left\{ \frac{3b_0}{8\epsilon} \left(\frac{\mu^2}{|\mathbf{p}_4|^2} \right)^{\epsilon} \left[\left(\frac{\mu^2}{|\mathbf{p}_4|^2} \right)^{\epsilon} - 1 \right] \right. \\ \left. - \frac{\alpha_g^{(1)} C_A}{2} \log \frac{|\mathbf{p}_4|^2}{\tau} \left(\frac{\mu^2}{|\mathbf{p}_4|^2} \right)^{2\epsilon} \left[\left(\frac{|\mathbf{p}_4|^2}{-t_1} \right)^{\epsilon} + \left(\frac{|\mathbf{p}_4|^2}{-t_2} \right)^{\epsilon} \right] \right\} \\ + \frac{3b_0^2}{128\epsilon^2} \left[\left(\frac{\mu^2}{|\mathbf{p}_4|^2} \right)^{\epsilon} - 1 \right]^2 + \frac{b_1}{64\epsilon} \left[\left(\frac{\mu^2}{|\mathbf{p}_4|^2} \right)^{2\epsilon} - 1 \right] \\ - \frac{\alpha_g^{(1)} C_A b_0}{16\epsilon} \left(\frac{\mu^2}{|\mathbf{p}_4|^2} \right)^{\epsilon} \log \frac{|\mathbf{p}_4|^2}{\tau} \left\{ \left(\frac{\mu^2}{|\mathbf{p}_4|^2} \right)^{\epsilon} \left[\left(\frac{|\mathbf{p}_4|^2}{-t_1} \right)^{\epsilon} + \left(\frac{|\mathbf{p}_4|^2}{-t_2} \right)^{\epsilon} \right] \right. \\ \left. + 2 \left(\frac{|\mathbf{p}_4|^2}{-t_1} \right)^{2\epsilon} + 2 \left(\frac{|\mathbf{p}_4|^2}{-t_2} \right)^{2\epsilon} \right] - 3 \left[\left(\frac{|\mathbf{p}_4|^2}{-t_1} \right)^{\epsilon} + \left(\frac{|\mathbf{p}_4|^2}{-t_2} \right)^{\epsilon} \right] \right\} \\ + \frac{C_A}{8} \left(\frac{\mu^2}{|\mathbf{p}_4|^2} \right)^{2\epsilon} \log \frac{|\mathbf{p}_4|^2}{\tau} \left\{ C_A (\alpha_g^{(1)})^2 \log \frac{|\mathbf{p}_4|^2}{\tau} \left[\left(\frac{|\mathbf{p}_4|^2}{-t_1} \right)^{\epsilon} + \left(\frac{|\mathbf{p}_4|^2}{-t_2} \right)^{\epsilon} \right]^2 \right. \\ \left. - 4\alpha_g^{(2)} \left[\left(\frac{|\mathbf{p}_4|^2}{-t_1} \right)^{2\epsilon} + \left(\frac{|\mathbf{p}_4|^2}{-t_2} \right)^{2\epsilon} \right] \right\}. \quad (\text{D.21c})$$

E The dipole formula in multi-Regge kinematics

According to the infrared factorization theorem an n -particle scattering amplitude has the following multiplicative structure [23, 132–143]

$$\mathcal{M}_n(\{p_i\}, \mu, \alpha_s(\mu^2)) = \mathbf{Z}_n(\{p_i\}, \mu, \alpha_s(\mu^2)) \mathcal{H}_n(\{p_i\}, \mu, \alpha_s(\mu^2)), \quad (\text{E.1})$$

where on the left-hand side one has the infrared divergent n -particle amplitude in dimensional regularization \mathcal{M}_n , while on the right-hand side \mathcal{H}_n is the finite remainder, and infrared divergences are factorized in the renormalization factor \mathbf{Z}_n , which has the exponential structure

$$\mathbf{Z}_n(\{p_i\}, \mu, \alpha_s(\mu^2)) = \mathcal{P} \exp \left\{ -\frac{1}{2} \int_0^{\mu^2} \frac{d\lambda^2}{\lambda^2} \mathbf{\Gamma}_n(\{p_i\}, \lambda, \alpha_s(\lambda^2)) \right\}, \quad (\text{E.2})$$

and in turn $\mathbf{\Gamma}_n$ represents the soft anomalous dimension for scattering of massless partons ($p_i^2 = 0$). Through three loops, it is given by

$$\mathbf{\Gamma}_n(\{p_i\}, \lambda, \alpha_s(\lambda^2)) = \mathbf{\Gamma}_n^{\text{dip.}}(\{p_i\}, \lambda, \alpha_s(\lambda^2)) + \mathbf{\Delta}_n(\{\rho_{ijkl}\}), \quad (\text{E.3})$$

where

$$\mathbf{\Gamma}_n^{\text{dip.}}(\{p_i\}, \lambda, \alpha_s(\lambda^2)) = -\frac{\gamma_K(\alpha_s)}{2} \sum_{i < j} \log\left(\frac{-s_{ij}}{\lambda^2}\right) \mathbf{T}_i \cdot \mathbf{T}_j + \sum_i \gamma_i(\alpha_s), \quad (\text{E.4})$$

and the argument of the functions indicates that the dependence on the scale is both explicit and via the $4 - 2\epsilon$ dimensional coupling, which obeys the renormalization group equation

$$\beta(\alpha_s, \epsilon) \equiv \frac{d\alpha_s}{d\ln\mu} = -2\epsilon\alpha_s - \frac{\alpha_s^2}{2\pi} \sum_{n=0}^{\infty} b_n \left(\frac{\alpha_s}{\pi}\right)^n, \quad (\text{E.5})$$

with $b_0 = \frac{11}{3}C_A - \frac{2}{3}n_f$.

Aim of this appendix is to specialise eq. (E.3) to the $2 \rightarrow 3$ parton amplitudes considered in this paper. We focus in particular on the dipole component, eq. (E.4), and neglect the quadrupole term $\mathbf{\Delta}_n(\{\rho_{ijkl}\})$. The latter starts at three loops and therefore it is not relevant for the analysis of the high-energy limit considered in the main text, which concerns scattering amplitudes up to two loops. For the purpose of this section we follow closely [56, 75] and parameterize the external momenta P_1, \dots, P_5 in the lab frame as follows:

$$P_1 = (0, x_1\sqrt{S}, \mathbf{0}), \quad P_2 = (x_2\sqrt{S}, 0, \mathbf{0}), \quad (\text{E.6})$$

where S is the hadronic centre of mass energy, such that $s_{12} = x_1x_2S$, and

$$P_i = (|\mathbf{p}_i| e^{y_i}, |\mathbf{p}_i| e^{-y_i}, \mathbf{p}_i), \quad \text{with} \quad i = 3, 4, 5. \quad (\text{E.7})$$

In turn, the transverse momenta \mathbf{p}_i are parameterized as $\mathbf{p}_i = |\mathbf{p}_i|(\cos\phi_i, \sin\phi_i)$, where ϕ_i is the azimuthal angle between the vector \mathbf{p}_i and an arbitrary vector in the transverse plane. Momentum conservation requires

$$\begin{aligned} \mathbf{0} &= \mathbf{p}_3 + \mathbf{p}_4 + \mathbf{p}_5, \\ x_1 &= \frac{1}{\sqrt{S}} \left(|\mathbf{p}_3| e^{-y_3} + |\mathbf{p}_4| e^{-y_4} + |\mathbf{p}_5| e^{-y_5} \right), \\ x_2 &= \frac{1}{\sqrt{S}} \left(|\mathbf{p}_3| e^{y_3} + |\mathbf{p}_4| e^{y_4} + |\mathbf{p}_5| e^{y_5} \right), \end{aligned} \quad (\text{E.8})$$

and the kinematic invariants of eq. (2.7) reads

$$\begin{aligned} s_{12} &= x_1x_2S = \sum_{i,j=3}^5 |\mathbf{p}_i||\mathbf{p}_j| e^{y_i-y_j}, \\ s_{1i} &= -2P_1 \cdot P_i = -\sum_{j=3}^5 |\mathbf{p}_i||\mathbf{p}_j| e^{y_i-y_j}, \quad i = 3, 4, 5, \end{aligned}$$

$$s_{2i} = -2P_2 \cdot P_i = -\sum_{j=3}^5 |\mathbf{p}_i| |\mathbf{p}_j| e^{-(y_i - y_j)}, \quad i = 3, 4, 5 \quad (\text{E.9})$$

$$s_{ij} = 2P_i \cdot P_j = |\mathbf{p}_i| |\mathbf{p}_j| [\cosh(y_i - y_j) - \cos(\phi_i - \phi_j)], \quad i, j = 3, 4, 5.$$

In terms of the rapidity variables y_i , the multi-Regge limit of eq. (2.6) reads

$$y_3 \gg y_4 \gg y_5. \quad (\text{E.10})$$

In this limit $x_1 \simeq |\mathbf{p}_5|/\sqrt{S} e^{-y_5}$, $x_2 \simeq |\mathbf{p}_3|/\sqrt{S} e^{y_3}$, and the invariants of eq. (E.9) can be approximated as

$$\begin{aligned} s_{12} &\simeq |\mathbf{p}_3| |\mathbf{p}_5| e^{y_3 - y_5}, \\ s_{1i} &\simeq -|\mathbf{p}_i| |\mathbf{p}_5| e^{y_i - y_5}, \quad i = 3, 4, 5 \\ s_{2i} &\simeq -|\mathbf{p}_3| |\mathbf{p}_i| e^{y_3 - y_i}, \quad i = 3, 4, 5 \\ s_{ij} &\simeq |\mathbf{p}_i| |\mathbf{p}_j| e^{|y_i - y_j|}, \quad i, j = 3, 4, 5. \end{aligned} \quad (\text{E.11})$$

Specialising eq. (E.4) to the case $n = 5$ and taking the high-energy limit according to eq. (E.11) one has

$$\begin{aligned} \mathbf{\Gamma}_5^{\text{dip.}}(\{p_i\}, \lambda, \alpha_s(\lambda^2)) &= -\frac{\gamma_K(\alpha_s)}{2} \left\{ \left[\log \frac{|\mathbf{p}_3|}{\lambda} + \log \frac{|\mathbf{p}_5|}{\lambda} - i\pi + y_3 - y_5 \right] \mathbf{T}_1 \cdot \mathbf{T}_2 \right. \\ &\quad + \left[\log \frac{|\mathbf{p}_3|}{\lambda} + \log \frac{|\mathbf{p}_5|}{\lambda} + y_3 - y_5 \right] \mathbf{T}_1 \cdot \mathbf{T}_3 \\ &\quad + \left[\log \frac{|\mathbf{p}_4|}{\lambda} + \log \frac{|\mathbf{p}_5|}{\lambda} + y_4 - y_5 \right] \mathbf{T}_1 \cdot \mathbf{T}_4 \\ &\quad + 2 \log \frac{|\mathbf{p}_5|}{\lambda} \mathbf{T}_1 \cdot \mathbf{T}_5 + 2 \log \frac{|\mathbf{p}_3|}{\lambda} \mathbf{T}_2 \cdot \mathbf{T}_3 \\ &\quad + \left[\log \frac{|\mathbf{p}_3|}{\lambda} + \log \frac{|\mathbf{p}_4|}{\lambda} + y_3 - y_4 \right] \mathbf{T}_2 \cdot \mathbf{T}_4 \\ &\quad + \left[\log \frac{|\mathbf{p}_3|}{\lambda} + \log \frac{|\mathbf{p}_3|}{\lambda} + y_3 - y_5 \right] \mathbf{T}_2 \cdot \mathbf{T}_5 \\ &\quad + \left[\log \frac{|\mathbf{p}_3|}{\lambda} + \log \frac{|\mathbf{p}_4|}{\lambda} - i\pi + y_3 - y_4 \right] \mathbf{T}_3 \cdot \mathbf{T}_4 \\ &\quad + \left[\log \frac{|\mathbf{p}_3|}{\lambda} + \log \frac{|\mathbf{p}_5|}{\lambda} - i\pi + y_3 - y_5 \right] \mathbf{T}_3 \cdot \mathbf{T}_5 \\ &\quad \left. + \left[\log \frac{|\mathbf{p}_4|}{\lambda} + \log \frac{|\mathbf{p}_5|}{\lambda} - i\pi + y_4 - y_5 \right] \mathbf{T}_4 \cdot \mathbf{T}_5 \right\} + \sum_{i=1}^5 \gamma_i(\alpha_s). \end{aligned} \quad (\text{E.12})$$

The expression in eq. (E.12) can be expressed in terms of the colour operators in eqs. (2.32), (2.33) and (2.35) by means of the identities

$$\sum_{i=1}^5 \mathbf{T}_i = 0, \quad \left(\sum_{i=1}^5 \mathbf{T}_i \right)^2 = \sum_{i=1}^5 C_i + 2 \sum_{j>i=1}^5 \mathbf{T}_i \cdot \mathbf{T}_j. \quad (\text{E.13})$$

After some elaboration one has

$$\begin{aligned} \mathbf{\Gamma}_5^{\text{dip.}}(\{p_i\}, \lambda, \alpha_s(\lambda^2)) = & -\frac{\gamma_K(\alpha_s)}{2} \left[- (y_4 - y_5) \mathbf{T}_{t_1}^2 - (y_3 - y_4) \mathbf{T}_{t_2}^2 - i\pi \mathbf{T}_s^2 \right. \\ & - \frac{1}{2} \left(\log \frac{|\mathbf{P}_5|^2}{\lambda^2} - i\pi \right) (C_1 + C_5) - \frac{1}{2} \left(\log \frac{|\mathbf{P}_4|^2}{\lambda^2} - i\pi \right) C_4 \\ & \left. - \frac{1}{2} \left(\log \frac{|\mathbf{P}_3|^2}{\lambda^2} - i\pi \right) (C_2 + C_3) \right] + \sum_{i=1}^5 \gamma_i(\alpha_s), \end{aligned} \quad (\text{E.14})$$

which is consistent with eq. (6.8) of [75]. Using eq. (2.41) it is possible to write the dipole formula in terms of the operators $\mathbf{T}_{(\pm, \pm)}$ introduced in eq. (2.40), in such a way to make symmetries under the exchanges $2 \leftrightarrow 3$ and $1 \leftrightarrow 5$ manifest. Taking into account that in the high-energy limit $C_1 = C_5 \equiv C_i$, $C_2 = C_3 \equiv C_j$, and identifying $C_4 \equiv C_v = C_A$, one obtains

$$\begin{aligned} \mathbf{\Gamma}_5^{\text{dip.}}(\{p_i\}, \lambda, \alpha_s(\lambda^2)) = & -\frac{\gamma_K(\alpha_s)}{2} \left[- (y_4 - y_5) \mathbf{T}_{t_1}^2 - (y_3 - y_4) \mathbf{T}_{t_2}^2 \right. \\ & \left. - \frac{i\pi}{2} \left(\mathbf{T}_{(++)} + \mathbf{T}_{(+-)} + \mathbf{T}_{(-+)} + \mathbf{T}_{(--) } \right) \right. \\ & \left. - C_i \log \frac{|\mathbf{P}_5|^2}{\lambda^2} - C_j \log \frac{|\mathbf{P}_3|^2}{\lambda^2} - \frac{C_v}{2} \left(\log \frac{|\mathbf{P}_4|^2}{\lambda^2} - i\pi \right) \right] + \sum_{i=1}^5 \gamma_i(\alpha_s). \end{aligned} \quad (\text{E.15})$$

The operator $\mathbf{T}_{(++)}$ commutes with $\mathbf{T}_{t_1}^2$ and $\mathbf{T}_{t_2}^2$, furthermore one has

$$\mathbf{T}_{(++)} = -\frac{1}{2} (\mathbf{T}_{t_1}^2 + \mathbf{T}_{t_2}^2 - C_4). \quad (\text{E.16})$$

This relation can be used in eq. (E.15) to obtain

$$\begin{aligned} \mathbf{\Gamma}_5^{\text{dip.}}(\{p_i\}, \lambda, \alpha_s(\lambda^2)) = & -\frac{\gamma_K(\alpha_s)}{2} \left[- \left(y_4 - y_5 - \frac{i\pi}{4} \right) \mathbf{T}_{t_1}^2 - \left(y_3 - y_4 - \frac{i\pi}{4} \right) \mathbf{T}_{t_2}^2 \right. \\ & \left. - \frac{i\pi}{2} \left(\mathbf{T}_{(+-)} + \mathbf{T}_{(-+)} + \mathbf{T}_{(--) } \right) \right. \\ & \left. - C_i \log \frac{|\mathbf{P}_5|^2}{\lambda^2} - C_j \log \frac{|\mathbf{P}_3|^2}{\lambda^2} - \frac{C_v}{2} \left(\log \frac{|\mathbf{P}_4|^2}{\lambda^2} - \frac{i\pi}{2} \right) \right] + \sum_{i=1}^5 \gamma_i(\alpha_s). \end{aligned} \quad (\text{E.17})$$

Using this result it appears natural, in the high-energy limit, to factorize the dipole renormalization factor $\mathbf{Z}_5^{\text{dip.}}$ in eq. (E.2) as follows:

$$\begin{aligned} \mathbf{Z}_5^{\text{dip.}}(\{p_i\}, \mu, \alpha_s(\mu^2)) = & Z_i \left(\frac{|\mathbf{P}_5|}{\mu}, \alpha_s(\mu^2), \epsilon \right) Z_j \left(\frac{|\mathbf{P}_3|}{\mu}, \alpha_s(\mu^2), \epsilon \right) \\ & \times Z_v \left(\frac{p_{4\perp}}{\mu}, \alpha_s(\mu^2), \epsilon \right) \hat{\mathbf{Z}}(\{y_i - y_j\}, \alpha_s(\mu^2), \epsilon). \end{aligned} \quad (\text{E.18})$$

In this equation the last factor $\hat{\mathbf{Z}}$ reads

$$\hat{\mathbf{Z}}(\{y_i - y_j\}, \alpha_s(\mu^2), \epsilon) = \exp \left\{ K(\alpha_s(\mu^2), \epsilon) \left[\tilde{\eta}_1 \mathbf{T}_{t_1}^2 + \tilde{\eta}_2 \mathbf{T}_{t_2}^2 \right] \right.$$

$$+ \frac{i\pi}{2} \left(\mathbf{T}_{(+-)} + \mathbf{T}_{(-+)} + \mathbf{T}_{(--)} \right) \Big] \Big\}, \quad (\text{E.19})$$

where

$$\tilde{\eta}_1 = y_4 - y_5 - \frac{i\pi}{4}, \quad \tilde{\eta}_2 = y_3 - y_4 - \frac{i\pi}{4}, \quad (\text{E.20})$$

and the factor $K(\alpha_s(\mu^2), \epsilon)$ is the well-known integral over the scale of the cusp anomalous dimension:

$$K(\alpha_s(\mu^2), \epsilon) = -\frac{1}{4} \int_0^{\mu^2} \frac{d\lambda^2}{\lambda^2} \hat{\gamma}_K(\alpha_s(\lambda^2)). \quad (\text{E.21})$$

The rapidity differences $\tilde{\eta}_1, \tilde{\eta}_2$ in eq. (E.20) constitutes the natural generalization of the signature-even combination of logarithms $L = \log(s/|t|) - i\pi/2$, introduced in case of $2 \rightarrow 2$ parton scattering (cf. with eq. (2.9) of [23]). The relation with the rapidity factors in eq. (4.11) can be easily found to be

$$\begin{aligned} \eta_1 &= \frac{1}{2} [\log(1-z) + \log(1-\bar{z})] + \log \frac{|\mathbf{p}_4|^2}{\tau} + \tilde{\eta}_1, \\ \eta_2 &= \frac{1}{2} [\log(z) + \log(\bar{z})] + \log \frac{|\mathbf{p}_4|^2}{\tau} + \tilde{\eta}_2. \end{aligned} \quad (\text{E.22})$$

Let us also point out that in this section we keep explicit dependence on the IR renormalisation scale μ , and fix the Regge factorization scale to $\tau = |\mathbf{p}_4|^2$. Next, we define

$$\gamma_i(\alpha_s) \equiv \gamma_1(\alpha_s) = \gamma_5(\alpha_s), \quad \gamma_j(\alpha_s) \equiv \gamma_2(\alpha_s) = \gamma_3(\alpha_s), \quad (\text{E.23})$$

such that the factors $Z_{i/j}$ in eq. (E.18) reads

$$Z_{i/j} \left(\frac{|\mathbf{p}_{5/3}|}{\mu}, \alpha_s(\mu^2), \epsilon \right) = \exp \left\{ -\frac{1}{2} \int_0^{\mu^2} \frac{d\lambda^2}{\lambda^2} \left[C_{i/j} \frac{\gamma_K(\alpha_s)}{2} \log \frac{|\mathbf{p}_{5/3}|^2}{\lambda^2} + 2\gamma_{i/j}(\alpha_s) \right] \right\}, \quad (\text{E.24})$$

and correspond to the collinear singularities associated to the impact factors $C_{i/j}$, according to eqs. (6.19) and (6.20). Last, the factor Z_v in eq. (E.18) reads

$$Z_v \left(\frac{|\mathbf{p}_4|}{\mu}, \alpha_s(\mu^2), \epsilon \right) = \exp \left\{ -\frac{1}{2} \int_0^{\mu^2} \frac{d\lambda^2}{\lambda^2} \left[C_v \frac{\gamma_K(\alpha_s)}{4} \left(\log \frac{|\mathbf{p}_4|^2}{\lambda^2} - \frac{i\pi}{2} \right) + \gamma_v(\alpha_s) \right] \right\}, \quad (\text{E.25})$$

where we identified

$$\gamma_v(\alpha_s) \equiv \gamma_4(\alpha_s). \quad (\text{E.26})$$

Eqs. (E.24) and (E.25) can be expressed in terms of the factors

$$K_D(\alpha_s(\mu^2), \epsilon) = -\frac{1}{4} \int_0^{\mu^2} \frac{d\lambda^2}{\lambda^2} \hat{\gamma}_K(\alpha_s(\lambda^2)) \log \frac{\mu^2}{\lambda^2}, \quad (\text{E.27})$$

$$K_{B_i}(\alpha_s(\mu^2), \epsilon) = -\frac{1}{2} \int_0^{\mu^2} \frac{d\lambda^2}{\lambda^2} \hat{\gamma}_i(\alpha_s(\lambda^2)). \quad (\text{E.28})$$

Then we have

$$Z_{i/j}\left(\frac{|\mathbf{p}_{5/3}|}{\mu}, \alpha_s(\mu^2), \epsilon\right) = \exp\left\{\left[K\left(\alpha_s(\mu^2), \epsilon\right) \log \frac{|\mathbf{p}_{5/3}|^2}{\mu^2} + K_D\left(\alpha_s(\mu^2), \epsilon\right)\right] C_{i/j} + 2K_{B_i}\left(\alpha_s(\mu^2), \epsilon\right)\right\}, \quad (\text{E.29})$$

and

$$Z_v\left(\frac{|\mathbf{p}_4|}{\mu}, \alpha_s(\mu^2), \epsilon\right) = \exp\left\{\left[K\left(\alpha_s(\mu^2), \epsilon\right) \left(\log \frac{|\mathbf{p}_4|^2}{\lambda^2} - \frac{i\pi}{2}\right) + K_D\left(\alpha_s(\mu^2), \epsilon\right)\right] \frac{C_v}{2} + K_{B_v}\left(\alpha_s(\mu^2), \epsilon\right)\right\}. \quad (\text{E.30})$$

Perturbative expansion

Given the non-commuting nature of the color operators in eq. (E.19), the expansion in powers of α_s of eq. (E.18) requires the repeated application of the Zassenhaus formula:

$$e^{k(X+Y)} = e^{kX} e^{kY} e^{-\frac{k^2}{2}[X,Y]} e^{\mathcal{O}(k^3)}, \quad (\text{E.31})$$

where X, Y represent two non-commuting color operators, and k a c-number. In what follows we define the perturbative expansion of the factors $K_m(\alpha_s)$ in eqs. (E.21), (E.27) and (E.28) as follows:

$$K_m\left(\alpha_s(\mu^2), \epsilon\right) = \sum_n \left(\frac{\alpha_s(\mu^2)}{\pi}\right)^n K_m^{(n)}\left(\mu^2, \epsilon\right), \quad (\text{E.32})$$

then we have

$$\begin{aligned} K^{(1)} &= \frac{\gamma_K^{(1)}}{4\epsilon}, \\ K^{(2)} &= -\frac{b_0 \gamma_K^{(1)}}{32\epsilon^2} + \frac{\gamma_K^{(2)}}{8\epsilon}, \end{aligned} \quad (\text{E.33})$$

$$\begin{aligned} K_D^{(1)} &= -\frac{\gamma_K^{(1)}}{4\epsilon^2}, \\ K_D^{(2)} &= \frac{3b_0 \gamma_K^{(1)}}{64\epsilon^3} - \frac{\gamma_K^{(2)}}{16\epsilon^2}, \end{aligned} \quad (\text{E.34})$$

$$\begin{aligned} K_{B_q}^{(1)} &= \frac{\gamma_q^{(1)}}{2\epsilon}, \\ K_{B_q}^{(2)} &= -\frac{b_0 \gamma_q^{(1)}}{16\epsilon^2} + \frac{\gamma_q^{(2)}}{4\epsilon}, \end{aligned} \quad (\text{E.35})$$

$$\begin{aligned}
K_{B_g}^{(1)} &= \frac{\gamma_g^{(1)}}{2\epsilon}, \\
K_{B_g}^{(2)} &= -\frac{b_0\gamma_g^{(1)}}{16\epsilon^2} + \frac{\gamma_g^{(2)}}{4\epsilon},
\end{aligned} \tag{E.36}$$

where in turn

$$\begin{aligned}
\gamma_K^{(1)} &= 2, \\
\gamma_K^{(2)} &= \left(\frac{67}{18} - \frac{\pi^2}{6}\right)C_A - \frac{5}{9}n_f,
\end{aligned} \tag{E.37}$$

$$\begin{aligned}
\gamma_q^{(1)} &= -\frac{3}{4}C_F, \\
\gamma_q^{(2)} &= \frac{C_F^2}{16} \left(-\frac{3}{2} + 2\pi^2 - 24\zeta_3\right) + \frac{C_A C_F}{16} \left(-\frac{961}{54} - \frac{11}{6}\pi^2 26\zeta_3\right) \\
&\quad + \frac{C_F T_R n_f}{16} \left(\frac{130}{27} + \frac{2}{3}\pi^2\right),
\end{aligned} \tag{E.38}$$

$$\begin{aligned}
\gamma_g^{(1)} &= -\frac{b_0}{4}, \\
\gamma_g^{(2)} &= \frac{C_A^2}{16} \left(-\frac{692}{27} + \frac{11}{18}\pi^2 + 2\zeta_3\right) + \frac{C_A n_f}{32} \left(\frac{256}{27} - \frac{2}{9}\pi^2\right) + \frac{C_F n_f}{8},
\end{aligned} \tag{E.39}$$

and in turn

$$b_0 = \frac{1}{3}(11C_A - 2n_f), \quad b_1 = \frac{1}{6}\left[17C_A^2 - (10C_A + 6C_F)T_R n_f\right]. \tag{E.40}$$

Then, at tree level and first order in perturbation theory one has

$$\begin{aligned}
\mathcal{M}^{(0)} &= \mathcal{H}^{(0)}, \\
\mathcal{M}^{(1)} &= \left\{ K^{(1)} \left[(\eta_1 \mathbf{T}_{t_1}^2 + \eta_2 \mathbf{T}_{t_2}^2) + \frac{i\pi}{2} (\mathbf{T}_{(--)} + \mathbf{T}_{(+-)} + \mathbf{T}_{(++)}) \right. \right. \\
&\quad \left. \left. + C_i \log \frac{|\mathbf{p}_5|^2}{\mu^2} + \frac{C_v}{2} \left(\log \frac{|\mathbf{p}_4|^2}{\mu^2} - \frac{i\pi}{2} \right) + C_j \log \frac{|\mathbf{p}_3|^2}{\lambda^2} \right] \right. \\
&\quad \left. + K_D^{(1)} \left(C_i + \frac{C_v}{2} + C_j \right) + 2K_{B_i}^{(1)} + K_{B_v}^{(1)} + 2K_{B_j}^{(1)} \right\} \mathcal{H}^{(0)} + \mathcal{H}^{(1)}, \tag{E.41}
\end{aligned}$$

and second order the factorization formula gives

$$\begin{aligned}
\mathcal{M}^{(2)} &= \left\{ \frac{1}{2} (K^{(1)})^2 \left[\eta_1^2 (\mathbf{T}_{t_1}^2)^2 + \eta_1 \eta_2 \{ \mathbf{T}_{t_1}^2, \mathbf{T}_{t_2}^2 \} + \eta_2^2 (\mathbf{T}_{t_2}^2)^2 \right. \right. \\
&\quad \left. \left. + \frac{i\pi}{2} \left(\eta_1 \{ \mathbf{T}_{(--)} + \mathbf{T}_{(-+)} + \mathbf{T}_{(+-)}, \mathbf{T}_{t_1}^2 \} + \eta_2 \{ \mathbf{T}_{(--)} + \mathbf{T}_{(-+)} + \mathbf{T}_{(+-)}, \mathbf{T}_{t_2}^2 \} \right) \right. \right. \\
&\quad \left. \left. - \frac{\pi^2}{4} (\mathbf{T}_{(--)} + \mathbf{T}_{(-+)} + \mathbf{T}_{(+-)})^2 \right] + K^{(2)} \left[\eta_1 \mathbf{T}_{t_1}^2 + \eta_2 \mathbf{T}_{t_2}^2 \right] \right\}
\end{aligned}$$

$$\begin{aligned}
& + \frac{i\pi}{2} \left(\mathbf{T}_{(--)} + \mathbf{T}_{(-+)} + \mathbf{T}_{(+-)} \right) \Big] + \frac{C_i^2}{2} \left[\left(K_D^{(1)} \right)^2 + 2K_D^{(1)} K^{(1)} \log \left(\frac{|\mathbf{p}_5|^2}{\mu^2} \right) \right. \\
& + \left. \left(K^{(1)} \right)^2 \log^2 \left(\frac{|\mathbf{p}_5|^2}{\mu^2} \right) \right] + \frac{C_v^2}{4} \left[\frac{1}{2} \left(K_D^{(1)} \right)^2 + K^{(1)} K_D^{(1)} \left(\log \left(\frac{|\mathbf{p}_4|^2}{\mu^2} \right) - \frac{i\pi}{2} \right) \right. \\
& + \left. \frac{1}{2} \left(K^{(1)} \right)^2 \left(\log^2 \left(\frac{|\mathbf{p}_4|^2}{\mu^2} \right) - i\pi \log \left(\frac{|\mathbf{p}_4|^2}{\mu^2} \right) - \frac{\pi^2}{4} \right) \right] \\
& + \frac{C_j^2}{2} \left[\left(K_D^{(1)} \right)^2 + 2K_D^{(1)} K^{(1)} \log \left(\frac{|\mathbf{p}_3|^2}{\mu^2} \right) + \left(K^{(1)} \right)^2 \log^2 \left(\frac{|\mathbf{p}_3|^2}{\mu^2} \right) \right] \\
& + C_i \left[\left(K^{(1)} K_D^{(1)} + \left(K^{(1)} \right)^2 \log \left(\frac{|\mathbf{p}_5|^2}{\mu^2} \right) \right) \left(\eta_1 \mathbf{T}_{t_1}^2 + \eta_2 \mathbf{T}_{t_2}^2 \right. \right. \\
& + \left. \left. \frac{i\pi}{2} \left(\mathbf{T}_{(--)} + \mathbf{T}_{(-+)} + \mathbf{T}_{(+-)} \right) \right) + K^{(2)} \log \left(\frac{|\mathbf{p}_5|^2}{\mu^2} \right) \right. \\
& + \left. \left(K^{(1)} \log \left(\frac{|\mathbf{p}_5|^2}{\mu^2} \right) + K_D^{(1)} \right) \left(2B_i^{(1)} + 2B_j^{(1)} + B_v^{(1)} \right) + K_D^{(2)} \right. \\
& + \left. \frac{C_v}{2} \left[\left(K_D^{(1)} \right)^2 + K^{(1)} K_D^{(1)} \left(\log \left(\frac{|\mathbf{p}_4|^2}{\mu^2} \right) + \log \left(\frac{|\mathbf{p}_5|^2}{\mu^2} \right) - \frac{i\pi}{2} \right) \right. \right. \\
& + \left. \left. \left(K^{(1)} \right)^2 \log \left(\frac{|\mathbf{p}_5|^2}{\mu^2} \right) \left(\log \left(\frac{|\mathbf{p}_4|^2}{\mu^2} \right) - \frac{i\pi}{2} \right) \right] \right] \\
& + C_v \left[\frac{1}{2} \left(K^{(1)} \right)^2 \left(\left(\eta_1 \mathbf{T}_{t_1}^2 + \eta_2 \mathbf{T}_{t_2}^2 \right) \log \left(\frac{|\mathbf{p}_4|^2}{\mu^2} \right) - \frac{i\pi}{2} \left(\eta_1 \mathbf{T}_{t_1}^2 + \eta_2 \mathbf{T}_{t_2}^2 \right. \right. \right. \\
& - \left. \left. \left(\mathbf{T}_{(--)} + \mathbf{T}_{(-+)} + \mathbf{T}_{(+-)} \right) \log \left(\frac{|\mathbf{p}_4|^2}{\mu^2} \right) \right) + \frac{\pi^2}{4} \left(\mathbf{T}_{(--)} + \mathbf{T}_{(-+)} + \mathbf{T}_{(+-)} \right) \right) \\
& + K^{(1)} \left(\frac{1}{2} K_D^{(1)} \left(\eta_1 \mathbf{T}_{t_1}^2 + \eta_2 \mathbf{T}_{t_2}^2 \right) - \frac{i\pi}{2} \left(B_i^{(1)} + B_j^{(1)} + \frac{1}{2} B_v^{(1)} \right) \right. \\
& - \left. \frac{1}{2} K_D^{(1)} \left(\mathbf{T}_{(--)} + \mathbf{T}_{(-+)} + \mathbf{T}_{(+-)} \right) \right) + \left(B_i^{(1)} + B_j^{(1)} + \frac{1}{2} B_v^{(1)} \right) \log \left(\frac{|\mathbf{p}_4|^2}{\mu^2} \right) \\
& + \left. \frac{K^{(2)}}{2} \left(\log \left(\frac{|\mathbf{p}_4|^2}{\mu^2} \right) - \frac{i\pi}{2} \right) + K_D^{(1)} \left(B_i^{(1)} + B_j^{(1)} + \frac{1}{2} B_v^{(1)} \right) + \frac{1}{2} K_D^{(2)} \right] \\
& + C_j \left[\left(K^{(1)} K_D^{(1)} + \left(K^{(1)} \right)^2 \log \left(\frac{|\mathbf{p}_3|^2}{\mu^2} \right) \right) \left(\eta_1 \mathbf{T}_{t_1}^2 + \eta_2 \mathbf{T}_{t_2}^2 \right. \right. \\
& + \left. \left. \frac{i\pi}{2} \left(\mathbf{T}_{(--)} + \mathbf{T}_{(-+)} + \mathbf{T}_{(+-)} \right) \right) + K^{(2)} \log \left(\frac{|\mathbf{p}_3|^2}{\mu^2} \right) \right. \\
& + \left. \left(K^{(1)} \log \left(\frac{|\mathbf{p}_3|^2}{\mu^2} \right) + K_D^{(1)} \right) \left(2B_i^{(1)} + 2B_j^{(1)} + B_v^{(1)} \right) + K_D^{(2)} \right. \\
& + \left. \frac{C_v}{2} \left[\left(K_D^{(1)} \right)^2 + K^{(1)} K_D^{(1)} \left(\log \left(\frac{|\mathbf{p}_3|^2}{\mu^2} \right) + \log \left(\frac{|\mathbf{p}_4|^2}{\mu^2} \right) - \frac{i\pi}{2} \right) \right. \right. \\
& + \left. \left. \left(K^{(1)} \right)^2 \log \left(\frac{|\mathbf{p}_3|^2}{\mu^2} \right) \left(\log \left(\frac{|\mathbf{p}_4|^2}{\mu^2} \right) - \frac{i\pi}{2} \right) \right] \right]
\end{aligned}$$

$$\begin{aligned}
& + C_i C_j \left[\left(K_D^{(1)} \right)^2 + K_D^{(1)} K^{(1)} \left(\log \left(\frac{|\mathbf{p}_3|^2}{\mu^2} \right) + \log \left(\frac{|\mathbf{p}_5|^2}{\mu^2} \right) \right) \right. \\
& + \left(K^{(1)} \right)^2 \log \left(\frac{|\mathbf{p}_3|^2}{\mu^2} \right) \log \left(\frac{|\mathbf{p}_5|^2}{\mu^2} \right) + 2 \left(B_i^{(1)} \right)^2 + 4 B_i^{(1)} B_j^{(1)} + 2 \left(B_j^{(1)} \right)^2 \\
& + 2 B_i^{(2)} + 2 B_j^{(2)} + 2 B_i^{(1)} B_v^{(1)} + 2 B_j^{(1)} B_v^{(1)} + \frac{1}{2} \left(B_v^{(1)} \right)^2 + B_v^{(2)} \\
& + K^{(1)} \left(\eta_1 \mathbf{T}_{t_1}^2 + \eta_2 \mathbf{T}_{t_2}^2 + \frac{i\pi}{2} \left(\mathbf{T}_{(- -)} + \mathbf{T}_{(- +)} + \mathbf{T}_{(+ -)} \right) \right) \\
& \left. \times \left(2 B_i^{(1)} + 2 B_j^{(1)} + B_v^{(1)} \right) \right] \mathcal{H}^{(0)} \\
& + \left\{ K^{(1)} \left[\left(\eta_1 \mathbf{T}_{t_1}^2 + \eta_2 \mathbf{T}_{t_2}^2 \right) + \frac{i\pi}{2} \left(\mathbf{T}_{(- -)} + \mathbf{T}_{(- +)} + \mathbf{T}_{(+ -)} \right) \right] \right. \\
& + C_i \left[K_D^{(1)} + K^{(1)} \log \frac{|\mathbf{p}_5|^2}{\mu^2} \right] + \frac{C_v}{2} \left[K_D^{(1)} + K^{(1)} \left(\log \frac{|\mathbf{p}_4|^2}{\mu^2} - \frac{i\pi}{2} \right) \right] \\
& \left. + C_j \left[K_D^{(1)} + K^{(1)} \log \frac{|\mathbf{p}_3|^2}{\lambda^2} \right] + 2 K_{B_i}^{(1)} + K_{B_v}^{(1)} + 2 K_{B_j}^{(1)} \right\} \mathcal{H}^{(1)} + \mathcal{H}^{(2)}, \quad (\text{E.42})
\end{aligned}$$

where we have defined

$$\{\mathcal{O}_1, \mathcal{O}_2\} = \mathcal{O}_1 \mathcal{O}_2 + \mathcal{O}_2 \mathcal{O}_1, \quad (\text{E.43})$$

with $\mathcal{O}_1, \mathcal{O}_2$ two non-commuting color operators.

To conclude this section, let us recall that in section 7.3 we have evaluated only the odd-odd amplitude at two loops, thus we need to extract the $\mathcal{M}^{(-,-)}$ component from eq.(E.42). In general, at all orders in perturbation theory this is obtained expanding systematically \mathbf{Z} and \mathcal{H} into their (\pm, pm) components. Then one has

$$\mathcal{M}^{(-,-)} = \mathbf{Z}^{(-,-)} \mathcal{H}^{(+,+)} + \mathbf{Z}^{(-,+)} \mathcal{H}^{(+,-)} + \mathbf{Z}^{(+,-)} \mathcal{H}^{(-,+)} + \mathbf{Z}^{(+,+)} \mathcal{H}^{(-,-)}. \quad (\text{E.44})$$

In practice, at two loops we have

$$\begin{aligned}
\mathcal{M}^{(-,-,2)} & = \left\{ \frac{1}{2} \left(K^{(1)} \right)^2 \left[\eta_1^2 \left(\mathbf{T}_{t_1}^2 \right)^2 + \eta_1 \eta_2 \left\{ \mathbf{T}_{t_1}^2, \mathbf{T}_{t_2}^2 \right\} + \eta_2^2 \left(\mathbf{T}_{t_2}^2 \right)^2 \right. \right. \\
& \left. \left. - \frac{\pi^2}{4} \left(\mathbf{T}_{(- -)}^2 + \mathbf{T}_{(- +)}^2 + \mathbf{T}_{(+ -)}^2 \right) \right] + K^{(2)} \left[\eta_1 \mathbf{T}_{t_1}^2 + \eta_2 \mathbf{T}_{t_2}^2 \right] \right. \\
& + \frac{C_i^2}{2} \left[\left(K_D^{(1)} \right)^2 + 2 K_D^{(1)} K^{(1)} \log \left(\frac{|\mathbf{p}_5|^2}{\mu^2} \right) + \left(K^{(1)} \right)^2 \log^2 \left(\frac{|\mathbf{p}_5|^2}{\mu^2} \right) \right] \\
& + \frac{C_v^2}{4} \left[\frac{1}{2} \left(K_D^{(1)} \right)^2 + K^{(1)} K_D^{(1)} \left(\log \left(\frac{|\mathbf{p}_4|^2}{\mu^2} \right) - \frac{i\pi}{2} \right) \right. \\
& \left. + \frac{1}{2} \left(K^{(1)} \right)^2 \left(\log^2 \left(\frac{|\mathbf{p}_4|^2}{\mu^2} \right) - i\pi \log \left(\frac{|\mathbf{p}_4|^2}{\mu^2} \right) - \frac{\pi^2}{4} \right) \right] \\
& \left. + \frac{C_j^2}{2} \left[\left(K_D^{(1)} \right)^2 + 2 K_D^{(1)} K^{(1)} \log \left(\frac{|\mathbf{p}_3|^2}{\mu^2} \right) + \left(K^{(1)} \right)^2 \log^2 \left(\frac{|\mathbf{p}_3|^2}{\mu^2} \right) \right] \right\}
\end{aligned}$$

$$\begin{aligned}
& + C_i \left[\left(K^{(1)} K_D^{(1)} + \left(K^{(1)} \right)^2 \log \left(\frac{|\mathbf{p}_5|^2}{\mu^2} \right) \right) \left(\eta_1 \mathbf{T}_{t_1}^2 + \eta_2 \mathbf{T}_{t_2}^2 \right) \right. \\
& + K^{(2)} \log \left(\frac{|\mathbf{p}_5|^2}{\mu^2} \right) + \left(K^{(1)} \log \left(\frac{|\mathbf{p}_5|^2}{\mu^2} \right) + K_D^{(1)} \right) \left(2B_i^{(1)} + 2B_j^{(1)} + B_v^{(1)} \right) \\
& + K_D^{(2)} + \frac{C_v}{2} \left[\left(K_D^{(1)} \right)^2 + K^{(1)} K_D^{(1)} \left(\log \left(\frac{|\mathbf{p}_4|^2}{\mu^2} \right) + \log \left(\frac{|\mathbf{p}_5|^2}{\mu^2} \right) - \frac{i\pi}{2} \right) \right. \\
& \left. \left. + \left(K^{(1)} \right)^2 \log \left(\frac{|\mathbf{p}_5|^2}{\mu^2} \right) \left(\log \left(\frac{|\mathbf{p}_4|^2}{\mu^2} \right) - \frac{i\pi}{2} \right) \right] \right] \\
& + C_v \left[\frac{1}{2} \left(K^{(1)} \right)^2 \left(\eta_1 \mathbf{T}_{t_1}^2 + \eta_2 \mathbf{T}_{t_2}^2 \right) \left(\log \left(\frac{|\mathbf{p}_4|^2}{\mu^2} \right) - \frac{i\pi}{2} \right) \right. \\
& + K^{(1)} \left(\frac{1}{2} K_D^{(1)} \left(\eta_1 \mathbf{T}_{t_1}^2 + \eta_2 \mathbf{T}_{t_2}^2 \right) - \frac{i\pi}{2} \left(B_i^{(1)} + B_j^{(1)} + \frac{1}{2} B_v^{(1)} \right) \right) \\
& + \left(B_i^{(1)} + B_j^{(1)} + \frac{1}{2} B_v^{(1)} \right) \log \left(\frac{|\mathbf{p}_4|^2}{\mu^2} \right) + \frac{K^{(2)}}{2} \left(\log \left(\frac{|\mathbf{p}_4|^2}{\mu^2} \right) - \frac{i\pi}{2} \right) \\
& \left. \left. + K_D^{(1)} \left(B_i^{(1)} + B_j^{(1)} + \frac{1}{2} B_v^{(1)} \right) + \frac{1}{2} K_D^{(2)} \right) \right] \\
& + C_j \left[\left(K^{(1)} K_D^{(1)} + \left(K^{(1)} \right)^2 \log \left(\frac{|\mathbf{p}_3|^2}{\mu^2} \right) \right) \left(\eta_1 \mathbf{T}_{t_1}^2 + \eta_2 \mathbf{T}_{t_2}^2 \right) \right. \\
& + K^{(2)} \log \left(\frac{|\mathbf{p}_3|^2}{\mu^2} \right) + \left(K^{(1)} \log \left(\frac{|\mathbf{p}_3|^2}{\mu^2} \right) + K_D^{(1)} \right) \left(2B_i^{(1)} + 2B_j^{(1)} + B_v^{(1)} \right) \\
& + K_D^{(2)} + \frac{C_v}{2} \left[\left(K_D^{(1)} \right)^2 + K^{(1)} K_D^{(1)} \left(\log \left(\frac{|\mathbf{p}_3|^2}{\mu^2} \right) + \log \left(\frac{|\mathbf{p}_4|^2}{\mu^2} \right) - \frac{i\pi}{2} \right) \right. \\
& \left. \left. + \left(K^{(1)} \right)^2 \log \left(\frac{|\mathbf{p}_3|^2}{\mu^2} \right) \left(\log \left(\frac{|\mathbf{p}_4|^2}{\mu^2} \right) - \frac{i\pi}{2} \right) \right] \right] \\
& + C_i C_j \left[\left(K_D^{(1)} \right)^2 + K_D^{(1)} K^{(1)} \left(\log \left(\frac{|\mathbf{p}_3|^2}{\mu^2} \right) + \log \left(\frac{|\mathbf{p}_5|^2}{\mu^2} \right) \right) \right. \\
& + \left(K^{(1)} \right)^2 \log \left(\frac{|\mathbf{p}_3|^2}{\mu^2} \right) \log \left(\frac{|\mathbf{p}_5|^2}{\mu^2} \right) + 2 \left(B_i^{(1)} \right)^2 + 4 B_i^{(1)} B_j^{(1)} + 2 \left(B_j^{(1)} \right)^2 \\
& + 2 B_i^{(2)} + 2 B_j^{(2)} + 2 B_i^{(1)} B_v^{(1)} + 2 B_j^{(1)} B_v^{(1)} + \frac{1}{2} \left(B_v^{(1)} \right)^2 + B_v^{(2)} \\
& \left. \left. + K^{(1)} \left(\eta_1 \mathbf{T}_{t_1}^2 + \eta_2 \mathbf{T}_{t_2}^2 \right) \left(2B_i^{(1)} + 2B_j^{(1)} + B_v^{(1)} \right) \right] \right\} \mathcal{H}^{(0)} \\
& + \left\{ K^{(1)} \left[\left(\eta_1 \mathbf{T}_{t_1}^2 + \eta_2 \mathbf{T}_{t_2}^2 \right) \right] + C_i \left[K_D^{(1)} + K^{(1)} \log \frac{|\mathbf{p}_5|^2}{\mu^2} \right] \right. \\
& + \frac{C_v}{2} \left[K_D^{(1)} + K^{(1)} \left(\log \frac{|\mathbf{p}_4|^2}{\mu^2} - \frac{i\pi}{2} \right) \right] + C_j \left[K_D^{(1)} + K^{(1)} \log \frac{|\mathbf{p}_3|^2}{\lambda^2} \right] \\
& \left. + 2K_{B_i}^{(1)} + K_{B_v}^{(1)} + 2K_{B_j}^{(1)} \right\} \mathcal{H}^{(-,-,1)} + K^{(1)} \frac{i\pi}{2} \left[\mathbf{T}_{(+,-)} \mathcal{H}^{(-,+,-1)} \right]
\end{aligned}$$

$$+ \mathbf{T}_{(-+)} \mathcal{H}^{(+,-,1)} + \mathbf{T}_{(--)} \mathcal{H}^{(+,+,1)} \Big] + \mathcal{H}^{(-,-,2)}. \quad (\text{E.45})$$

References

- [1] P.D.B. Collins, *An Introduction to Regge Theory and High-Energy Physics*, Cambridge Monographs on Mathematical Physics, Cambridge Univ. Press, Cambridge, UK (2009).
- [2] L. Lipatov, *Reggeization of the Vector Meson and the Vacuum Singularity in Nonabelian Gauge Theories*, *Sov. J. Nucl. Phys.* **23** (1976) 338.
- [3] V.S. Fadin, R. Fiore and A. Quartarolo, *Reggeization of quark quark scattering amplitude in QCD*, *Phys. Rev. D* **53** (1996) 2729 [[hep-ph/9506432](#)].
- [4] V.S. Fadin, R. Fiore and M. Kotsky, *Gluon Regge trajectory in the two loop approximation*, *Phys. Lett. B* **387** (1996) 593 [[hep-ph/9605357](#)].
- [5] V.S. Fadin, M. Kotsky and R. Fiore, *Gluon Reggeization in QCD in the next-to-leading order*, *Phys. Lett. B* **359** (1995) 181.
- [6] V.S. Fadin, *Regge trajectory of a gluon in the two loop approximation*, *JETP Lett.* **61** (1995) 346.
- [7] V.S. Fadin, *BFKL news*, in *LAFEX International School on High-Energy Physics (LISHEP 98) Session A: Particle Physics for High School Teachers - Session B: Advanced School in HEP - Session C: Workshop on Diffractive Physics*, pp. 742–776, 7, 1998 [[hep-ph/9807528](#)].
- [8] V. Fadin, M. Kozlov and A. Reznichenko, *Gluon Reggeization in Yang-Mills Theories*, *Phys. Rev. D* **92** (2015) 085044 [[1507.00823](#)].
- [9] V. Fadin, R. Fiore, M. Kozlov and A. Reznichenko, *Proof of the multi-Regge form of QCD amplitudes with gluon exchanges in the NLA*, *Phys. Lett. B* **639** (2006) 74 [[hep-ph/0602006](#)].
- [10] J.R. Forshaw and D.A. Ross, *Quantum Chromodynamics and the Pomeron*, vol. 9, Oxford University Press (1998), [10.1017/9781009290111](#).
- [11] V.S. Fadin, E.A. Kuraev and L.N. Lipatov, *On the Pomeranchuk Singularity in Asymptotically Free Theories*, *Phys. Lett. B* **60** (1975) 50.
- [12] E.A. Kuraev, L.N. Lipatov and V.S. Fadin, *Multi - Reggeon Processes in the Yang-Mills Theory*, *Sov. Phys. JETP* **44** (1976) 443.
- [13] E.A. Kuraev, L.N. Lipatov and V.S. Fadin, *The Pomeranchuk Singularity in Nonabelian Gauge Theories*, *Sov. Phys. JETP* **45** (1977) 199.
- [14] I.I. Balitsky and L.N. Lipatov, *The Pomeranchuk Singularity in Quantum Chromodynamics*, *Sov. J. Nucl. Phys.* **28** (1978) 822.
- [15] V.S. Fadin and L.N. Lipatov, *BFKL pomeron in the next-to-leading approximation*, *Phys. Lett. B* **429** (1998) 127 [[hep-ph/9802290](#)].
- [16] Y.V. Kovchegov and E. Levin, *Quantum Chromodynamics at High Energy*, vol. 33, Oxford University Press (2013), [10.1017/9781009291446](#).
- [17] S. Caron-Huot, *When does the gluon reggeize?*, *JHEP* **05** (2015) 093 [[1309.6521](#)].
- [18] S. Caron-Huot, E. Gardi and L. Vernazza, *Two-parton scattering in the high-energy limit*, *JHEP* **06** (2017) 016 [[1701.05241](#)].

- [19] S. Caron-Huot, E. Gardi, J. Reichel and L. Vernazza, *Infrared singularities of QCD scattering amplitudes in the Regge limit to all orders*, *JHEP* **03** (2018) 098 [[1711.04850](#)].
- [20] S. Caron-Huot, E. Gardi, J. Reichel and L. Vernazza, *Two-parton scattering amplitudes in the Regge limit to high loop orders*, *JHEP* **08** (2020) 116 [[2006.01267](#)].
- [21] S. Caron-Huot, D. Chicherin, J. Henn, Y. Zhang and S. Zoia, *Multi-Regge Limit of the Two-Loop Five-Point Amplitudes in $\mathcal{N} = 4$ Super Yang-Mills and $\mathcal{N} = 8$ Supergravity*, *JHEP* **10** (2020) 188 [[2003.03120](#)].
- [22] G. Falcioni, E. Gardi, C. Milloy and L. Vernazza, *Climbing three-Reggeon ladders: four-loop amplitudes in the high-energy limit in full colour*, *Phys. Rev. D* **103** (2021) L111501 [[2012.00613](#)].
- [23] G. Falcioni, E. Gardi, N. Maher, C. Milloy and L. Vernazza, *Scattering amplitudes in the Regge limit and the soft anomalous dimension through four loops*, *JHEP* **03** (2022) 053 [[2111.10664](#)].
- [24] G. Falcioni, E. Gardi, N. Maher, C. Milloy and L. Vernazza, *Disentangling the Regge Cut and Regge Pole in Perturbative QCD*, *Phys. Rev. Lett.* **128** (2022) 132001 [[2112.11098](#)].
- [25] S. Abreu, G. Falcioni, E. Gardi, C. Milloy and L. Vernazza, *Regge poles and cuts and the Lipatov vertex*, *PoS* **LL2024** (2024) 085.
- [26] F. Buccioni, F. Caola, F. Devoto and G. Gambuti, *Investigating the universality of five-point QCD scattering amplitudes at high energy*, [2411.14050](#).
- [27] V. Fadin and L. Lipatov, *Reggeon cuts in QCD amplitudes with negative signature*, *Eur. Phys. J. C* **78** (2018) 439 [[1712.09805](#)].
- [28] V.S. Fadin, *Regge Cuts in QCD*, *Phys. Part. Nucl. Lett.* **20** (2023) 341.
- [29] V. Fadin, *Colour structure of three-reggeon cuts in QCD*, *PoS* **ICPPCRubakov2023** (2024) 037.
- [30] I.Z. Rothstein and I.W. Stewart, *An Effective Field Theory for Forward Scattering and Factorization Violation*, *JHEP* **08** (2016) 025 [[1601.04695](#)].
- [31] I. Moutl, S. Raman, G. Ridgway and I.W. Stewart, *Anomalous dimensions from soft Regge constants*, *JHEP* **05** (2023) 025 [[2207.02859](#)].
- [32] A. Gao, I. Moutl, S. Raman, G. Ridgway and I.W. Stewart, *A collinear perspective on the Regge limit*, *JHEP* **05** (2024) 328 [[2401.00931](#)].
- [33] A. Gao, I. Moutl, S. Raman, G. Ridgway and I.W. Stewart, *Reggeization in Color*, [2411.09692](#).
- [34] V. Del Duca and E. Glover, *The High-energy limit of QCD at two loops*, *JHEP* **10** (2001) 035 [[hep-ph/0109028](#)].
- [35] V. Del Duca, C. Duhr, E. Gardi, L. Magnea and C.D. White, *An infrared approach to Reggeization*, *Phys. Rev. D* **85** (2012) 071104 [[1108.5947](#)].
- [36] V. Del Duca, G. Falcioni, L. Magnea and L. Vernazza, *High-energy QCD amplitudes at two loops and beyond*, *Phys. Lett. B* **732** (2014) 233 [[1311.0304](#)].
- [37] V. Del Duca, G. Falcioni, L. Magnea and L. Vernazza, *Analyzing high-energy factorization beyond next-to-leading logarithmic accuracy*, *JHEP* **02** (2015) 029 [[1409.8330](#)].

- [38] I. Balitsky, *Operator expansion for high-energy scattering*, *Nucl. Phys.* **B463** (1996) 99 [[hep-ph/9509348](#)].
- [39] J. Jalilian-Marian, A. Kovner, L.D. McLerran and H. Weigert, *The Intrinsic glue distribution at very small x* , *Phys. Rev. D* **55** (1997) 5414 [[hep-ph/9606337](#)].
- [40] J. Jalilian-Marian, A. Kovner, L.D. McLerran and H. Weigert, *The Intrinsic glue distribution at very small x* , *Phys. Rev.* **D55** (1997) 5414 [[hep-ph/9606337](#)].
- [41] J. Jalilian-Marian, A. Kovner, A. Leonidov and H. Weigert, *The Wilson renormalization group for low x physics: Towards the high density regime*, *Phys. Rev.* **D59** (1998) 014014 [[hep-ph/9706377](#)].
- [42] L.N. Lipatov, *Gauge invariant effective action for high-energy processes in QCD*, *Nucl. Phys. B* **452** (1995) 369 [[hep-ph/9502308](#)].
- [43] J. Bartels, L.N. Lipatov and A. Sabio Vera, *BFKL Pomeron, Reggeized gluons and Bern-Dixon-Smirnov amplitudes*, *Phys. Rev. D* **80** (2009) 045002 [[0802.2065](#)].
- [44] J. Bartels, L.N. Lipatov and A. Sabio Vera, *$N=4$ supersymmetric Yang Mills scattering amplitudes at high energies: The Regge cut contribution*, *Eur. Phys. J. C* **65** (2010) 587 [[0807.0894](#)].
- [45] L.N. Lipatov, *Integrability of scattering amplitudes in $N=4$ SUSY*, *J. Phys. A* **42** (2009) 304020 [[0902.1444](#)].
- [46] L.J. Dixon, J.M. Drummond, C. Duhr and J. Pennington, *The four-loop remainder function and multi-Regge behavior at NNLLA in planar $N = 4$ super-Yang-Mills theory*, *JHEP* **06** (2014) 116 [[1402.3300](#)].
- [47] V. Del Duca, S. Druc, J. Drummond, C. Duhr, F. Dulat, R. Marzucca et al., *All-order amplitudes at any multiplicity in the multi-Regge limit*, *Phys. Rev. Lett.* **124** (2020) 161602 [[1912.00188](#)].
- [48] J. Bartels, *$N = 4$ SYM Gauge Theories: The $2 \rightarrow 6$ Amplitude in the Regge Limit*, (2021), [DOI](#).
- [49] Z. Bern, L.J. Dixon and V.A. Smirnov, *Iteration of planar amplitudes in maximally supersymmetric Yang-Mills theory at three loops and beyond*, *Phys. Rev. D* **72** (2005) 085001 [[hep-th/0505205](#)].
- [50] F. Caola, A. Chakraborty, G. Gambuti, A. von Manteuffel and L. Tancredi, *Three-Loop Gluon Scattering in QCD and the Gluon Regge Trajectory*, *Phys. Rev. Lett.* **128** (2022) 212001 [[2112.11097](#)].
- [51] F. Caola, A. Chakraborty, G. Gambuti, A. von Manteuffel and L. Tancredi, *Three-loop helicity amplitudes for four-quark scattering in massless QCD*, [2108.00055](#).
- [52] F. Caola, A. Chakraborty, G. Gambuti, A. von Manteuffel and L. Tancredi, *Three-loop helicity amplitudes for quark-gluon scattering in QCD*, *JHEP* **12** (2022) 082 [[2207.03503](#)].
- [53] J. Bartels, *High-Energy Behavior in a Nonabelian Gauge Theory (I): $T_{n \rightarrow m}$ in the Leading $\ln s$ Approximation*, *Nucl. Phys. B* **151** (1979) 293.
- [54] J. Bartels, *High-Energy Behavior in a Nonabelian Gauge Theory (II): First Corrections to $T_{n \rightarrow m}$ Beyond the Leading $\ln s$ Approximation*, *Nucl. Phys. B* **175** (1980) 365.
- [55] V.S. Fadin and L.N. Lipatov, *Radiative corrections to QCD scattering amplitudes in a multi-Regge kinematics*, *Nucl. Phys. B* **406** (1993) 259.

- [56] V. Del Duca, *An introduction to the perturbative QCD pomeron and to jet physics at large rapidities*, [hep-ph/9503226](#).
- [57] V.S. Fadin, R. Fiore and A. Quartarolo, *Quark contribution to the reggeon - reggeon - gluon vertex in QCD*, *Phys. Rev. D* **50** (1994) 5893 [[hep-th/9405127](#)].
- [58] V.S. Fadin, R. Fiore and M.I. Kotsky, *Gribov's theorem on soft emission and the reggeon-reggeon - gluon vertex at small transverse momentum*, *Phys. Lett. B* **389** (1996) 737 [[hep-ph/9608229](#)].
- [59] V. Del Duca and C.R. Schmidt, *Virtual next-to-leading corrections to the Lipatov vertex*, *Phys. Rev. D* **59** (1999) 074004 [[hep-ph/9810215](#)].
- [60] V. Del Duca, C. Duhr, E.W. Nigel Glover and V.A. Smirnov, *The One-loop pentagon to higher orders in epsilon*, *JHEP* **01** (2010) 042 [[0905.0097](#)].
- [61] V. Del Duca, C. Duhr and E.W. Nigel Glover, *The Five-gluon amplitude in the high-energy limit*, *JHEP* **12** (2009) 023 [[0905.0100](#)].
- [62] V.S. Fadin, M. Fucilla and A. Papa, *One-loop Lipatov vertex in QCD with higher ϵ -accuracy*, [2302.09868](#).
- [63] S. Abreu, J. Dormans, F. Febres Cordero, H. Ita and B. Page, *Analytic Form of Planar Two-Loop Five-Gluon Scattering Amplitudes in QCD*, *Phys. Rev. Lett.* **122** (2019) 082002 [[1812.04586](#)].
- [64] S. Abreu, J. Dormans, F. Febres Cordero, H. Ita, B. Page and V. Sotnikov, *Analytic Form of the Planar Two-Loop Five-Parton Scattering Amplitudes in QCD*, *JHEP* **05** (2019) 084 [[1904.00945](#)].
- [65] S. Abreu, F. Febres Cordero, H. Ita, B. Page and V. Sotnikov, *Leading-color two-loop QCD corrections for three-jet production at hadron colliders*, *JHEP* **07** (2021) 095 [[2102.13609](#)].
- [66] B. Agarwal, F. Buccioni, F. Devoto, G. Gambuti, A. von Manteuffel and L. Tancredi, *Five-parton scattering in QCD at two loops*, *Phys. Rev. D* **109** (2024) 094025 [[2311.09870](#)].
- [67] G. De Laurentis, H. Ita, M. Klinkert and V. Sotnikov, *Double-virtual NNLO QCD corrections for five-parton scattering. I. The gluon channel*, *Phys. Rev. D* **109** (2024) 094023 [[2311.10086](#)].
- [68] G. De Laurentis, H. Ita and V. Sotnikov, *Double-virtual NNLO QCD corrections for five-parton scattering. II. The quark channels*, *Phys. Rev. D* **109** (2024) 094024 [[2311.18752](#)].
- [69] G. De Laurentis, *Non-Planar Two-Loop Amplitudes for Five-Parton Scattering*, in *Loops and Legs in Quantum Field Theory*, 6, 2024 [[2406.18374](#)].
- [70] S. Abreu, G. De Laurentis, G. Falcioni, E. Gardi, C. Milloy and L. Vernazza, *The Two-Loop Lipatov Vertex in QCD*, 2024. <https://doi.org/10.5281/zenodo.14568484>.
- [71] V. Del Duca, *Equivalence of the Parke-Taylor and the Fadin-Kuraev-Lipatov amplitudes in the high-energy limit*, *Phys. Rev. D* **52** (1995) 1527 [[hep-ph/9503340](#)].
- [72] A. Bassetto, M. Ciafaloni and G. Marchesini, *Jet Structure and Infrared Sensitive Quantities in Perturbative QCD*, *Phys. Rept.* **100** (1983) 201.
- [73] S. Catani and M.H. Seymour, *The Dipole formalism for the calculation of QCD jet cross-sections at next-to-leading order*, *Phys. Lett. B* **378** (1996) 287 [[hep-ph/9602277](#)].

- [74] S. Catani and M.H. Seymour, *A General algorithm for calculating jet cross-sections in NLO QCD*, *Nucl. Phys. B* **485** (1997) 291 [[hep-ph/9605323](#)].
- [75] V. Del Duca, C. Duhr, E. Gardi, L. Magnea and C.D. White, *The Infrared structure of gauge theory amplitudes in the high-energy limit*, *JHEP* **12** (2011) 021 [[1109.3581](#)].
- [76] D. Chicherin and V. Sotnikov, *Pentagon Functions for Scattering of Five Massless Particles*, *JHEP* **20** (2020) 167 [[2009.07803](#)].
- [77] W. Wasow, *Asymptotic expansions for ordinary differential equations*, vol. XIV, Interscience Publishers John Wiley & Sons, Inc. (1965).
- [78] M. Hidding, *DiffExp, a Mathematica package for computing Feynman integrals in terms of one-dimensional series expansions*, *Comput. Phys. Commun.* **269** (2021) 108125 [[2006.05510](#)].
- [79] C. Duhr and F. Dulat, *PolyLogTools — polylogs for the masses*, *JHEP* **08** (2019) 135 [[1904.07279](#)].
- [80] E. Panzer, *Algorithms for the symbolic integration of hyperlogarithms with applications to Feynman integrals*, *Comput. Phys. Commun.* **188** (2015) 148 [[1403.3385](#)].
- [81] G. De Laurentis and B. Page, *Ansätze for scattering amplitudes from p -adic numbers and algebraic geometry*, *JHEP* **12** (2022) 140 [[2203.04269](#)].
- [82] H.A. Chawdhry, *p -adic reconstruction of rational functions in multiloop amplitudes*, *Phys. Rev. D* **110** (2024) 056028 [[2312.03672](#)].
- [83] E.P. Byrne, G. De Laurentis, E. Gardi and J.M. Smillie, *Work in progress*, .
- [84] G. Laurentis and D. Maître, *Extracting analytical one-loop amplitudes from numerical evaluations*, *JHEP* **07** (2019) 123 [[1904.04067](#)].
- [85] E.P. Byrne, V. Del Duca, L.J. Dixon, E. Gardi and J.M. Smillie, *One-loop central-emission vertex for two gluons in $\mathcal{N} = 4$ super Yang-Mills theory*, *JHEP* **08** (2022) 271 [[2204.12459](#)].
- [86] E.P. Byrne, *One-loop five-parton amplitudes in the NMRK limit*, *JHEP* **07** (2024) 284 [[2312.15051](#)].
- [87] A. von Manteuffel and R.M. Schabinger, *A novel approach to integration by parts reduction*, *Phys. Lett. B* **744** (2015) 101 [[1406.4513](#)].
- [88] T. Peraro, *Scattering amplitudes over finite fields and multivariate functional reconstruction*, *JHEP* **12** (2016) 030 [[1608.01902](#)].
- [89] <https://github.com/GDeLaurentis/antares>.
<https://doi.org/10.5281/zenodo.14501989>.
- [90] <https://github.com/GDeLaurentis/antares-results>.
<https://doi.org/10.5281/zenodo.14536697>.
- [91] <https://github.com/GDeLaurentis/lips>.
<https://zenodo.org/doi/10.5281/zenodo.11518261>.
- [92] <https://github.com/GDeLaurentis/pyadic>.
<https://zenodo.org/doi/10.5281/zenodo.11114230>.
- [93] S. Abreu, J. Dormans, F. Febres Cordero, H. Ita, M. Kraus, B. Page et al., *Caravel: A C++ framework for the computation of multi-loop amplitudes with numerical unitarity*, *Comput. Phys. Commun.* **267** (2021) 108069 [[2009.11957](#)].

- [94] M.T. Grisaru, H.J. Schnitzer and H.-S. Tsao, *The Reggeization of elementary particles in renormalizable gauge theories: scalars*, *Phys. Rev. D* **9** (1974) 2864.
- [95] M.T. Grisaru, H.J. Schnitzer and H.-S. Tsao, *Reggeization of yang-mills gauge mesons in theories with a spontaneously broken symmetry*, *Phys. Rev. Lett.* **30** (1973) 811.
- [96] M.T. Grisaru, H.J. Schnitzer and H.-S. Tsao, *Reggeization of elementary particles in renormalizable gauge theories - vectors and spinors*, *Phys. Rev. D* **8** (1973) 4498.
- [97] I.T. Drummond, P.V. Landshoff and W.J. Zakrzewski, *Signature in production amplitudes*, *Phys. Lett. B* **28** (1969) 676.
- [98] J. Bartels, *A Reggeon Calculus for the Production Amplitude. 1.*, *Phys. Rev. D* **11** (1975) 2977.
- [99] V.S. Fadin, R. Fiore and A. Papa, *One loop Reggeon-Reggeon gluon vertex at arbitrary space-time dimension*, *Phys. Rev. D* **63** (2001) 034001 [[hep-ph/0008006](#)].
- [100] Z. Bern, V. Del Duca and C.R. Schmidt, *The Infrared behavior of one loop gluon amplitudes at next-to-next-to-leading order*, *Phys. Lett. B* **445** (1998) 168 [[hep-ph/9810409](#)].
- [101] A.B. Goncharov, *Multiple polylogarithms, cyclotomy and modular complexes*, *Math. Res. Lett.* **5** (1998) 497 [[1105.2076](#)].
- [102] A.B. Goncharov, *Multiple polylogarithms and mixed Tate motives*, [math/0103059](#).
- [103] O. Schnetz, *Generalized single-valued hyperlogarithms*, [2111.11246](#).
- [104] F.C.S. Brown, *Polylogarithmes multiples uniformes en une variable*, *Compt. Rend. Math.* **338** (2004) 527.
- [105] J. Pennington, *The six-point remainder function to all loop orders in the multi-Regge limit*, *JHEP* **01** (2013) 059 [[1209.5357](#)].
- [106] L.J. Dixon, C. Duhr and J. Pennington, *Single-valued harmonic polylogarithms and the multi-Regge limit*, *JHEP* **10** (2012) 074 [[1207.0186](#)].
- [107] F. Brown, *Single-valued Motivic Periods and Multiple Zeta Values*, *SIGMA* **2** (2014) e25 [[1309.5309](#)].
- [108] O. Schnetz, *Graphical functions and single-valued multiple polylogarithms*, *Commun. Num. Theor. Phys.* **08** (2014) 589 [[1302.6445](#)].
- [109] V. Del Duca, L.J. Dixon, C. Duhr and J. Pennington, *The BFKL equation, Mueller-Navelet jets and single-valued harmonic polylogarithms*, *JHEP* **02** (2014) 086 [[1309.6647](#)].
- [110] C.W. Bauer, A. Frink and R. Kreckel, *Introduction to the GiNaC framework for symbolic computation within the C++ programming language*, *J. Symb. Comput.* **33** (2002) 1 [[cs/0004015](#)].
- [111] A.V. Kotikov and L.N. Lipatov, *DGLAP and BFKL evolution equations in the N=4 supersymmetric gauge theory*, in *35th Annual Winter School on Nuclear and Particle Physics*, 12, 2001 [[hep-ph/0112346](#)].
- [112] A.V. Kotikov and L.N. Lipatov, *DGLAP and BFKL equations in the N = 4 supersymmetric gauge theory*, *Nucl. Phys. B* **661** (2003) 19 [[hep-ph/0208220](#)].
- [113] E. Gardi, S. Caron-Huot, J. Reichel and L. Vernazza, *The High-Energy Limit of 2-to-2 Partonic Scattering Amplitudes*, *PoS RADCOR2019* (2019) 050 [[1912.10883](#)].

- [114] C. Anastasiou, E.W.N. Glover and C. Oleari, *Application of the negative dimension approach to massless scalar box integrals*, *Nucl. Phys. B* **565** (2000) 445 [[hep-ph/9907523](#)].
- [115] C. Anastasiou, E.W.N. Glover and C. Oleari, *Scalar one loop integrals using the negative dimension approach*, *Nucl. Phys. B* **572** (2000) 307 [[hep-ph/9907494](#)].
- [116] S. Bloch, *Higher Regulators, Algebraic K-Theory, and Zeta Functions of Elliptic Curves*, CRM Monograph Series, American Mathematical Society (2011).
- [117] V. Del Duca, G. Falcioni, L. Magnea and L. Vernazza, *Beyond Reggeization for two- and three-loop QCD amplitudes*, *PoS RADCOR2013* (2013) 046 [[1312.5098](#)].
- [118] V. Fadin, *Particularities of the NNLLA BFKL*, *AIP Conf. Proc.* **1819** (2017) 060003 [[1612.04481](#)].
- [119] V. Fadin, *Chapter 4: BFKL — Past and Future*, in *From the Past to the Future*, J. Bartels, V. Fadin, E. Levin, A. Levy, V. Kim and A. Sabio-Vera, eds., pp. 63–90 (2021), DOI [[2012.11931](#)].
- [120] V.S. Fadin, *Three-Reggeon Cuts in QCD Amplitudes*, *Phys. Atom. Nucl.* **84** (2021) 100.
- [121] R.J. Eden, P.V. Landshoff, D.I. Olive and J.C. Polkinghorne, *The analytic S-matrix*, Cambridge Univ. Press, Cambridge (1966).
- [122] J. Kwiecinski and M. Praszalowicz, *Three Gluon Integral Equation and Odd c Singlet Regge Singularities in QCD*, *Phys. Lett. B* **94** (1980) 413.
- [123] L.N. Lipatov, *Asymptotic behavior of multicolor QCD at high energies in connection with exactly solvable spin models*, *JETP Lett.* **59** (1994) 596 [[hep-th/9311037](#)].
- [124] L.D. Faddeev and G.P. Korchemsky, *High-energy QCD as a completely integrable model*, *Phys. Lett.* **B342** (1995) 311 [[hep-th/9404173](#)].
- [125] S.E. Derkachov, G.P. Korchemsky and A.N. Manashov, *Noncompact Heisenberg spin magnets from high-energy QCD: 1. Baxter Q operator and separation of variables*, *Nucl. Phys. B* **617** (2001) 375 [[hep-th/0107193](#)].
- [126] S.E. Derkachov, G.P. Korchemsky, J. Kotanski and A.N. Manashov, *Noncompact Heisenberg spin magnets from high-energy QCD. 2. Quantization conditions and energy spectrum*, *Nucl. Phys. B* **645** (2002) 237 [[hep-th/0204124](#)].
- [127] S. Mandelstam, *Cuts in the Angular Momentum Plane. 2*, *Nuovo Cim.* **30** (1963) 1148.
- [128] M. Ciafaloni and G. Camici, *Energy scale(s) and next-to-leading BFKL equation*, *Phys. Lett. B* **430** (1998) 349 [[hep-ph/9803389](#)].
- [129] A.V. Kotikov and L.N. Lipatov, *NLO corrections to the BFKL equation in QCD and in supersymmetric gauge theories*, *Nucl. Phys. B* **582** (2000) 19 [[hep-ph/0004008](#)].
- [130] V. Del Duca, *Real next-to-leading corrections to the multi - gluon amplitudes in the helicity formalism*, *Phys. Rev. D* **54** (1996) 989 [[hep-ph/9601211](#)].
- [131] V. Del Duca and C.R. Schmidt, *Virtual next-to-leading corrections to the impact factors in the high-energy limit*, *Phys. Rev. D* **57** (1998) 4069 [[hep-ph/9711309](#)].
- [132] S. Catani, *The Singular behavior of QCD amplitudes at two loop order*, *Phys. Lett. B* **427** (1998) 161 [[hep-ph/9802439](#)].
- [133] G.F. Sterman and M.E. Tejeda-Yeomans, *Multiloop amplitudes and resummation*, *Phys. Lett. B* **552** (2003) 48 [[hep-ph/0210130](#)].

- [134] S. Aybat, L.J. Dixon and G.F. Sterman, *The Two-loop soft anomalous dimension matrix and resummation at next-to-next-to leading pole*, *Phys. Rev. D* **74** (2006) 074004 [[hep-ph/0607309](#)].
- [135] S. Aybat, L.J. Dixon and G.F. Sterman, *The Two-loop anomalous dimension matrix for soft gluon exchange*, *Phys. Rev. Lett.* **97** (2006) 072001 [[hep-ph/0606254](#)].
- [136] E. Gardi and L. Magnea, *Factorization constraints for soft anomalous dimensions in QCD scattering amplitudes*, *JHEP* **03** (2009) 079 [[0901.1091](#)].
- [137] E. Gardi and L. Magnea, *Infrared singularities in QCD amplitudes*, *Frascati Phys. Ser.* **50** (2010) 137 [[0908.3273](#)].
- [138] L.J. Dixon, E. Gardi and L. Magnea, *On soft singularities at three loops and beyond*, *JHEP* **02** (2010) 081 [[0910.3653](#)].
- [139] T. Becher and M. Neubert, *Infrared singularities of scattering amplitudes in perturbative QCD*, *Phys. Rev. Lett.* **102** (2009) 162001 [[0901.0722](#)].
- [140] T. Becher and M. Neubert, *Infrared singularities of scattering amplitudes and N^3LL resummation for n -jet processes*, *JHEP* **01** (2020) 025 [[1908.11379](#)].
- [141] O. Almelid, C. Duhr and E. Gardi, *Three-loop corrections to the soft anomalous dimension in multileg scattering*, *Phys. Rev. Lett.* **117** (2016) 172002 [[1507.00047](#)].
- [142] O. Almelid, C. Duhr, E. Gardi, A. McLeod and C.D. White, *Bootstrapping the QCD soft anomalous dimension*, *JHEP* **09** (2017) 073 [[1706.10162](#)].
- [143] L. Magnea, *Non-abelian infrared divergences on the celestial sphere*, *JHEP* **05** (2021) 282 [[2104.10254](#)].